



**4<sup>th</sup> Conference of the EFRC  
June 9<sup>th</sup> / 10<sup>th</sup>, 2005, Antwerp**

## Contents

### Hydrogen

- Upgrading Hydrogen Booster Compressors at the BP/ Innovene Grangemouth Hydrocracker Complex** - 7 -  
*J. Jones, J. Campbell; BP Grangemouth Refinery*
- Hydrogen Compression in Refining, Petrochemical and Chemical Applications** - 17 -  
*J. Khor; BASF Petronas Chemicals Sdn. Bhd.*
- Service Life Improvement of Piston-Rod Sealing Systems by Means of Pressure-Relieved Sealing Elements** - 23 -  
*N. Feistel; Burckhardt Compression*

### Operation & Maintenance

- Concept Selection and Design Considerations for Compression Facilities for FPSO Glas Dowl** - 33 -  
*J. de Roos, J. Gillis; Bluewater Energy Services*  
*A. Eijk; TNO Science & Industry*
- Technical Improvement of Hyper Compressor in LDPE Plant** - 43 -  
*J. Bojan, S. Dragan; HIP-Petrohemija*
- The Use of HydroCom to Determine the Root Cause of K6301 Compressor Failure** - 49 -  
*P. Melvin; Shell UK, Stanlow Manufacturing Complex*

### Fundamentals

- CFD Simulation of the Two Phase Pulsating Flow in the Reciprocating Compressor Installation** - 59 -  
*P. Cyklis, K. Ryszard; Cracow University of Technology*
- Simulation Methods for Piston Compressors** - 65 -  
*Th. Steidten, S. Pischinger, W. Wiese; VKA – Technical University of Aachen*  
*M. Hopp; FEV Motorentechnik*
- Fundamental Research on Tribology of PTFE Wear Parts Opens Windows of Opportunity for Improved Materials** - 75 -  
*A. Dittmann, B. Spiegl, P. Steinrück; Hoerbiger Ventilwerke*

### Operation & Maintenance

- Free Floating Piston™ Case History of Revamp of Existing Compressors** - 85 -  
*L. Koop; Thomassen Compression Systems*
- Construction Unit Damage and Corrosion Attack at CO<sub>2</sub> Reciprocating Compressors** - 93 -  
*H. Ochs, J. Titz; BASF*
- Detection of Concealed Damages in Early Stages on Reciprocating Machinery** - 101 -  
*E. Drewes; PROGNOST Systems*



## Innovation & Technology

- Solutions Developed to Meet Very Stringent Requirements for an Offshore Application of a Reciprocating Compressor System** - 109 -  
*H. Elferink; Thomassen Compression Systems*  
*A. Eijk; TNO*
- Advanced Monitoring and Diagnostic System for Reciprocating Compressors** - 119 -  
*E. Giacomelli, E. Calamai, D. Martinelli, N. Monachino; GE Energy*
- Analysis of Torsional Vibrations in Reciprocating Compressors driven by Electric Motors and Gas Engines** - 127 -  
*A. Laschet; ARLA Maschinentechnik*

## Operation & Maintenance

- Increased Reliability and Extended Service Intervals in an Ethylene Oxide Plant** - 137 -  
*M. Seedorf, U. Bartsch; Sasol Germany*
- Noise Reduction at a NAM-compressor Station** - 143 -  
*H. Korst; TNO Science & Industry*  
*W. Brocatus; Nederlandse Aardolie Maatschappij*

## Education at EFRC

- Educating Reciprocating Compressor Engineers at the EFRC** - 153 -  
*Siegmond Cierniak*

## EFRC Research

- Thermodynamic Simulation of Reciprocating Compressors to enable Diagnostic based on Measured Temperatures and Pressures** - 159 -  
*M. Huschenbett, G. Will; Technical University of Dresden*
- Valve Dynamics and Internal Waves in a Reciprocating Compressor** - 169 -  
*H. Steinrück, R. Aigner, G. Meyer; Institute of Fluid Mechanics and Heat Transfer – Technical University of Vienna*
- Effect of Pulsations on Separator Efficiency** - 179 -  
*G. Alberts, S.P.C. Belfroid; TNO Science & Industry*

## Operation & Maintenance

- Modification of a Reciprocating Compressor due to process Changes in the TOTAL Refinery in Spergau/ Germany** - 187 -

*S. Gast; Borsig ZM Compression  
P.M. Rainer; TRM Total Raffinerie Mitteldeutschland*

- Pulsation Study for Two 2250 bar Hyper Compressors – Measurement, Theory, Measures** - 197 -

*A. Brümmer; KÖTTER Consulting Engineers*

## Selection & Sizing

- Automatic Strength Calculation of Pistons for Reciprocating Compressors** - 207 -

*K. Hoff, P. Houba, G. Knop, F. Ohler, E. Steinbusch; NEUMAN & ESSER*

- Development of a New Gas Compressor – Design of a Crankshaft and Strength Test by Means of FEM** - 215 -

*G. Braun; Josef Mehrer Maschinenfabrik*

- Operating History of Moderate-speed API-618 Compressors in Refinery Service** - 219 -

*G.M. Kopsick; ARIEL Corporation*

- Repair, Revamp or Replace Natural Gas Reciprocating Compressors for Underground Storage** - 237 -

*S. Cierniak; HGC Hamburg Gas Consult  
T. Knebel; VNG Verbundnetz Gas*

## Fundamentals

- Experimental Study of a Resonating Ring Plate Valve** - 247 -

*R. Habing; University of Twente  
J. Bolle, J. Smeulers; TNO Science & Industry*

- Reciprocating Compressor Valve Plate Life and Performance Analysis** - 257 -

*K. Brun, J.P. Platt, A.J. Smalley, M.G. Nored; Southwest Research Institute,  
BP company*

## Selection & Sizing

- Sizing and Optimization of Compressors in IdPE Plants and Validation by Measurement** - 267 -

*C. Krockner, A. Allenspach; Burckhardt Compression*

- Economical Pipe Stress Analysis using Parametric Modelling and Design Standards** - 277 -

*V. Kacani, E. Huttar; Leobersdorfer Maschinenfabrik*



# **Upgrading Hydrogen Booster Compressors at the BP / Innovene Grangemouth Hydrocracker Complex**

**by:**

**Jerry Jones**

**Senior Rotating Machinery Engineer**

**Jim Campbell**

**Refinery Maintenance Manager**

**Innovene Grangemouth Refinery**

**Scotland**

**4<sup>th</sup> Conference of the EFRC  
June 9<sup>th</sup> / 10<sup>th</sup>, 2005, Antwerp**

## **Abstract:**

Hydrogen forms the building block of a lot of the processes in Refining. As such, the compression of hydrogen is an essential part of most Refining processes, and the compressors used for this duty form the backbone of the unit availability and reliability.

This paper reviews the upgrades that have had to be made to two Worthington Simpson hydrogen booster compressors that form the heart of the BP / Innovene Grangemouth Hydrocracker complex. These machines boost the hydrogen supply pressure from 15.75 barg to 149 barg for the Hydrocracker loop. The reliability of these machines has historically been very poor. With proposed increases in production operating run lengths, there is less and less opportunity for preventative maintenance activity to take place; the unreliability of these machines has therefore had to be engineered out so that they will achieve in excess of 18 months uninterrupted operation.

## 1 Introduction

The GM-H2MU-C-202 A & B are two Worthington Simpson BDC – 3 OF6 16 – 6 reciprocating compressors – affectionately known as the “Booster compressors”. They were built during 1968 and installed and commissioned the following year. Their duty is to take hydrogen from the Hydrogen Manufacturing unit and the Catalytic Reformer / Cryogenic Unit and pressurise it to Hydrocracker loop pressure. They originally ran as main and stand-by, but as time went by and the plants were de-bottlenecked, they now run in parallel.

The compressors are three stage six cylinder machines. Stage 1 cylinders are 18 ½” (cylinders 1 & 2), stage cylinders are 12 ½” (cylinders 3 & 5) and stage 3 cylinders are 9 ¼” (cylinders 4 & 6).

6 pockets on the first stage cylinders give capacity control. These pockets are controlled by a progressive cam system. This gives a total of 18 steps from 60% to 100% load.

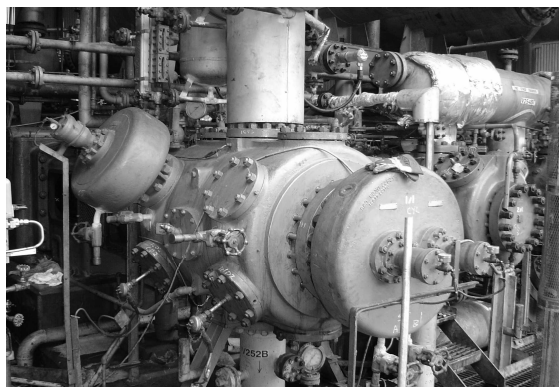


**Figure 1:** View of “A” machine capacity control pockets and control pistons

The compressors are direct coupled to single bearing 11kV electric motors rated at 6.6 MW. Each motor weighs in at 65 tons.



**Figure 2:** View of Booster compressor house from the North

## 2 Background

### 2.1 History

Because of the compact nature of the installation, the suction knock-outs and dampers are combined into one snubberator vessel for each of the second and third stages, but one for each of the first stage cylinders. These vessels are a work of art internally, but how effective they are is open to conjecture.

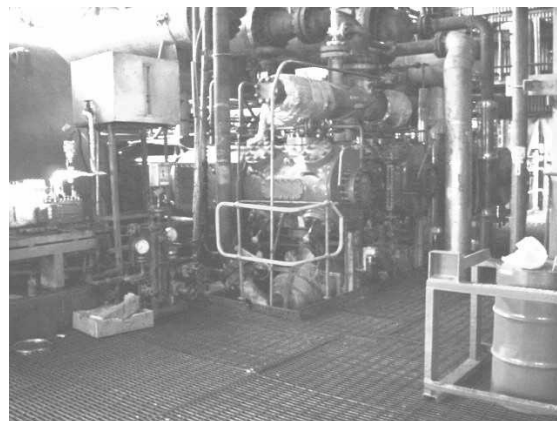


**Figure 3:** View of 3<sup>rd</sup> stage cylinders and common snubberator

During the 80’s and 90’s, these machines suffered because of the management regime that was driven by the universal mantra at the time of cutting costs and reducing head counts – what we have referred to as the “dark ages” for our machinery. This resulted in the significant machinery outages during 1999 and 2000 and poor maintenance records.

The problems in 1999 & 2000 resulted in a reappraisal of how we carried out maintenance on these machines, with the result that there is now a renewed focus on these machines.

### 2.2 Original specification

Originally these machines were designed for single machine operation with a capacity of 32,900 SCFM and a total gas power of 7290 hp (5.43MW).

### 2.3 Maintenance regime

During the good old days of the 70’s and 80’s, these machines were maintained by their own dedicated compressor squad. Because they were operated as an on-line machine and stand-by, the stand-by could be overhauled during its “rest” period. This led to a culture of continuous maintenance and a masking of underlying problems with the machine design and operation.

During the 80's and 90's there was the de-manning of the maintenance teams and the cutbacks in maintenance expenditure. This coupled with the use of less experienced Engineers in positions of responsibility stored up trouble for later. At the end of 1999 and beginning of 2000, both machines suffered extensive failures of big-end bearings and the failure of one of the drive motors. Both motors were re-wound and significant work was done in the crankcase, but more of that later.

## 2.4 Piston rods locking system

During the early life of the compressors there were a number of piston rod failures. Some were the result of a weak design at the threaded section, but incorrect tensioning of the locking system caused some of the failures. This was resolved by paying very close attention to the procedure for installing the locking ring.

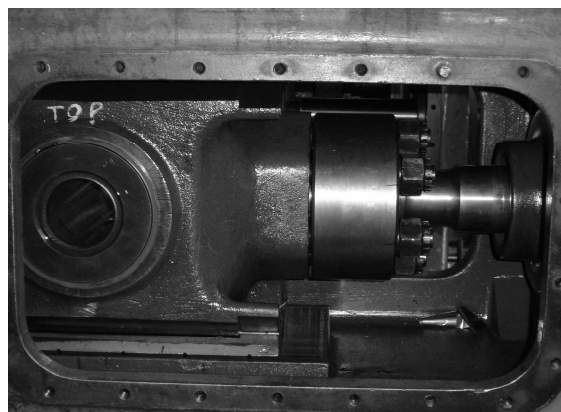


**Figure 4:** Crosshead / piston rod and piston rod locking ring

## 2.5 Liners and head fits

The liners on these machines have created hours of amusement for our maintenance personnel. The liners are all in-situ shrink fits. We have had a number of liner failures around the head end flange of the liner, where the liners have cracked circumferentially. The liners were re-designed around the change of section of the liner to reduce the stress raiser at the flange section.

These compressors have always suffered from intermittent leakage from the third stage cylinder head gaskets, especially the No 6 cylinders. When the heads have been removed, the aluminium gaskets have been badly extruded. The most probable root cause is thought to be liquid carry-over. This has resulted in a stretching of the head cover bolts as liquid passes through the machine, with a resultant hammering of the head cover gasket, reducing the effectiveness of the gasket and

reducing the amount of pre-stretch on the head cover bolting.

In an attempt to reduce the effect of the thinning of the aluminium gaskets, soft iron gaskets were tried. This resulted in a cracked liner at the head end. As a short-term measure, we have reverted back to the aluminium gaskets, but increased the thickness, which seems to be working at the moment.

## 3 Liquid carry over

### 3.1 Process outline

The compressors source their feed from two plants. The Cryogenic hydrogen is almost pure hydrogen, but the Hydrogen unit hydrogen also contains water vapour and Methane. It is the hydrogen from the later source that causes us problems. During the compression process the water tends to condense out especially at the third stage cylinders.

### 3.2 Snubberators

#### 3.2.1 Snubberator drain system

The snubberators are a combination of damper and knock out drum. Traditional arrangements have these two duties carried out by separate entities, but on these machines they are combined. The snubberator sectional drawings reveal a nightmare of Bernoulli tubes, cyclones, baffles and coalescers. Because of the compact nature of these vessels, there is a question mark over their effectiveness.

Originally, drain pigs were used to drain liquid from these vessels, but these used to block up or stop working effectively. This would cause the separator sections to become flooded and liquid could be drawn into the machine before it could trip out on high level in the knockouts. The drain system was modified with high capacity drums external to the compressor house and the removal of the pigs.

#### 3.2.2 Super heaters

The steam driven super-heaters were removed from the snubberators following a heater failure, which released hydrogen into the steam system. This has resulted in an increase in liquid condensing out between the coalescers and the cylinder inlet manifolds. This has been partially mitigated by tracing and lagging the snubberators and connecting pipework. But the real cure will be an improved separation system inter-stage.



### 3.2.3 Effects on the valves

The valve problems that we experience now are normally related to liquid ingress – broken springs, buttons and outer rings. There is also evidence from the CM data of valve event phase shifting. This is most likely related to the over-lubrication to counter the condensate washout.

We have historically changed out one machine set of valves each year, regardless of condition – 40 valves in total. Since we have started to send the valves off-site for overhaul by an external company, we have seen a significant increase in the reliability of the valves.



**Figure 5:** Cylinder 5 HE suction valve 1 with liquid slugging damage (oil and condensate)

With the change in the operating regime of the plants, the valves will now be expected to operate for 36 months. This will be a test of valves and our ability to eliminate the liquid ingress issues.

### 3.2.4 Cylinder lubrication

Manzel point-to-point lubricators lubricate the compressor cylinders. This design of lubricator has proved to be a little variable at times and constantly requires adjustment to keep the drip rate correct. Because of the liquid ingress, we have had to increase the lubrication rates to compensate. This additional lubrication has to go somewhere, and that is usually into the discharge dampers and intercoolers, from whence it periodically makes an appearance at the suction to the next stage cylinders.

## 3.3 Cylinder Jacket cooling

This cylinder jacket cooling system is a closed cooling system, which is shared with two other compressors. The system is common to all cylinders. The system is now operated such that there is a 5 – 10 DegC differential between the

lowest process gas suction temperature and the cylinder cooling jacket inlet temperature. This is to prevent the chilling of the process stream entering the cylinders, which causes additional liquid knockout.

## 4 Areas of development

### 4.1 Valves

Originally the compressors were fitted with Worthington metal plate valves. These were reported to be unreliable and valve breakages resulted in occasional cylinder damage from the ingress of metal components

Since the installation of the Manley valves in the 1980's, valve reliability has been good, although we did have an issue with overhaul quality, so we now pay particular attention to controlling the valve movements during overhaul, as some of the second and third stage valves are identical in size, but the spring rates are different. We also now have some valves fitted with through valve porting for the PT tappings. The moral of the story is that the correct overhaul procedures are required and control of components is vitally important to these machines.

### 4.2 Wear components

#### 4.2.1 Rider Rings

These machines were originally equipped with dual rider rings at each end of the piston. The rings were also single piece with no pressure relieving grooves.

Rider ring breakages were a regular occurrence, so a modification to alter the design of the rider ring bands and piston rings to improve their reliability was developed.

#### 4.2.2 Rider Rings Re-design

The Rider Ring problems stem from three areas:

- The current rings have to be heated and stretched onto the piston, incurring unnecessary stresses;
- The rings are too thin to be designed with pressure relief grooves causing the rider rings to act as piston rings thereby attempting to seal the pressure (particularly when pressure gets below the rider rings and lifts them from the piston), which they are not designed to do;
- The current arrangement has two rider rings at each end of the piston causing some outside rings to have almost 100% over-run on the valve ports.

The re-designed pistons enable the use of angle cut rider rings, which are thick enough to incorporate pressure-relieving grooves in line with API618. This design required a slight reduction of the diameter of piston at the rider ring locations and the 2nd Stage Rider Rings were reduced in length (despite the reduction in length the rider ring bearing loads remain below the API618 recommended levels).

The alteration also incorporated changing from two rider rings at each end of the piston to one ring. This has the benefit of reducing the amount of rider ring over-run of the valve ports to less than 30% (API618 requirement is less than 50%). In order to achieve this reduction in over-run, modifications to the ring stack were incorporated on the 2nd and 3rd Stage pistons.

### 4.2.3 Piston Rings Re-design

The primary design modification was to thicken (radially) the piston rings in all stages to provide greater strength to the ring. In the 2nd and 3rd Stages the ring width and groove width were reduced in order to allow a reduction in the amount of rider ring over-run on the valve ports. However, this reduction had the added benefit of spreading the pressure letdown to further into the ring stack, easing the stress on the outer rings.

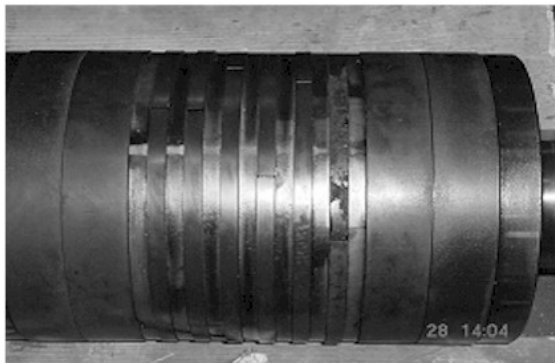


**Figure 6:** Original piston design showing double rider band arrangement

### 4.2.4 Results

The reliability improvement in these rings has been dramatic. In the three years since the modifications were implemented there has not been a single failure of a rider ring in either machine.

## 4.3 Bearings

The original bearings fitted to the machine have lasted really well. The problem was that no one checked them. Therefore, after a period of time some of bearings decided to take some time out

with a resultant big bang. Both machines lost their throw 6 big end bearings within a matter of 6 months. The investigation points to old age combined with high loading when we started up with saturated hydrogen from the hydrogen unit. Because we couldn't obtain the original bearings, we have worked closely with D+R to come up with a suitable replacement design of bearings.



**Figure 7:** One of the cylinder 6 bearings that failed in 2000

We were extremely lucky on both occasions in that the crankshaft journals were not damaged beyond a few light score marks.

## 5 Foundations

### 5.1 Introduction

Foundations are a crucial part of a reciprocating compressor. In addition to supporting the machine weight, the foundations are required to restrain the vibration forces generated by the movement of the compressor motion-works. This is achieved by generating friction at the interface between the foundation and the compressor base. Hold-down bolts are required to pre-load this interface, thereby increasing the friction force at the interface and allowing greater loads to be transmitted to the foundation block. The hold-down bolts are not there to restrain the vibration by themselves. Having good foundations is also critical for achieving and maintaining good alignment of the compressor's various components. It is therefore a necessity for good reliability to have correctly designed, installed and maintained foundations.

It should be pointed out at this point that the work outlined as follows was all carried out with the sister compressor operating on full load, and the plant still operating on partial throughput. If for any reason the running compressor was brought down because of the work being carried out on the non-running machine, then a major commercial impact would result.

## 5.2 Condition of the C202 A/B Foundations

The foundations of these compressors had deteriorated to such a degree that a high level of vibration was clearly evident between the machine base and the foundation block.

Oil had penetrated the interface between the compressor base and the foundation block. This “lubrication” almost totally eliminated the friction between the surfaces, making it impossible to tighten the holding down bolts sufficiently to eliminate compressor movement.

This amount of vibration had created three areas of major concern:

1. The crankcase was now being required to absorb very high levels of vibration, increasing the stresses and risk of major mechanical component failure.
2. The hold-down bolts were required to absorb the remaining vibration. Not only was this over-stressing the bolts (a number of hold-down bolt failures had been experienced) but it also created stress concentrations in the foundations leading to cracking of the concrete base.
3. Excess oil from the machine had made its way into the cracks in the foundations and with each cycle of the machine, the oil, by hydraulic action, was causing further expansion of the cracks. In addition the oil had impregnated the foundations further weakening the concrete.
4. Maintaining machine component alignment was becoming a losing battle.



**Figure 8:** Grouting condition upon breakout showing oil impregnation

The foundations were in a poor condition, and repairs had to be carried out before a major failure of the foundations or one of the compressor components occurred.

## 5.3 Repair Proposal

The C202 compressors each weigh upwards of 100 tons. To remove the crankshaft and crankcase is a major operation requiring not only a complex disassembly and re-build, but also a difficult re-alignment process. This could not be achieved within the available outage window.

In 2002 and 2003, 28 days annual unit commercial turn-down windows would be available for all civil related work on one machine plus any annual maintenance work that had to be carried out on the sister. Any extension to this duration would cost the Refinery many millions of dollars in added downtime. In order to carry out this work, it was also planned to carry out the remedial work with the machines in place.

The scope of each repair was as follows:

- 1) Break-out the grouting and remove concrete until sound concrete is found.
- 2) During the breakout, the machine is floated on jacking screws and heavy duty spacers fixed to the foundation block.
- 3) Drill holes of varying depth (2,5 & 8ft) to allow reinforcing rods to be forced through the foundations and allow epoxy compound to be injected into the foundation block to stabilise the block.
- 4) New rebar reinforcement cage to be installed under the compressor.
- 5) Install a three pour epoxy grouting.
- 6) Replace any failed holding down bolts.

## 5.4 Preparation

Prior to the civil engineering work, a number of mechanical activities had to be carried out. In order to reduce the weight on the compressor jacking screws and temporary supports when the foundation had been chipped-out, the overhead vessels and pipework was removed. To help with access around the machine during the civils works, cylinders 3, 4, 5 and 6 were also removed.

In order to protect the machine internals, all possible ingress paths were sealed. To prevent the dust escaping from the area local to the machine and affecting the surrounding machinery, in particular the sister machine, a double skinned and sealed habitat was built around each machine in turn. To remove the generated dust from the habitat, extraction fans were installed.



## 5.5 Chip-Out

As the foundations were chipped-out, it was found that the foundations had very little grout capping. What grout was there was badly oil soaked. Around the 'B' machine, 8" was sufficient to reach good concrete, whilst around the 'A' machine a 12" chip-out was required.

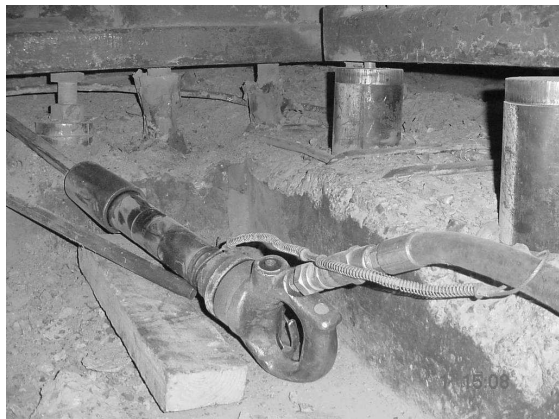


**Figure 9:** Support spacers installed under compressor components during chip-out

## 5.6 Crack Repairs

The main foundation block was cracked in a number of planes. In order to repair the cracks, holes were drilled and block injected under pressure to squeeze out the contaminants and fill the cracks. In some places a number of injections were required because of the severity of the cracking.

## 5.7 Removal of Veneer

After the foundation block injection, a final chip-out was required. This was to remove the excess epoxy over pour and to ensure a good surface bond between the old and new concrete. Concrete was also removed of the sides of the foundation block for 1-4 inches to ensure the new epoxy cap established a good anchorage to the existing block.

## 5.8 Preparation for Epoxy Pour

The base of the compressor was grit-blasted following breakout. This was to remove any oil and rust debris from the underside of the compressor and provide a good bonding surface.

Rebar cages were installed to bring the critical load bearing areas rebar densities upto current normally accepted levels.

The shuttering was installed with a release coating and expansion joint forms in the high stress areas.



**Figure 10:** Additional rebar cage installed prior to shuttering

Finally the holding down bolts and jacking screws were taped up to ensure the epoxy does not bind to the bolts. It would ensure that the jacking screws can be loosened after the epoxy has cured.

## 5.9 Epoxy Pouring

The epoxy was applied in three pours for this depth since the curing is an exothermic reaction and applying too large a mass results in too rapid a curing.

The foundation block and compressor casing was heated at temperatures above 70oF (20oC) by applying hot air into the enclosure habitat using large air blowers heated by plant steam.

After the first pour was carried out it was allowed to cure for 12 hours. Immediately after this curing period the second pour was completed. When the second pour had cured, the compressor was aligned.

## 5.10 Compressor Re-alignment

The alignment philosophy reflected that this work had a short-time frame and is a maintenance repair rather than a new installation.

The machine was levelled from the crankcase through the distance pieces to the cylinders. The web deflections were used as corroboration that the crankcase was level in each plane. The rod run out were also used to confirm the relative position of the cylinder and the distance piece. Because the B machine train was lying down by the oil pump end and canted over to the North, the decision was taken to maintain the train relative alignment and correct within the planes. The change in absolute alignment of the compressor train was caused by the settling of the support raft at the North / East end.

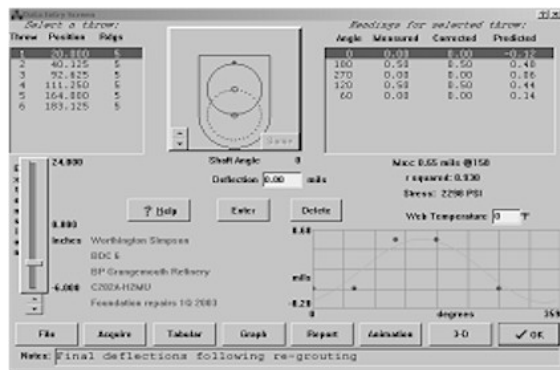


**Figure 11:** Webmap display of web deflection following final grouting of the A machine

## 5.11 Capping Pour

After a satisfactory alignment, the third and final pour was carried out. The epoxy was cured for 48 hours at temperatures no less than 70oF (20oC). The jacking screws were loosened back and the hold-down bolts tightened down and a final set of web deflections were taken.



**Figure 12:** Final grouting installation

Oil resistant silicone sealant was applied over the expansion joints and between the machine and the new foundation to prevent oil getting in between the foundation.

Following the successful foundation repairs, the machines were re-built and any routine maintenance required was carried out.

## 6 Condition Monitoring

On the Booster compressors we were operating blind as far as the key component condition was concerned. In order to rectify this we fitted a key phaser onto each machine and start taking vibration and ultrasonic data from each of the valves. Originally our only monitoring for the valves was temperature readings from the suction valves. This

tended to be very erratic and would only show up a problem once the valve had failed and we had a significant problem, which would require an immediate shutdown.

Because of the age and design of the compressor, the fitting of indicator ports through the cylinder wall was not feasible. The only available option was to fit indicator ports through the suction valves. This was eventually carried out after extensive risk assessments.

The system has been in place now for just over two years, and has resulted in significant early identification of problems. We now can identify failing valves early on in the failure cycle and often we have months to plan a suitable operational window so the machine can be taken off-line and the valve changed out.

It isn't just valves that we have had success with, we recently overhauled the machine and the CM indicated a problem with the throw 4 crosshead. There was a knock at the 180 degree position. When we went into the machine we found the bottom slipper had worn unevenly at the head-end, resulting in a rocking of the crosshead at the change of direction at TDC.

An example of a defective valve and the associated traces can be seen. The temperature of the discharge valve was slightly higher than the rest (5HD2). Close inspection of the ultrasonic trace for valve 5HS2 shows that a wider than normal display can be seen during the valve quiet period. There is also a slight mismatch on the actual PT diagram when compared to the theoretical diagram. This mismatch also indicates a faulty valve. When the valve was changed out broken springs and a damaged ring face were found.

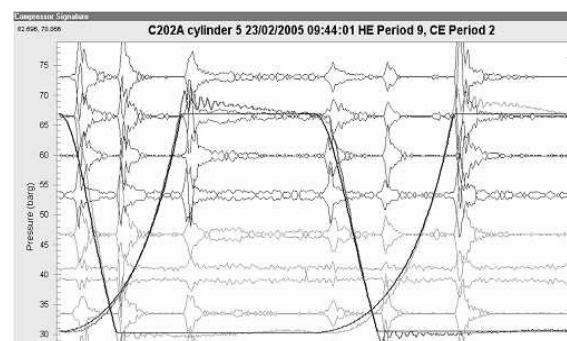


**Figure 13:** 5HD2 trace showing valve passing

The following pictures indicate why it is important to consider more than one set of data. The vibration traces indicate raised impacts, but no other problems with the valves, but if you now look at the

ultrasonic traces, you will see that there is considerable noise during the compression / discharge part of the cycle. This indicates a badly leaking valve. The valve was removed and found to be slightly distressed – see following picture – another good call for CM!

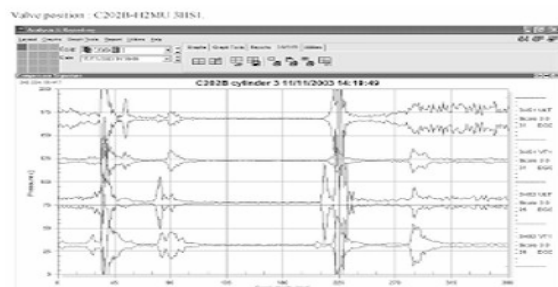


**Figure 14:** 3HS1 trace showing ultrasonic leaking valve indication



**Figure 15:** 3HS1 valve internals

Unusual patterns are very, important indications of faults when using this particular system, this is more important because of the need to rely heavily on trend information. Below is a plot that represents a fault detected on the crosshead of the B machine just prior to the March 2005 Outage. Although the fault doesn't look severe it nonetheless growing and it was seen to be a very important part of the machine. Failure of this part could have caused catastrophic failure and several days if not weeks of lost production. The problem was a worn crosshead shoe.

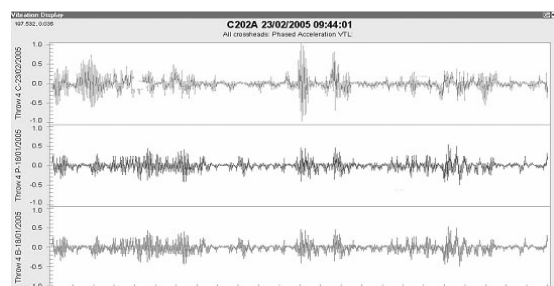


**Figure 16:** Knock detected at 180 degree position – worn crosshead shoe

For machines of this criticality, the obvious next move is to go to a hard wired system. We have looked a quite a few, and have yet to see a system which can achieve as comprehensive analysis as we can achieve with the Recip Trap. We might be proved wrong during this conference though!

## 7 Conclusion

The development of compressors is an ongoing process, and being Engineers we can always come up with ways to improve things! These compressors are over thirty years old, and if new machines were installed, then we would probably do things differently. The fact that they have run this long is a testament to the people who have operated these machines before – that doesn't stop them being a real pain to work on.

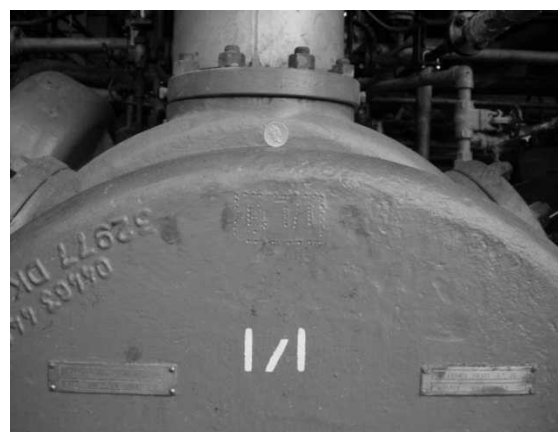


**Figure 17:** Cylinder 1 on the A machine under full load with a pound coin balancing on its edge – no glue was used!

## 8 Acknowledgements

Work like this is not the sole preserve of one person, but can only happen with the assistance of other people and disciplines. The recent rogues gallery associated with these machines include: Brian Arnott, Ewan Warbeck, Kevin Martin (The Tash), Willie Lochhead, Dave Wilson, Hugh Wakker, Stuart Bennie (Hoerbiger) & Robin Wilson (CPI) without whom the wheels of progress would not have turned.

## 9 Bibliographies

GMRC Foundation guidelines AJ Smally, PJ Pantermuehl

GMRC Reciprocating compressor foundations: Loading, Design, Analysis, Monitoring & Repair

## Hydrogen

J. Jones, J. Campbell: Upgrading Hydrogen Booster Compressors at the BP / Innovene Grangemouth Hydrocracker Complex

---

A.J. Smallye, J.S.Mandke, P.J.Pantermuehl, R.D.  
Drummond

Adhesive Services Co Good foundations reduce  
machinery maintenance E.M.Renfro

Compressor Tech Foundation renewal at Coastal's  
ANR Pipeline station April 2000 P.Burnside Arrow  
Industries Inc

Repairing cracked foundations under reciprocating  
compressors D.Smith & E.M.Renfro ASC



# **Hydrogen Compression in Refining, Petrochemical and Chemical Applications**

**by:**

**Jeffrey Khor**

**Oxo-/Syngas Plants**

**BASF PETRONAS Chemicals Sdn. Bhd.**

**Kuantan**

**Malaysia**

**khorcb@basf-petronas.com.my**

**4<sup>th</sup> Conference of the EFRC  
June 9<sup>th</sup> / 10<sup>th</sup>, 2005, Antwerp**

## **Abstract:**

With more stringent environmental legislation there is undoubtedly significant impact on the hydrogen balance in refineries. The need for ever-lower sulphur levels in both gasoline and diesel would mean an increase in process using hydrogen and the need for more high purity hydrogen.

Thus this gives rise to a need for oil free hydrogen gas compression for bottle-filling, pipelines, hydrogenation processes and other applications. The need for a simple and robust compressor design for long life, easy maintenance and the ability to cope with a flexible process condition are of great importance to the industries.

This paper reports from the BASF Petronas Chemicals (BPC) operations perspective the challenges encountered during the start-up, commissioning and optimization phases of our horizontal, 2-stage, high purity hydrogen gas reciprocating compressors.

Aim of the paper is to share the achievements through our continuous improvement on a journey towards excellence.



## 1 Introduction

To enable gas compression at the NAM-Grooteagst Synthesis Gas Plant of BASF Petronas Chemicals Sdn. Bhd. in Kuantan, Malaysia, was commissioned in April 2001. The plant produces hydrogen and carbon monoxide. The numerous hydrogen clients request bone-dry oil-free high purity hydrogen ( $H_2 > 99.99\%$ ) at higher pressure. The raw syngas is generated in a steam-methane reformer.  $CO_2$  removal is done via the aMDEA process. Downstream the aMDEA-unit hydrogen is separated from the synthesis gas via Pressure Swing Adsorption (PSA).

This paper describes the selection of an appropriate compressor type to meet the request for moisture and oil-free high purity hydrogen, the commissioning and start-up problems and the path how to finally assure that these compressors run without interruption throughout the year. High reliability of such compressors can only be assured if the right maintenance actions are being taken. The paper also discusses the various aspects of adequate maintenance.

## 2 Compressor Configuration

### 2.1 Selection of an appropriate compressor design

Kuantan Synthesis Gas Plant has a number of clients who consume hydrogen at a volume that can change quite significantly on daily basis. Basically there are two bigger consumers who consume in the order of magnitude of 12,000 to 17,000  $Nm^3/h$  and a couple of smaller ones who consume between 1,000 to 5,000  $Nm^3/h$  on an on/off-basis. Maximum requested pressure is 42 bar.

Since production of the downstream clients is on continuous basis and they unfortunately never intend to schedule their turnarounds congruently a highly reliable and available system had to be chosen. Due to its known outstanding availability a centrifugal compressor would have been choice number 1. However, due to the molecular weight of hydrogen and the relatively small volume it is technically and economically not feasible to realize a centrifugal compressor for such application.

Therefore, in order to best suit the clients volume requirements and to assure maximum availability it was decided to configure a compressor set-up with 3 similar compressors each of them being able to compress 50 % of the maximum required product flow at 100 % load.

Load control of the compressor was realized via the Hoerbigger HydroCOM system.

**Table 1:** Design criteria of the compressors

No of stages	2
Max Flow [ $Nm^3/h$ ]	17,800
Suction pressure stage 1 [bar]	15.8
Discharge pressure stage 1 [bar]	26.3
Discharge pressure stage 2 [bar]	43.3
Compressor speed [ $min^{-1}$ ]	327
Motor rating [kW]	920

The compressor is provided with suction and discharge dampeners on both stages. Since the gas is processed in a PSA unit it is moisture-free. Therefore, no interstage separators are required. In the inlet suction pipe of stage 1 a strainer with mesh size 40 microns is installed.



**Figure 1:** Overview of installation of one hydrogen compressor unit. The location of the local operator console is in the back ground on the right

### 2.2 Description of compressor features

Some key features of the compressors are described which we consider to be key-elements for high reliability and availability of reciprocating compressors.

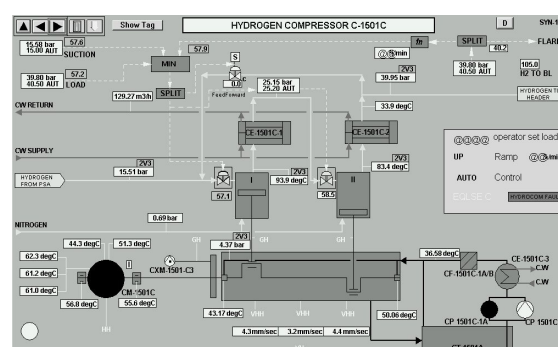
#### 2.2.1 Capacity Control

The capacity of the individual compressor is controlled with a suction pressure controller in the DCS.

As the energy consumption of a compressor is essentially proportional to the quantity of gas compressed per compression cycle, this system realizes an energy saving compressor control method.

The rod drop is measured with one proximity probe on each cylinder rod. The probes are mounted in vertical position on top of the cylinder rod. The rod drop measurement generates either a DCS alarm or DCS trip once certain thresholds are being exceeded.

However, compressor start-up is only possible at the local operating console in the field. This is to make sure the operating personnel can immediately identify all kinds of problems other than those being indicated in the DCS during start-up and act accordingly.



After opening of the compressor we detected quite significant wear and tear of the piston- and rider rings. Also we had to notice that the piston already touched the cylinder liner.



**Figure 3:** 2<sup>nd</sup> stage piston showing significant wear and tear at piston and rider rings also scratch marks there piston touched the cylinder liner

Closer inspection revealed that the rider rings at some point of time discontinued their rotational movement around the piston. Therefore, they showed uneven localized wear. The thickness difference around the circumference was up to 3 mm (see Figure 4).



**Figure 4:** 1st stage rider ring showing significant localized loss of thickness

For the HydroCOM unit the realized significant accumulation of dust in all moving parts. This was probably the reason why it didn't function properly any more previously. Figure 5 is giving an overview of the dismantled valve unit and figure 6 shows in more detail the dust and dirt deposits on the valve plate.

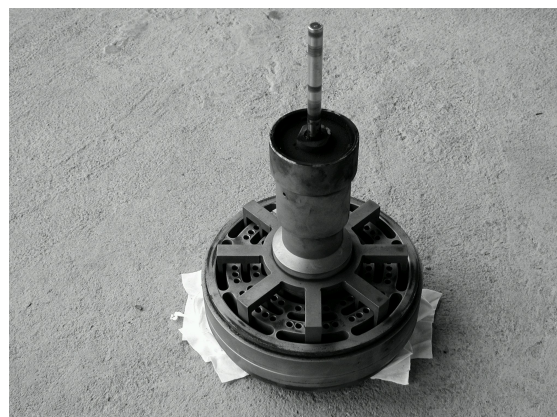


**Figure 5:** Accumulation of dust in HydroCom unit



**Figure 6:** Closer look at valve plate from figure 5

The material of the piston- and rider rings was a PTFE/PPS-type of material. In doing the failure analysis together with the vendor it was initially suspected that a carry over of dust from the PSA unit might have caused the excessive wear of the rings. However, neither in the filter unit downstream the PSA significant amounts neither of dust nor in the filter at the inlet of stage 1 any amount of dust was found. Finally, we agreed to cut down the rider rings by a couple of millimetres and to modify the material of the rings to a harder grade.

Cutting down was already done in early 2003. Since then velocity of rod drop has significantly decreased. During the last shutdown the piston- and rider rings of one of the compressors were inspected. For the same number of running hours this time the wear was remarkable smaller. Also it appeared as if the rotational movement did take place according to the expectations. The rings with the modified material will be installed on occasion of next periodic overhaul.



## 4 Operation and Maintenance Issues

### 4.1 Grid operation

Grid operation can become a major issue in case there are several clients and consumption volumes change quite rapidly. The load of a synthesis gas plant can only be modified in increments. These increments are far smaller than the volume that will be in surplus if one consumer is suddenly lost or is suddenly fully opening its intake valve.

Also the pulsations caused by the reciprocating compressor can become a hurdle for downstream applications. The pulsation dampeners we installed at the suction and discharge side of each individual compressor already helped to minimize these pulsations.

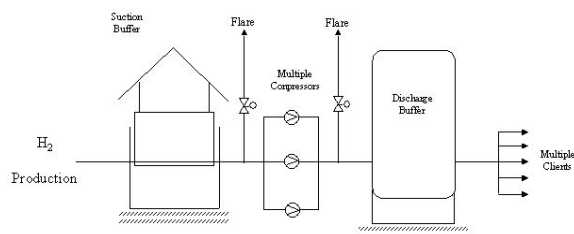


**Figure 7:** Typical set-up in optimized gas distribution system

In case that the consumers change their gas intake quite rapidly a pressure spike or dip is the consequence. For some of the clients such spikes or trips can already have the consequence to run into their low- or high-pressure trip. The case “sudden oversupply” due to one client is cutting back can be solved quite easily in simply flaring up- or downstream the compressor (see fig. 7). However, this is quite costly and should be avoided. The case “sudden undersupply” due to one client is suddenly fully opening its intake valve immediately causes a pressure dip. In order to allow the Hydrogen producer to adjust its production it is advisable to have some intermediate buffer capacity as illustrated in fig. 7. The buffer capacity at suction and discharge shall be able to cater for the Synthesis Gas plant load adjustment rate. Most important is the buffer capacity at the suction. The buffer capacity at the discharge only helps to balance out smaller spikes.

### 4.2 Maintenance

In today’s highly competitive world plant operations requests to run their machines as long as possible without any need for servicing. In remote places like Kuantan in Malaysia there are a couple of issues being crucial for outstanding compressor availability,

- Maintenance intervals/preventive maintenance
- Online check of compressor condition
- Spare parts stocking
- Records of maintenance history

Only to name a few of them.

#### 4.2.1 Maintenance intervals/preventive maintenance

It is established industrial practice to shutdown and service reciprocating compressors once every 8000 hours of operation. This becomes crucially essential when talking about oil-free compression. We discussed to extend this period to 16,000 hrs. However, the described wear and tear issue recommended sticking to 8,000 hrs. For the future we will carefully monitor the wear and tear issue and if possible extend the maintenance interval. We believe it is essential that qualified personnel are at least checking the condition of the running compressor once a week to assure trouble-free operation.

#### 4.2.2 Online check of compressor condition

We believe that the sensors we installed to check for vibration and rod-drop are essential to operate a reciprocating compressor reliable. Especially in today’s world where there is a tendency to operate whole compressor stations unmanned these sensors play a more and more important role. After some extensive calibration work we believe the sensors have now reached a level of reliability that realizing trips is no more a risk. Previously the chance was quite high that such trips were already triggered by false alarms.

#### 4.2.3 Spare parts stocking

We recommend planning carefully for spare parts. This is especially to keep short shutdowns and to reach a high availability. We made very good experience stocking the compressor vendors’ recommended spare parts list. Well planned overhaul work and a clear registration of wear values allow best utilisation of spare parts. Another important issue is the proper storage of the spare parts in order to avoid corrosion or other modes of degradation (i.e. evaporation of plasticizer from O-Rings to make them brittle etc.). Denomination that allows easy identification is another important topic.

## 4.2.4 Records of maintenance history

Experience shows that a maintenance log file in which it is easy to find the running hours of different parts is essential. It doesn't matter if such log files are simple and "hand-made" (see figure 8). Of course modern databank software can help a lot. However, most important is not the tool but the accuracy of filing.

Basf Petronas Chemicals Sdn Bhd									
OOM EQUIPMENT HISTORY CARD									
Equipment Tag No.		C-1001 C	Manufacturer		Sulzer Blackhardt		Plant : Syngas		
Description		Reciprocating compressor	Model						
Service		Hydrogen	Type						
Location		Compressor house	Serial no.						
Item	Date of stopping	Description of stopping	Reason for stopping	Spare parts changed	Material no.	Quantity	Date put back to operation	Remarks	
1	25-Mar-02	Rod drop alarm	Check rod drop	1st piston ring	80040511	4 pcs	Aug 02		
				1st slider ring	80040510	2 pcs			
				Oil scraper ring	80040508	2 sets			
				Lock washer	80040495	4 pcs			
				Red packing	80040516	10 pcs			
				Supporting ring	80040509	10 pcs			
				Breaker ring	80040503	2 pcs			
				Spin washer ring	80040471	2 sets			
				1st Valve cover gasket	80040506	0 pcs			
				2nd piston ring	80040517	6 pcs			
				2nd slider ring	80040515	3 pcs			
				2nd Head gasket	80040514	1 pc			
				Coupe gasket	80040514	2 pcs			
				Plug NPT 1/2"	80052512	1 pc			
				2nd Unloaden spindle	80061143	2 pcs			
2	10-Jan-03	Oil sampling (No breakdown)	Predictive maintenance						
3	24-Feb-03	Change CW piping to packing							
4	7-Mar-03	Inspection	Inspection by vendor	7-Mar-03					

Figure 8: Example of simple log file

## 5 Conclusion

The biggest obstacles for a successful trouble-free compressor operation are already the shortcomings made during the initial design phase. The most important thing is the clear concept how to realize the configuration to achieve highest availability and reliability. Here, we have to bear in mind that up to today hydrogen has still to be compressed via reciprocating compressors and that this compressor type requires significant more maintenance shutdowns than centrifugal ones. In order to assure full clients volume availability the installation of spare capacity is unavoidable.

Today's vibration and rod drop sensors have reached the required level of reliability. This allows extending maintenance intervals and makes it possible to move from the fixed periodic maintenance to a more flexible "on-need" basis, finally to help reducing maintenance costs.

## 6 Acknowledgements

We would like to express our thanks and gratitude to all our staffs in BASF Petronas Chemicals Sdn. Bhd. who contributed very hard in bringing up this plants from grassroots to today's level of excellence in only a couple of years. We also like to thank our mother companies for the continuous support over all this years. Finally we also like to thank the contractor, Lurgi Oil and Gas, Frankfurt, Germany and the compressor vendor, Sulzer Burckhardt, Switzerland for their contribution to finally make this project a success.

# **Service Life Improvement of Piston-Rod Sealing Systems by Means of Pressure-Relieved Sealing Elements**

by:

**Dr. Norbert Feistel**  
**Research and Development**  
**Burckhardt Compression AG**  
**CH-8404 Winterthur**  
**Switzerland**  
**[norbert.feistel@burckhardtcompression.com](mailto:norbert.feistel@burckhardtcompression.com)**

**4<sup>th</sup> Conference of the EFRC**  
**June 9<sup>th</sup> / 10<sup>th</sup>, 2005, Antwerp**

## **Abstract:**

Pressure relief of frictional sealing elements, i.e. a deliberate introduction of the gas to be sealed into the friction surface in order to reduce contact pressure, is a well-known method for improving service life of sealing systems. It is used for piston rings as well as packing rings. However, more common are applications inside cylinders, where pressure-relieved sealing elements are used to seal gases with high pressure differences. Experiments with pressure-relieved packing rings have shown that their favourable wear characteristics are frequently offset by poor or even unacceptable sealing efficiency. Obtained results make it clear that the pressure-relief principle should not be applied to all sealing elements, especially when it comes to dry-running packings for sealing hydrogen. At the same time, pressure-relieved sealing elements employed specifically for sealing the dynamic pressure component improve the service life of the entire packing. Especially favourable operating characteristics are exhibited here by the crown ring developed by BCA, in combination with the widely known step bridge design (penguin ring).

## 1 Introduction

Of sealing systems used in crosshead compressors, the piston-rod sealing system (packing) is often the component whose life cycle limits the machine's service interval. Accordingly, measures to improve the packing's critical life cycle can prove beneficial in attempts to maximize periods of trouble-free operation. A suitable method here is to equip packings with pressure-relieved sealing elements. To provide a frictional sealing element with pressure relief, the gas to be sealed is channelled to the friction surface so as to lower radial contact pressure; this results in improved wear characteristics and, consequently, less material loss. For many years now, this method has been used to improve the service life of piston rings as well as packing rings. However, more common are applications inside the cylinder, a typical one being the sealing of gases with high pressure differences by means of piston rings made of filled PTFE. On an introduction of high-temperature polymers and polymer blends to sealing technology, the pressure-relief principle initially had to take a back seat. However, steadily rising demands on the performance of dry-running sealing systems have restored the appeal of pressure-relief as a means of lengthening life cycles.

The investigations described next were intended to reveal the advantages and disadvantages of the pressure-relief principle as a technique of improving packing service life. These investigations focus on a sophisticated, dry-running sealing system for hydrogen. Another important objective was to ascertain the potential benefit offered by a simple upgrading of existent packings.

## 2 Principles and properties of pressure-relief mechanisms

In the case of contactless seals, the sealing gap's axial dimensions play a major role in increasing the flow resistance and, consequently, sealing efficiency. By contrast, the sealing efficiency of frictional sealing elements cannot be enhanced significantly by enlarging axial dimensions. Their leakage rates are influenced, in particular, by joint sealing quality and – with increasing wear – the quality of wear compensation. To achieve the necessary reduction in friction power during dry running, unnecessarily large axial dimensions of the friction area should accordingly be avoided wherever possible.

However, there are limits to optimization of axial dimensions of frictional sealing elements, imposed, for example, by a requirement to maintain certain minimum dimensions in order to adhere to strength specifications. This entails unfavourably large dimensions, especially in the case of the commonly

used, filled PTFE materials, characterized by a very low thermal strength. Consequently, design measures to improve frictional sealing elements should focus on using only a defined part of their axial dimension for the actual sealing function. This can be achieved, for instance, by channelling the gas to be sealed toward the friction surface such that it is partly relieved by the radial pressure vectors.

No longer experiencing a forced flow of gas, the pressure-relieved area now serves as an integrated bearing surface. A positive effect of this measure is a reduction of the resulting radial forces acting on the sealing element, whose size can be manipulated by the ratio between the relieved and loaded friction surfaces (Fig. 1). The reduction in contact pressure, combined with the resulting improvement in wear characteristics, lowers the rate of material loss of the sealing elements.

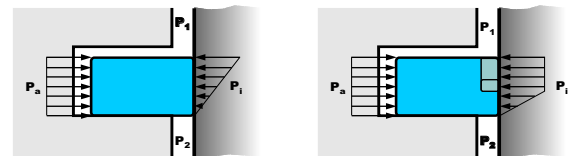


**Figure 1:** Pressure characteristic at the friction surface of a conventional (left) and pressure-relieved sealing element

However, Fig. 1 also reveals a negative effect in comparison with conventional designs: The radial contact pressure is now concentrated on an even smaller part of the axial sealing element dimension lying outside the centre of gravity. For the sake of simplification, our treatment assumes a linear pressure characteristic at the friction surface.

The pressure-relief technique is employed for piston rings and packing rings. More common, however, are applications inside the cylinder, where pressure-relieved sealing elements are used to seal gases with high pressure differences, frequently in conjunction with the two-piece design. Fig. 2 shows a common configuration with differently arranged pressure-relief channels.

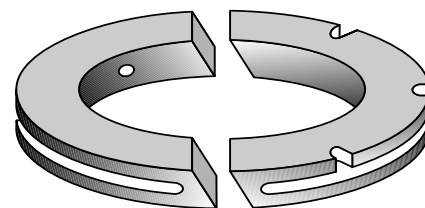


**Figure 2:** Pressure-relief of a two-piece piston ring by means of radial bores (left) for double-acting compression, or axial grooves for single-acting compression

### 3 Application of the pressure-relief principle to the TID design

In addition to the primary goal of improving life cycles, the following criteria were defined for applications of the pressure-relief principle to piston-rod sealing systems (packings):

- Economical design of sealing elements
- Suitability for lubricated and dry-running applications
- Suitability for manufacture from of all common dry-running materials
- High sealing efficiency, even during dry-running compression of hydrogen
- Simple upgrading for existent packings

The well-known packing-ring design comprising segment sections tangential with respect to the internal diameter (TID) is especially suitable for realizing sealing elements with just a few segments (to reduce the risk of failure by fracture, the sections are usually not precisely tangential in practice). This design achieves a high degree of sealing efficiency even without an additional cover ring. By nature, however, the special kind of wear compensation of the TID design typically results in an uneven material removal along the sealing element segments, the maximum wear occurring at the segment ends facing the piston rod (Fig. 3).

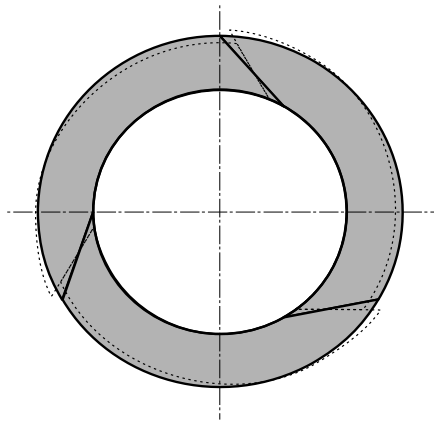


**Figure 3:** Conventional TID packing ring with a typical wear profile exhibiting maximum values at the segment ends facing the piston rod

The TID sealing element's special type of wear compensation not entailing any additional cover segments permits easy integration of a pressure-relieved bearing surface. Fig. 4 shows a TID segment with a single bearing block facing the compression chamber. As a side-effect, the previously unlimited radial wear of the TID design is now limited to a value proportional to the total clearance between the bearing blocks.

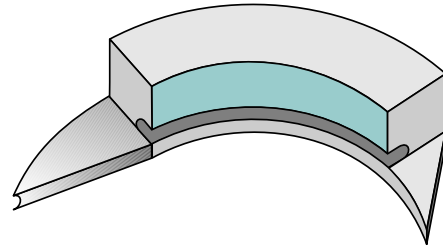


**Figure 4:** Application of the pressure-relief principle to a segment of a TID packing ring

Initial tests of a pressure-relieved TID version involving a piston-rod diameter of 50 mm were conducted, in each case, with just one sealing element subjected to purely static pressure difference in a nitrogen compressor incorporating elaborate measurement technology intended specially to investigate the operational behaviour of dry-running packings<sup>2</sup> ( $p_s = p_d = 2$  MPa,  $c_m = 3.18$  m/s). A use of packing cups with axial dimensions adapted to conventional sealing-ring pairs made it possible to roughly double the bearing area with respect to the sealing area. Fig. 5 shows a graph of the temperatures measured inside the sealing-element chamber, indicating that the prevailing conditions lead to a notable rise in temperature either immediately following test commencement, or a few hours later. Conventional sealing-ring pairs of identical axial dimensions did not exhibit this effect, suggesting that the rapid temperature rise is due to the fact that the bearing surface not experiencing a forced flow of gas is relatively large compared with the sealing surface.

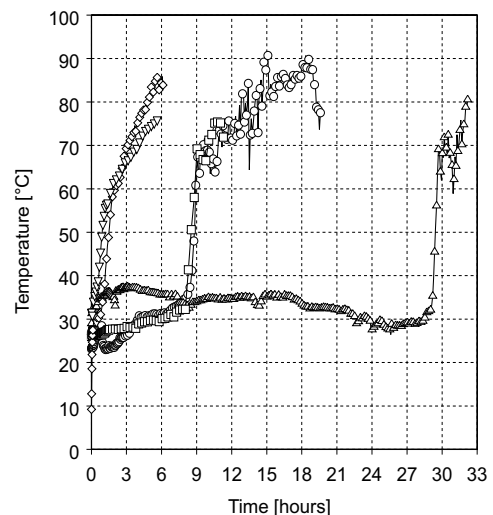


**Figure 5:** Temperatures measured in a sealing-element chamber during various tests involving, in each case, one sealing element of the first version of a pressure-relieved TID ring made of carbon/graphite-filled PTFE ( $p_s = p_d = 2$  MPa,  $c_m = 3.18$  m/s)



## 4 Development of the crown packing ring

To eliminate thermal problems, it proves expedient to reduce the bearing surface and chamfer it<sup>1</sup>. Geometric variations in chamfer make it possible to determine the initial and maximum proportions of the bearing area. This makes it very easy to achieve a favourable ratio between the sealing and bearing areas while adhering to the specified sealing-element geometry, even when upgrading existent packings.

As a result of chamfering, the conditions prevailing during the running-in period are similar to those accompanying non-relieved TID packing rings, thus positively influencing temperatures and leakage rates. As wear progresses, the bearing area increases gradually until attainment of the maximum value. To further improve thermal conditions, the single-piece bearing block was divided into two smaller ones. Fig. 6 shows this type of sealing-element segment.

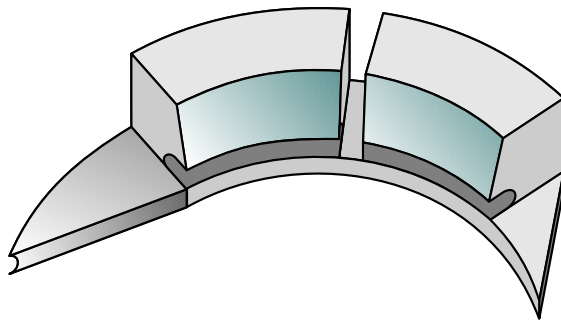


**Figure 6:** Thermal problems during the running-in period were eliminated by dividing the bearing surface into two bearing blocks and chamfering them

These improvements eliminated thermal problems, from the time of commissioning to attainment of the maximum bearing area. This optimized packing-ring design subsequently underwent further tests in a dry-running hydrogen compressor<sup>5</sup>. As in the case of the nitrogen compressor, the nitride-steel piston rod had a diameter of 50 mm, and its surface roughness was set to a value  $0.20 \leq Ra \leq 0.30 \mu\text{m}$  before each test. Already on commissioning of the new sealing elements, though, disappointingly high leakage values of more than 10 standard cubic meters per hour (scm/h) were measured (Fig. 7).

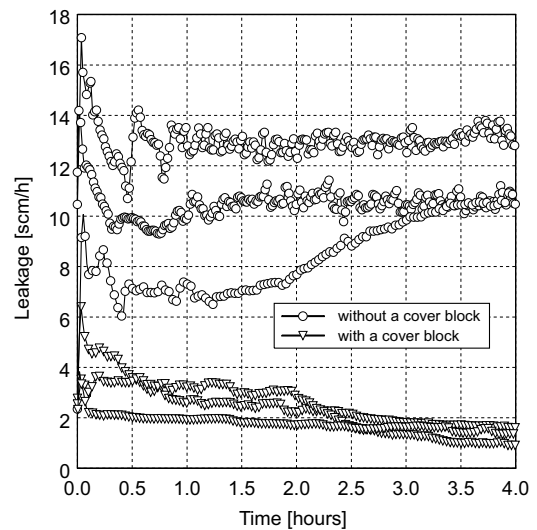


**Figure 7:** Comparison between hydrogen leakage rates of crown versions with and without a cover block

The high leakage was attributable to gaps in the vicinity of the segment joints caused by the production and/or installation of the sealing elements, which frequently impair sealing efficiency even in the case of conventional TID sealing elements. To remedy this, the two existent bearing blocks were supplemented by a further block for sealing the joint axially at the segment end facing away from the piston rod. This cover block was not furnished with a pressure relief groove, thus resulting in a higher radial contact pressure here. In conjunction with the two bearing blocks, this generates an effect which counteracts the typical wear characteristic of a TID profile by harmonizing material removal along the segment and simultaneously improving sealing efficiency (Fig. 8). This technique also made it possible to commission the sealing elements in hydrogen with low leakage rates of about 2 scm/h (Fig. 7). Because the sealing element with the array of blocks on the circumference resembles a small crown (Fig. 9), the packing ring was accordingly named "crown ring".

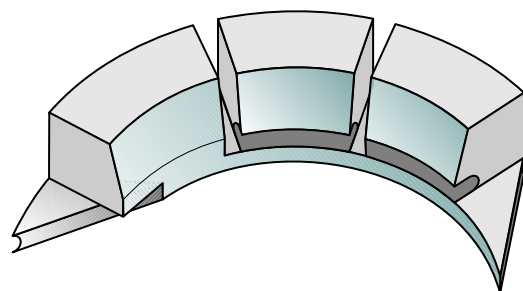


**Figure 8:** Crown segment with two pressure-relieved bearing blocks and one cover block (left end)

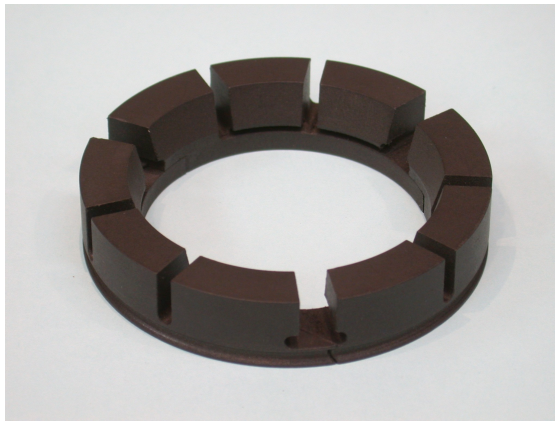


**Figure 9:** The array of blocks on the circumference led to the name "crown ring"

## 5 Homogeneous crown piston-rod sealing system

Six crown rings made of polymer blend were to be tested over an extended period in the dry-running hydrogen compressor at a suction pressure of 1.4 MPa, discharge pressure of 4 MPa and an average piston velocity of 3.4 m/s. At first, it was possible to achieve stable operation at the low leakage rates familiar from the previous tests. After 250 hours however, operation became unstable, accompanied by a notable rise in the leakage rate, which attained a peak value of 15 scm/h after roughly 900 hours, making it necessary to abort testing (Fig. 10). Under the same conditions, leakage rates of just 2 - 4 scm/h were measured on sealing systems comprising conventional packing rings of the step bridge design.

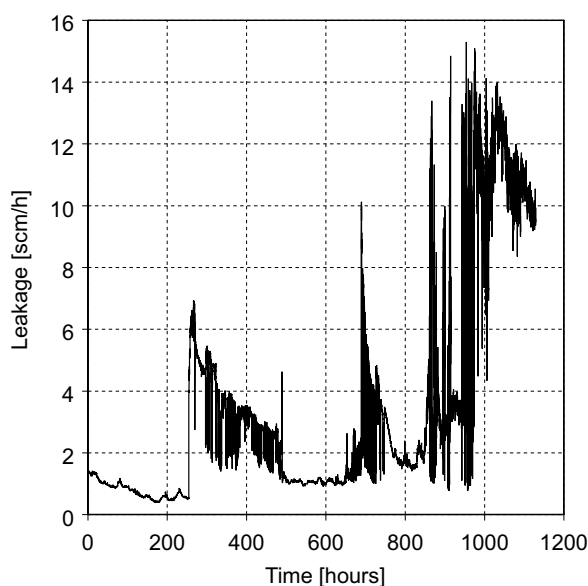


**Figure 10:** Hydrogen leakage vs. time of a homogeneous packing comprising six crown rings

After the removal of the packing, the reason for the high leakage did not become apparent immediately: All sealing elements were undamaged, and the average wear of the overall sealing system turned out to be just 0.35 mm. A detailed analysis of material loss on the individual sealing elements then revealed that the radial wear in the area of the sealing surface was roughly 0.05 to 0.10 mm higher than in the area of the bearing surface. This uneven material removal is due to the pressure distribution over the friction surface indicated in Fig. 1, which – in the case of conventional sealing-ring pairs – gives rise to the familiar phenomenon of different wear levels on the sealing ring and cover ring.

Whereas in the case of non-relieved sealing-ring pairs, uneven material removal in the axial direction can be compensated through radial displacement of the sealing segments and cover segments, the even less favourable pressure distribution in pressure-relieved designs leads to a formation of gaps in the sealing surfaces. The tests clearly reveal that – especially in the case of dry-running hydrogen sealing systems – even small deviations from the ideal sealing-element arrangement can significantly increase the leakage. Although uneven material removal has a weaker impact on nitrogen sealing systems, they also exhibit higher leakage rates in comparison with non-relieved sealing elements. The test results make it evident that the association frequently drawn between reduced wear and increased service life is not always valid; instead the sealing efficiency represents the primary service life criterion. Consequently, the versatility of pressure-relieved packing rings is compromised by relatively high leakage rates which limit the permissible range of application of such rings.

## 6 Heterogeneous crown-penguin piston rod sealing system

Nevertheless, the characteristic operational behaviour of gas-tight friction seals permits the use of pressure-relieved packing rings in a way advantageous for the overall sealing system. Packings are subjected typically to combinations of static and dynamic pressure components (Fig. 11). In an absence of sealing elements with a particularly elaborate joint sealing, the various pressure components distribute themselves at the two ends of the sealing system, especially in the case of the new sealing elements. Investigations have shown that common, contactless throttle rings do not contribute significantly toward sealing the dynamic pressure component, this function being performed to the greatest extent by the first frictional sealing element<sup>3</sup>. With progressive wear, a constantly increasing part of the dynamic pressure

component will be taken over by the subsequently arranged sealing element. In contrast, the static pressure difference tends to be sealed by the sealing element currently providing the highest sealing efficiency; under identical conditions, however, the last sealing element located furthest away from the compression chamber is preferred.

The two pressure components also differ considerably in terms of their influence on the sealing system's operational behaviour. During the suction stroke, the dynamic pressure component can be reduced by means of pressure-relief grooves located on the pressure-facing side of the sealing elements. The grooves enable the gas to flow back to the cylinder, thus exerting no influence on the leakage rate of a packing. Especially in the case of segmented packing rings, however, it results in a high degree of wear, failure by fracture or creep. In contrast, the static pressure difference constitutes the primary load parameter influencing the leakage rate, therefore placing the highest possible demands on sealing technology<sup>5</sup>.

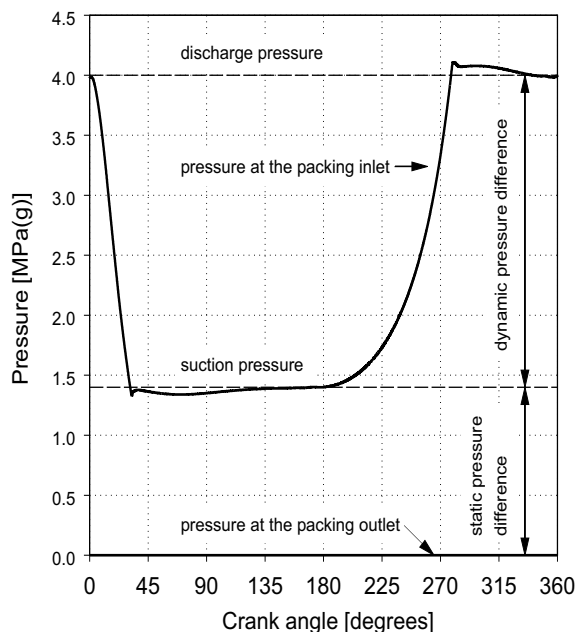


**Figure 11:** Dynamic and static pressure components of a packing experiencing a suction pressure of 1.4 MPa and a discharge pressure of 4 MPa

Typical of a serial arrangement of gas-tight sealing elements, this distribution of the two pressure components among various sealing elements can be used to optimize overall sealing systems through an employment of different designs each possessing the most favourable properties for handling a particular pressure component. Although packing rings of the step bridge design (penguin ring) have proven very suitable for the use with static pressure differences<sup>4</sup>, they are excessively susceptible to

wear when subjected to dynamic pressure differences.

It would hence appear advisable to combine the sealing efficiency of penguin rings with the favourable wear characteristics of pressure-relieved packing rings. For this purpose, the latter are arranged in the vicinity of the compression chamber to withstand the dynamic pressure difference, while the subsequent penguin rings are intended for handling the static pressure difference responsible for the leakage. Fig. 12 shows this type of heterogeneous packing comprising crown rings and penguin rings.

Of special interest was the potential usefulness of the remaining pressure-relieved packing rings to the service life of the overall sealing system. This potential was to be examined in hydrogen tests involving homogeneous packings each comprising six penguin rings and six crown rings made of a polymer blend, in comparison with a heterogeneous packing corresponding to Fig. 12. A throttle ring was not used in any of these tests.

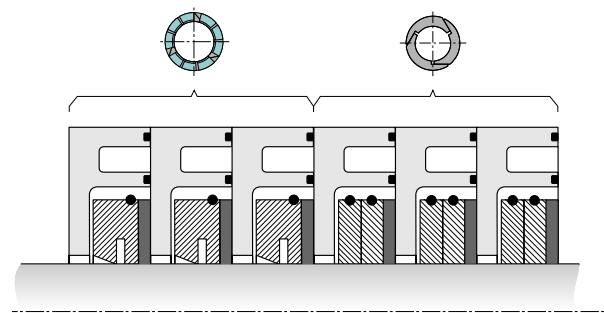


**Figure 12:** Heterogeneous packing comprising three crown rings and three penguin rings

Fig. 13 shows the radial wear determined on the individual sealing elements after 500 hours of operation. In each case, the first sealing element located right next to the compression chamber exhibits considerably lower values for the two crown rings compared with the penguin ring, the crown ring of the heterogeneous packing achieving the best result of all. For the specific use with the dynamic pressure component, the bearing blocks of the crown rings in this variant were designed to be somewhat more robust than the crown version of the homogeneous packing, thus further reducing wear.



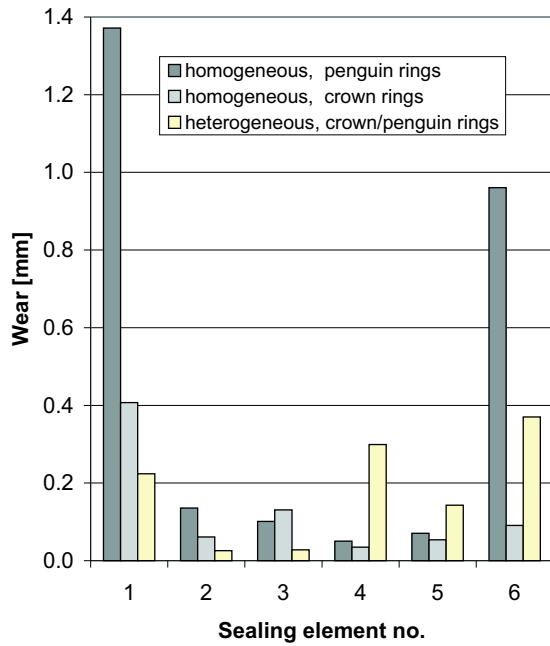


**Figure 13:** Average wear on sealing elements of homogeneous and heterogeneous packings after 500 hours of operation (sealing element number 1 next to the compression chamber,  $p_s = 1.4$  MPa,  $p_d = 4$  MPa,  $c_m = 3.4$  m/s)

If the average wear of the sealing elements and the sliding distance are used to form the sealing system's average wear rate, the lowest value is achieved by the homogeneous crown variant (Fig. 14); however, their operational behaviour is characterized by an increased, strongly fluctuating leakage. The average wear rate of the heterogeneous packing is slightly higher than that of the homogeneous crown variant, but nearly three times lower than that of a conventional, homogeneous packing comprising penguin rings. To maximize the period of high sealing efficiency of penguin rings, it is necessary to protect them effectively against the wear-intensive effect of the dynamic pressure difference. The ratio between the numbers of crown and penguin rings therefore needs to be adapted in accordance with the composition of the pressure difference. Tests have shown that a minimum number of penguin rings need to be present. Given proper design, however, a use of crown rings notably improves the wear characteristics of overall sealing systems while maintaining high sealing efficiency. Depending on the extent to which production has been optimized, crown rings also offer a cost advantage which can be considerable compared with six-segment penguin sealing-ring pairs.

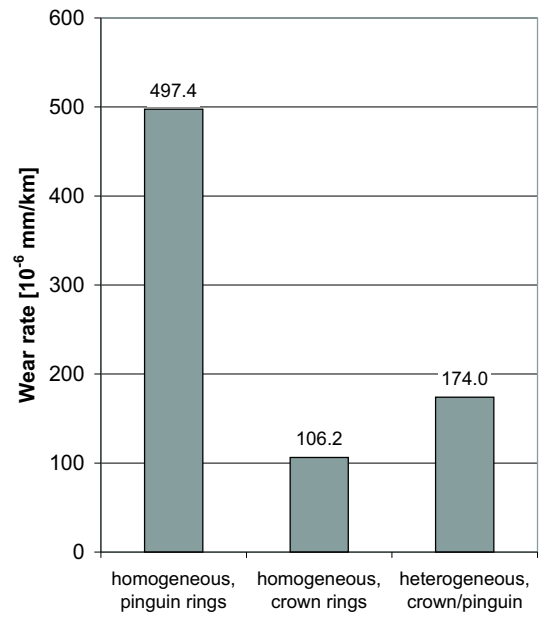


**Figure 14:** Average wear rate on homogeneous and heterogeneous packings made of polymer blend after 500 operating hours

## 7 Conclusion

Pressure-relief of frictional sealing elements reduces the resulting radial forces acting on these elements. Although this lowers material loss in general, the radial contact pressure is focused on a smaller axial cross-section lying outside the sealing elements' centre of gravity. In addition, the bearing surfaces not experiencing a forced flow of gas can cause temperatures to rise sharply.

For use in piston-rod sealing systems, the pressure-relief principle was applied to the packing ring design possessing a tangential section with respect to the internal diameter (TID). Thermal problems observed in the beginning were eliminated later by dividing the bearing surface into individual bearing blocks and chamfering these blocks. To improve sealing efficiency for hydrogen applications, the bearing blocks were supplemented by an additional cover block in the vicinity of the joints. The line-up of blocks along the circumference of the optimized sealing element gave it the name "crown ring". As operation progresses, the uneven material removal on the sealing and bearing surfaces resulting from large variances in pressure distribution over the friction surface leads to a formation of gaps between the sealing surfaces. The consequential increase in leakage rates compared with non-relieved designs can assume unacceptable proportions, at least when it comes to dry-running compression of hydrogen.

Nevertheless, the characteristic operational behaviour of gas-tight friction seals permits the use

of pressure-relieved packing rings in a way advantageous for the overall sealing system. The typical distribution of pressure differences – usually comprising dynamic and static components – among various sealing elements can be made to contribute toward optimizing the overall sealing system if the normally homogeneous packings are replaced by a heterogeneous combination of designs each possessing the most favourable properties for handling a particular pressure component. Tests on this type of heterogeneous packing comprising crown rings and the familiar packing ring of the step bridge design (penguin ring) revealed notably better wear characteristics – given the same, high sealing efficiency – compared with homogeneous packings comprising penguin sealing-ring pairs.

## Notation

$p_s$	suction pressure
$p_d$	discharge pressure
$p_1$	pressure before the sealing element ( $p_1 > p_2$ )
$p_2$	pressure after the sealing element
$p_a$	radial pressure acting on the sealing element ( $p_a = p_1$ )
$p_i$	pressure acting on the sealing element's friction surface
$c_m$	average piston velocity

---

## References

- <sup>1</sup> Burckhardt Compression AG: Sealing Ring PCT-Patent WO 97/00395, 1997
- <sup>2</sup> Feistel, N.: Comparative measurements of the piston rod surface temperature during the operation of a dry-running crosshead compressor 2<sup>nd</sup> EFRC-Conference, Den Haag, The Netherlands, 2001, S. 175 – 183
- <sup>3</sup> Feistel, N.: Beitrag zum Betriebsverhalten trocken laufender Dichtsysteme zur Abdichtung der Arbeitsräume von Kreuzkopfkompressoren Dissertation Universität Erlangen-Nürnberg, 2002
- <sup>4</sup> Vetter, G.; Feistel, N.: Investigation of the operational behaviour of dry-running piston-rod sealing systems in crosshead compressors 3<sup>rd</sup> EFRC-Conference, Vienna, Austria, 2003, S. 11 – 21
- <sup>5</sup> Feistel, N.: Influence of piston-ring design on the capacity of a dry-running hydrogen compressor 3<sup>rd</sup> EFRC-Conference, Vienna, Austria, 2003, S. 141 – 149



# **Concept Selection and Design Considerations for Compression Facilities for FPSO Glas Dowl<sup>1</sup>**

by:

**André Eijk**  
**Flow and Structural Dynamics**  
**TNO Science and Industry**  
**Delft**  
**The Netherlands**  
**andre.eijk@tno.nl**

**Jan de Roos, Jerry Gillis**  
**Process and Piping Section**  
**Bluewater Energy Services B.V.**  
**Hoofddorp**  
**The Netherlands**  
**Jan.deRoos@bluewater.com**

**4<sup>th</sup> Conference of the EFRC**  
**June 9<sup>th</sup> / 10<sup>th</sup>, 2005, Antwerp**

## **Abstract:**

As part of the modification of the Floating Production Storage and Offloading Unit (FPSO) Glas Dowl for operation on the Sable Field (offshore South Africa), a new gas compression system was installed. Associated gas is compressed for use as lift gas and re-injection back into the reservoir for pressure maintenance and optimizing liquid recovery.

Concept selection of the compression facilities was based on technical and commercial criteria in combination with the specific requirements of the Sable field. Large variations in gas molecular weight, compressor efficiency and overall system availability favored the use of reciprocating compressors, despite space constraints and potential vibration problems. A configuration based on 4 x 33% MP/HP reciprocating compressors which includes a spare compressor, was selected.

During the design, specific attention was given to pulsation and vibration control as this was considered crucial for the success of the project. A dynamic analysis of the compression system according API 618 Design Approach 3 was included in the scope of the compressor Original Equipment Manufacturer (OEM). In addition an independent verification study was awarded to TNO, acting as 3<sup>rd</sup> party.

The required modifications to the piping system resulting from the analysis were implemented as far as practically possible. An extensive field measurement program during the operational phase was conducted which showed vibration levels well within the allowable range.

The application of multiple large reciprocating compressors on the FPSO Glas Dowl showed to be a success. Compressor and piping system vibrations were controlled successfully which resulted in vibration levels well within allowable limits. The stringent space restrictions and high system availability requirements were met in full.

## 1 Introduction

In 2001 a project was initiated to develop a marginal field offshore South-Africa. With a relative short field life, the development scenarios showed that the application of a leased FPSO was the most suitable option. At that time the existing FPSO Glas Dowr, owned and operated by Bluewater was available for a new contract and showed to have a good basic match with the project requirements. The main modifications to the existing topsides facilities consisted of new gas compression facilities, additional power generation and some modifications to the crude separation system.

To meet the challenging technical and commercial constraints a challenging gas compression system based on reciprocating compressors was selected. Due to the relative small area available for the compressors and the pulsations and vibrations that can be expected with the application of reciprocating compressors, a thorough investigation of the pulsation and vibration behavior of the compressors and the piping system was considered crucial. High pulsations and vibrations may lead to reduced compressor efficiency, pipe failures and possibly unsafe operating conditions. Recognizing this risk, in addition to the analysis that was conducted by the OEM, a similar analysis study was awarded to TNO for the purpose of verification by an independent party.

This paper presents the process of concept development which led to the selection of the optimum compression solution. Further, the methodology used for pulsation and vibration control of the compressors and connected piping system is outlined. Results of the analysis as well as results of field measurements are presented.

## 2 Field Development

The Sable Field Development lies in the Bredasdorp Basin in Block 9, off the coast of South Africa. It is located in approximately 100 meters water depth and consists of two reservoirs: the E-BD oil reservoir and the E-CE oil and gas reservoir. With recoverable reserves estimated at between 20 million and 25 million barrels, the field is expected to have an economic life of three to five years. The field has been developed using six sub-sea wells tied back to the Bluewater owned and operated (FPSO) vessel, Glas Dowr. PetroSA, the South African state-owned Exploration and Production Company is Field Operator with the majority share in the field and Pioneer Natural Resources holds the remaining interest.

Of the two reservoirs, the E-BD reservoir is a typical oil reservoir characterized by a relative low and fairly constant Gas-Oil-Ratio (GOR) throughout the field life. The reservoir holds oil in the upper part and water in the lower part of the reservoir. Pressure maintenance of the E-BD reservoir is by means of injecting treated seawater.

The E-CE reservoir is an oil and gas reservoir and is characterized by a relative high and increasing GOR throughout the field life. Reference is made to Figure 1.

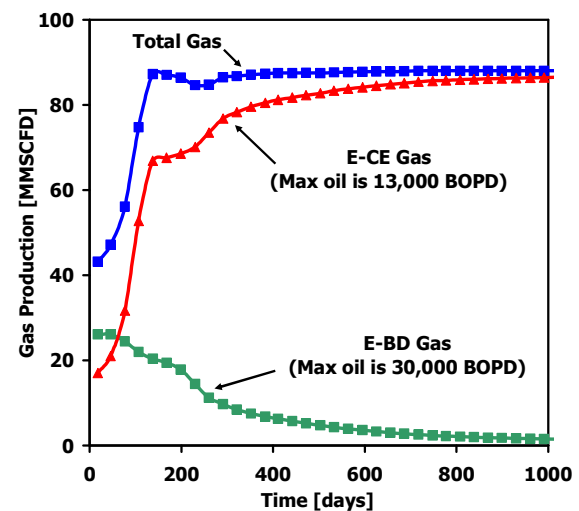


Figure 1: Associated gas flow rate - first 3 years

It holds a gas cap in which gas is re-injected for pressure maintenance and for optimizing liquid recovery. Not only the GOR but also the composition of the E-CE fluids changes throughout field life resulting in a challenging set of process characteristics for design and operation of the separation and compression systems.

## 3 Project Overview

### FPSO Glas Dowr

The existing topsides facilities of the FPSO Glas Dowr consisted of a two-stage separation train, water injection system and the supporting utilities. No gas compression system was installed.

For development of the Sable Field, the existing FPSO Glas Dowr was contracted including the required modifications to make it suitable for handling the specific oil and gas properties and the production requirements.



**Figure 2:** FPSO Glas Dowr

## Project Drivers

The main project drivers which influenced the final design of the topsides facilities are listed below:

- Fast Track Project (18 months)
- Short Field Life (minimum 3 years with upside case to 5 years)
- Low Cost Solution
- Performance Driven
- Modification of an existing facility
- Flexibility (also for future relocation)

The required first oil date for the project implied a fast track project of around 18 months. As usual, the schedule of a project of this kind is driven by the lead time of the long lead equipment, in this case the gas compression facilities. The relative short field life and required flexibility to meet the specific process characteristics and future relocation enforced the requirement of a flexible design of the topsides. With the FPSO Glas Dowr, being an existing facility, due consideration had to be given to the optimum balance between adding equipment versus modifying equipment. Furthermore, as for every production facility, the design was driven by striving after optimum performance in the operational phase with regards to availability of systems and uptime of the overall production facilities. Finally, budget indication of the client reflected the requirement for a low cost solution in order to meet the financial requirement of the project.

## Topsides Facilities Upgrade

In order to meet the new production requirements and handling the specific oil and gas properties, an upgrade of the topsides facilities (2000 tonnes in total) was required. The upgrade was mainly related to the crude separation plant, the compression system and the supporting utilities.

The typical oil and gas properties and the relatively high Flowing Well Head Pressure (FWHP) of the E-CE reservoir resulted in the process schematic as outlined in the next section. A gas compression system was installed to handle the associated gas and boost the pressure to the required injection pressure.

## Separation and Compression Scheme

The oil and gas is produced from two separate reservoirs. The fluids from the E-BD reservoir are separated in two stages using the existing separation train. Separation of the E-CE fluids consists of three stages. The additional separation stage for the E-CE fluids is placed upstream of the existing separation train and not only enhances liquid recovery but it also enables separation of the major part of the E-CE gas upstream the existing separation system at a higher pressure. The E-CE reservoir allows for the higher operating pressure of 58 barg due to its higher FWHP and relative low fluid density. A large benefit of the higher separation pressure of the major part of the gas is that it limits the actual gas flow rate and, hence, saves in required compression power.

The liquids from the E-CE separator are routed to the inlet of the existing first stage separator (operating pressure 8.5 barg) where it is commingled with the fluids from the E-BD reservoir. The final crude product requirements are obtained in the second stage separator (operating pressure of 1.0 barg)

All gas evolving from the fluids needed to be compressed for re-injection. With the three levels of separator operating pressure (1 barg, 8.5 barg and 58 barg), three levels of compression can be distinguished, hereafter called LP, MP and HP compression. Reference is made to the figure below presenting the overall crude separation and compression scheme.

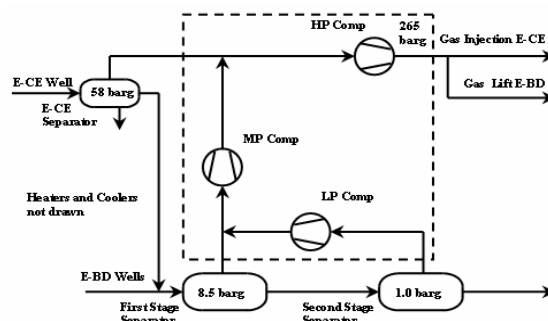


**Figure 3:** Selected crude separation and gas compression scheme

The associated gas is re-injected in the E-CE reservoir for reservoir pressure maintenance requiring a compressor discharge pressure of 264



barg. A small portion of the associated gas is used as fuel gas for power and heat generation and as lift gas for artificial lift of the E-BD reservoir.

The compressor discharge was driven by the required re-injection pressure into the E-CE reservoir which is 264 barg. The compressor design flow rate is 85 MMSCFD.

## Topsides Constraints

With the FPSO Glas Dowr being an existing installation, modifications had to be designed within the margins of the facility. As usual on an offshore installation, space is limited which sets the available footprint for new compression equipment. Further, with only one slot with specified footprint available for additional power generation, limiting the absorbed power was a selection criterion for the new compression facilities as well.

## Compressor Type Evaluation

The combination of a relatively high compressor discharge pressure of 264 barg and a flow rate of 85 MMSCFD allowed for selecting either aerodynamic or a positive displacement compressor type. The total gas flow rate is rather high for the application of positive displacement compressors, especially in combination with space constraints. But due to the fact that the larger part of the associated gas is flashed off at 58 barg, the actual gas flow rate, especially for the MP compression stage, is kept to a minimum. In the table below the main criteria for the compression system are listed and evaluated for the aerodynamic and the positive displacement compressor type.

**Table 1:** Compressor type - technical comparison

	Flexibility to Gas MW variation	Efficiency at high Pressure	Weight & Size / Capacity Ratio	Vibration Levels	Availability
Aerodynamic Type Compressor (Centrifugal)	-	-	++	++	+
Positive Displacement Type Compressor (Screw or Reciprocating)	++	+	--	--	+/-

## Gas Molecular Weight Range

The well fluid composition and, even more important, the gas composition showed to have a large variation throughout field life. This was an important design requirement for the crude separation and gas compression system. In below table an overview is given of the gas MW (Molecular Weight) which formed part of the design basis for the three compression stages.

**Table 2:** Gas MW design range

	LP Compressor	MP Compressor	HP Compressor
Gas MW Range	39.5 - 51.3	27.3 - 37.2	22.0 - 24.8

In the concept design phase it became evident that for the LP compressor only a positive displacement type compressor suited the gas molecular weight variation. For the MP and HP compressor stages, either a positive displacement (fixed speed) or an aerodynamic compressor (variable speed) showed to be able to supply the required flexibility.

## Compressor Efficiency

As indicated earlier, available electric power for powering the new consumers was limited due to space constraints. At higher operating pressure, the positive displacement type compressors show significantly better efficiency compared to the aerodynamic type compressor. In the concept design phase it became clear that the higher consumed power for the aerodynamic type compressor did not allow for an electric driven aerodynamic type compressor.

## Weight & Size / Capacity Ratio

Clearly with the high operating speed of the aerodynamic compressor type and the fully balanced features, this compressor type has a much better weight & size / capacity ratio compared to the positive displacement compressors. Nevertheless, during the concept design phase it showed that both compressor types would meet the space and weight constraints with the capacity requirements. Since the major part of the associated gas is flashed off at 58 barg, the actual gas flow rate is kept to a minimum, especially in the MP compression stage, and positively supports the application of the positive displacement compressor type.

## Vibration Levels

Gas pulsations and mechanical unbalance will induce forces and related vibrations in positive displacement type compressor while the aerodynamic type compressor is mechanically fully balanced and the flow is continuous. Hereto the vibrations of a positive displacement type compressor are of a much larger magnitude.

## Availability

Since for every production facility the production availability is of utmost importance, the availability of the compressors is weighed heavily in the concept decision. Reference is made to the section

of chapter 4 where the availability of the considered compressor types and of the overall compression system is outlined. It should be noted that, referring to the three compression stages, the criticality of the MP and HP compression stages are the most critical for production as well as for the related contractual requirements.

#### 4 Compression System

As indicated before the compression system consists of three compression stages being the LP, MP and HP compression stage.

##### LP Compressor

The main driver for selecting the LP compressor is maximum flexibility towards variation in gas molecular weight as well as turndown capability. A reciprocating compressor was selected. The compressor was designed with valve un-loaders and variable clearance pockets to meet the required turndown capability and to minimize the absorbed power at reduced capacity. Final capacity turndown (beyond the turndown of the valve un-loaders and variable clearance pockets) and fine tuning between the capacity steps is obtained by means of recycling.

##### MP and HP Compressor

At an early stage in the concept design it became evident that the optimum solution with regards to footprint for the MP and HP compression stage is to integrate these two compression stages on one shaft. This yielded mainly for the positive displacement type compressor. But this combination also implied extensive attention had to be given to the operability and flexibility of the compressors.

The required compression flow rate and discharge pressure depicted centrifugal type compressor for the aerodynamic type and reciprocating compressor for the positive displacement compressor. These compressor types will be considered from hereon.

Due to the reduced efficiency (at higher discharge pressure) of a centrifugal type compressor, the only solution using a centrifugal compressor is a direct driven compressor train incorporating the MP and HP compressor on one shaft.

Combining the MP and HP compressor on one shaft showed also to be feasible for the reciprocating type compressor and fitted in the available space. The big advantage of this combination was its compactness which allowed for installation of a 4 x 33% concept which includes a spare compressor. This spare compressor was the key to a high overall availability of a concept based on reciprocating compressors, an availability higher

than the availability of a single train direct driven centrifugal compressor (Reference is made to the next section). The concept with 2 x 100% direct driven centrifugal compressors would offer a higher availability but was not cost effective.

As a result of the overall initial screening of potential compression solutions, the number of concepts was brought down to the following two concepts. These were compared in more detail in order to conclude on the concept to be finally selected:

- 1 x 100% Gas Turbine driven Centrifugal Compression Train (MP and HP body on one shaft).
- 4 x 33% E-motor driven Reciprocating Compressors (MP and HP stages on one shaft).

##### Compression System Availability

The difficulty with calculating equipment availability in general is to obtain good and representative data. For the concept selection it was decided to use reliability data from the OREDA database<sup>7</sup>. The reliability together with the Mean Time To Repair (MTTR) can be used to calculate the unplanned downtime of equipment. For the planned downtime (for planned maintenance) data from the OEM was used. For both concepts the system production availability is calculated based on the unit availability. Based on these calculations, the differences between the two concepts are the following:

1. The unit availability of an E-motor driven reciprocating compressor (90.76%) is lower (more planned maintenance required) than the unit availability of a gas turbine driven centrifugal type compressor (96.70%)
2. The partial capacity availability for a single full capacity compression train is equal to the full capacity availability whereas for 3 x 33% parallel units the partial capacity availability (0 – 66.6%) is higher than the full capacity availability.
3. The concept using reciprocating compressors includes one spare compressor which is very beneficial for the overall availability.

Since the financial compensation schemes in the contract use pro-ratio compensation for partial production and the availability of the oil production system is directly related to the availability of the gas compression system, the partial availability of gas compression is used to calculate the (partial) availability of oil production. The difference in oil production is then translated in an accumulated

difference in turnover using an oil price of 20 USD/barrel. From Figure 4 it becomes clear that for this field development analysis:

- The availability of the 4 x 33% E-motor driven reciprocating compressor concept (an availability of power generation of 98.5% is included in the calculation) is higher than of the 1 x 100% GT driven centrifugal compressor concept.
- The accumulated difference in turnover due to difference in availability (resulting difference in actual production time) in 3 years was found to be close to US\$ 9 million in favor of the reciprocating compression system.
- The difference mainly develops in early field life where the associated gas rate is relatively low (see figure 1). This is the period where the partial capacity advantage of the reciprocating compressor concept (multiple units) shows its large benefit.

Based on above evaluation, the 4 x 33% E-motor (3.2 MW) driven reciprocating compressor concept was selected as the most attractive solution, meeting the technical and commercial criteria for the project.

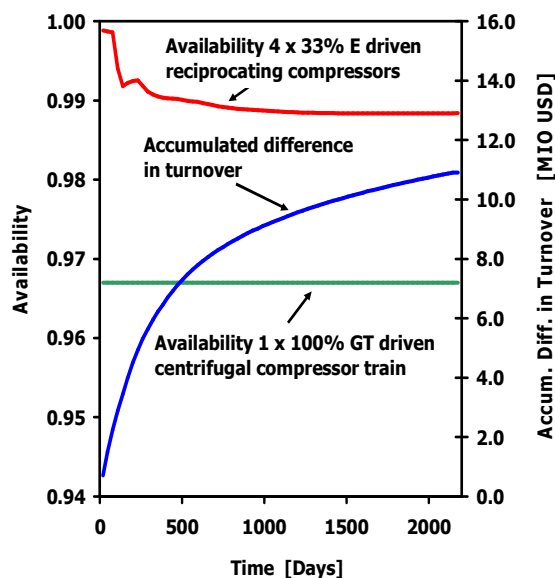


**Figure 4:** Concept availability comparison (theoretical)

## Compressor (package) design

With the selection of the reciprocating compressor type, special attention had to be given to the design of the compressor and the package. Reciprocating compressors are well known for higher vibration

levels due to unbalanced forces as well as due to the gas pulsation-induced forces.

- The MP/HP compressors as selected are 6-cylinder compressors which by nature give the advantage of being mechanically nearly fully balanced features (inherent to a 6-cylinder machine).
- Mechanical vibrations are further reduced by applying a 3-point support system. Hereby the likelihood of compressor string misalignment and the occurrence of related vibrations are minimized.
- The package is of a two layer design in order to meet the space constraint. Reference is made to Figure 5 which shows a complete MP/HP compressor package.
- Extensive attention was given to pulsation and vibration control of the compressor and connecting piping system. A pulsation and mechanical response analysis was specified in the scope of the OEM. Furthermore a 3<sup>rd</sup> party verification study of the pulsation and mechanical response analysis was awarded to TNO. The results of this verification study are presented in detail in the next chapter.

## Compression System Performance

In actual operation, the overall compression system shows very good performance. The compression system availability is currently on average in excess of 98%.



**Figure 5:** One of the four MP/HP compressor packages.  $L \times W \times H = 10.5 \times 4.7 \times 6$  meter and an operational weight of 150 tonnes.



### 5 Pulsation and vibration control

#### Introduction

Vigorous flow variation in time and space make reciprocating compressors and its responsive piping system an intimately connected system and demands effective system design, especially for offshore installations such as FPSO's. If mismanaged, the pulsed energy input can cause pipe failures, inefficiency and capacity limitations. This challenge has led to many innovations in the past, including the acoustic analog, acoustic filtering techniques and more recently the digital simulation technique. The API Standard 618<sup>2</sup> reflects much of the knowledge developed in applying these design tools.

Due to the rather complex installation and operating conditions of varying gas molecular weight, varying pressures, several unloading conditions and a number of operation modes of the compressors (single and parallel operation), potential vibrations problems should be recognized and solved in an early stage of the design. Therefore, the pulsation and mechanical response analyses were specified in the vendor scope and in addition a 3<sup>rd</sup> party verification by TNO was required.

Both the pulsation and mechanical response analysis had very strong information/data dependency and the timing and alignment in the project was of great essence. Essential is therefore a good and extensive communication between all parties involved.

TNO has carried out the following steps in the dynamic analysis of the piping system to achieve a reliable, efficient and safe installation:

- Step 1: Pre-study<sup>3,6</sup> or damper check
- Step 2: Pulsation analysis of the piping system<sup>4</sup>
- Step 3: Mechanical response analysis

In the following sections each step will be explained in short and the results will be summarized.

#### Pre-study or damper check

The first step in the pulsation study is a check of the performance of the initial design of the pulsation dampers for the specified operation conditions. During this check in the model the piping system has been replaced by an "endless" line, representing a reflection free termination point. This step is necessary to avoid that, in a later stage of the analysis when the piping system is connected to the dampers, a redesign might be necessary. Optimizing the design and performance of the

pulsation dampers in an early stage of the design is of utmost importance in order to prevent potential significant additional costs in a later stage.

The results of the damper check are the pulsation levels at the compressor valves and line connections, pulsation-forces acting on the damper and the power consumption of the compressor (PV charts).

If the calculated levels exceed allowable levels, modifications will be investigated. E.g. when during the damper check the pulsations near the compressor valves exceed the allowable levels, they can be effectively reduced by the installation of orifice plates or other damping devices at the cylinder flange. The increased power consumption of these damping devices can be calculated, optimized and discussed with the compressor vendor. As indicated the damper check is carried out for the initial design of the dampers.

Although the evaluation of the dampers showed that a number of dampers were undersized according the API requirements, the overall on-skid damper/piping/scrubber design showed to be satisfactory from a pulsation and vibration point of view. This resulted mainly from the fact that the scrubbers act as good acoustic filters. The measure taken to decrease the pulsations levels even further (in case deemed necessary) was the installation of orifice plates at the inlet/outlet of the dampers and of the scrubbers.

#### Pulsation (acoustic) modeling of the complete piping system

Acoustical modeling defines the particle velocity and plane wave dynamic pressure variation in time and space from piston face to the piping system extremity. Both compressor and piping system have been modeled using simulation elements like compressor cylinders, pipe elements, T-branches, elbows, volumes, valves, etc. A compressor piping system comprises a complex configuration of tubes filled with an acoustic media, driven by discontinuous velocity pulses.

For the acoustic analysis the computer program called PULSIM<sup>4,5</sup>, which has been developed by TNO, has been applied.

During the analysis special attention has been given to resonance conditions that can occur within the range of speed of sound in which the system can operate. The pulsation levels at these worst-case conditions have been compared with the allowable API 618 levels. Measures to eliminate or to dampen these resonances have been investigated in case the allowable limits have been exceeded.

The calculations have been carried out for all specified operation conditions, unloading conditions and single and parallel operation of the compressors.

An overview of the system for which the pulsation and mechanical response analysis has been carried out is shown in Figure 6.

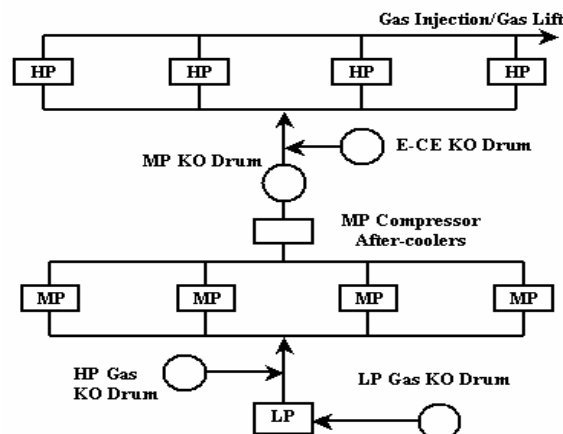


**Figure 6:** System for which the dynamic pipe analyses have been carried out

Due to acoustical separation between several parts of the system, the system has been split up into the following 8 parts: suction 1<sup>st</sup> stage LP, interstage LP, discharge 2<sup>nd</sup> stage LP/suction 1<sup>st</sup> stage MP, interstage MP, discharge 2<sup>nd</sup> stage MP, suction 1<sup>st</sup> stage HP, interstage HP and discharge 2<sup>nd</sup> stage HP. As an example, the investigated piping of interstage LP compressor is shown in Figure 7.

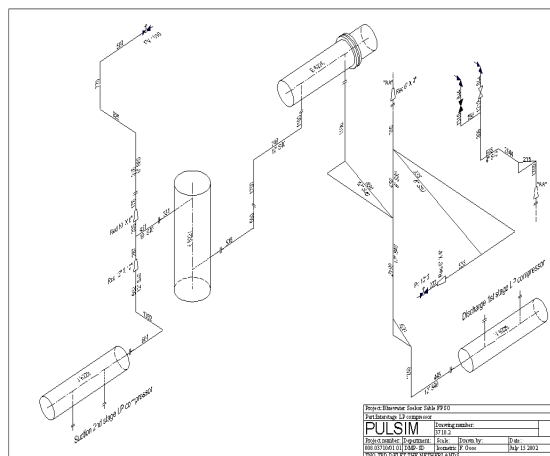


**Figure 7:** Model of interstage LP piping

## Results

The results of the original system showed exceedance of the allowable level at certain locations in all investigated parts. High exceedance occurred in relief lines; blow down lines and other side branches which were caused by acoustic

resonances. The maximum exceedance was 14 times the allowable API 618 level and was caused by the fact that the pipe diameters of these lines were too small.

Several modifications have been investigated to decrease the pulsation levels to acceptable levels e.g. the installation of orifice plates and increase of pipe diameters. Orifice plates at the damper inlet/outlet and in the side branches close to the headers and an increase of the diameter of most of the relief lines showed satisfactory results and were included in the design.

The installation of all advised modifications was not always feasible and the final number of accepted modifications was 20 out of a recommended number of 25. This implies that some exceedance of the allowable pulsations occur at specific locations and under specific operating conditions. However, the effect of these exceedances on the vibration and cyclic stress levels has been finally investigated in the mechanical response analysis. This approach is also accepted in the 5<sup>th</sup> edition of the API Standard 618<sup>6</sup>.

## Mechanical response analysis of the off-skid piping system

One of the objectives of the pulsation analysis is to reduce the pulsation-induced vibration forces to a minimum. However, unallowable vibrations and cyclic stresses can occur in case a mechanical natural frequency is close to or coincides with a frequency component of the pulsation-induced vibration forces, even in case the pulsation levels itself are below the allowable level.

The objective of the mechanical response analysis is therefore to check the design of the piping system, including the pipe supports and the construction on which the supports are mounted in order to make sure that the vibration and cyclic stress levels are lower than the applicable allowable levels.

The advantage of a mechanical analysis during the design stage is that the support layout can be optimized for all possible operation conditions. Hereby, potential fatigue failures can be recognized and avoided in an early stage of the design since the dynamic stresses are also calculated. The experience of TNO is that 90-95% of the vibration and fatigue problems can be solved during the design stage with this approach.

Special attention has been paid to local flexible parts<sup>3</sup> such as nozzle/shell intersections, compressor flange and local flexible steel structures. Upon decision of the customer which of the recommended modifications of the pulsation

analysis will be implemented, the mechanical response analysis has been carried out according to the API Standard 618, design approach 3.

For the above mentioned calculations the general-purpose finite element (FE) program ANSYS has been used. The piping system is divided into basic parts (finite elements) such as straight pipe sections, elbows, T-joints, flanges, reducers, constructions on which pipe supports are mounted. When the vibration and cyclic stress levels exceed allowable levels, it was investigated to include modifications to decrease the levels to allowable levels. This can be achieved by shifting the natural frequencies far enough from the excitation frequency.

## Results

The overall system (as in Figure 6) has been split up into 20 separate mechanical models of which an example of the discharge 2<sup>nd</sup> stage MP piping is shown in Figure 8. The results of the analysis showed that the allowable vibration and cyclic stress level were exceeded for several models. The exceedance mainly occurred in the relief lines; blow down lines, other side branches and in the main header (at parallel operation). This was mainly caused by the fact that these parts were too flexible to restrain the dynamic forces in case of resonance and because not all advised acoustical recommendations could be implemented.

The maximum calculated vibration and cyclic stress levels were respectively 12.8 times and 1.4 times the allowable level which means that fatigue failure can occur. A mode shape at which the vibration level exceeds the allowable level is shown in Figure 9.

Several modifications have been investigated and shifting of the natural frequencies was achieved by the installation of extra pipe supports and by increasing the stiffness of the structures on which the supports are mounted. To decrease the vibration and cyclic stress levels, 18 additional supports were added and 7 beam structures were added or modified.

Unfortunately it was not feasible to carry out all the advised modifications but in general the calculated vibration levels were satisfactory. Some exceedances of the allowable vibration level remained but the maximum calculated cyclic stresses were within the allowable level. This means that fatigue failure, caused by pulsations, will not occur.

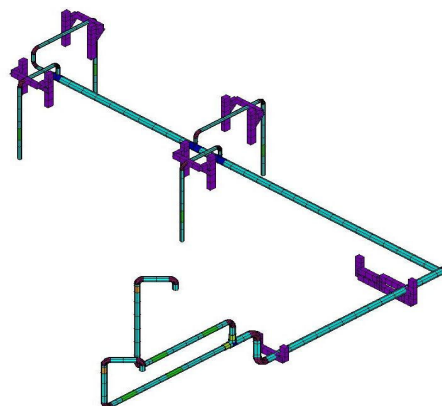


**Figure 8:** Mechanical (FE) model – Piping system discharge 2<sup>nd</sup> stage MP compressor

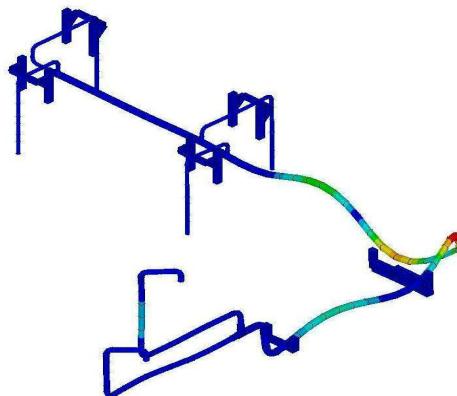


**Figure 9:** Mode shape at 57.5 Hz – Piping system discharge 2<sup>nd</sup> stage MP compressor

## 6 Field Measurements

The last step in the project consisted of field measurements. The purpose of the measurements was to check the actual boundary conditions as assumed in the pulsation and mechanical response analysis (supports, orifices etc) and the measurement of the actual vibration levels and check against the calculated values.

The measurements were limited to the actual field situations but 3 sets of measurements have been carried out at different combinations of parallel running compressors at various unloading conditions and at two discharge 2<sup>nd</sup> stage HP pressures.

From the results of gas samples, which have been taken during the site survey, it appeared that the actual gas molecular weights throughout the compression system were close to the design values used in the acoustical analysis. It could therefore be concluded that the actual process conditions during the field measurements were close to the simulation conditions.

Since the quality of the pipe support and of its installation is important for controlling the pipe vibrations, the first step in the field survey was a check of the pipe supports. It appeared that several supports were loose and that some U-bolts were too flexible to restrain the vibrations. It was advised to tighten the pipe clamps and to include this procedure in maintenance routines. It was also advised to change out U-bolts into rigid clamps for the large diameter piping. The results of the measured vibration levels showed that the vibration levels are generally in line with the results of the analysis and well within the allowable range.



**Figure 10:** Photo of a part of the system with a loose clamp

## 7 Conclusions

Large size and multiple reciprocating compressors are suitable for application on Floating Production Systems providing due consideration is given to the specific design requirements.

The overall performance of the compression system on the FPSO Glas Dowr is very good; it shows production availability in excess of 98%.

Pulsation and vibration control is considered essential for successful application of reciprocating compressors on FPSO's and should be initiated as early as possible in a project i.e. in the concept development phase.

The advantage of a simulation according to the API Standard 618 is that prediction and avoiding of fatigue failure is possible in an early stage of the design. It is also possible to optimize complex systems as installed on FPSO's with a broad operating envelop in process and operating conditions. This is not possible when only vibration measurements are carried out after the facilities have been put into operation but also require analysis in the engineering phase of a project. From

the results of the pulsation and mechanical response analysis it appeared that several modifications were necessary to achieve acceptable levels.

The results of the field measurements confirm that the reciprocating compression system on the FPSO Glas Dowr shows very good performance and vibration levels are satisfactory low. These results promise a safe, efficient and reliable long term operation.

## 8 Acknowledgements

The authors wish to thank Bluewater Energy Systems B.V. for their permission to use the results of this project and Nuovo Pignone, the compressor OEM, for providing the supporting information for this paper. Bluewater Energy Services B.V. would like to thank TNO for the successful co-operation during the project and for the joint effort of writing this paper.

## References

- <sup>1</sup> J. de Roos and J. Gillis, Bluewater Energy Services B.V., A. Eijk, TNO Science and Industry. "Concept Selection and Design Considerations for Compression Facilities for FPSO Glas Dowr", OTC 2005, Houston, 2 - 5 May 2005
- <sup>2</sup> API Standard 618, 4<sup>th</sup> Edition, June 1995
- <sup>3</sup> A. Eijk, J.P.M. Smeulers, L.E. Blodgett (Southwest Research Institute), A.J. Smalley (Southwest Research Institute), "Improvements and Extensions to API 618 Related to Pulsation and Mechanical Response Studies", The Recip – a State of the Art Compressor, 4-5 November 1999, Dresden, pp 85-94
- <sup>4</sup> Egas, G., "Building Acoustical Models and Simulation of Pulsations in Pipe Systems with PULSIM3", Workshop Kolbenverdichter, 27-28 October 1999, Rheine, pp 82-108
- <sup>5</sup> E. van Bokhorst, H.J. Korst, J.P.M. Smeulers, "PULSIM3, a program for the design and optimization of pulsation dampers and pipe systems", Euronoise '95
- <sup>6</sup> A. Pyle (Shell Chemicals Houston), A. Eijk and H. Elferink (Thomassen Compression Systems B.V.), "Coming 5<sup>th</sup> Edition of the API Standard 618", 3<sup>rd</sup> EFRC-Conference, March 27-28, 2003, Vienna, Austria, pp 25-33
- <sup>7</sup> OREDA-92, Offshore Reliability Data Handbook, 2<sup>nd</sup> edition 1992



# **Technical Improvement of Hyper Compressor in LDPE Plant**

by:

**Janjic Bojan, control department in  
LDPE plant, HIP-Petrohemija,  
Pancevo, Serbia and Montenegro,  
janjicb@verat.net**

**Stojakov Dragan, maintenance  
department in LDPE plant,  
HIP-Petrohemija, Pancevo, Serbia  
and Montenegro**

**4<sup>th</sup> Conference of the EFRC  
June 9<sup>th</sup> / 10<sup>th</sup>, 2005, Antwerp**

## **Abstract:**

Reciprocating compressors play very important role in the petrochemical industry. Unfortunately, compressors are one of the most frequent reasons for plant shutdowns. Having said that, it is of the utmost importance to keep them constantly operating. Simultaneously with correct maintenance practice, the best way to achieve high performances is upgrading compressors.

This report informs about upgrading hyper compressor (4 HHE-2, Ingersoll-Rand, 1974) in LDPE plant that has been accomplished by home know-how powered by market leader in compression technology from Austria. The focus was to increase running period (up to 20000 hours) between replacing cylinders through the use of redesigned sealing rings. Report also presents tremendous decrease (savings of 200000 € per year) of cooling oil consumption, using up-to-date sealing rings design. In it we will refer to the problem solution of not sliding of the greased metallic plate across the anchor plate, too.



## 1 Introduction

In Europe, most of petrochemical plants were built many years ago. Nevertheless, through the ongoing efforts of dedicated maintenance engineers, the majority of this machinery continues to operate reliably and efficiently. Such is the case in Petrochemical complex, HIP-Petrohemija a.d. Pancevo, Serbia and Montenegro. HIP-Petrohemija a.d. with its plants is the leading producer of petrochemicals and polymers in the country, having annual production of approximately 700 k tons per year of petrochemicals of highest quality.

Every year the petrochemical industries spend billions of euros in maintenance. Businesses are continually forced to look for ways to optimize the performance of their processes and reduce their maintenance cost. In a difficult economic environment, minute process improvements can impact dramatically upon operating profits. In today's climate, effective plant maintenance, and thus process efficiency, takes perhaps a higher priority than ever.

This paper informs how small technical improvements on hyper compressor in low density polyethylene (LDPE) plant can make significant benefits.

## 2 LDPE plant process

In LDPE plant, HIP-Petrohemija a.d. Pancevo, the ethylene polymerization is performed in continual autoclave reactor under high pressure of 2000 bars. For 45 k tons per year low-density polyethylene plant, Ingersoll-Rand compressors are delivering the ethylene gas up to above mentioned value in two separate compression systems. The booster and primary section compress of ethylene up to 252 bars. Then ethylene is compressed in hyper compressor section from 241 bars to 2000 bar in two stages. General data of primary and hyper compressor in LDPE plant are listed in Table 1.

**Table 1:** Compressors general data

	primary compressor	hyper compressor
design	Ingersoll-Rand Company, 1972.	Ingersoll-Rand Company, 1974.
Type	6 HHE-3-2	4 HHE-2
motor	GE 932.5kW, synchronous, 50 Hz, 375 rpm	GE 5966kW, synchronous, 50 Hz, 200 rpm

## 3 Need for improvement

Even when a company has both the will and the money to spend, it is difficult to know where to start with investment in order to optimize process performance and increase reliability. Problem is even bigger if there is restricted budget. HIP-Petrohemija has very restricted budget.

LDPE plant in HIP-Petrohemija a.d. is one process reactor line plant. Every unplanned shut down puts company in tremendous losses. Having said that, it is of the utmost importance to keep key equipment constantly operating. Simultaneously with correct maintenance practice, the best way to achieve high process performances is upgrading compressors.

In order to reduce maintenance cost and increase running period (up to 20000 hours) between shut downs home engineers have achieved significant results.

How it starts? First step was dedicated to increase running period between replacing cylinders. According to compressor recommendation bronze packing rings are used in the hyper compressor cylinders. Refer to Figure 1. the packing ring set [1] consists of radially cut pressure breaker ring which is installed in cup and three pairs of rings. One of these is tangentially cut and the other is radially cut. Logically, radially cut ring always goes toward the pressure, ahead of the ring. The tangent ring consists of three segments. The total end gaps should be [1]:

- radial ring:  $0.254 \div 0.762$  mm,
- tangent ring:  $1.524 \div 2.28$  mm,
- breaker ring:  $0.13 \div 0.26$  mm.

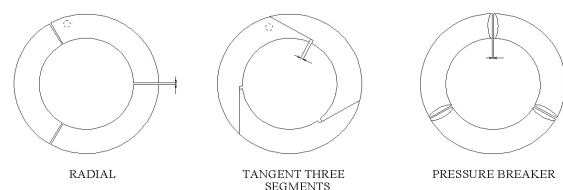


**Figure 1:** Packing rings

Ring side clearance in the ring groove should be  $0.203 \div 0.279$  mm. Clearance between the inside diameter of the packing ring and the outside diameter of the plunger to be used should not exceed 0.127 mm on the diameter.

Average cylinder running period, (see Table 2.), using above shown rings were unsatisfactory. Figure 2. shows layout of hyper compressor in LDPE plant.

**Table 2:** Average cylinder running period

cylinder	average running period (1982÷1997) (h)
L1	7461,8
L2	6395,3
L3	5217,8
L4	5549,8
H1	1088,5
H2	809,2
H3	1208,3
H4	667,5

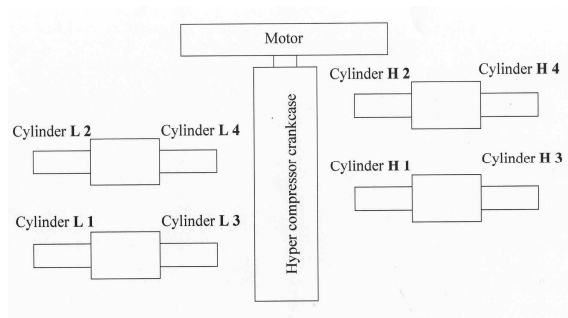


**Figure 2:** Layout of hyper compressor in LDPE plant

In 1998 home engineer have redesigned and developed packing rings. Redesigned packing rings (see Figure 3.) consist of the pressure breaker ring and three pairs of rings. One if these are tangentially cut and the other is radially cut. Opposite of compressor's producer recommendations, the total end gaps were changed as follows:

- radial ring: 6 mm,
- tangent ring: 15 mm,
- breaker ring: 0.8 mm.

As shown on Figure 3, tangentially cut ring shape was changed. This six-piece-tangent, radial and breaker rings are made of very special grade of bronze. This grade of bronze was recommended by engineers from the world market leader in compression technology from Austria. Both, design and material have extended the operating limits of hyper compressor.

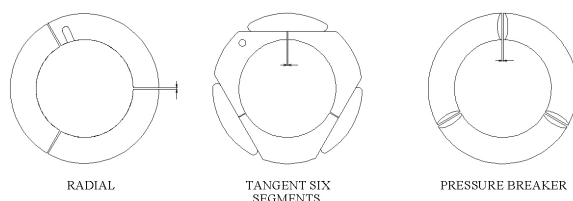


**Figure 3:** Redesigned packing rings

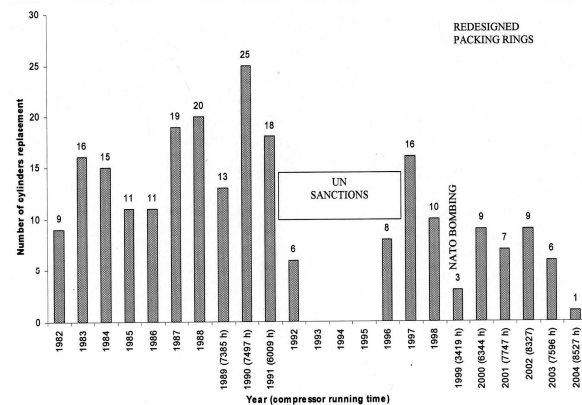
It should be stressed that radial cut ring slot for tangent ring dowel was changed. New design of slot provides maximum tangent ring gaps utilization.

All above mentioned changes have provided increased running period between replacing cylinders. Table 3. shows average running period in 1998 ÷ 2004. Best results were reached on H4 cylinder with average running period near 10 times greater than in 1982 ÷ 1997.

**Table 3:** Average cylinder running period

cylinder	average running period (1998÷2004) (h)
L1	6076,8
L2	5241,5
L3	9059,2
L4	5999,5
H1	4872,2
H2	5425,8
H3	7203,6
H4	6419,4

Figure 4 presents number of cylinders replacement on hyper compressor in LDPE plant. Here, it is evident how big are the differences between the number of replacements before the new design of packing rings and after it. In 2004. there was only one cylinder replacement.



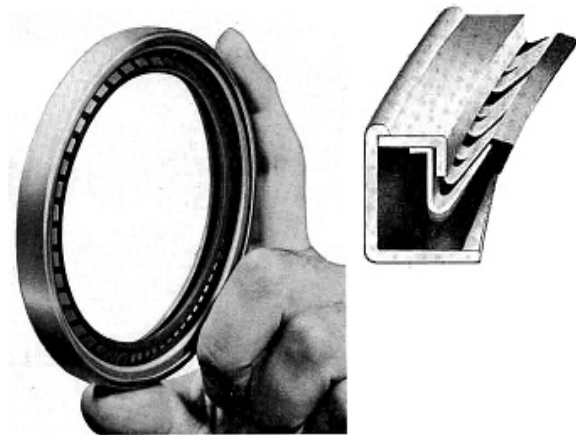
**Figure 4:** Influence of redesigned packing rings on number of cylinder replacement

Table 4 gives an overview of cylinder operating time in 2004. Last year was set a new record in cylinders operating time. It should be stressed that all cylinders are still (01.01.2005.) operating.

**Table 4:** Cylinder operating time at 01.01.2005.

	cylinder operating time (h)
L 1	6860
L 2	12239
L 3	9729
L 4	9729
H 1	9729
H 2	14696
H 3	14696
H 4	20150

The second improvement was significant result with tremendous decrease in cooling oil consumption, using state-of-the-art sealing rings design. Designer of hyper compressor in LDPE plant recommended ordinary oil seal (see Figure 5.) to minimize leakage of cooling oil between housing and plunger.



**Figure 5:** Oil seal

Using ordinary sealing elements cooling oil consumption in 2001. was 130410 kg. That year LDPE plant spent more at almost 214 000 € in cooling oil. Having said that, it was of the utmost importance to reduce cooling oil consumption. In 2002. home maintenance engineer and an engineer from the world market leader in compression technology found solution to make leakage of cooling oil between plunger and housing as low as possible. New sealing elements, so called step seal, consist of a profile ring with an O-ring as a buffer element, (see Figure 6.). Profile ring is made of PTFE, Bronze and MoS<sub>2</sub>.

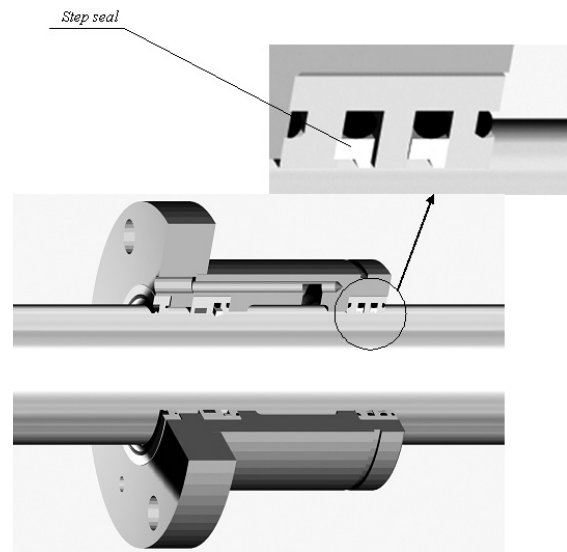


**Figure 6:** Step seal

Using step seal, cooling oil consumption was dramatically reduced. Figure 7. compares oil consumptions before and after oil seal upgrade. For instance, in 2004. oil consumption was 10980 kg (14561 €). It means that oil consumption was almost 12 times lower than 3 years before. In another words step seal made an 11943 kg (199407 €) difference. Those were installed progressively depending on cylinders replacement dynamic. Because of that, decrease in oil consumption was being reduced with time, too. The more we installed seals the better results were.

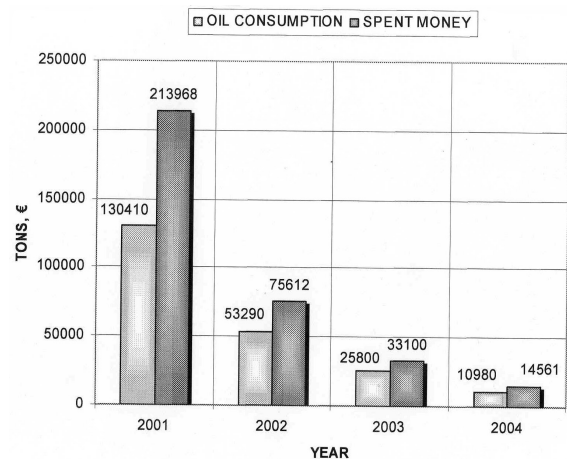


**Figure 7:** Influence of step seal on oil consumption

As mentioned before, hyper compressor in LDPE plant was made in 1974. Now, it is 31 years old with almost 25 years constantly operating. Fortunately, during that period there has been none serious accidents. But old age brings its problems. And since recently, there is tremendous problem with foundations shaking. Main reason for those shocks is not sliding of the greased metallic plates

across the anchor plates installed under the cylinder yoke supports, Figure 8a. 10 months ago home engineers, using experiences from engineers within Petrochemical complex in neighboring country, have found solution to eliminate existing problem using nonmetallic slide plates, Figure 8b. Instead of well known design with eight nonmetallic plates per cylinder made of long carbon fiber reinforced polyamide resin, our solution consists of four nonmetallic plate made of polyamide-imide (PAI) and four metallic plate covered by tungsten carbide (50 HRC). PAI is graphite powder and PTFE filled engineering thermoplastic. This grade excels in severe service wear applications such as non-lubricated bearings, seals, bearing cages and reciprocating compressor parts. After this improvement on hyper compressor supports, there was no foundations shaking.

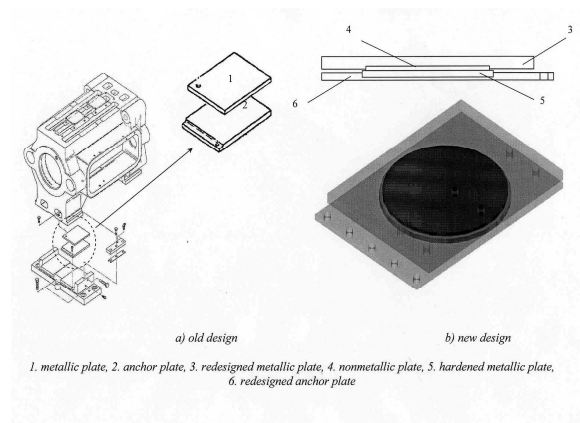


**Figure 8:** Compressor support

## 4 Conclusion

Generally speaking, there is a continuous need to increase production efficiency and maximize economic benefits for any given process plant. It is, one and only, way to increase profit. Increasing production efficiency is possible either through significant equipment reconstructions in order to debottleneck or make operation effectiveness exceed its design limits. Unfortunately, equipment reconstructions are not always payable. Sometimes factor ROI (return of investment) is not acceptable. In those cases increasing operation effectiveness is the best way.

Technical improvements on primary and hyper compressor, in order to achieve high performances, increase operation effectiveness. It should be stressed that technical improvements on primary compressor corresponding with less important benefits. Therefore, those improvements were not mentioned in this paper.

In 2004, compressors operation effectiveness was 99.6 % instead of annual 97.4 % during previous years. Difference of 2.2 % corresponding with 1288 tons of low density polyethylene (ldpe) per year. According with ldpe world market annual price in 2004, this increase in ldpe has earned 180320 € in net profit. Also, it should be added to the saving in 199407 € due to decreasing in cooling oil consumption. Finally, technical improvements on compressors has earned approximately 379727 € in net profit per year.

## 5 Look into the future

The 2005 will be point brake year in Petrochemical complex. In another words our company has to define strategic targets till the end of this year. After years of political instability in Serbia, Petrochemical complex has been identified as a high priority for the oil, gas and petrochemical sector. This is a result of the current and anticipated high level of investment, in both the oil-petrochemical and gas sectors. The focus will be on how to increase polymer production from existing equipment. Anyway, compressors upgrade will be one of the targets in LDPE plant. Increasing polymer production in this plant corresponding with increasing capacity of the booster and primary section. In order to increase compressors capacity in those sections it is necessary to make feasibility studies. That study has to identify all solutions for compressor upgrade. According to our expectations it should be necessary to increase either revolutions per minute of motor or cylinder and piston diameter. Somehow, both compressors in LDPE plant will operate at the boundary conditions. To operate compressors safely at peak load it necessary to install condition monitoring system. This is the only way to manage plant shutdowns in order to uproot reactive maintenance practice if possible.

## References

- [1] Ingersoll-Rand. ``Instructions for installation and operation'',1973.



# **The Use of HydroCom to Determine the Root Cause of K6301 Compressor Failure**

**By**  
**Paul Melvin**  
**Rotating Equipment Team**  
**Shell UK, Stanlow**  
**Ellesmere Port**  
**England**  
**Paul.Melvin@shell.com**

**4<sup>th</sup> Conference of the EFRC**  
**June 9<sup>th</sup> / 10<sup>th</sup>, 2005, Antwerp**

## **Abstract:**

K6301 is a Peter Brotherhood 2B2, 2 stage double acting compressor, it supplies 'fresh gas' Hydrogen on a Hydrogen De-Sulphurising Plant which produces Low Sulphur Diesel Fuels.

HydroCom was fitted in September 2004 to provide 'stepless' control capabilities during the process. As a result system pressures can be controlled without the need to recycle gas. The recycle gas contains H<sub>2</sub>S and Chlorides whilst 'Fresh Gas' is pure Hydrogen, therefore drastically reducing the H<sub>2</sub>S and Chlorides to K6301.

Re-cycling gas with Chlorides caused heavy fouling of the compressor valves and H<sub>2</sub>S contaminated the Hydrogen.

In December 2004, the compressor suffered a catastrophic failure.



### 1 Introduction

The failure was caused by loosening of the piston-to-piston-rod locking nut until the nut eventually became detached from the rod and fell into the cylinder as the piston was still reciprocating.

The impact of the piston onto the nut resulted in excessive loads on the crosshead 'web' at the piston rod to crosshead locking nut access port.

This 'web' failed due to high load low cyclic fatigue, causing the gudgeon pin to become loose eventually breaking through the casing and thrown out of the machine onto the ground.

Oil leaked from the machine through the opening of the fractured casing, the oil level reduced causing the compressor to trip due to the 'Low Lube Oil Trip' logic function.

This report describes the events causing the failure and compressor trip and discusses the recommendations that followed.

### 2 Findings

#### 2.1

The operator approached the compressor once it had tripped due to low lube oil pressure.

Oil had spilled onto the floor having leaked from the access door on the distance piece. The gudgeon pin was on the floor and the distance piece access door was peeled open like a tin can. See fig 1.

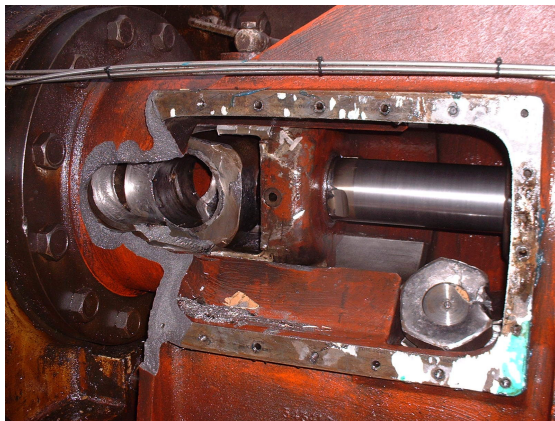


**Figure 1:** View via the Crosshead Distance Piece Access Panel

#### 2.2

The piston rod at the crosshead failed due to high load low cyclic fatigue, indicated by very few beach marks and a large final fracture area, also fracturing the nut required high loads. See fig 2.



**Figure 2**

#### 2.3

When the cylinder head was removed, the piston to rod locking nut was found detached from the rod and laying in the cylinder. See fig 3.

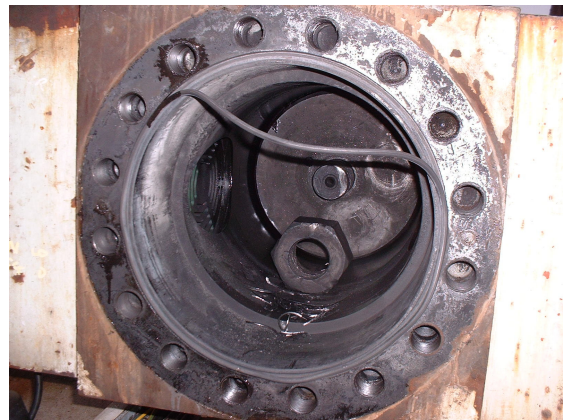


**Figure 3**

#### 2.4

There was also several pieces and several fragments of stripped thread from the nut and rod together with the tab washer which was in several pieces. See fig 4.



**Figure 4**

### 2.5

When the compressor was disassembled the spacer used to set the 'bump clearance' was found heavily thinned (reduced to 1 or 2 mm at the bore) and split due to excessive compression forces. The spacer should be approx. 16mm in thickness. See fig 5.



*Figure 5*

### 2.6

When the cylinder head was removed exposing the cylinder head face, clear indications of contact between the nut and the head could be seen in two locations.

A; in the recess of the head where the piston/nut would enter at top dead centre.

B; At the 6 o'clock position of the cylinder i.e. as the nut became detached from the rod and fell into the cylinder. See fig 6.



*Figure 6*

### 2.7

The crankcase top cover was removed, revealing the crank there was evidence of heavy rubbing indicating contact between the rotating counter balance mass and the detached crosshead. See fig 7.



*Figure 7*

### 2.8

The material of the piston nut was as per the manufacturers recommendations (EN8). The threads in the piston nut appear to be heavily corroded and approx. 50% of the length of the threaded bore had the thread peaks sheared followed by heavy rubbing both directions, the remaining 50% of the threads were relatively undamaged indicating that the nut became loose and unscrewed from the rod causing the piston to move on the rod. As the rod moved towards the crank end the piston impacted on the loosened nut before the piston begins to move.

As the rod moved towards the head the nut and rod start to impact on the inner surface of the cylinder head in the recessed area and the loads on the threads increased. See fig 8.

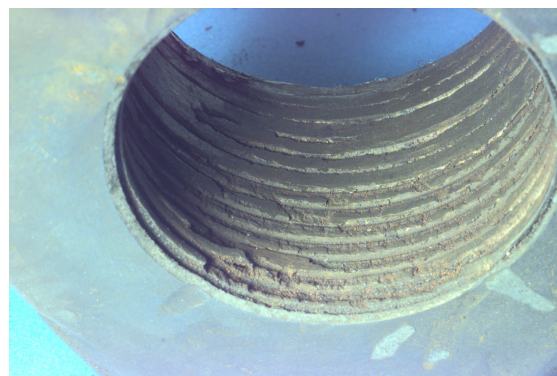


*Figure 8*

### 2.9

The piston nut was sectioned in order to analyse the threads closely.

All thread roots were found to contain numerous cracks of up to 0.5mm long.

As the crack propagates, the tension of the nut weakens and the nut can become loose. See fig 9.



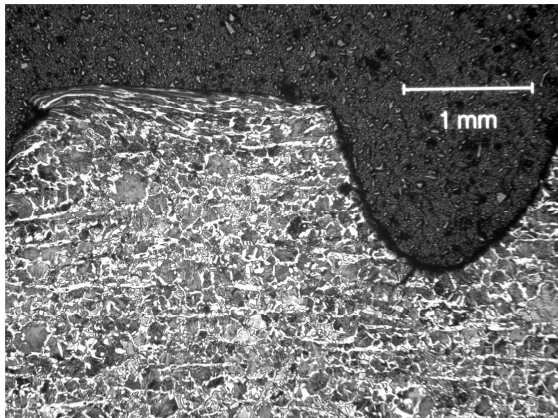


**Figure 9**

### 2.10

The cracks were found to be 'branched'. The material contained within the cracks was analysed and found to contain up to 20% Sulphur, 10% Iron and 1.5% Chlorides. - indicative of stress corrosion cracking. See fig 10.

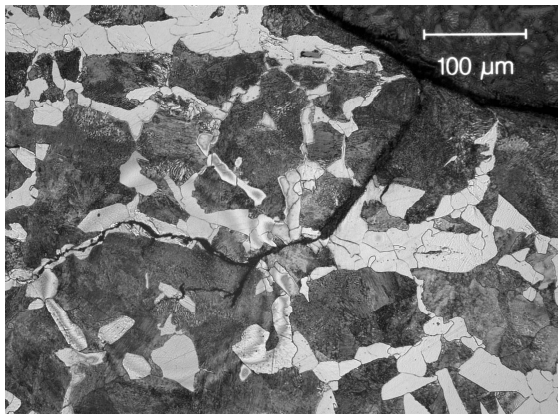


**Figure 10**

### 2.11

The threads on the rod at the piston end contained relatively few short cracks with a maximum length of 150 microns, levels of Sulphur, Chlorides and Iron contained within the cracks were a lot lower. See fig 11.



**Figure 11**

### 2.12

The threads on the rod at the crosshead end showed no evidence of containing cracks, the rod had suffered a high load, low cyclic fatigue failure. See fig 12.



**Figure 12**

### 2.13

The threads on the rod at the crosshead end were found to be heavily deformed in both directions, the 'whitened area on the thread peaks indicate some localised heat has taken place in that area. See fig13.

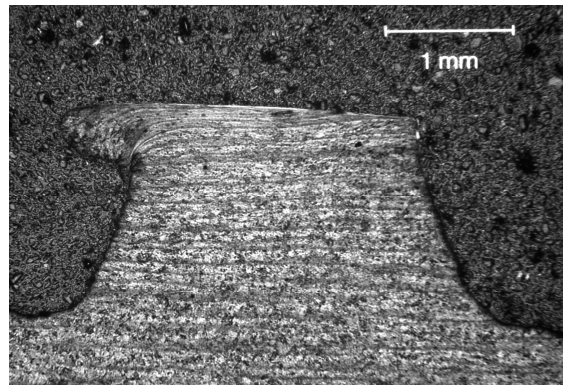


**Figure 13**

### 2.14

The material of the tab washer was NOT as per the manufacturers recommendations, EN2a - a soft malleable Iron but was made from stainless steel. The tab had failed due to fatigue. Part of the tab was found inside the hollow of the piston - the curve of the tab can be perfectly matched to the rod where it was forced into the hollow of the piston as the rod moved through the piston. See fig 14.

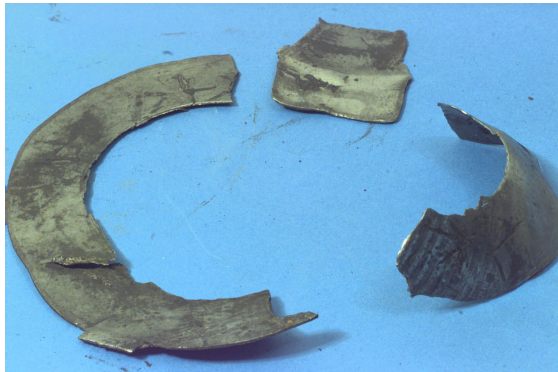


Figure 14

### 2.15

The tab washer was sectioned at the tab location. The grain structure revealed that the tab had been used more than once indicated by the 'dog leg' in the grain structure, repeated bending and straightening caused embrittlement in that area, therefore weakening the tab. See fig 15.

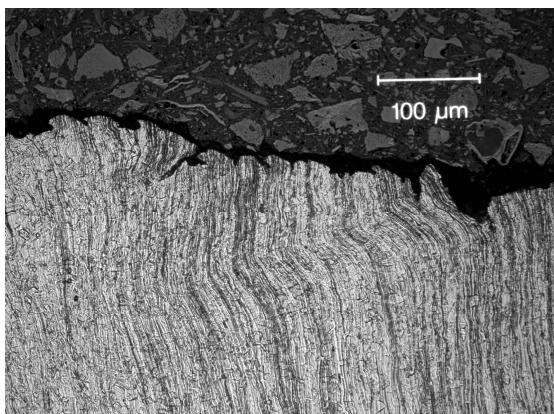


Figure 15

## 3 HydroCom

### 3.1

HydroCom was fitted to the compressor to enable 'stepless' capacity control, increased reliability; reduced operating costs and also provides condition monitoring information such as suction and

discharge gas temperatures and pressures. Individual valve temperatures, rod displacement and position as it reciprocates - indicating vibration and wear rates on rider rings. It can also produce Pressure Volume diagrams.

Since the compressor failure data from HydroCom was used to create a timeline of events prior to the failure.

HydroCom stores data at 5-second intervals and automatically saves 30 minutes of data prior to the compressor stopping; each time stamp is called a profile.

Profile 360/360 is equivalent to when the compressor stopped, profile 1/360 is equivalent to 30 minutes before it stopped.

The system was set up to view the cylinder pressure (crank end and head end) against crank position together with rod drop position.

Each profile was inspected closely. It was clear when a change in the normal signatures began i.e. when the piston nut started to become loose.

The rod displacement indicated when high impact loads began at certain positions within its stroke - the pressure curve changed dramatically from normal. The rod was seen to be reciprocating with high impact vibrations as it entered the stationary piston whilst there was zero gas compression in both directions.

The piston nut eventually fell into the cylinder.

During the next few strokes vibrations were seen to be very high, the impact of the piston on the nut caused excessive loads on the crosshead web at the locking nut access port causing high load, low cyclic fatigue failure of the web on the crosshead.

### 3.2

This is profile 1 of 360 prior to the failure of the compressor, normal compression on both the head end and crank end strokes as well low levels of rod displacement throughout the cycle. See fig 16.

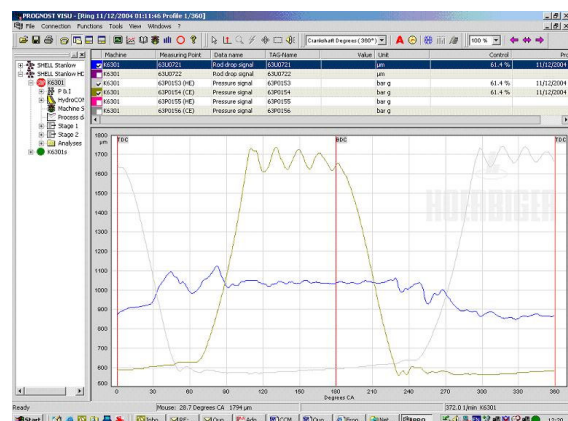


Figure 16



### 3.3

This is profile 186 of 360, here you can see that compression has ceased early during the crank end and compression stroke suggesting that the piston nut is loose and as the rod moves towards the crank end the piston remains stationary for a few degrees of rotation, therefore when at bottom dead centre the piston does not travel it's design distance but stops short.

Also, the rod displacement has increased dramatically.

As the piston rod moves towards the head end, the compression begins then stops for a few degrees of rotation then begins again. This due to the piston being loose on the rod, the rod begins to move towards the head, the piston moves for a short distance then the rod moves through the piston whilst the piston remains stationary, the rod and piston then move together for the remaining of the stroke, and compression is re-established again. See fig 17.

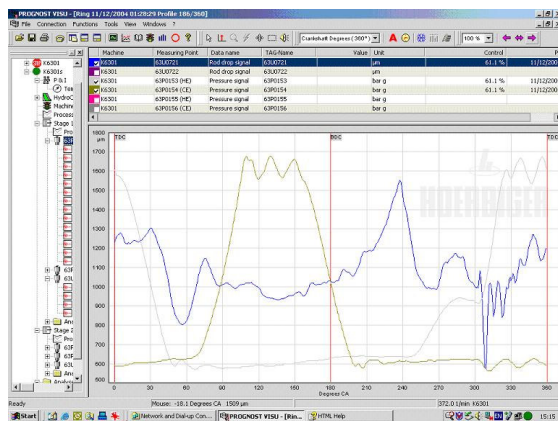


Figure 17

### 3.4

This is profile 250 of 360, compression stops in both directions but rod displacement is very high at approx. 2000 microns - suggested as being the clearance between the rod and packing bore.

The high levels of rod displacements are due to the rod impacting the stationary piston as the rod travels throughout its stroke.

Also, the very high displacement seen at 60 degrees before top dead centre is equivalent to a piston position of 2.5" (63mm) which is approx. equal to the thickness of the piston nut - At this point the piston nut has become detached and has fallen into the cylinder. As the piston moves towards top dead centre and impacts the nut, the loads generated cause the failure of the web at the crosshead gudgeon pin location; the piston now becomes detached from the crosshead. See fig 18.

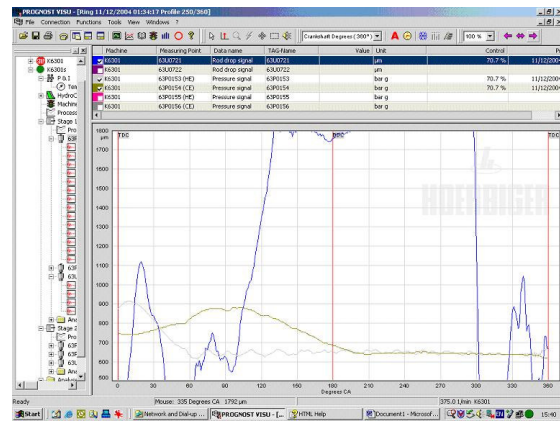


Figure 18

### 3.5

This is profile 308 of 360, there is zero compression and low levels of shaft displacement. The rod has become detached from the crank when the crosshead web failed.

The gudgeon pin was forced through the compressor distance piece access door onto the floor. Oil then leaked from the machine as it was still rotating until the low level trip was initiated and the machine stopped. See fig 19.

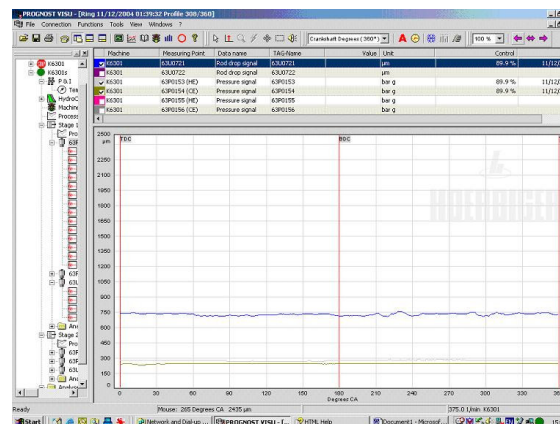


Figure 19

## 4 Discussion

It was confirmed with PU technicians that on occasion we have new rods or refurbished rods delivered to site without nuts or tab washers and that we may re-use old nuts and tab washers. We may on occasion have hand made tab washers to suit.

A number of presentations that have been carried out, resulted in several topics requiring attention in order to try to prevent this type of failure re-occurring.



1. New or Refurbished rods who supplies them?  
Should we have new nuts and tab washers fitted to the rods as standard practice?  
Should the individual components be 'date stamped' etc for future reference.  
Wrong rods (New, but not for this machine) and used rods (not refurbished) were delivered from stores, HOW.  
'Buy Desk Description' review are they accurate for the need.
2. Nut retaining device  
what type is the most effective. - B'Hood confirmed Tab washer is not an issue as long as it's new and made from the correct mat'l - theirs are made from EN2Ac (soft carbon steel. i.e. easily formed without raising stresses at the bend.
3. Review of relevant PSSR Work Instruction,  
Do we need to review our current 'Equipment Maintenance Plans, and our compliance with them?
4. Training and Competency of people undertaking compressor overhauls.
5. Review of the GET? What is the GET for - recording tech data?
6. Use of HydroCom as alarm/trip in DCS.
7. How did we end up with a new rod made at Brotherhood that was 1.5" too long, B'Hood questioned this at the time of ordering and their reply came from the P.U. no advice sourced from REG or PCR raised to cover the change.

## K-6301 Reciprocating Compressor Failure December 2004

### **Supplementary issues further to completed Technical Investigation, March 2005**

(As reviewed by A S Jones, J Swash, C Heald, P Hodgson 10/03/05)

Item No	Description	Action	Action by Whom	Action by When
1	Rod from Stores for LP/HP was for K-9302 which is 5" shorter (later found in K-9302 box lying in Bay 3. See 4)	Review existing WIs and processes with CWS and PCL for any gaps etc	OME/30 & PCL/50	
2	Rod from stores for HP/LP was correct rod BUT was in need of refurbishment How can this happen?	Review existing WIs and processes with CWS and PCL for any gaps etc	OME/30 & PCL/50	
3	In 2000 Stanlow, OMP requested Peter Brotherhood to supply rods 11 1/2" longer than design without PCR, which, due to confusion led to ALL rods being longer of two.	Remind OMP/00 of need for vigilance in this area. Onward cascade to OMP team	OMP/00	
4	Rod found in K-9302 box was correct length but piston fit was not square to it. Cannot confirm whether rod or piston issue. Corrected by PB as part of their works.	Completed by PB at overhaul		
5	Current BuyDesc requests rod to come with Nut, several instances of rods not coming with Nut. Likely incomplete/incorrect despatch controls	Review of CWS & PCL Repairable Stock & Insurance processes & procedures	OME/30 & PCL/50	
6	Continue to correct SAP BOM and BuyDesc descriptions to better describe items Generally as well as K-6301 in this instance			
7	Nut Retaining Device (Tab Washer) Currently don't stock on BOM, either separately or as part of Rod Assembly	Add to BOM & Rod Assembly BuyDesc	OME/30 & 93	
8	Cross Head Nut. Currently don't stock on BOM, either separately or as part of Rod Assembly	Include supply with Rod assembly BuyDesc	OME/30 & 93	



# **CFD Simulation of the Two Phase Pulsating Flow in the Reciprocating Compressor Installation**

by:

**Piotr Cyklis and Kantor Ryszard**

**Institute of Industrial Apparatus and Power Engineering**

**Cracow University of Technology**

**Cracow**

**Poland**

**E-mail: pcyklis@mech.pk.edu.pl, rkantor@mech.pk.edu.pl**

**4<sup>th</sup> Conference of the EFRC  
June 9<sup>th</sup> / 10<sup>th</sup>, 2005, Antwerp**

## **Abstract:**

The analysis of the pulsating flow in the reciprocating compressor installation is important for the technical exploitation compressor plants. One of the phenomena causing difficulties in modeling gas pulsations is the presence of liquid droplets in gas. For an example the oil remover designed for refrigerating reciprocating compressor is chosen for investigation. As the numerical tool the FLUENT software has been used and for verification the experimental identification method has been used. For multiphase flow several models have been compared. As the effect of this work we may conclude that the use of two-phase flow simulation has more influence in case of liquid mass fraction 10%-15% and more. With lower liquid contamination than 5% mass fraction the improvement of two- phase flow consideration in simulation of pulsations is not that important.

## 1 Introduction

The phenomenon of pressure pulsation significantly influences the functioning of the entire compressor manifold. This brings up the need to analyse the phenomena of pulsation wave propagation, and its damping. An important issue in analysing the pressure pulsations is the model the working gas<sup>1</sup>. The use of the proper equation of state for the gas, and the description of the real gas properties, as well as dispersed liquid contamination influence not only the accuracy of the obtained results, but also the quality of the solution. Dealing with pressure pulsation, it is important to know both: the real velocities of wave propagation, and the values of the thermal properties of the gas. Liquid contamination influences the wave propagation taking away part of the pulsation energy. The most common approach in analysing the phenomenon of pressure pulsation is the use of the ideal gas equation of state. However, in certain ranges of gas contamination, the error of results obtained through this equation, as compared with real values, becomes considerable. A need thus arises to carry out calculations using alternative models describing the behaviour of real gas with impurities<sup>2,3</sup>.

## 2 Theoretical basis of the method

The classic Helmholtz model is based on a solution, for a straight section of a pipeline, of the wave equation of the form (1). As a result, a four-pole matrix of the form (2) is obtained. Elements of this matrix  $\{a_{ij}\}$  are determined only for a segment of a pipeline. Concurrently with a four-pole matrix, a complex impedance matrix  $Z$  having the elements  $\{z_{ij}\}$  is defined by the relation (4).

$$\begin{cases} \frac{\partial \phi}{\partial x} = \frac{1}{S} \frac{\partial m}{\partial \tau} + \frac{b}{S} \cdot m \\ \frac{\partial m}{\partial x} = \frac{S}{c^2} \frac{\partial \phi}{\partial \tau} \end{cases} \quad (1)$$

$$\begin{bmatrix} P_1 \\ M_1 \end{bmatrix} = \begin{bmatrix} ch\gamma L & Z_f sh\gamma L \\ \frac{1}{Z_f} sh\gamma L & ch\gamma L \end{bmatrix} \cdot \begin{bmatrix} P_2 \\ M_2 \end{bmatrix} \quad (2)$$

$$\begin{bmatrix} P_1 \\ M_1 \end{bmatrix} = \begin{bmatrix} a_{11} & a_{12} \\ a_{21} & a_{22} \end{bmatrix} \cdot \begin{bmatrix} P_2 \\ M_2 \end{bmatrix} \quad (3)$$

$$\begin{bmatrix} P_1 \\ P_2 \end{bmatrix} = \begin{bmatrix} z_{11} & z_{12} \\ z_{21} & z_{22} \end{bmatrix} \cdot \begin{bmatrix} M_1 \\ M_2 \end{bmatrix} \quad (4)$$

where:  $p$  – pressure,  $m$  – mass flow rate,  $S$  – cross section area,  $b$  – damping factor,  $\tau$  – time,  $x$  – Cartesian coordinate,  $L$  – pipe length,  $Z_f$  – pipe impedance,  $c$  – speed of sound,  $\gamma$  – wave propagation coefficient,  $P$  – pressure in complex space,  $M$  – mass flow in complex space.

In order to generalize the model for an arbitrary geometry it has been assumed that the forms of matrices  $\{a_{ij}\}$ ,  $\{z_{ij}\}$  will not be based on equation (2), but that they will have a completely generalized form. This assumption means that for a unique determination of the interaction of an arbitrary component of a manifold it is sufficient to know four elements of the matrix, which must be identified for this component. The aim of the present work was to develop a method of the identification of these matrix elements.

The concept of the method developed here is following: for a considered element of a manifold a full multi-dimensional CFD simulation is carried out, solving the Navier-Stokes set of equations numerically together with the necessary closing models, i.e. gas state model, turbulence model, boundary conditions<sup>2,4</sup>. The results obtained are averaged at the inlet and outlet of the analysed element and next a complex transformation of the results is carried out, so that elements consistent with the generalized form of matrices  $\{a_{ij}\}$ ,  $\{z_{ij}\}$  are obtained. In this way the advantages of both methods can be combined: the Helmholtz model possibility of analysis of extended installations and the possibility of studying geometry of an arbitrary element, without a priori simplifications.

For further considerations it is necessary to define complex transmittances. Below, complex transmittances are defined: a flow and flow-pressure one for excitation for the forward and reverse flow.

- flow transmittance

$$\bar{T}_M(i\omega) = -\frac{M_{i+1}}{M_i} \quad (5)$$

- flow-pressure transmittance

$$T_{MP}(i\omega) = -\frac{P_{i+1}}{M_i} \quad (6)$$

For a symmetrical muffler (or other compressor manifold element) two transmittances would be sufficient (along the flow direction), for unsymmetrical four transmittances are necessary. These transmittances can be derived using CFD simulation, as all of them are determined having the flow excitation boundary condition:  $\dot{m}_i$ ,  $\dot{m}_{i+1}$ .

The second boundary condition is a free outflow or a total closing. Impedance of closed end  $Z_k = \infty$  and for open end  $Z_k = 0$ .

The four cases planned for the CFD simulation of the unsymmetrical compressor manifold element are shown on the Figure 1.

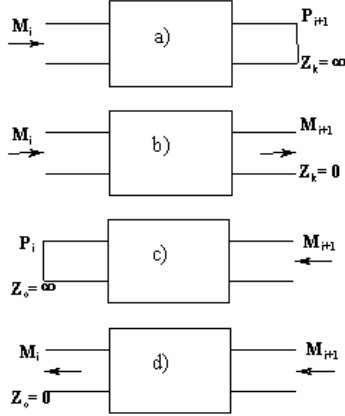


**Figure 1:** Four cases of simulation essential to complete determine of acoustic parameters

Each simulation allows to determine one transmittance according to the drawing, named respectively  $\bar{T}_a, \bar{T}_b, \bar{T}_c, \bar{T}_d$ .

Writing down impedance relations for the cases a, b, c, d as defined in Figure 1 one obtains:

$$\left. \begin{aligned} P_i &= z_{ii} \cdot M_i \\ P_{i+1} &= z_{i+1,i} \cdot M_i \end{aligned} \right\} \Rightarrow z_{i+1,i} = \bar{T}_a \quad (7a)$$

$$\left. \begin{aligned} P_i &= z_{ii} \cdot M_i + z_{i+1,i} \cdot M_{i+1} \\ 0 &= z_{i+1,i} \cdot M_i + z_{i+1,i+1} \cdot M_{i+1} \end{aligned} \right\} \Rightarrow z_{i+1,i+1} = \frac{\bar{T}_a}{\bar{T}_b} \quad (7b)$$

$$\left. \begin{aligned} P_i &= -z_{i,i+1} \cdot M_{i+1} \\ P_{i+1} &= -z_{i+1,i} \cdot M_{i+1} \end{aligned} \right\} \Rightarrow z_{i,i+1} = \bar{T}_c \quad (7c)$$

$$\left. \begin{aligned} 0 &= -z_{ii} \cdot M_i - z_{i+1,i} \cdot M_{i+1} \\ P_{i+1} &= -z_{i+1,i} \cdot M_i - z_{i+1,i+1} \cdot M_{i+1} \end{aligned} \right\} \Rightarrow z_{i,i} = \frac{\bar{T}_c}{\bar{T}_d} \quad (7d)$$

The derived relationships (7) allow a unique determination of complex impedance matrix  $Z$  that defines a linear lumped acoustic element. As the excitation for the CFD simulation the impulse or/and unit step function for mass flow rate is used, allowing for general element response calculation.

The general method for calculation all transmittances is the use of an impulse or a unit

step function as flow input excitation, for each of four cases a, b, c, d on Figure 1.

Since pressure and flow pulsations have damped oscillation characteristic it is obvious to use a general damped harmonic form for transmittances. The acoustic response of the installation element for an impulse inflow excitation have general form in the complex domain:

$$G(s) = \frac{K \omega_0^2}{s^2 + 2\zeta \omega_0 s + \omega_0^2} \cdot e^{-s\tau} \quad (8)$$

and in the real domain:

$$y(\tau) = K \cdot u_0 \cdot \frac{\omega_0}{\sqrt{1-\zeta^2}} e^{-\zeta \omega_0 \tau} \cdot \sin(\omega_0 \sqrt{1-\zeta^2} \tau + \tau_0) \quad (9)$$

The damping coefficient may be derived as:

$$\zeta = B \cdot \sqrt{\frac{1}{\left(\frac{2\pi}{\tau_c}\right)^2 + B^2}} \quad (10)$$

and the amplification:

$$K = \frac{A_0 \cdot \sqrt{1-\zeta^2}}{u_0 \cdot \Delta \tau \cdot \omega_0} \quad (11)$$

The natural harmonic frequency:

$$\omega_0 = \frac{2\pi}{\tau_c \sqrt{1-\zeta^2}} \quad (12)$$

The values  $\tau_0, \tau_c, B$  may be easily determined from the analysis of real system response shown on Figure 2.

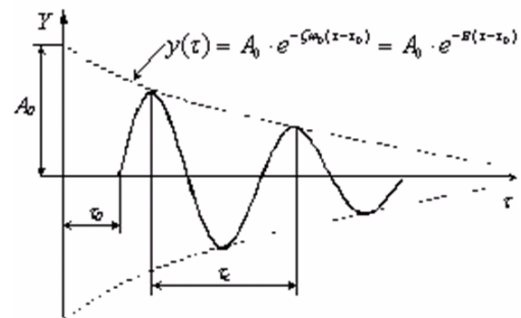


**Figure 2:** Curve of oscillating damped impulse response

However usually the system response for an impulse inflow excitation tends to form more then one basic natural frequency. In this case the response is decomposed using Fourier analysis, and each frequency is consequently analysed using above shown algorithm.

### 3 Difference between two-phase models

In most commercial packages for CFD simulations, three main two-phase flow models may be introduced:

- DPM (Discrete Phase Modeling) – where one phase is calculated in continuous basis (Euler model, Navier-Stokes equations), and for the second phase discrete Lagrange model is used,
- VOF (Volume of Fluid) – both phases are continuous (Euler model), the common momentum equation is solved for both phases and results are divided accordingly to the volume ratio of each phase,
- Mixture model - also both phases are continuous, but additionally equations for each phase content and diffusion equation for concentration are included. The comparison of models is shown in Table 1.

**Table 1:** Multiphase flow models

	<b>DPM</b>	<b>Mixture</b>	<b>VOF</b>
<b>Variables</b>	Euler-Lagrange	Euler	Euler
<b>Particle size determination</b>	yes, (also Rosin-Rammler distribution available)	yes (only uniform sized particles)	no
<b>Modelling of static systems</b>	no	yes	yes
<b>Compressible flow</b>	yes	yes	yes
<b>Sliding</b>	yes	yes	no
<b>Phase interaction</b>	yes (partial)	yes	yes
<b>Typical use</b>	dispersed gas bubbles, droplets and particles	dispersed gas bubbles, droplets and particles with higher volumetric ratio	slow flow with stratification

### 4 CFD simulation of oil remover acoustic reaction for an impulse flow excitation for varying oil contamination

Described model was used for numerous numerical experiments for nozzle, muffler and oil removers simulations<sup>2,3</sup>.

It finally occurred that from three described earlier two-phase models only Mixture model gave realistic results. Only this model was able to account for taking over part of pulsation energy by liquid phase dispersed in gas.

In this paper the oil remover for a refrigerant compressor is shown as an example. The geometry of this element is shown on the Figure 3 together with the finite volume mesh.

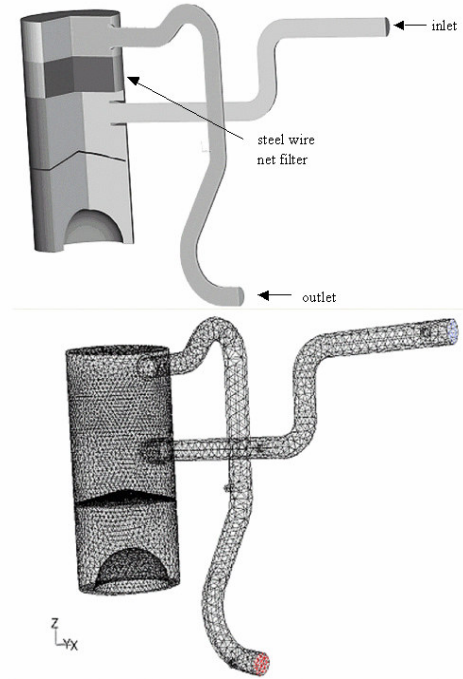


**Figure 3:** 3D geometry of oil remover (83 792 of finite volume elements)

The results of simulation for pure gas and 1, 5, 20 and 50 % of oil mass content in gas are shown. The results of 3D simulation are averaged within the inlet and outlet cross-section area in order to obtain one-dimensional mass flow and pressure curves. Calculated  $p(\tau)$  and  $\dot{m}(\tau)$  for inlet and outlet are shown on figures 4, 5, 6.



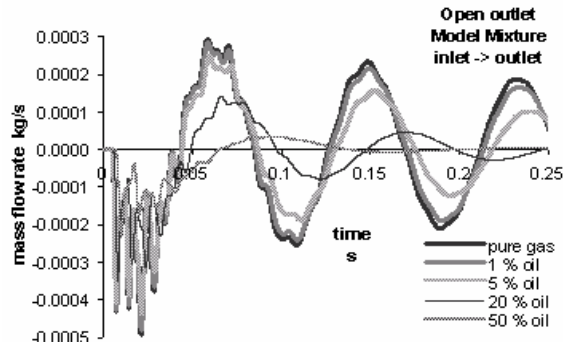


**Figure 4:** The impulse reaction (mass flow rate) on open outlet of oil remover - the excitation on inlet

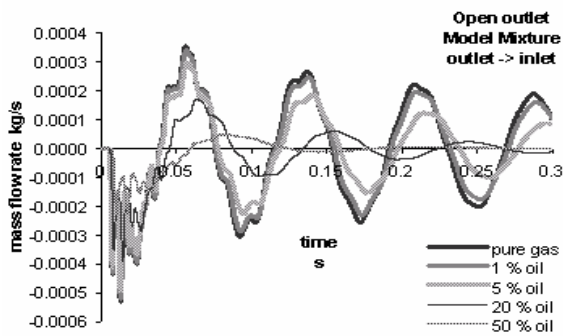


**Figure 5:** The impulse reaction (mass flow rate) on open outlet of oil remover - the excitation on outlet

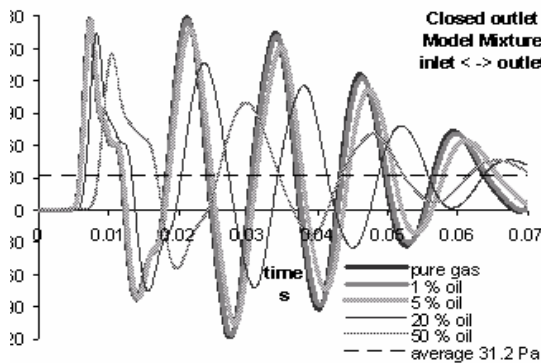


**Figure 6:** The impulse reaction (pressure) on closed outlet of oil remover

They are then used to calculate complex transmittances and four-pole matrix for the oil remover. On the figures 4, 5 and 6 it's clearly visible that the rise of oil contamination reduces the main response frequency. For simulation of closed end oil remover the pressure pulsation curves are mono-harmonic, what simplifies further analysis. In case of open end, the flow tends to form more than one basic harmonics. The calculated transmittances have physical explanation for its parameters. The figure 7 shows four parameters for open-end oil remover pressure-flow transmittance. More substantial analysis of various cases is shown in <sup>2</sup>.

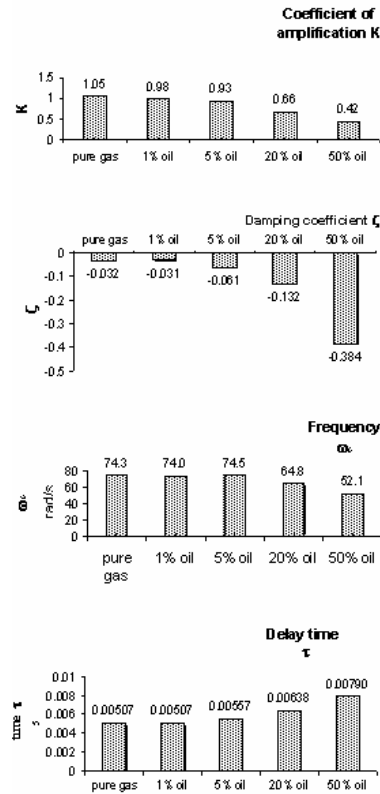


**Figure 7:** The comparison of transmittance parameters for different oil mass fraction for 1-st harmonic frequency

The important conclusion which may be derived is that the significant influence of the oil contamination on the acoustical response of the oil remover occurs close to 20 % of the oil to gas mean flow ratio. For lower values the tendency of changes is visible, but the quantitative difference are small enough to be neglected in the simplified technical analysis.

Generally the changes of transmittance parameter values with the respect to oil mass contamination is proportional to the oil mass fraction in gas. The linear characteristic is very convenient, while it can be used to estimate transmittance parameters for different oil content.

## 5 Experimental validation

The simulated oil remover (Fig. 3) for a refrigerant compressor has been also used to experimental identification. The method of this identification was shown earlier<sup>5</sup>. The oil content in refrigerant was assumed to be about 1% of mass flow rate. The comparison of the experimental results with Classic Helmholtz model and the model described in this paper is shown on the figures 8 and 9. The peak-to-peak amplitudes of pressure pulsations are also compared in Table 2.

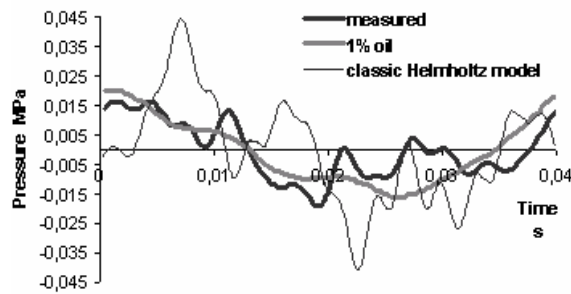


**Figure 8:** Pressure pulsations curves averaged in inlet cross section of oil remover

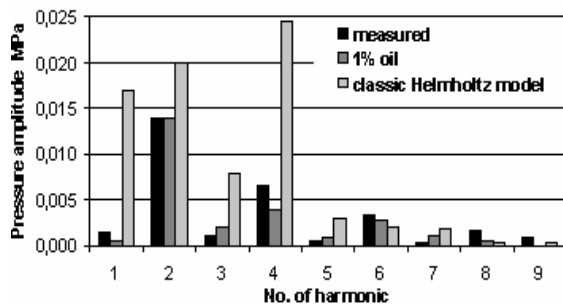


**Figure 9:** Pressure pulsations harmonic analysis averaged in inlet cross section of oil remover

**Table 2:** Peak-to-peak amplitudes comparison

	experiment	1% of oil mass fraction	Helmholtz ideal gas model
$\Delta p_{\max}$ [MPa]	0,035	0,036	0,085
Error [%]	—	2,9%	143,7%

Although there are discrepancies between presented model and experimental results, they are comparable.

The classic Helmholtz method in this case gave unrealistic results. Main cause of this is the oil remover geometry, which in case of 3D CFD simulation is properly modelled, but also oil contamination has its influence. The differences between the present model and experiment may be due to the fact that the oil contamination is not constant. It is higher at the oil remover inlet and lower at its outlet.

## 6 Summary and conclusions

In the paper only small part of numerous simulation results is shown. However on this basis some of important conclusions may be drawn. First, the CFD identification method proved to be a proper tool for the analysis of pressure pulsation

attenuation in the installation element. Second, the oil contamination in the compressed gas may influence the pressure pulsations propagation lowering its frequency response increasing dumping and time delay. The quantitative results have nearly linear dependency on the oil mean fraction. However we may also state that the influence of oil is worth considering for more than 5% of liquid mass fraction.

## References

- <sup>1</sup> LIU Z., SOEDEL W., 1994 International Compressor Engineering Conference at Purdue, West Lafayette, USA: Using a Gas Model to Predict the Supercharging Phenomenon in a Variable Speed Compressor.
- <sup>2</sup> Kantor R., CFD analysis of the influence of oil separator on the steady and pulsating flow in the volumetric compressor installation, PhD thesis, Cracow University of Technology, June 2004 (in polish).
- <sup>3</sup> Cyklis P., Hendla R., Kantor R., The analysis of the orifice flow measurement errors of the refrigerant using CFD simulation, Conference "Chłodnictwo Przemysłowe '2001" Wisła 2001 (in polish).
- <sup>4</sup> CYCLIS P., 2002 International Compressor Engineering Conference at Purdue, West Lafayette, USA: A CFD Based Identification Method of the Transmittances for the Pulsating Gas Installation Element Part I – Theory, Part II – Experimental.
- <sup>5</sup> CYKLIS P., 2001 Journal of Sound and Vibration, 244, 859-870: Experimental Identification of the Transmittance Matrix for any Element of the Pulsating Gas Manifold.

# **Simulation Methods for Piston Compressors**

**by:**

**Prof. Dr.-Ing. S. Pischinger**

**Dipl.-Ing. Th. Steidten**

**Dipl.-Ing. W. Wiese**

**VKA – RWTH Aachen**

**Dr.-Ing. M. Hopp**

**FEV Motorentchnik**

**Aachen**

**Germany**

**4<sup>th</sup> Conference of the EFRC  
June 9<sup>th</sup> / 10<sup>th</sup>, 2005, Antwerp**

## **Abstract:**

Minimizing the energy consumption of compressor units to decrease the operating costs and to protect the environment is a typical engineering task of today's compressor development<sup>1</sup>. A high volumetric efficiency and a compression process with high efficiency are two aspects to fulfill these requirements. To obtain such an optimized compression process a detailed analysis is necessary.

1-D gas exchange and CFD calculations are state of the art in the design product development of an internal combustion engine. These tools can even be used to simulate and to optimize a compressor station.

This paper reports the simulation results of a three stage compressor. It shows how the gas dynamic prediction helps to detect and avoid critical pressure pulsations and the improvement potential of a gas dynamic optimization. Furthermore different mass flow control strategies are implemented in the compressor model. A high efficient speed variation is discussed as well as intake pipe throttling and compression ratio variations with lower performance potential.

## 1 Introduction

Due to the rapidly growing cost pressure in the automotive industry coupled with a strong increase in complexity of the internal combustion engine, the efficiency of the product development processes has to be increased.

One way to implement and to assess complex engine layouts in the concept phase, or to decrease cost intensive test bench measurements, is the simulation of the engine process.

Beside structural calculations the thermodynamical prediction of the engines performance is of high interest especially in the early concept phase. In this context CFD calculations are used to optimize specific parts and to generate boundary conditions for several other development stages. Furthermore the gas exchange calculation helps to simulate and optimize the whole complex system.

Due to the similar design of piston compressors and internal combustion engines, the know-how gained at one application can help to speed up and improve the design process of the other application.

## 2 Base model build up

### 2.1 Gas exchange model build up

For the gas exchange simulations the commercial program GT-Power was used.

The base model for the gas exchange calculations was derived from a six cylinder inline engine. Aim of these modifications was to build up a three stage compressor with a final outlet pressure of 200 bar.

For compressor operation several geometry changes were made. The basic intake manifold was replaced by a new compressor inlet, so that the cylinder 1, 3, 4 and 5 represent the first stage. The second and the third stage are single cylinder stages (second stage: cylinder 2; third stage: cylinder 3). With this stage layout it is possible to implement the cooling devices and the piping easily.

After the cylinders of the first two stages intercoolers were implemented. The heat transfer of these intercoolers was modeled with a so called "Heat conduction object". This sub model allows an interactive calculation of the wall temperature in dependency of an external fluid temperature and a corresponding heat transfer coefficient.

The cylinder head with the positively controlled valves was replaced by a sheet metal and a self operating coupled intake/exhaust reed valve.

At the cylinder (i.e. the working chamber) orifices were attached to simulate the leakage.

For the in-cylinder calculation the general gas option was activated. With this option a sub model based on the theory of Redlich-Kwong is used for the fluid properties calculation during the compression process<sup>2</sup>.

The exhaust system of the engine had to be replaced. After the last stage an ideal pulse damper was implemented. A detailed muffler modeling is possible but is not part of this paper.

Figure 1 shows the layout of the GT-Power model.

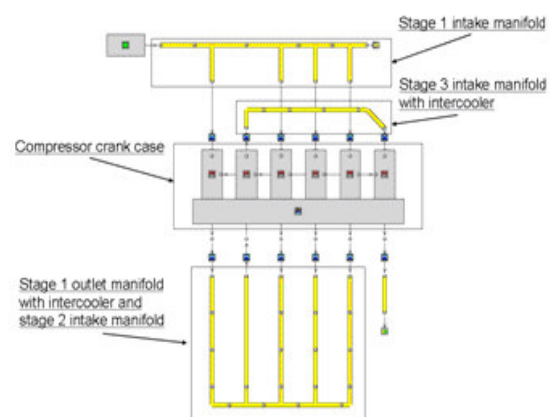


**Figure 1:** GT-Power model of the compressor

### 2.2 Compressor main dimensioning

After the build up of the rough geometries of the compressor the main dimensioning had to be done. To set a constant pressure ratio for the three stages the cylinder swept volume and the compression ratio of the cylinders were adjusted.

To keep the force on the connection rod low the stroke was kept constant in comparison to the internal combustion engine and only the cylinder bore was adjusted. Therefore five parameters (geometrical compression ratio of stage 1, 2 and 3; cylinder bore of stage 2 and 3) had to be specified<sup>3</sup>.

Because of a broad range of possible bore and compression ratio variations, a Design of Experiments (DoE) tool was used to determine suitable values. The final results are:

Bore:

- 1<sup>st</sup> stage: 108 mm
- 2<sup>nd</sup> stage: 93,3 mm
- 3<sup>rd</sup> stage: 67,4 mm

Geometrical compression ratio:

- 1<sup>st</sup> stage: 21,9
- 2<sup>nd</sup> stage: 14
- 3<sup>rd</sup> stage: 5,3

The stroke was kept constant at 130 mm for all cylinders.

These values result in a pressure ratio per stage of about 5,9.

The next dimensioning task was the determination of the valve flow coefficients. For the first calculations data from literature was used. In a second step CFD calculations were made to gain more experience with this kind of valve and to set up and prove a valid flow calculation model for the 1-D simulation.

### 3 CFD investigations

To model gas exchange calculations the important items to know are the flow coefficients of the valves. Therefore a reed valve has been built as a CFD model. CFD calculations offer the possibility to model the detailed three dimensional flow through special parts of interest. It is very useful to get information how to improve parts in terms of flow and heat transfer. So in this case the CFD calculations helped to determine the flow coefficients for the gas exchange calculations.

Due to the fact that the reed valve is symmetric, only one quarter of the valve was modeled in CFD. The mesh of the valve is pictured in Figure 2. The code used for the calculations was the commercial software StarCD version 3.24 from CD-Adapco.

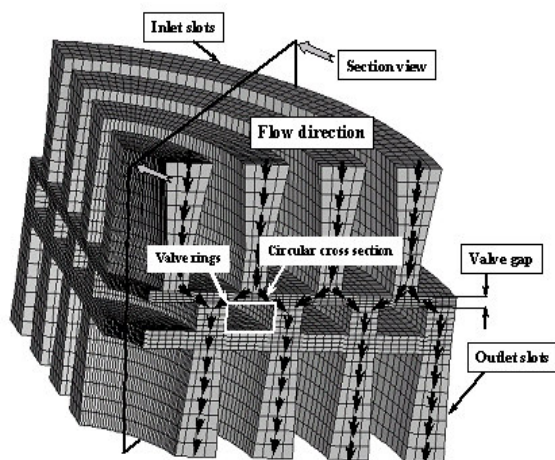


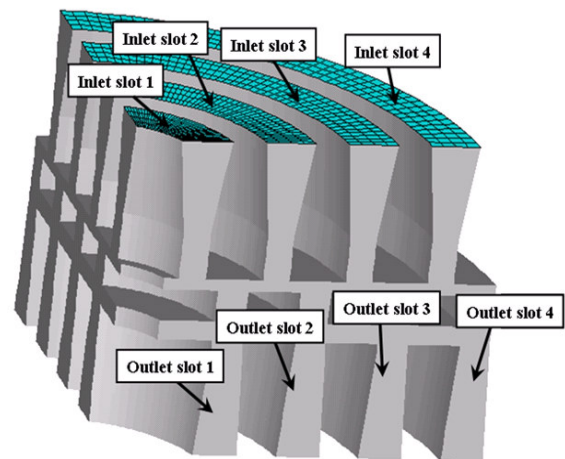
**Figure 2:** CFD model

The boundary condition for the simulation was a steady state flow through the valve with a constant pressure difference over the valve of 50 mbar and

an inlet temperature of 293 K. The walls were chosen to have the same temperature as the inlet temperature, whereas the main focus of the calculations was on the flow and the pressure losses over the valve. The investigated lifts varied from 0,5 mm to 2,5 mm.

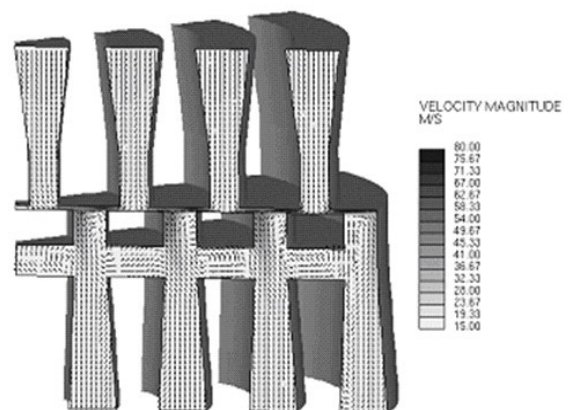
The gas flows through the inlet slots into the valve. Then, by the pressure difference over the valve, the valve rings are moved downwards against the spring force, as it can be seen in Figure 2. Now at the sides of each inlet slot a circular cross section opens and the flow is separated to both sides into the valve gap, as indicated by the arrows in Figure 2. In the outlet slots the flow is then merged together again.

Figure 3 shows the numbering of the inlet and outlet slots.



**Figure 3:** Numbering of slots in the CFD model

In Figure 4 the results for 0,5 mm lift are shown. It is a contour plot for the velocity magnitude plus vectors to indicate the direction of the flow.



**Figure 4:** Flow distribution for 0.5 mm valve lift



For the valve lift of 0,5 mm the velocity of the flow is very slow, about 15 m/s, in almost every zone except for the small valve gap. In the gap the flow is accelerated up to 80 m/s and is afterwards decelerated in the outlet slots down to 15 m/s again.

In the outlet slot 4 a recirculation of the flow is visible. A circulation of the flow can also be seen in the connection zones of the outlet slots below the valve rings.

Figure 5 and Figure 6 show the results for 1,5 mm and 2,5 mm valve lift.

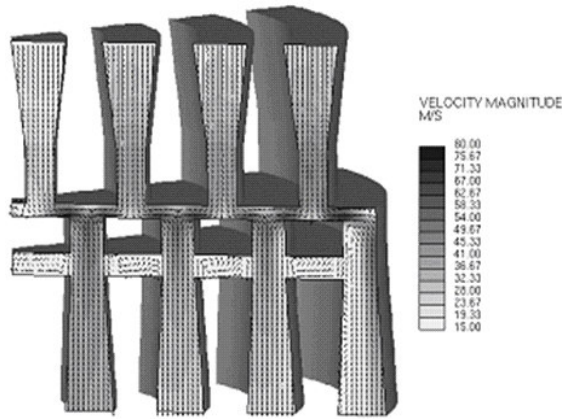


**Figure 5:** Flow distribution for 1.5 mm valve lift

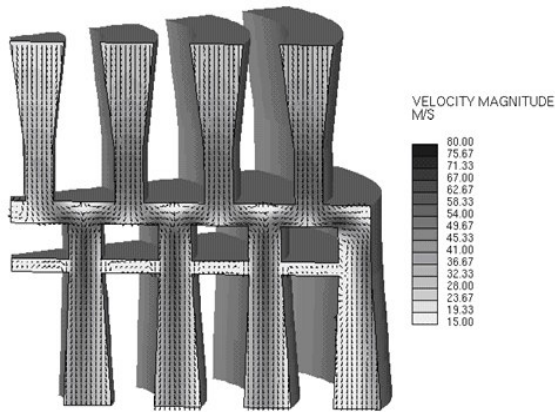


**Figure 6:** Flow distribution for 2.5 mm valve lift

For the 1,5 mm and 2,5 mm valve lift there are still high velocities of about 80 m/s in the valve gap. But now high velocities also occur in the slots. Only outlet slot 4 and inlet slot 1 do not show as high velocities as the others.

For outlet slot 4 the reason for the slower velocities is the recirculation at the inner side. This recirculation is caused by the flow coming only from one inlet slot into outlet slot 4. The flow is separated at the inner side and produces the recirculation.

For inlet slot 1 the reason for the slow velocities compared to the other inlet slots is different. At the other inlet slots the flow is separated to two sides in the valve gap. At inlet slot 1 this is not the case. This causes a higher back pressure and thus slower velocities in inlet slot 1.

In figure 7 the percentage mass flow through each slot can be seen at 1,5 mm valve lift. For the inlet slots the mass flow increases to the outer slots. This is due to the larger cross section of the outer slots.

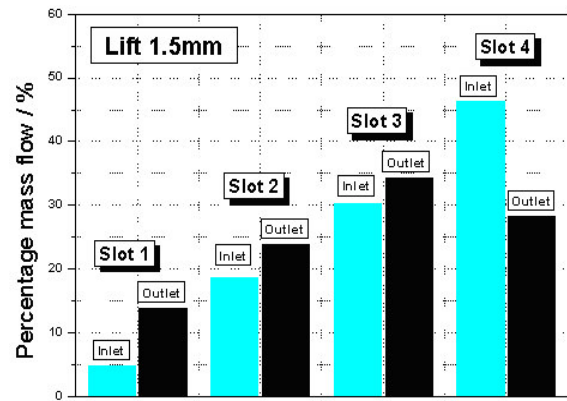


**Figure 7:** Mass flow through slots

For the outlet slots the mass flow increases also to the outer slots, except for outlet slot 4. There the mass flow drops down again to a percentage value of 28 %, even though outlet slot 4 has the largest geometrical cross section. The reason can be found in the recirculation of that slot.

The mass flow depending on the valve lift is the issue of interest for the gas exchange calculations, because it describes the efficiency of the valve. The flow coefficient is defined by the ratio of the isentropic flow cross section  $A_s$  to the valve cross section. The valve cross section  $A_v$  can be any constant reference value. In this case the diameter to calculate the cross section  $A_v$  was chosen to 120 mm, the fitting dimension of the valve.

$$\alpha_v = \frac{A_s}{A_v}$$

The isentropic flow cross section is dependant on the calculated mass flow, the pressure difference over the valve and the inlet temperature, whereas the equation for the isentropic velocity is only valid for subcritical pressure ratios. That was the case here. For overcritical pressure ratios the isentropic velocity depends only on the inlet temperature.

$$\dot{m} = A_s \cdot \rho_s \cdot c_s$$

$$c_s = \sqrt{\frac{2 \cdot \kappa}{\kappa - 1} \cdot R \cdot T_0 \left[ 1 - \left( \frac{p}{p_0} \right)^{\frac{\kappa - 1}{\kappa}} \right]} \quad \rho_s = \rho_0 \cdot \left( \frac{p}{p_0} \right)^{\frac{1}{\kappa}}$$

with:

$\alpha_v$  = flow coefficient  
 $A_s$  = isentropic flow cross section  
 $A_v$  = valve cross section  
 $c_s$  = isentropic velocity  
 $\kappa$  = isentropic exponent  
 $T_0$  = inlet temperature  
 $R$  = gas constant  
 $p$  = outlet pressure  
 $p_0$  = inlet pressure  
 $\rho$  = outlet density  
 $\rho_0$  = inlet density

In Figure 8 the resulting flow coefficients are depicted.

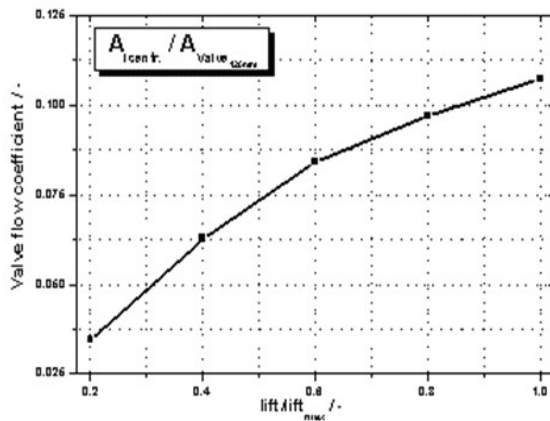


**Figure 8:** CFD results "Flow coefficients"

The flow coefficient increases with a rising lift of the valve. For small lifts the flow coefficient increases almost linearly. Then the slope decreases. The reason can be seen in Figure 9.

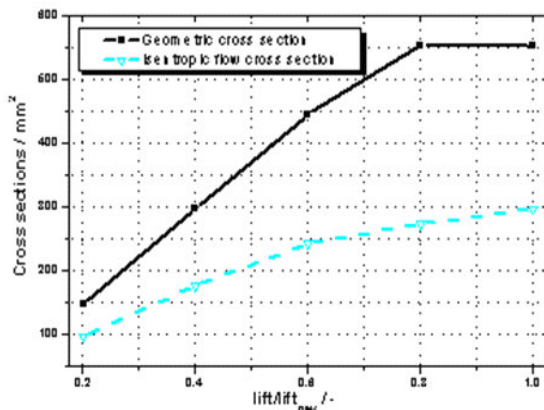


**Figure 9:** Valve cross sections

The geometric cross section and the isentropic cross section are plotted against the lift. The geometric cross section increases with rising lift and keeps constant at the end. Up to 60 % valve lift the limiting cross section is the circular cross section in Figure 2. Then the limiting cross sections are the slots themselves. So the geometric cross section cannot increase anymore, although the lift still increases. This phenomenon results in a decreasing slope of the flow coefficients.

Improvements on the valve and thus on the flow coefficients could be achieved by adding curvatures to the valve geometry, to reduce the redirection of the flow. Furthermore improvements of the flow coefficients could be achieved with a reduction of the losses caused by the merging flow in the valve gap.

## 4 Detailed analysis of the compression process

### 4.1 Pressure losses

The pipe diameters were dimensioned so that no significant pressure losses occur. Due to this restriction the pipe diameter after stage 1 and stage 2 was set to 54 mm. For the base calculation the average maximum velocity in the pipes and the intercoolers is below 10 m/s with this diameter.

The intercooler was modeled as tube bundle heat exchanger with ten identical pipes. This results in a pressure drop over the cooler of max. 30 mbar between the first two stages and of 70 mbar between stage 2 and 3. With this arrangement the heat transfer per stage has to be 10 kW to realize the desired temperature drop of 150 K.

More emphasis should be put on the pressure drop in the reed valves. Figure 10 – Figure 12 show the pressure traces of the intake manifold resp. the inlet pipe of each stage and the working chamber of the cylinder together with the intake valve lift of the corresponding intake valve.

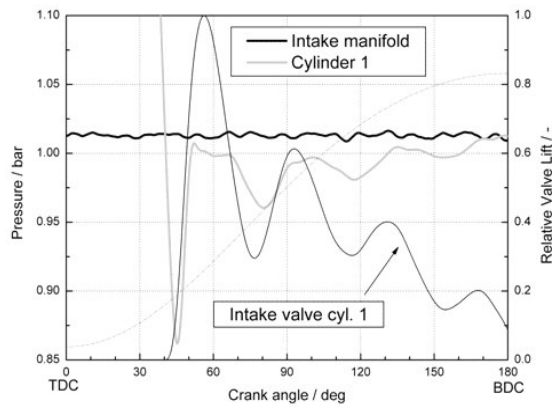


**Figure 10:** Gas dynamic in front of stage 1

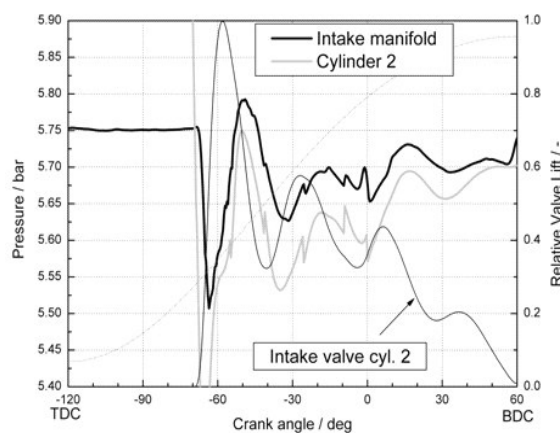


**Figure 11:** Gas dynamic in front of stage 2

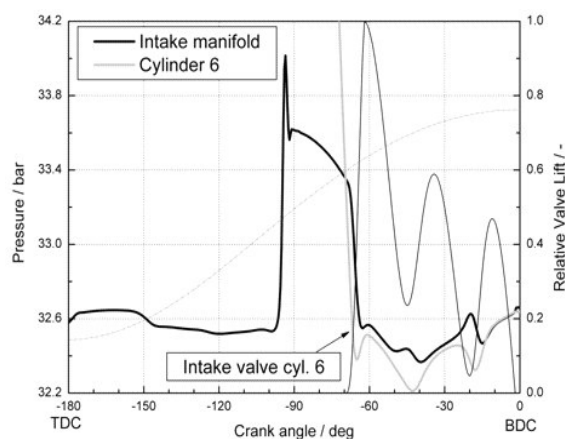


**Figure 12:** Gas dynamic in front of stage 3

At the first stage the pressure before the cylinder is nearly constant. Parallel the in-cylinder pressure drops with increasing working chamber volume until the pressure difference is sufficient to open the valve against the spring force. The intake valve lift can be described by a damped oscillation. The maximum pressure drop is about 50 mbar.

At the second and third stage a pressure drop can be seen, when comparing the pressure in-cylinder with the pressure in the intake manifold. While the maximum pressure loss at stage 2 is about 100 mbar the loss at stage 3 reaches 300 mbar.

## 4.2 Influence and analysis of the gas dynamics

A more detailed look at Figure 12 shows that the gas dynamic has got a significant influence. While the pressure amplitude before stage 1 and 2 does not exceed 300 mbar the amplitude before stage 3 reaches 1,6 bar.

There are several effects which are induced by this pressure pulse. First of all such pressure pulses may damage the intercooler and piping between the stages. Second, this pulse has got an influence on the valve opening and on the NVH behavior.

Figure 13 shows the results of a variation of the pipe length before stage 3. Due to the movement of the piston the cylinder pressure drops until the pressure difference between inlet pipe and working chamber is sufficient to open the inlet valve. This process is supported by a pressure peak coming from the outlet valve of stage 2. For the base calculation this peak reaches the inlet valve 90 °CABDC. When increasing the pipe length between stage 2 and 3 two effects can be seen:

1. Due to the increased volume the pressure peak is slightly decreased (damping effect).
2. Corresponding to the increasing acoustic length of the piping the peak reaches the inlet valve at later crank angles.

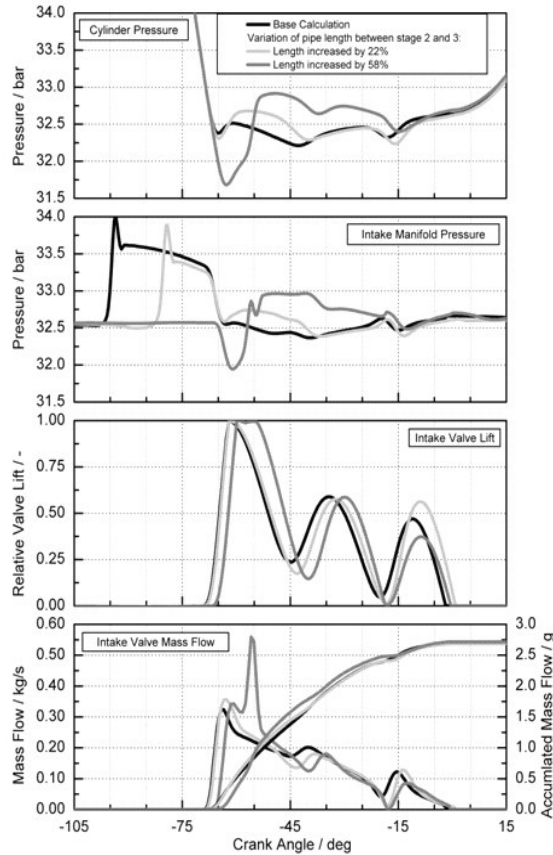


**Figure 13:** Results of pipe length variation between stage 2 and 3 "Gas dynamic"

Figure 14 shows the influence of this variation on the effective volumetric efficiency of stage 3 and on the effective isothermal efficiency of the compressor.

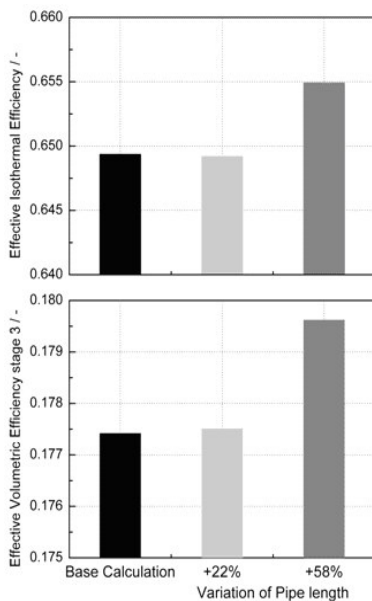


**Figure 14:** Results of pipe length variation between stage 2 and 3 "Performance"

The first increase in pipe length of 22 % does not influence the performance of the compressor significantly. When looking on the pressure traces (Figure 13) it can be seen that the intake valve opening is induced by the high pressure in the intake manifold due to the pressure peak coupled with the in-cylinder pressure and therefore similar to the base calculation.

An increase in pipe length of 58 % on the other hand leads to an increase in the effective volumetric efficiency of stage 3. This can be explained by the pressure traces. In this case the pressure difference which opens the valve is build up by the decreasing cylinder pressure and a constant intake pipe pressure. The pressure peak of cylinder 2 reaches cylinder 3 when the inlet valve is fully opened and therefore does not influence the valve opening. This results in a strong mass flow peak (at the bottom graph of Figure 14) which leads to a higher filling of cylinder 3 and therefore to an increase of 0,5 % in isothermal efficiency and 0,2 % in volumetric efficiency.

## 5 Parameter variations

To investigate the influence of different parameters on the compressor performance several variations were done.

The comparison between the different setups will be done by the inner isothermal efficiency:

$$\eta_{T,e} = \frac{P_T}{P_e}$$

where  $P_T$  is the isothermal power of a one stage compression of an ideal gas and  $P_e$  is the effective shaft power of the compressor. This measure describes the quality of the process in comparison to an ideal process with isothermal change of state. The second measure which will be used is the effective volumetric efficiency:

$$\lambda_e = \frac{V_{1e}}{V_h}$$

where  $V_{1e}$  is the effective conveyed volume and  $V_h$  is the swept volume. This is a measure for the quality of gas exchange and includes flow losses.

Moreover the effective power itself is used for benchmarking the different variations.

### 5.1 Influence of structure temperatures

The heat transfer simulation was done with a sub model based on the theory of Woschni<sup>4</sup>. Herein the walls of the working chamber are separated in three parts: cylinder head, cylinder liner and piston.



In a first step the cylinder liner temperature was varied to simulate different cooling of the compressor block itself. The temperature of the base calculation was 400 K. In this case the head and piston temperatures remain constant (400 K).

The second step was to vary the whole temperature set (head, liner and piston). The results for these variations can be seen in Figure 15 and Figure 16.

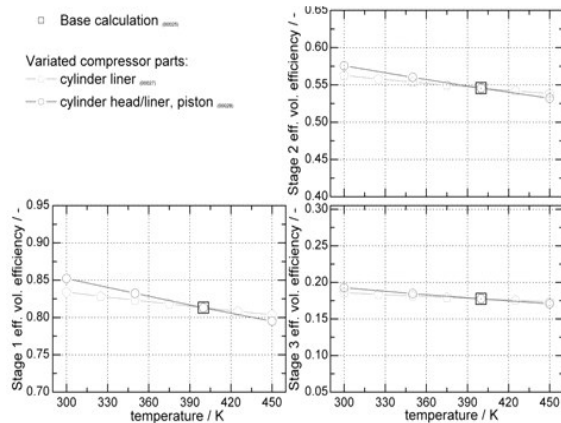


**Figure 15:** Results of temperature variation "Eff. volumetric efficiency"

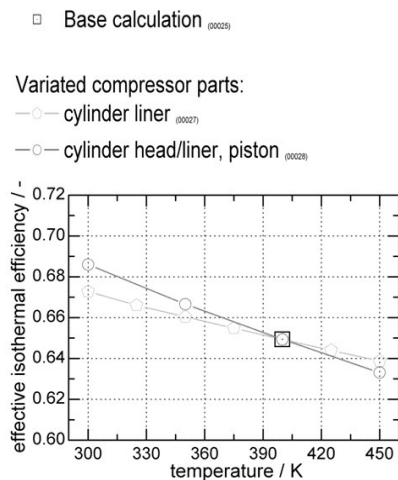


**Figure 16:** Results of temperature variation "Eff. isothermal efficiency"

With an increasing temperature the effective isothermal efficiency drops. One reason for this loss of performance is the smaller cooling effect during the compression process with higher wall temperatures, which results in a higher compression work.

Furthermore the effective volumetric efficiency drops with higher wall temperatures. This can be explained by the heating-up of the incoming fluid during the suction phase with the correlating decrease of the fluid density ("thermal throttling").

The influences with decreasing structure temperatures are vice versa.

When comparing the two steps of temperature variation, it can be seen that the cylinder liner temperature has the dominating influence on the compressor performance. While the effective isothermal efficiency drops 1 % when heating up the liner to 450 K, the decrease when heating up the whole engine block is only 0,6 % higher.

To sum up these results, it can be said that both effective isothermal efficiency and the effective volumetric efficiency of each stage show a linear dependency on the wall temperatures of the working chamber.

## 5.2 Controlling strategy

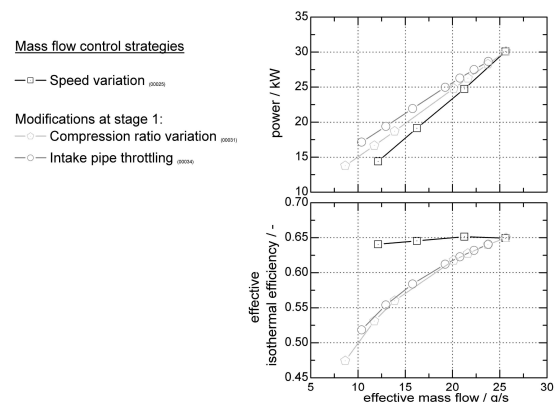
Beside the temperature variation several strategies for the mass flow controlling were investigated.

The easiest way to reduce the mass flow is to throttle the intake pipe. The density before compressor drops and the mass flow is reduced. This variation was done by reducing the ambient inlet pressure for the given compressor. The inlet temperature was kept constant.

Another way of reducing the mass flow is to decrease the compressor speed, which requires a suitable engine.

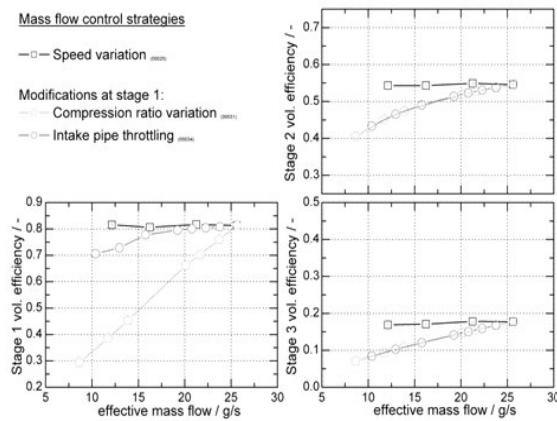
The third kind of mass flow controlling is an activation of dead space or a variation of the geometrical compression ratio<sup>5</sup>.

Figure 17 to Figure 19 show a comparison of these three strategies for the given compressor.



**Figure 17:** Results of the flow control variations „Power and eff. isothermal efficiency “





**Figure 18:** Results of the flow control variations  
„Eff. volumetric efficiency“

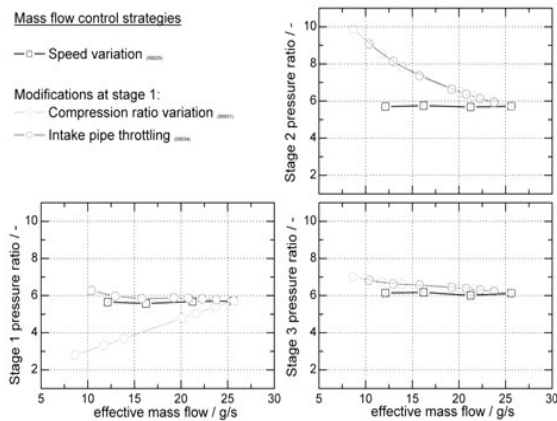


**Figure 19:** Results of the flow control variations  
„Stage pressure ratio“

The comparison shows that the speed variation has got the highest performance, i.e. the lowest power consumption and the best effective isothermal efficiency. With this controlling strategy the effective volumetric efficiency as well as the stage pressure ratio can be kept constant over the mass flow range. Another benefit is the decreasing friction at lower compressor speeds. Comparing this variation to the geometrical compression ratio variation and the intake pipe throttling, a strongly increasing advantage in effective isothermal efficiency towards small mass flows is observed.

The highest power consumption is seen by the control via intake pipe throttling. The low pressure in front of the first stage coupled with the constant outlet pressure of 200 bar leads to a very high effective work. On the other hand the effective isothermal efficiency of the control by intake pipe throttling is higher than with the compression ratio variation. This measure is also influenced by the isothermal work (for an ideal gas), which is growing with higher overall pressure ratios.

Another effect which can be seen in these variations is the shifting of operating points of each stage when changing the boundary conditions. Both geometry and throttling variation decrease the outlet pressure of the first stage, due to the smaller conveyed mass flow. This results in a lower pressure ratio for the first stage, when the inlet pressure is held constant and in a slightly increased pressure ratio when the inlet pressure drops. Due to the constant outlet pressure, this pressure drop has to be compensated by the other stages. Therefore the pressure ratios of stage 2 and 3 increase for both control strategies. A further effect is a decreasing effective volumetric efficiency, which is one reason for the lower effective isothermal efficiency.

## 6 Conclusion and outlook

To keep the operation costs for a compressor station low, a highly efficient compression process is needed. To increase this efficiency of today's well engineered compressors a detailed analysis and a fundamental understanding of the process is necessary.

This paper describes how CAE tools from the development of internal combustion engines can help to increase the efficiency of the optimization process of a piston compressor.

It was shown that CFD calculation can be used to simulate and optimize specific parts such as reed valves of compressors.

Moreover the potential of gas dynamic simulation was shown in this abstract with some examples. By a pipe length variation, using gas dynamical phenomena, an effective isothermal efficiency increase of 0,5 % could be realized. Further more it was shown in which way structure temperatures influence the performance of the given compressor.

In another variation the efficiency with different control strategies was computed and the potential for high efficient operation was pointed out.

It can be stated that modern CAE tools can help to minimize development time and therefore costs by maximizing the performance and efficiency under specific boundary conditions.

In this paper results of a process analysis of a compressor were shown. The tools, especially the gas exchange software, due to the flexible and modular build up of those models, can also be used for the simulation of a full compressed air system. The pipe system of a plant, condensers or consumers can be added to the model to optimize the whole system for steady state and transient

operation. Moreover, these programs can be used to generate compressor station maps for the use in other control or simulation tools.

---

## References

- <sup>1</sup> Fraunhofer ISI: „Compressed air facts“.  
<http://www.druckluft-effizient.de/e/facts/fakten-dl.php> (18.03.2005)
- <sup>2</sup> GT-Power User's Manual Version 6.1, Gamma Technologies, August 2004
- <sup>3</sup> Fröhlich, F.: „Kolbenverdichter – Thermodynamische Grundlagen, Berechnung, Konstruktion und Betriebsverhalten“. Berlin, Göttingen, Heidelberg: Springer Verlag 1961
- <sup>4</sup> Woschni, G.: „A universally applicable equation for the instantaneous heat transfer coefficient in the internal combustion engine“. SAE Transaction Vol. 76, 1967
- <sup>5</sup> Haas, A.: „Kolbenarbeitsmaschinen“. Vorlesungsumdruck, Lehrstuhl für Verbrennungskraftmaschinen, RWTH Aachen 1995



# **Fundamental Research on Tribology of PTFE Wear Parts Opens Windows of Opportunity for Improved Materials**

by:

**Andreas Dittmann, Bernhard Spiegl, Peter Steinrück**

**Research & Development**

**HOERBIGER Ventilwerke GmbH & Co KG**

**Vienna**

**Austria**

**dit@hvw.hoerbiger.com**

**4<sup>th</sup> Conference of the EFRC  
June 9<sup>th</sup> / 10<sup>th</sup>, 2005, Antwerp**

## **Abstract:**

Rings and Packing materials based on Polytetrafluoroethylene (PTFE) compounds have become the standard in the compressor industry, in lubricated compressors as well as in demanding non lube installations.

Despite the comprehensive research on PTFE wear over the last decades, many topics like the fundamental mechanisms of wear, the chemical reactions in the friction area, the load and temperature distribution on micro scale, the transient behaviour of the transfer film, the filler working principles and the interactions of these effects are not yet fully understood.

The investigation of wear probes prepared under controlled conditions (speed, load, gas atmosphere, moisture, counter surface, direction of motion,..) by using most recent analysing techniques (SEM, TEM, IR, TOF-SIMS, Auger,..) permits the insight into the governing mechanisms of wear and influencing parameters. In this paper the fundamental new findings are presented and conclusions for improved materials are drawn.

## 1 Introduction

Rings and Packing materials based on Polytetrafluoroethylene (PTFE) compounds have become the standard in the compressor industry, in lubricated compressors as well as in demanding non-lube installations. The general trend towards oil-free compression in many applications and the boom of PET compressors force the suppliers to continuously improve the materials and to extend the application range of PTFE based materials.

The tribological behaviour of the sealing materials is influenced by a number of factors and a lot of literature has been published in recent years on tribology and wear rate of polymers<sup>1, 2, 3</sup>. Most of it is based on low speed stationary wear tests. However, in general correlation between test results and real life performance is poor.

The target of this work is the investigation of selected polymer-based wear samples that have been prepared under compressor specific wear test conditions (speed, load, gas atmosphere, moisture, counter surface, direction of motion,...). Detailed structure and formation of transfer films and the effect of filler addition were investigated by using most recent analysing techniques. Additionally the underlying physical and chemical effects that form the basis for improved materials in the future have been identified.

## 2 Tribology

### 2.1 Tribology fundamentals

Tribology is defined as the science and technology of interacting surfaces in relative motion (Figure 1) and of related subjects and particles<sup>4</sup>.

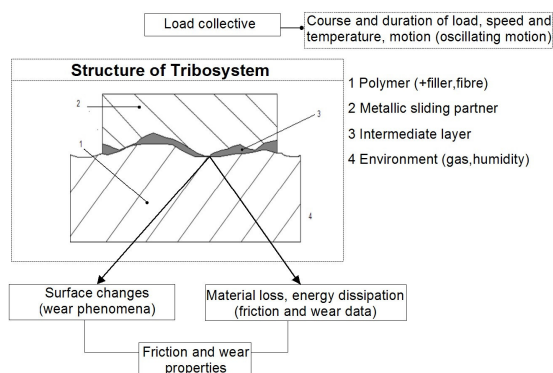


**Figure 1:** Features and parameter groups of a tribological system

Wear is the progressive loss of substance from the operating surface of a body occurring as a result of relative motion of surfaces. The most often used references are running time, covered distance and

number of cycles. Commonly a simple relation (1) between wear  $\Delta l$ , pressure  $p$ , sliding velocity  $v$  and time  $t$  is postulated that defines the so called wear factor  $k^5$

$$k = \frac{\Delta l}{p \cdot v \cdot \Delta t} \quad (1)$$

However, the wear rate may depend on  $p$  and  $v$  in non-linear manner, so that wear factor  $k$  may also depend on  $p$  and  $v$ . This should be taken into account when comparing different tribological systems.

Friction and wear cannot be used as material specific terms as tribology results from the properties of a compound system defined by a complex set of parameters. Thus it is possible that the same material used for a component in one system may show deviating friction and wear rates in another even under the same load conditions.

The practical value of laboratory results is also limited by the strong influence of test conditions on wear results. Figure 2 shows the influence of sliding speed and temperature on specific wear rate  $k$  and friction coefficient  $\mu$ . Thus laboratory conditions must match real conditions within rather close limits.

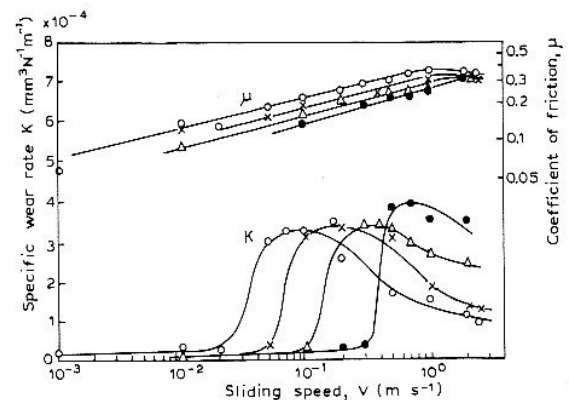


**Figure 2:** Variations in specific wear rate  $K$ , and coefficient of friction  $\mu$ , with sliding speed for PTFE against a glass surface at 23°C (o); 50°C (x); 70°C ( $\Delta$ ); 100°C (●)<sup>6</sup>

In general there are three possibilities for improving a tribological system leading to longer lifetime and higher reliability:

- At first change of process conditions, e.g. elimination of presence of liquids, to attain a changed tribological system and thus other wear mechanisms.
- Secondly changes and improvement in design and reduction of applied load, e.g. to lower the

mechanical load by balanced designs or to decrease temperature by improved cooling means.

- Thirdly changes and improvement of the material.

The first and the second options are design and application specific. The emphasis of this work is put on material issues.

## 2.2 Transfer film

Some polymers used for tribological applications have a special property: the formation of a so called “transfer film”. The particularity of PTFE is that the composite material exhibits excellent wear properties whenever such a polymer film on the counter surface is formed. It has also to be considered that fillers may cause abrasion and thereby disrupt this transfer film. Therefore it is of great importance to study and understand formation of the transfer film, the topology and structure of this boundary layer, its physical/chemical bonding to the counter surface and the transient stage during running time. The comprehensive understanding of the transfer film is the foundation for the development of improved materials.

## 3 Experimental

### 3.1 Material

Although the scope of this work comprises a wide range of PTFE based wear materials, this paper will deal only with one very specific, but characteristic material, which is typically used in wet and dry air applications. The investigated material consists of PTFE filled with 20 wt% modified Polyphenylenesulphide (PPS), a sulphur containing polymer, and 5 wt% of an experimental carbon fibre grade. The blended material grade is characterised by irregular fibre and filler distribution. It has been cold compression moulded and then free sintered.

### 3.2 Wear testing

For many reasons wear tests using field equipment are impractical not to say impossible in an early stage of material development. However, they are a must for the final prove of a new concept or product. Thus a carefully designed test process has been set up: It starts with easily accessible and fast rig testing under well defined and well monitored conditions, leading over to functional testing in a laboratory test compressor, which permits precise control of operating conditions with the disadvantage of long test cycles and thus decreased test productivity, towards final product verification in carefully selected and monitored field trials.

Despite the advantages of using test rigs, several challenges in correlating the results from test rigs to service performance have to be faced and small differences in the test set-up may have significant influence on tribological properties.

Comprehensive studies<sup>7</sup> on different wear test rigs carried out clearly prove a reciprocating wear tester (TE77/S/, Phoenix Tribology, Newbury, UK) working at high frequency to yield good correlation with practical results and thus to be a viable tool for studying material wear (Figure 3).

The sliding link design enables a horizontal, pure sinusoidal, periodic motion (50 mm stroke) of the specimen carrier. The fixed counterface is located on two screw fittings in a stainless steel container, heated by electrical resistance elements and exposed to user selectable various gas atmospheres.

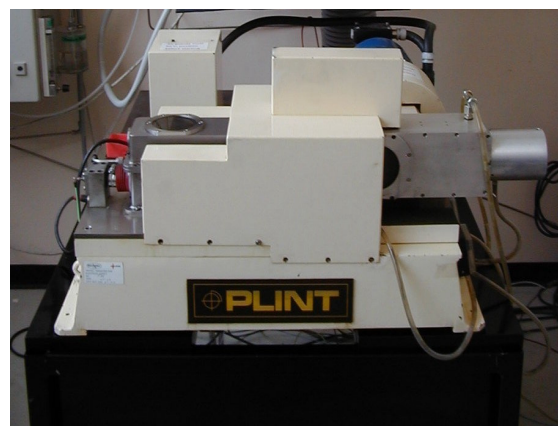


**Figure 3:** Reciprocating wear test rig

### 3.3 Test set-up

The test sample was mounted on the specimen head. Cast iron (CI, grey cast iron from strand casting) with a Brinell hardness HB187.5/2.5 of 220 and a roughness  $R_a$  of  $0.4\text{ }\mu\text{m}$  was used as counterface material. Before testing the counterface material was cleaned ultrasonically in an acetone bath.

Tests were conducted in technical air with a humidity of 1000 ppm. After initially heating up the system to operation temperature ( $120^\circ\text{C}$ ) under low load for about 2 hours, the rig was switched to full speed and full load (20 Hz, contact pressure of 1.6 bar) followed by 48 hours test time. Friction force, wear, temperature and humidity were monitored, allowing continuous monitoring of conditions to stay constant over the test period.



## 4 Investigation findings

After the test the specimen and the counterface were analysed regarding transfer film and related wear phenomena using the methods discussed in the sections below.

### 4.1 Scanning electron microscopy (SEM)

In the SEM a finely focused electron beam scans across the surface of the sample generating secondary electrons, backscattered electrons, and characteristic X-ray radiation that can be directly used for spotted chemical analysis and imaging.

Surprisingly after wear testing the polymer surface showed that the modified PPS filler particles were coated with a bright, back transferred material layer mainly consisting of iron (Figure 4) protecting the polymeric material. The energy dispersive X-ray (EDX) analysis proved the thickness of this layer to be much smaller than 1  $\mu\text{m}$ . In addition the fibre free grade of the same polymer was investigated. On this sample the metallic coating was found to be inhomogeneous and more particle-shaped. So this effect is to a certain extent related to the carbon fibre reinforcement too.

SEM pictures reveal the load carrying mechanism of fibre enforced PTFE material. Since the matrix polymer has a lower modulus than the fibres, the latter carry the largest amount of the contact load. Load transfer between fibres and matrix is facilitated by shear stress along the cylindrical fibre surface and contact pressure at the end surfaces of the fibres.

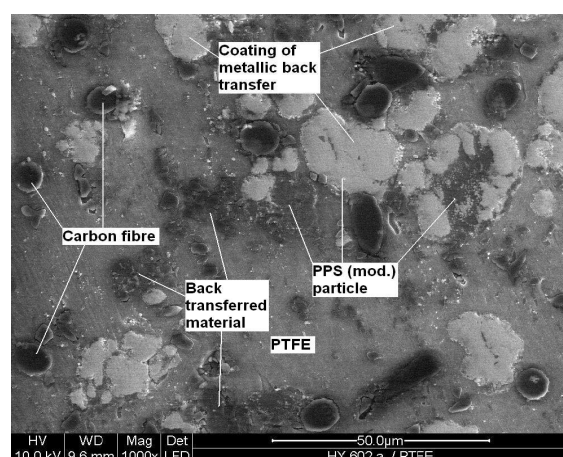


**Figure 4:** SEM picture of the polymer material post wear testing. PTFE is grey, carbon fibres appear black and the modified PPS is covered with a bright iron based back transferred layer. Some of the PTFE is covered with back transferred wear debris (dark grey). Mag. 1000x

The fibre content in the material investigated was rather low. It is, however, the content of filler particles that contributes significantly to load carrying: During wear testing the rather hard filler particles take some of the applied load. They are elastically pressed into the PTFE matrix. So the rather soft PTFE in the areas between the filler particles is almost relieved from load carrying. After removal of the load the elastic deformation of the system recovers and the PPS particles can be found to have a prominence of several  $\mu\text{m}$ . In addition wear debris transferred back onto the specimen, is found on the PTFE. This back transferred layer, consisting of metallic and organic debris might protect the pure PTFE as well.

In Figure 5 the corresponding counterface is shown. It can be deduced that the transfer film on the cast iron is far from being homogenous and of varying thickness (maybe partly even zero thickness). Further the film consists of lumps with rather great thickness and polymer material filling the grooves. This effect was found to be a quite characteristic feature of high-speed reciprocating motion. However, the EDX effect was strongly affected by the subsurface layers and thus it was not possible to identify the elemental composition or presence of small debris and layers thinner than 1  $\mu\text{m}$  on the counterface.

Also the lumps, sheared off due to inter-lamellar shear stress, without softening or melting, might be connected to pits and additionally sharp scales effectively abrading material from the polymer.

Figure 5 indicates that the lumps are very often attached to grooves. Thus the surface roughness might strongly influence the formation of the transfer film, especially its thickness variations.

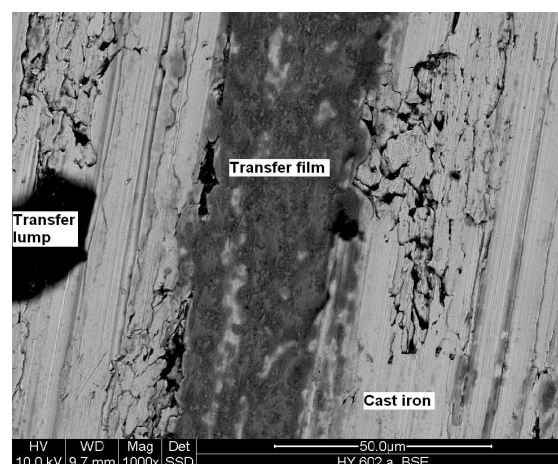


**Figure 5:** SEM picture of the cast iron surface post wear testing. The transfer layer (dark grey) appears to be band shaped, transfer lumps are black. Mag. 1000x

It may be concluded that there is an alternating wear process ongoing:

In the beginning the soft matrix is removed. Next the outstanding fibres (and also hard filler particles) are sheared off or quarried out and the matrix carries most of the load again and hence is removed, thus quickly passing load carrying back to the fibres and filler (Figure 6).

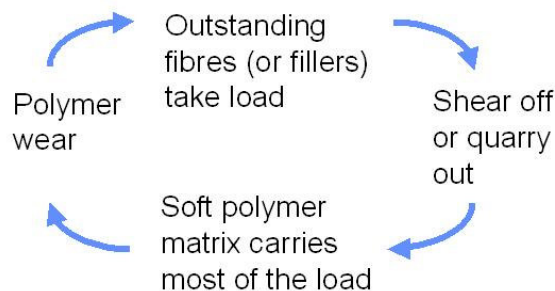


**Figure 6:** The wear mechanism alternates matrix and filler wear due to changing load-supporting mechanisms

A rough estimation of the thickness of the transfer film could be obtained with the aid of an EDX signal. In theory the ratio between the F-signal of the polymer film and that of the Fe-signal of the cast iron can be used for this purpose. Unfortunately the F and the Fe peaks did overlap severely preventing a quantitative analysis of transfer film thickness. However, comparison of several signals clearly showed the presence of a PTFE originated signal. Thus the observed transfer lumps definitely originate from the PTFE matrix of the polymer sample.

It should be noted that a certain amount of carbon could always be detected with EDX even on the pure metallic material. It results from contamination of specimens stored at air. In case of cast iron a carbon signal is also to be expected from the material itself.

## 4.2 Time of flight – Secondary ion mass spectroscopy (TOF-SIMS)

In order to overcome this difficulty TOF-SIMS has been applied. TOS-SIMS is a surface analytical technique that uses a pulsed primary ion beam to desorb and ionise species (secondary ions) from a sample surface that are then detected in a mass spectrometer. This method, which can be used for obtaining elemental and molecular chemical information about surfaces, has been applied to evaluate the transfer film distribution on the counterface.

Findings revealed that all fluorine related signals are not homogenous nor is the transfer film (Figure 7). This is of course contrary to the initial assumption of a homogenous transfer film and might be related to the nature of high speed reciprocating wear tests. Further slight chemical changes, mainly oxidation, of the filler particles could be observed.

In this case, the TOF-SIMS analysis did not work to measure transfer film thickness, for the following reasons: a) it was not equipped with a sufficiently powerful sputtering tool, b) the sputtering effect is material related and c) the available equipment lacked digital image processing.

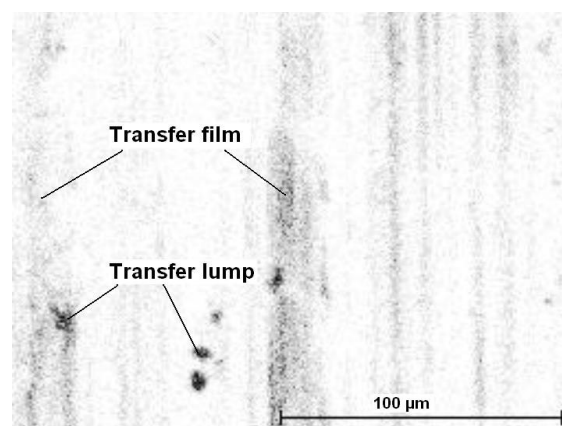


**Figure 7:** TOF-SIMS image of the cast iron specimen. On the surface an inhomogeneous transfer film (dark regions) is visible after wear testing. Mag. 500x

## 4.3 Auger electron spectroscopy (AES)

In a next step AES has been employed to yield the expected answer on transfer film thickness. AES is a surface specific technique utilising the emission of low energy electrons in the Auger process and is a commonly employed surface analytical technique. It was applied to analyse the surface layer of the counterface and to determine the distribution of both polymers in lateral as well as depth direction.

The modified PPS created a very thin surface layer (several nm). The presence of this layer is opposed to the presence of PTFE. Due to sputtering the transfer film on the spot investigated could be confirmed to be at least 100 nm thick (Figure 8).

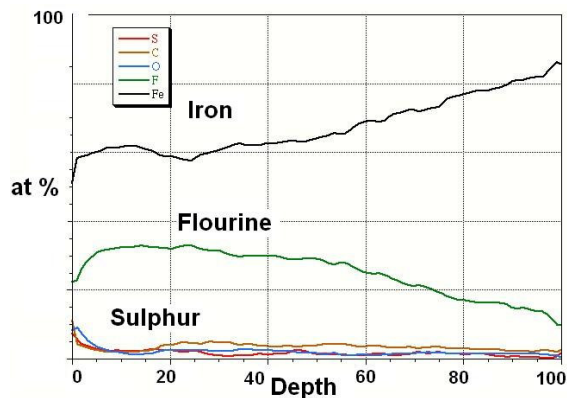


**Figure 8:** Qualitative depth profile of the transfer film formed on the cast iron counterface. The transfer film has a thickness of about 100 nm

The results showed that the PTFE is mainly distributed along grooves and other topographical structures, whereas a more precise attribution to topographical structures was not possible. Also with AES the Fe and the F peak overlapped and so no conclusion regarding the chemical state could be drawn.

## 4.4 Transmission electron microscopy (TEM)

All characterisation methods presented and discussed in the foregoing sections had certain disadvantages. The SEM did not give results regarding lay-up, composition, bonding and chemical state of the transfer layer. Nor did TOF-SIMS and AES. So the application of TEM, which requires a relatively time consuming sample preparation, became inevitable.

The TEM allows to determine the internal structure of materials, materials for TEM must be specially prepared to a thickness, which allow electrons to transmit through the sample. Then the optimal resolution attainable is many orders of magnitude better than any other microscopy.

A thin section (cf. Figure 9) for TEM was prepared by focused ion-beam milling (FIB). The region chosen for the TEM section was covered with a thin Pt-film, which is necessary to protect the sample surface during ion-beam milling and to avoid rounded edges at the specimen surface.

The image of the thin section clearly demonstrates that the transfer film thickness varies in lateral direction.

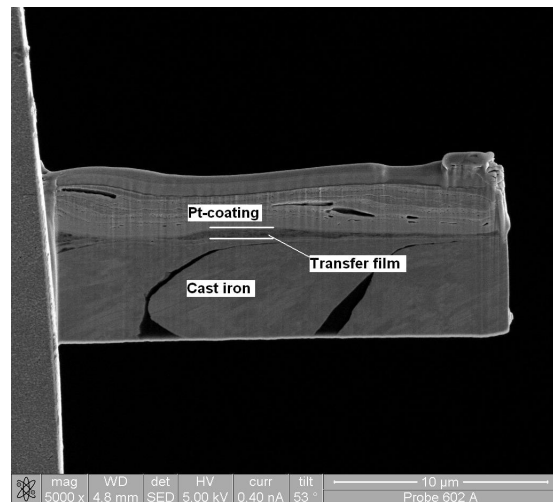


**Figure 9:** TEM lamellae prior to characterisation. The transfer film developed on the cast iron surface was protected with a Pt-layer. Mag. 5000x

The TEM image shown in Figure 10 allows unique tribological insights, demonstrating that the overall transfer layer on the cast iron is not homogenous, but composed of a maximum of the three individual layers with different composition on top of each other. The distribution of single elements was investigated by elemental analysis and it was found that carbon is enriched in the top layer, although not in a homogenous way, but in individual spots. This might be due to fragments from the carbon fibres. The high oxygen concentration found in the intermediate layer originates from iron oxide. Most of the iron seems to be very fine grained, a kind of “nanometer filler” with a high load carrying capacity.

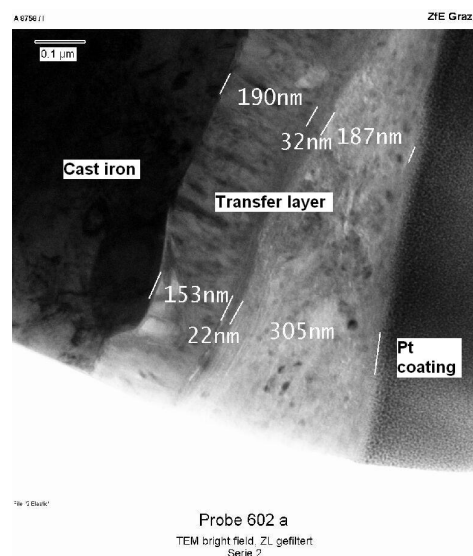


**Figure 10:** Cross-section cut of a transfer film. The transfer layer is not homogenous and consists of several individual layers of different chemical nature. Mag. 150000x



Fluorine is found in approximately the same concentration in both the top and the bottom layer. The sulphur concentration is too low to be seen in the elemental maps but could be detected by Electron Energy Loss Spectroscopy (EELS). This permits the conclusion that fillers in the polymer material and the counterface material also influence the transfer film.

The surface of the cast iron was very smooth over the whole cross section and so the thickness variations of the layer could not be related to the surface topography. Its layered structure and the presence of iron in this layer proves that its formation is also related to abrasion of cast iron and not only a filling cavities.

The missing carbon content in the base layer, i.e. just the presence of iron and fluoride, allows to conclude that the nature of this part of the transfer film differs completely. So the polymer is most likely chemically bonded to the cast iron as metal fluorides form strong adherence. This can be regarded as the basis for the so called “transfer film” that would of course be difficult to destroy. Later several “nanofilled” PTFE layers with a high load carrying capacity emerge that cover as well as protect the metallic base material.

## 4.5 Infrared (IR) investigations

So far the nature of the transfer film found on the counterface has been discussed. To identify any changes of the molecular structure and to trace variations in chemical composition of wear partners infrared spectroscopy (IR) may be used. This method exploits the difference in response to infrared radiation of different polymer materials. ATR (attenuated total reflection) has been used here because sample preparation is simple and the frequency specific attenuation of reflected IR light yields a very useful fingerprint of chemical changes the sample has been exposed to.

In the fibre containing material no evidence for a major material degradation was found. There can be a lot of different reasons. The high thermal conductivity of the carbon fibres conducts the temperature of the flash zone into deeper material layers and on the other hand, the “iron coated” PPS particles might also have a positive influence.

Therefore additionally a fibre free material of the same kind was investigated, as shown in Figure 11. Tribochemical effects, mainly chemical and thermal damage of PTFE, as result of the change in the aspect ratio between several bands, could be identified on a very small level but quantitative evaluations were almost impossible. The content of the modified PPS on the surface (also coming from the material transferred back) seemed to increase

because all material specific bands got stronger. The PPS was pressed into the softer PTFE material and the softer PTFE was removed more easily. Additionally, new infrared bands were found as a result of tribochemically induced material degradation.

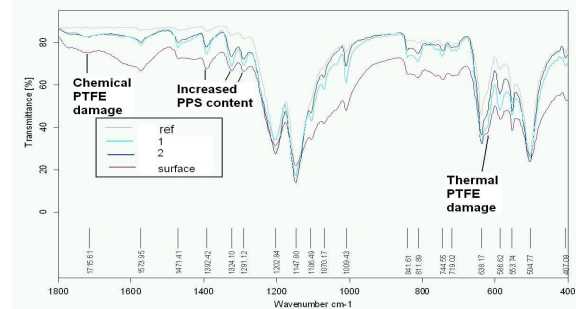


**Figure 11:** IR spectra of polymer surface. The PTFE is damaged thermally and chemically, while the PPS content in surface regions is increased due to the wear process

## 4.6 Tribochemistry

During the wear process new debris particles are generated and milled, thus generating a large surface area. The frictional energy induced increases the temperature level and local temperature peaks (flash temperature) increase the likelihood of chemical reactions. And so a tribological system has the same function as a catalyst.

During friction, especially at elevated temperatures, molecules at polymer surfaces are subjected to mechanical compression, tension and shear, deformed and even broken at different positions in the molecule chains, producing different molecule radicals (cf. IR results). PTFE starts decomposing above 400°C into fragments that can cause several side reactions that also have to be regarded. Highly active radicals could react with unbroken chains, giving rise to a series of new chain breakage events (Figure 12), and could also produce new polymer molecules together with other radicals.

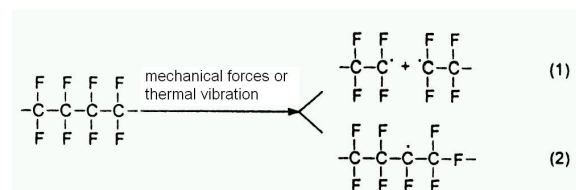


**Figure 12:** PTFE chain break mechanism

In dry friction of polymers/metals other substances might also take part in reactions on friction surfaces, for example oxygen, humidity, metal oxides on the counterface or in the composite, and

so may fresh metal surfaces formed after the wear of metal surface oxides.

SEM pictures show that the surface of the cast iron counterface is partly oxidised. The activation energy for oxidation is rather high (54 kJ/mol) but under tribochemical conditions it may shrink significantly (0.7 kJ/mol)<sup>8</sup>. This example demonstrates how difficult it is to argue on the likelihood and extent of tribochemical reactions.

Under the action of external forces, the chain breakdown could take place at the  $-C-C-$  or  $-C-F-$  bond. The PTFE molecule fragments containing radicals could give rise to a series of chain reactions, as stated above. F-ions generated from later breakdown react with metal oxide or fresh metal surface to form metal fluorides (TEM results) as shown in Figure 13.

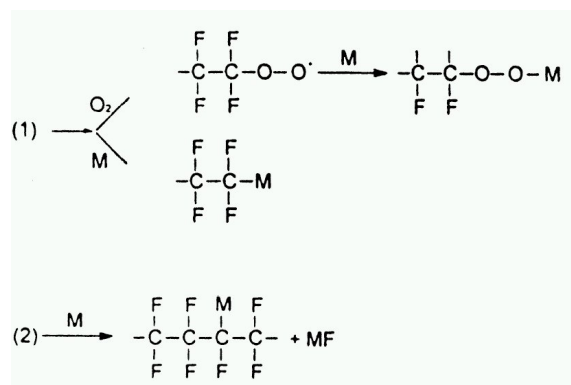


**Figure 13:** Broken PTFE chains either react with oxygen and metals or directly with the metal linking the polymer chain to the sliding partner or form metal fluorides

## 5 Conclusions and Outlook

Despite the comprehensive research on PTFE wear over the last decades, many topics like the fundamental mechanisms of wear, the chemical reactions in the friction area, the transient behaviour of the transfer film, the filler working principles and the interactions of these effects are not yet fully understood. Thus an intensive fundamental investigation on rings and packings wear probes became necessary and was initiated.

SEM was found to give valuable results in the beginning of the investigation. By careful selection of most modern analysis techniques like AES or TOF-SIMS additional transfer film related information could be gained. Finally TEM revealed groundbreaking results concerning bonding, lay-up and composition of the transfer film. The IR was found to be useful to support tribochemical considerations and previous findings.

Starting from the initial tribological system - filled PTFE sliding against a metallic counterface - some of the polymer is carried over to the metallic sliding partner. This polymer is most likely chemically bonded as metal fluorides form strong adherence. This can be regarded as the basis for the so called “transfer film”, which would of course be difficult to destroy. Later several “nanofilled” PTFE layers with a high load carrying capacity emerge covering and protecting the metallic base material.

Simultaneously uncovered metallic areas are oxidised from rather soft cast iron to harder iron oxide. At the same time milled metallic debris is transferred back to the polymer counterpart covering the hard elastic components, mainly the modified PPS filler, protecting the material from severe wear.

This allows to conclude that the material requires a load-supporting component with a very high thermal stability. The kind, size and shape of filler selected should have an optimum bonding to the PTFE matrix to minimize particle breakout and to be effective in reducing wear in dry sliding conditions where adhesion transfer and fatigue is involved. The filler selection, composition and distribution has always to be an application specific (counterface material, gas type, humidity, temperature) process.

Similar transfer films with different functionality especially in bone dry applications were found for non-PTFE based materials. These materials also exhibit excellent wear properties.

The identification of material and fibre/filler functions as presented in this work was found to be most promising approach so far. However, plenty of work has still to be done with regards to the creation of comprehensive wear models and ultimate design guidelines for improved material behaviour.

## 6 Acknowledgements

This project was sponsored by the Austrian Industrial Research Promotion Fund (FFF). Any support by various scientists at Graz University of Technology, WFT Research Traun, Vienna University of Technology and University of Leoben is grateful acknowledged.

## References

- <sup>1</sup> Friedrich, K. (1986). “Friction and wear of polymer composites”, Elsevier, Amsterdam.



---

<sup>2</sup> Uetz, H., Wiedemeyer, J. (1984). Tribologie der Polymere, Hanser, München.

<sup>3</sup> Arkles, B. (1974). Adv. in polymer friction and wear (Lee, ed.), 33, New York, London, 1974.

<sup>4</sup> Czichos, H. (2002). In „Tribologie der Polymere“, Hanser, München.

<sup>5</sup> Kriegl, G. (1978). „Beitrag zur Berechnung des Radialverschleißes von Trockenlaufkolbenringen“, Dissertation, Technische Universität Dresden, D.

<sup>6</sup> Tanaka, K. (1986). In „Friction and wear of polymer composites“, (Friedrich, K., ed.), S.137ff, Elsevier, Amsterdam.

<sup>7</sup> Dittmann, A. (2003). „Wear failure characterisation of polymer based materials for use in reciprocating compressors by conventional and novel test methods“, Master thesis, Institute of Materials Science and Testing of Plastics, Montanuniversität Leoben, A.

<sup>8</sup> Heinicke, G. (1984). Tribochemistry, Hanser, München.



# **Free Floating Piston<sup>TM</sup> Case History of Revamp of Existing Compressors**

by:

**Lau G.M. Koop**  
**Technology Department**  
**Thomassen Compression Systems**  
**Rheden**  
**The Netherlands**  
**tcs@thomassen.com**

**4<sup>th</sup> Conference of the EFRC**  
**June 9<sup>th</sup> / 10<sup>th</sup>, 2005, Antwerp**

## **Abstract:**

Reciprocating compressors for refinery and oil- and gas services are expected, in the API 618 Standard, to operate for 24000 hours without maintenance. This expected uninterrupted running time will only seldom be met, and most of the time only by compressors provided with cylinder lubrication. A few major wearing parts are responsible for the stops that decrease the availability, namely the valves, stuffing boxes and piston/rider ring assembly. Cylinder and stuffing box lubrication generally improves the life time of the piston/rider rings and the stuffing box, however lubricating oil has an adverse effect on the life of the valves. Sometimes the process permits no oil contamination, the lubricating oil is used only once and is relatively expensive, environmental requirements make the removal of drain oil expensive. Lubricators require maintenance and must be regularly filled. All reasons to aim for non lubricated cylinders.

This paper describes the retrofit of reciprocating compressors at two BP refineries with free-floating pistons in an attempt to eliminate the ring wear and so extend maintenance intervals to a minimum of three years.

## 1 Introduction

The presentation of the Maintenance Fair Prize in Rotterdam in 2001, where BP Chembel received the award for there plant process, and Thomassen received a maintenance innovation award for the Free Floating Piston™, was the occasion for BP to contact Thomassen, to explore the possibility of considerably increasing the reliability of one of their compressors. The objective of a revamp was to decrease the down time of the compressor. In particular the unpredictable wear of the rider rings made the continuity of the compressor operation and therewith the process, very uncertain.

The first item is in the chemical plant of BP Chembel in Geel, Belgium. It is a 3-stage, 4-cylinder compressor in Nitrogen duty. It is in operation since 1995. The process gas contains aggressive substances. The compressor in question was not constructed by Thomassen. There is no spare or standby compressor. The compressor cylinders are not lubricated, the process permits absolutely no oil. Specific details are shown in table 1.

The second item is a compressor in the BP refinery in Gelsenkirchen Germany, the former VEBA Oel refinery. This user wanted to increase the reliability of their Methane/Hydrogen compressor. It is a two-stage two cylinder compressor. Again there is no spare compressor. The cylinders at not lubricated. The compressor is not constructed by Thomassen. Specific details are shown in table 2.

The life time of the rider rings was absolutely unpredictable. The maintenance departments tried out a large number of design and material modifications, including changes of the number of rider rings per piston, pressure equalization grooves and the introduction of a tail rod. Thomassen reliability engineering could persuade the maintenance management to retrofit the compressor with Free Floating Pistons. The convincing argument for the investment was the increased reliability and by that the saving on maintenance cost.

This paper briefly describes the design, installation and the operating experiences including the problems encountered, of the revamp of FFP™ in the subject compressors. It is explained that communication between the compressor user and the designer is of major importance for each party to be successful.

## 2 Case history BP Chembel

### 2.1 Wear of the existing rider rings

The life time of the rider rings on the originally supplied piston design, was very short. It varied between 3 days and 3 month's, depending on the brand of the material. The liner is made of Ni-resist material, due to the corrosivity of the gas. The running and wear properties of this material in combination with a non lubricated cylinder is questionable, and by that unpredictable. The API requirements for non lubricated cylinders requires a low surface pressure of the rider rings on the liner, and therewith a large width. As a result of this, three rider rings were selected. The relatively high discharge temperatures, the short stroke and the large total width of the rider rings, resulting in rider band masking of the bearing section, the temperature of the contact area between liner and rider rings, rose to high values. This is a major reason for rapid wear.

Inspection of a 1<sup>st</sup> stage cylinder liner showed a severe deviation of the roundness unevenly distributed along the length of the liner. In fact locally, the bore became smaller than the nominal design value. It appeared that this was caused by the uneven local heating of the Ni-resist liner. The heat transfer from the liner to the cylinder wall is limited by the low transfer coefficient and the local space between the liner and the cylinder.

### 2.2 Customer Requirements

The aggressive components in the gas dictate special demands to the material of the piston, piston rod, liner and cylinder. As the client already had gone through several corrosive problems and failures, they requested special expertise in selecting and application of the material of the piston and rod.

After discussions concerning the proposed materials, Thomassen received the order for the revamp of the compressor cylinders.

#### Materials:

Piston rod	17-4 PH and HVOF special anti-corrosive coating Rod-end at piston side, silver plated.
Liner	Ni- resist
Piston	Cast Stainless Steel X5CrNiMo 13-4

The use of free-floating pistons was proposed and accepted by the refinery as a means to reduce or eliminate the piston/rider ring wear.

## 2.3 The operating conditions

There are two gas duties specified, and three part load operating cases. There is a 75%, 50%, and 25 % load case, achieved by suction valve depressors.

**Table 1:** Gas and compressor data Nitrogen compressor BP Chembel

Nitrogen compressor BP Chembel			
Operating conditions	Stage 1	Stage 2	Stage 3
Nr of cylinders	2	1	1
Duty: PTA			
Suction pressure (bara)	0.85	2.75	7.39
Discharge pressure (bara)	3.49	8.56	15.53
Suction temperature	23	40	40
Discharge temperature	169	156	111
Duty: PIA			
Suction pressure (bara)	0.99	3.023	7.65
Discharge pressure (bara)	3.23	7.86	13.9
Suction temperature	23	40	40
Discharge temperature	179	154	103
Compressor Data	Stage 1	Stage 2	Stage 3
Bore [mm]	560	430	260
Stroke [mm]	160		
Speed [RPM]	590		
Year of installation	1995		
Year of revamp	2002		
Gas Data			
Nitrogen	94 %		
Carbon Dioxide	2.5 %		
Water	3.3 %		
Carbon Monoxide	0.3 %		
Benzene	58 mg/Nm <sup>3</sup>		
Toluene	4.1 mg/Nm <sup>3</sup>		
Xylene	1.6 mg/Nm <sup>3</sup>		
Methyl Acetate	510 mg/Nm <sup>3</sup>		
Methyl Bromide	250-800 mg/Nm <sup>3</sup>		
Acetic Acid	250-3000 mg/Nm <sup>3</sup>		
Molecular weight	28.9		

## 2.4 Changes on the design

- The clearance of the liner in the cylinder of a 1<sup>st</sup> stage cylinder appeared to be too small. The liner was not free to expand. The cylinder was

transported to Thomassen. The clearance was changed without removing the liner. The diameter was corrected by increasing the bore with 1 mm. The piston diameter remained the original value. The 2<sup>nd</sup> stage liner was replaced by a new one.

- Originally the 1<sup>st</sup> stage piston was provided with a tailrod to carry part of the load of the piston weight. This rod end has already been removed already in an earlier stage.
- The piston rod design deviates considerably from the Thomassen design. Piston rods of revised design were supplied. At the crosshead side they are in accordance to the original manufacturers design, the piston side is in accordance with the Thomassen hydraulic fit design.
- Each stage is provided with a Free Floating Piston™. It consists of three sections. The centre part can be replaced for repair or maintenance. A spare section can be held in stock. The non-return valves are mounted in Headend side or Crankend side depending on the side which is always in operation during partial load.
- The FFP's are provided with two rider rings. The total width is such that the API surface pressure requirement for non lubricated condition is not exceeded, even though they do not actually bear on the liner.
- The number of piston rings for the 1<sup>st</sup> and 2<sup>nd</sup> stage has been increased from 3 to 4.

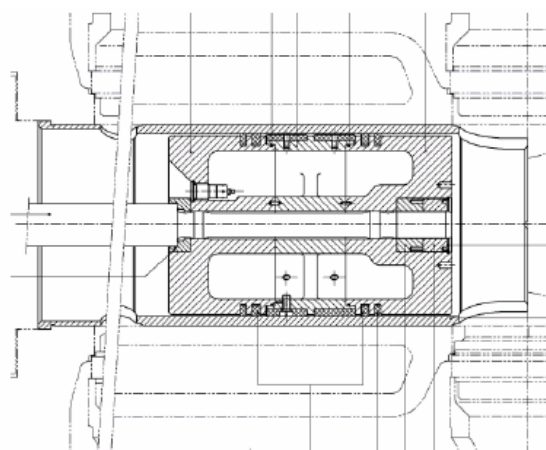


**Figure 1:** Free Floating Piston in cylinder

## 2.5 Operation of the retrofitted pistons

In December 2002 the compressor was put into operation, with new parts installed. High discharge temperatures and vibrations were encountered. As at first instance the correct action of the FFP™ was



suspected, pressure measurements in the cylinders were performed. Discharge valves lift height appeared to be low. The excessive temperatures that were encountered, (>180 C) led to some damage on the rider rings.

The wear of the rider rings can be measured by measuring the gap between liner and piston. The gap was not significantly changed compared to the newly installed value. So it was decided to replace the discharge valves, and to continue the start-up procedure of the process. Pressures and temperatures were thereafter as expected.

The compressor is provided with a rod drop monitoring system. The operating conditions and the rod drop were monitored and supplied to Thomassen for analysis. The line representing the rod drop showed some decay during the first three month's of operation. The machine was stopped and opened for inspection. It appeared that some wear already has occurred. Especially the rider rings of the 1<sup>st</sup> stage pistons showed signs of severe overheating. Analysis of the operating data showed that the stage differential pressures were below the specified values. This was the result of the partial load operating condition, and plant throughput. During operation on 75% load the discharge temperature of the unloaded cylinder was high, and the differential pressure in the cylinder is lower than the absolute minimum which is required for the FFP™ to maintain a sufficient lifting force. After discussion with BP it was decided to delete this case.

Thomassen adapted the design of the 1<sup>st</sup> stage FFP™ in such a way that it is suitable for lower differential pressures. The 1<sup>st</sup> stage rider rings and piston rings were replaced.

To avoid the critical process conditions for the FFP™, differential pressure alarms have been implemented.

After the start-up occurrences, the compressor is now in operation for more than two years.

The contract basis was no cure/no pay with a bonus after two years of uninterrupted operation. BP has granted Thomassen with the bonus.



**Figure 2:** Photograph of the 1<sup>st</sup> stage FFP™, showing rider rings with grooves and nozzles, and the non return valve

## 3 Case history BP Gelsenkirchen

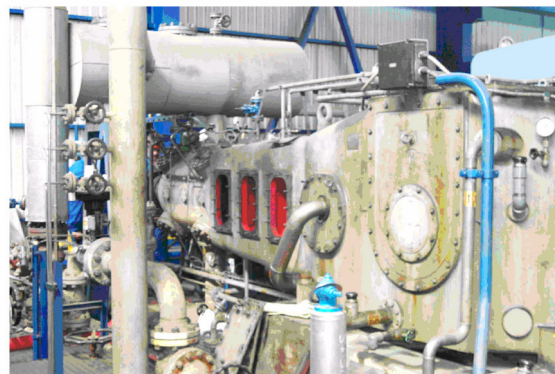


**Figure 3:** GB-220 compressor in Gelsenkirchen

The 2<sup>nd</sup> example of another compressor is installed at BP Gelsenkirchen, Germany. This compressor is part of a hydrogen plant. It is a two-stage two-cylinder compressor. For the compressor data and operating conditions, see table 4.

The gas is not corrosive, but does contain a relative large amount of catalyst dust. This was the major reason that the machine has not been provided with cylinder lubrication. Dust and oil would lead to the formation an abrasive sludge which would deposit on the valves and the piston.

The compressor operates with a side stream between the 1<sup>st</sup> and 2<sup>nd</sup> stage. The side stream extracts gas to approximately 50% of the maximum flow. The capacity of each stage is controlled separately by means of the Hoerbiger "Staudruck regelung".

### 3.1 Wear of the rider rings

The machine has been in operation since 1983. The maximum uninterrupted operating time varied with the brand of rider rings. Changes have been made to the piston and rider ring design. Experiments with materials of several suppliers has been performed. BP has built a test rig on which materials under the process gas and dust conditions could be tested. Finally the maximum operation time ever achieved was 4500 hours, but remained totally unpredictable. Sometimes the replacement of identical rider rings lasted for only 1000 hours. Extensive damage on the liner and piston once occurred after unexpected fast wear of the rider rings. (see figure 4.)

Thomassen was requested to investigate the possibilities for the reduction of the down time of this compressor.



**Figure 4:** Photographs of the damage on the liner after mechanical contact

**Table 2:** Gas and compressor data Hydrogen/Methane compressor BP Gelsenkirchen

BP Gelsenkirchen Hydrogen/Methane compressor		
Compressor data	Stage 1	Stage 2
Bore [mm]	680	400
Stroke [mm]	325	
Speed [RPM]	367	
Year of installation	1982	
Year of revamp	2003	
Process data		
Suction pressure	3.5	10.3
Discharge pressure	10.6	31
Suction temperature	40	40
Discharge temperature	126	133

Gas data	
Hydrogen	20.4 %
Methane	66.1 %
Mixture of hydrocarbons up to pentane	13.5 %
Molecular Weight	16.51

## 3.2 Customer requirements

The new Free Floating Pistons™ were to fit on the existing piston rods, the reinstallation of the existing piston must be possible at any time. The new pistons had to be fabricated from steel.

## 3.3 Site survey

Site survey was done prior to the design of the FFP's. The wear of the rider rings is clearly shown. The wear pattern of the rider rings is not equally

divided over the width of the ring. The rings show signs of overheating. During inspection, it appeared that the 2<sup>nd</sup> stage Ni-resist liner showed the same deformation pattern as the liner at BP Chembel. As the capacity control system is separate for both stages, the pressure ratio of the 2<sup>nd</sup> stage could rise to high values, which caused high discharge temperatures. The side stream extraction between the 1<sup>st</sup> and 2<sup>nd</sup> stage could induce this.



**Figure 5:** Photographs showing the wear pattern of the rider rings.

## 3.4 Design

The replacement pistons had to be suitable for the existing piston rods, as well as suitable for the FFP™ gas bearing concept. The 1<sup>st</sup> stage piston is constructed in three sections, the 2<sup>nd</sup> stage in four sections. The centre part can be replaced by a spare section. The sections are clamped together by means of tie rods. (see figures 6 and 7).

As the process did not require the corrosive resistant properties for the material, the 2nd stage liner was replaced by a standard Cast Iron one. The 1<sup>st</sup> stage liner was still in good condition.

To fulfill the formal API 618 requirements for maximum allowable surface pressure, while, strictly speaking not applicable with an FFP™ design, the 2<sup>nd</sup> stage piston was provided with four rider bands, of which the two outer ones were "FFP™" rings. The inner ones were installed on the piston identical to the two outer ones, only not provided with nozzles and grooves.

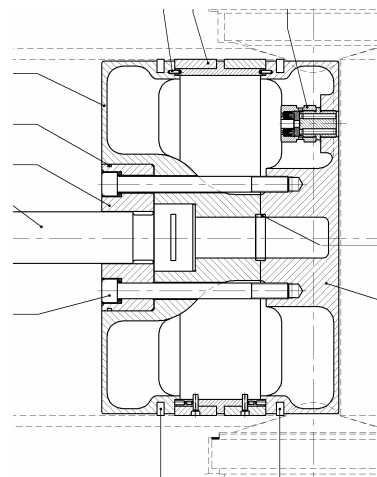


**Figure 6:** 1<sup>st</sup> stage FFP™

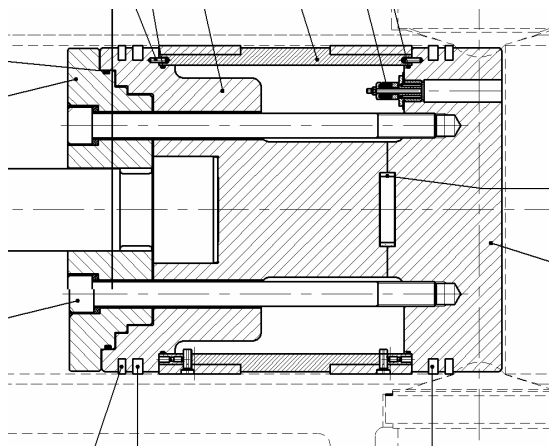


**Figure 7:** 2<sup>nd</sup> stage FFP™

### 3.5 Operation

After installation the compressor was running app. 10 days when high discharge temperatures were encountered. The machine was stopped and inspected. The rider rings were heavily damaged. The pistons were shipped back.

The piston assembly appeared to be leaking in such a way that the proper working of the gas bearing was disturbed. After discussion with BP it also appeared that the capacity of the 1<sup>st</sup> stage was almost completely extracted by the side stream, and that consequentially the 2<sup>nd</sup> stage was operating at very low load. Overheating occurred and consequentially the rider rings were damaged. (see figure 8).

The design of the piston had been changed to alleviate this problem, and in addition, more compensation for thermal expansion was created on the rider ring assembly.

The two center rings of the 2<sup>nd</sup> stage have been removed. The stability of the bearing proved to be negatively influenced by rings not having a gas bearing. BP has adjusted the process to overcome the problem of too much extraction of gas between the 1<sup>st</sup> and 2<sup>nd</sup> stage.

After reinstallation and restart, the stuffing box temperature appeared to rise to high values. At first instance this was expected to be caused by the running properties of the FFP's™. Since the only part that was changed were the pistons. After evaluation with all party's involved showed it turned out however that the sealing elements of the stuffing box had also been changed and that the origin of the high temperatures was not FFP™ related, but that the clearance of the stuffing box sealing elements had been marginal.

The compressor has been put into operation in February 2003, and has run continuously since. The piston rings have been checked once and showed almost no signs of wear.

The rod drop monitoring system shows a very stable characteristic. The reading of the rod drop

monitoring system has taught us that when the FFP's are not working well or when normal pistons are in use, the signal shows high scatter during operation.



**Figure 8:** damaged rider rings 1st stage

### 4 Conclusions

- Dry running compressors are common practice in chemical plants. In refinery and the oil and gas applications the majority of the compressor cylinders is lubricated. Besides from the major advantage of lubrication, that is the reliability of the piston rings, rider rings and stuffing boxes, the disadvantages are numerous. Especially in the case where dust comes with the process gas, the oil-dust mixture forms an abrasive sludge which affects the reliable operation of the valve. More and more processes no longer permit any contamination of the gas by lubricating oil. At present many situations are being evaluated for a potential changeover to non-lubricated duties. Increased wear rates as a result of a changeover however, require fundamental solutions.
- Altering the design of an existing compressor requires intensive study, sometimes reverse engineering of the compressor, good communication and information transfer with the user. Experience is, that machines that are already in operation for a longer period of time.



- always manage to show some surprises. Operating conditions and operating philosophy must be discussed and recorded. Operating conditions which are obvious for the user, can have far reaching consequences, especially if not suitably defined, for the compressor designer.
- In the case of BP Gelsenkirchen, savings of 70000-80000 Euro on working hours and parts are reached per stop, by the deletion of repair and maintenance intervals after the application of the FFP's. This is hardly to be termed as a trivial improvement.
- The FFP™ rider rings need not to meet the API 618 requirements on the surface pressure for non lubricated cylinders.
- Doubts or skepticism about the reliability of FFP™ in dusty environment has been taken away.
- The barrier for the application of non lubricated cylinders, regarding the unpredictable wear, is taken away by the application of FFP™.

## 5 Acknowledgement

- The maintenance department of BP Chembel, Geel Belgium. Mr. E. van der Look and Mr. A. Nevelsteen
- The maintenance department of BP Gelsenkirchen, Germany. Mr. M. Grafe, Mr. R. Pancerzynski, Mr B. Schleifenbauer

---

## References

Free Floating Piston™:A technology to prevent rider ring wear presented during the 1<sup>st</sup> EFRC conference (1999).

Retrofit of a Reciprocating Compressor with Free Floating Pistons

Authors:E.W.Brown, CSD,S.H.Janbi, JRD

Presented during the Rotating Equipment Technical Exchange Meeting 2004 In Damman Saudi Arabia





The Chemical Company

# **Construction Unit Damage and Corrosion Attack at CO<sub>2</sub> Reciprocating Compressors**

by:

**Dipl. Ing. Heinrich Ochs**

**Dr. Jörg-Thomas Titz**

**Rotating Equipment**

**BASF Aktiengesellschaft**

**Ludwigshafen**

**Deutschland**

**4<sup>th</sup> Conference of the EFRC  
June 9<sup>th</sup> / 10<sup>th</sup>, 2005, Antwerp**

## **Abstract:**

At the Ludwigshafen Verbund site of BASF Aktiengesellschaft, saturated carbon dioxide is compressed at about 250 barg. This process has been working since 1975 without any problems. In 2003 unexpectedly high corrosion rates of up to 8 mm/year occurred. The causes, the automatic effect of CO<sub>2</sub> corrosion, and remedy measures were recorded.

## 1 Introduction

At the Ludwigshafen Verbund site of BASF Aktiengesellschaft, saturated carbon dioxide (CO<sub>2</sub>) resulted in ammonia production is fed into the pressureless CO<sub>2</sub> piping network. In the further Verbund chain (see Figure 1), the gas is compressed at about 250 barg and is supplied to the urea plant. The manufactured urea is raw material for the production of melamine, glues, resins and fertilizers.

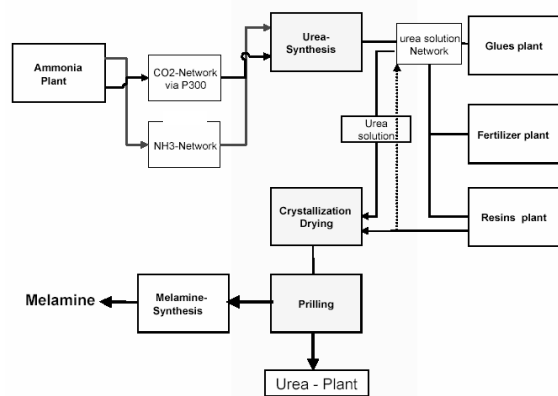


**Figure 1:** CO<sub>2</sub> Verbund structure

CO<sub>2</sub> gas compression occurs in 7-stages, uniformly-built reciprocating compressor units (Borsig Company, driving power of 3 MW, stroke of 800 mm, oil-lubricated). The reciprocating compressors were adapted over decades to raw material developments in the area of materials for packing rings, pistons rings and coatings.

## 2 Incident

A loud bang resulting in a strong expansion noise and the activation of CO<sub>2</sub> gas warning devices led to the shutdown of reciprocating compressor units in early 2003. The compressor units were able to be safely shut down and released, and no-one was injured.

The following Figure 2 shows the location:



**Figure 2:** Torn safety valve inflow pipe of the 5th stage

The safety valve inflow pipe of the 5th stage was torn on the underside for a length of about 40 cm. The overall piping was bent upwards about 30° and the underlying pipes were torn from their fixtures.

## 3 Cause

The piping branch of the safety valve inflow pipe of the 5th stage is located before the entry into the heat exchanger. The operating overpressure varies between 60 barg, and the operating temperature is about 120°C. The safety valve inflow pipe is made out of a low-alloyed steel pipe (St.35.8) with a wall thickness of 7.1 mm. It occurs only a flow current in case of safety valve lifting. Therefore it has to do with a “dead branch”, so that forming a condensate with corrosive attack is possible.

In Figure 3, the details of the interior side in the 06-00-h position directly next to the damage point are shown. A strong corrosion attack is noticeable with flat bursting points and hollows. In the marked area, a so-called “mesa attack” (mesa = table in Spanish) can be seen.



**Figure 3:** Corrosion attack at the damage point

$$\begin{array}{l} \text{CO}_2 + \text{H}_2\text{O} \leftrightarrow \text{H}_2\text{CO}_3 \\ \quad \quad \quad \swarrow \searrow \\ \quad \quad \quad \text{H}^+ + \text{HCO}_3^- \\ \quad \quad \quad \nearrow \nwarrow \\ 2 \text{H}^+ + \text{CO}_3^{2-} \end{array}$$

The graph plots Temperature (K) on the y-axis against Carbonic Acid ( $\text{CO}_2$ ) concentration in  $\text{mg/l}$  on the x-axis. The y-axis ranges from 273 to 333 K in increments of 10 K. The x-axis ranges from 600 to 3400  $\text{mg/l}$  in increments of 400  $\text{mg/l}$ . A smooth, downward-sloping curve represents the relationship. A specific point on the curve is highlighted with a horizontal arrow pointing to 293 K on the y-axis and a vertical arrow pointing to 1800  $\text{mg/l}$  on the x-axis.

Temperature (K)	Carbonic Acid ( $\text{CO}_2$ ) in $\text{mg/l}$
273	3400
283	2600
293	1800
303	1200
313	800
323	600
333	600

A line graph showing the relationship between pH and CO<sub>2</sub> pressure at a constant temperature of 298 K. The y-axis is labeled 'pH' with an upward arrow, ranging from 3.0 to 5.0. The x-axis is labeled 'CO<sub>2</sub> - Druck (bar)', ranging from 0 to 1.0. The curve starts at a pH of 5.0 for a pressure of approximately 0.1 bar and decreases sharply, reaching a plateau of about 3.8 at pressures above 0.6 bar.

CO <sub>2</sub> - Druck (bar)	pH
0.1	5.0
0.2	4.5
0.4	4.0
0.6	3.85
0.8	3.8
1.0	3.8

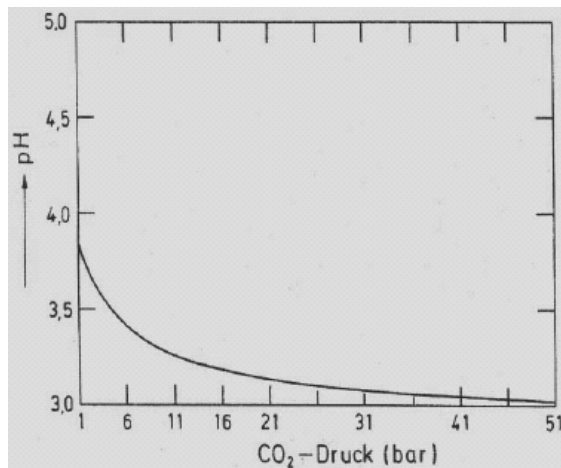


**Figure 8:** pH values under pressure [4]

At these pH values, non-alloyed steel is continuously attacked by CO<sub>2</sub>-saturated water at a rate of 0.2 – 0.5 mm/year up to 1 mm/year.

### 3.3 Automatic effect in the phase limit

The “slight” corrosiveness of carbonic acid which has been identified is not sufficient to explain the corrosion attack on the CO<sub>2</sub> compressor unit described above.

As far as that goes, it is questionable if there are conditions under which carbonic acid can have significantly greater corrosive effects.

It is described in the literature that carbonic acid can be as corrosive as hydrochloric acid in the area of the phase limit with a steel surface and water.

“In the phase limit which is saturated with ferrous carbonate (FeCO<sub>3</sub>), the corrosiveness of carbonic acid (H<sub>2</sub>CO<sub>3</sub>) is higher than that of hydrochloric acid (HCl) for a given pH value. Carbonic acid is directly reduced, so that twice as many acid H<sup>+</sup> ions exist (see Figure 9)“ [1].

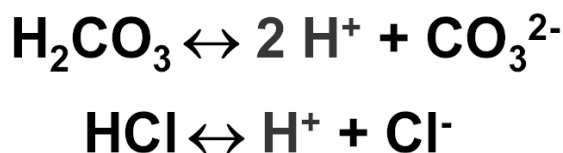


**Figure 9:** Conditions in the phase limit [1]

### 3.4 Phase limit of steel surface – water

In the phase limit of steel surface – water, other conditions prevail than in the solution. The corrosiveness of carbonic acid in the phase limit, with a thickness of about 0.5 mm, is also affected by:

- Ionic interactions between carbonic acid molecules and ferric ions
- Saturation of the phase limit with ferric carbonate, leading to precipitation of ferric carbonate and a ferric carbonate coating.
- Electrochemical anode and cathode reactions in the ferric carbonate coating

In the investigations conducted by [1], the corrosion rate was calculated in relation to the CO<sub>2</sub> pressure. As in Figure 10, the corrosion rate apparently lies in the model calculation and in the data determined in experiments of >10 mm/year.

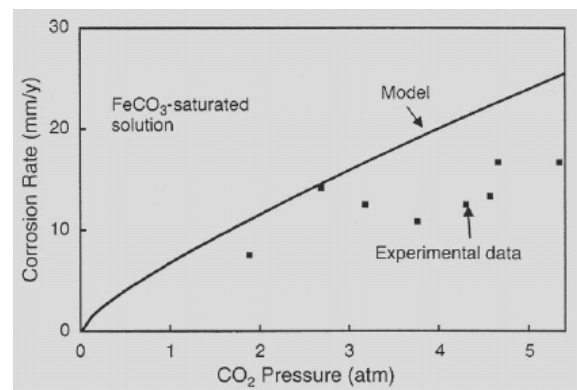


**Figure 10:** Corrosion rate in relation to CO<sub>2</sub> pressure [1]

Therefore, carbonic acid does not work in the phase limit as “slightly” corrosive weak acid, but as strong acid and thereby basically more corrosive. In the following table (see Figure 11) are the measured pH values of carbonic acid and, as a comparison, of hydrochloric acid as well as the calculated pH values of carbonic acid as weak or strong acid opposed.

CO <sub>2</sub> or HCl	CO <sub>2</sub> dissolved in H <sub>2</sub> O	pH - value		
		weak acid (1)	strong acid (2)	HCl
3 mg/L	6,0	7,2	4,3	4,1
50 mg/L	5,0	6,7	3,1	2,8
1610 mg/L	3,7	5,9	1,6	1,3

(1)  $\text{pH} = \frac{1}{2} (\text{pK}_s - \log C_s)$ ,  $K_s = 5,61 \times 10^{-11} \text{ mol/L}$

(2)  $\text{pH} = -\log C_s$ ,  $K_1 = 4,31 \times 10^{-7} \text{ mol/L}$

**Figure 11:** Calculated/measured comparison of pH value

As shown, there are conditions under which carbonic acid works significantly more corrosively than calculated from the CO<sub>2</sub> dissociation for a weak acid. These conditions are found in the phase limit.



The corrosion behavior of steel in carbonic acid is still affected by additional parameters.

In a pH value  $>4.2$ , a stable coating is formed on the material surface by ferrous carbonate ( $\text{FeCO}_3$ ), which works passively and protects against corrosion. The corrosion attack also can be reduced by the addition of oils or greases. In a pH value  $<4.2$ , the outside coating is incomplete or an available ferric carbonate coating is locally attacked with perforations. The perforations are corroded out into hallows over time, since at the perforated point it leads to the formation of ferric ions and a pH reduction. Galvanic effects also are conceivable between the passive ferric carbonate coating and the active, corroding area. The development of the so-called “mesa attack” also helps this.

### 3.5 Further parameters affected by corrosion

Further parameters affected by corrosion are temperature (see Figure 12), flow speed (see Figure 13), and the content of oxygen (see Figure 14 and Figure 15).

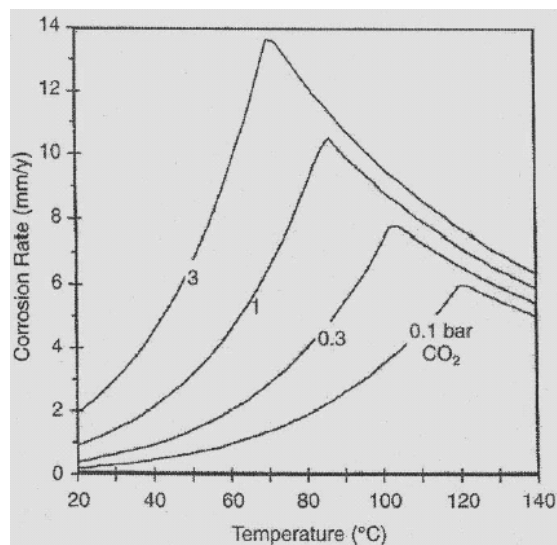


**Figure 12:** Corrosion rate related to temperature [2]

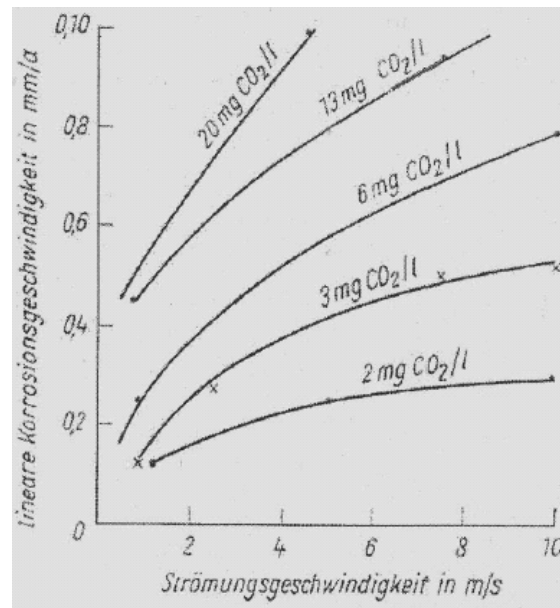


**Figure 13:** Corrosion rate related to flow speed [4]

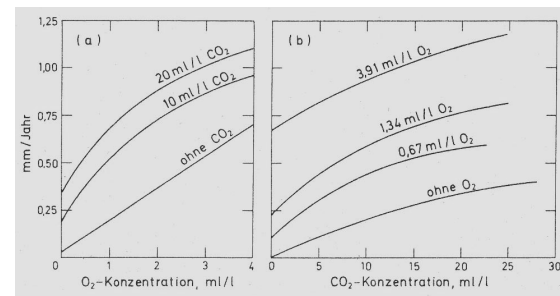


**Figure 14:** Corrosion rate related to the concentration of oxygen with CO<sub>2</sub> (a) [4]

**Figure 15:** Corrosion rate related to the concentration of CO<sub>2</sub> with oxygen (b) [4]

## 4 From theory back to practice

The pipes and equipment of the oil-lubricated CO<sub>2</sub> compressor units are made out of non-alloyed steel, the cylinders out of cast iron or forged steel, and have been operating since 1975 with saturated CO<sub>2</sub> gas without unusual damage or incidents.

In accordance with the guidelines, the equipment and pipes are periodically tested by measuring the wall thickness, among other things, and reserve strengths are checked by using measurement datas. In periodic internal tests, the equipment and pipes are opened, examined, put through a water-pressure test, and put back into operation.

The corrosion rates of  $>10$  mm/year given in the literature could not be observed up to 2003.

However, in 2003 questions were raised about all the experiences and results gained up to that time.

## 4.1 Findings

In the summer of 2003, a periodic test was conducted on a separator in the 4th step (see Figure 16) and a brightly shining surface was discovered in the area of the gas inlet.

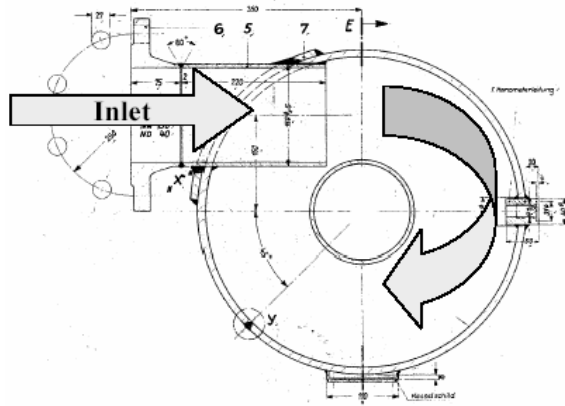


**Figure 16:** Cross-section of a separator in the 4th stage with gas inlet

The aerial measurements of wall thickness which were conducted showed in the upper equipment part (see Figure 17) in the gas rechanneling an unexpected corrosion rate of 4 mm within the previous half-year.



**Figure 17:** Aerial excavation on the jacket

Furthermore, the welded joint of the upper surface was also severely corroded to a degree of about 300°. A thickness reduction of the welded joint to 5 mm from about 12 mm was noticed.

Because of this high corrosion rate, aerial measurements of the wall thickness were conducted in stages on the entire CO<sub>2</sub> compressor units. Ultrasound scanners which showed the measurement results online were used, and in a very short time provided reliable, reproducible results (see Figure 18).



**Figure 18:** Ultrasonic scanner at 06-00-h position

The measurements produced unexpected results. On the equipment and pipes of the 1st to 4th stage, aerial and local reductions of minimum wall thicknesses were detected. Serious damage was also found on the heat exchanger of the 2nd stage (contents: 8.200 liters, length: 6.00 m, diameter: 1.40 m) in the area of the lower condensate drain along the 05-00-h to 07-00-h position in about 50% of the overall length (see Figure 21) The designed wall thickness is about 10 mm according to drawings, and the remaining wall thicknesses measured were less than 3 mm.

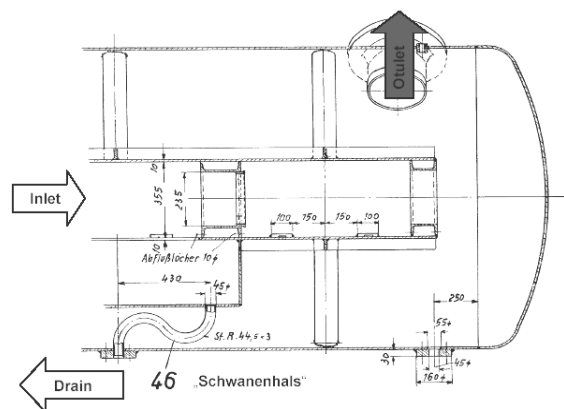


**Figure 19:** Heat exchanger of 2nd stage, detailed view of condensate drain

The area of the condensate drain (see Figure 19, position 46 of the “goose neck”) was particularly jeopardized. The pipe connection between the two

shells (see Figure 20) was corroded through and the underlying area was heavily damaged (see Figure 21).

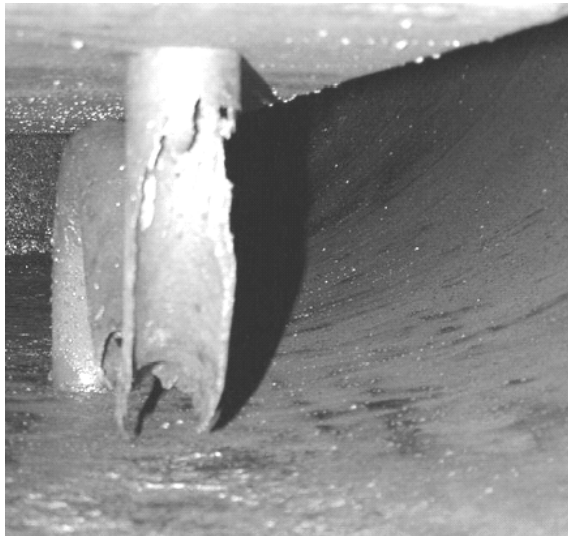


**Figure 20:** Heat exchanger of 2nd stage, corroded "goose neck"

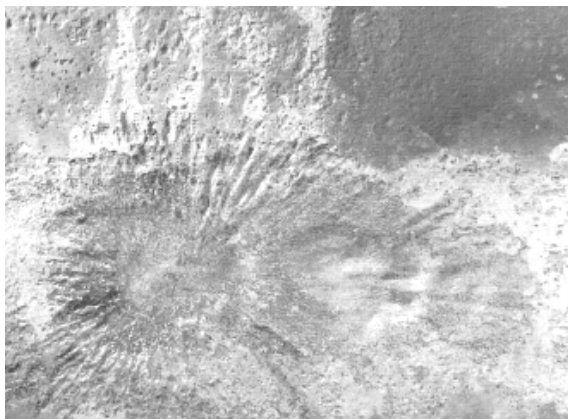


**Figure 21:** Heat exchanger of 2nd stage, 05-00-h to 07-00-h position

## 4.2 Changes in operating conditions

Apparently in the previous operating period from 1975 to 2002, conditions prevailed in the CO<sub>2</sub> compressor units which hindered this type of a corrosion attack. Although it could not be conclusively explained how the spontaneously occurring high corrosiveness of carbonic acid was set off, the following clues were given:

- Because of the use of piston rings made from high-performance plastics and increasingly occurring valve plate damage as a result of sticking oil, the amount of cylinder lubricating oil was reduced in the past by about 8%.

- In comparison to previous years, the capacity utilization of the compressor units had increased by about 30% since May 2002, whereby the flow rate per compressor had been increased.
- Affected by the summer 2002 and the once-in-a-lifetime summer of 2003 with the accompanying high cooling water temperatures, the gas intake temperature rose to 60°C from time to time. The water content in the saturated gas rose by 100g/Nm<sup>3</sup> as compared with the compressor unit's previous conditions. Because of this, the remaining condensation of the proportionate water content was shifted to the later 4th and 6th stage (see Figure 22).

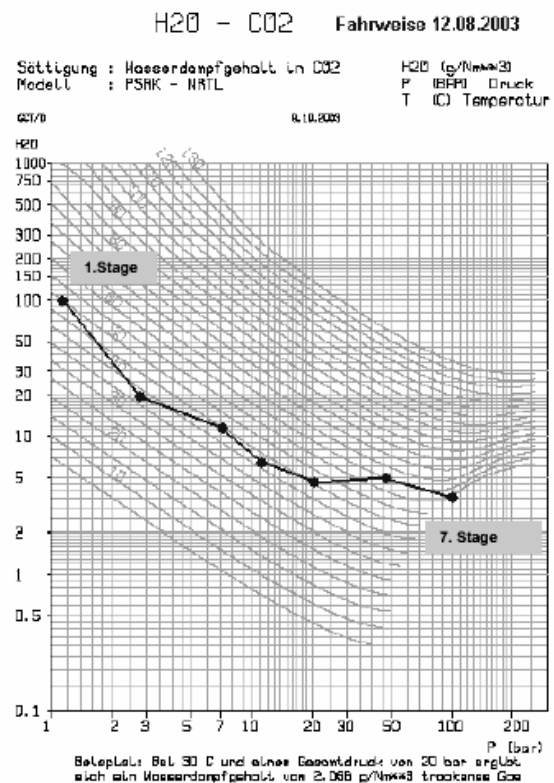


**Figure 22:** Water content in CO<sub>2</sub>, operating procedure in summer of 2003

## 5 Measures

The repair works of the heat exchangers of the 1st to 3rd stage and pipes took place in the BASF workshops. The equipment of the 4th stage was replaced and water pressure tests at 1.5 times the operating overpressure were conducted in the entire units. After 12 working days, production was able to be resumed with reduced gas volume and increased amounts of cylinder lubricating oil, whereby the testing intervals of internal tests were shortened from 5 years to 6 months.



For the replacement of equipment of the 4th step, a highly-alloyed type of steel (1.4462) was specified and an Online Corrosion Monitoring System (Force Technology Company, Netherlands B.V.) was installed (see Figure 23).

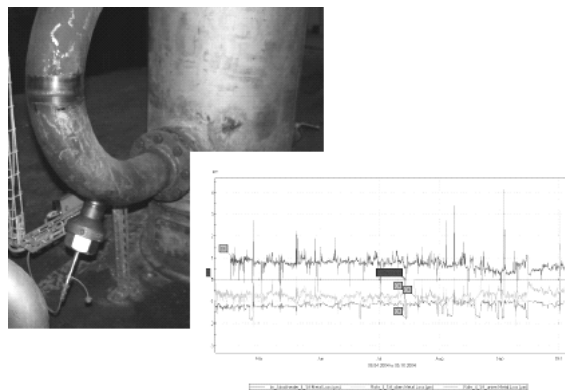


**Figure 23:** Online Corrosion Monitoring

To avoid remaining condensation after the 4th to 7th stage, the units were operated above the dew point (see Figure 24), whereby the installation of a cooling system was required.

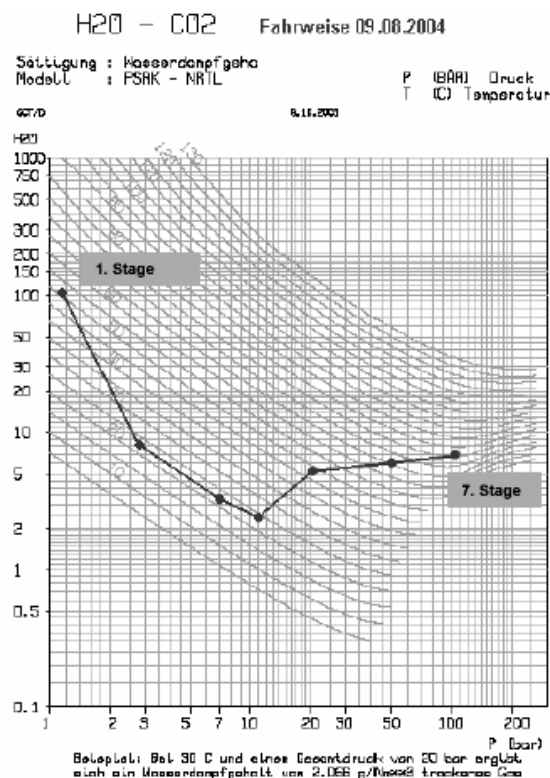


**Figure 24:** Water content in CO<sub>2</sub>, operating procedure in summer of 2004

## 6 Results

Now after about 1.5 years of operation, there are positive operating experiences concerning the measures which were introduced. The results of the locally implemented wall thickness measurements are nearly identical with the measurement values of the Online Corrosion Monitoring System and are in the area of about 0.3 mm/year. In the internal tests, no bright, active corrosion attack has been detected. The examined areas were covered with an oily coating. Based on these results, the testing intervals of the internal tests and pressure test were able to be increased.

## 7 Summary

The use of non-alloyed and low-alloyed steels in existing compressor units for the compression and transport of saturated CO<sub>2</sub> can be safely realized if the mentioned precautions are realized. The testing intervals were able to be increased because the unusual working condition are controlled and monitored. The temperature behavior in the individual compression steps and the performance of the condensate drain are important parameters here. As far as possible from a technical standpoint, cylinder lubricating oils containing additives with viscosities greater than ISO VG 320 are preferred. For the projection of new units, high-alloyed steels and gas-driven compressor construction units are necessary – also in pipes and equipment.

## 8 Literature

- [1] F.M. Song, D.W. Kirk, J.W. Graydon, D.E. Cormack, Corrosion 60 (2004), 736–748
- [2] C. de Waard, U. Lotz, Prediction of CO<sub>2</sub>-Corrosion of Carbon Steel, Paper No 69,NACE Conference 93
- [3] M.B. Kermani, A.Morshed, CO<sub>2</sub>-Corrosion in Oil and Gas Production – A Compendium, Corrosion, Vol. 59, No 8, 659–683
- [4] VEB Deutscher Verlag für Grundstoffindustrie Leipzig, Werkstoffeinsatz und Korrosionsschutz in der chemischen Industrie
- [5] J. Greven, K. Hoff, 3. EFRC Conference (2003), 151–159





# **Detection of Concealed Damages in Early Stages on Reciprocating Machinery**

**by:**

**Eike Drewes**

**PROGNOST Systems GmbH**

**Rheine, Germany**

**[eike.drewes@prognost.com](mailto:eike.drewes@prognost.com)**

**4<sup>th</sup> Conference of the EFRC  
June 9<sup>th</sup> / 10<sup>th</sup>, 2005, Antwerp**

## **Abstract:**

A key factor to reliable and safe machine operation is the detection of concealed damages providing an early detection of component failures. Results and efficiency of maintenance strategies such as preventive and predictive maintenance can be significantly improved by the early failure detection capabilities of monitoring equipment. This paper deals with two detected incidents occurred on different types of machines - an integral and a horizontal reciprocating compressor. In both cases the continuous online monitoring provided root cause information and pinpointed the damage; one on the bolted cylinder/crankcase connection and the other at the piston rod/crosshead connection. Both damages were not discovered during first inspections even after opening the machine and only the objective information from the monitoring initiated further inspections which finally revealed the failure. The early detection of the failures prevented catastrophic failures and minimized the damage and shutdown time to repair.

## 1 Introduction

Today finding the right maintenance strategy is a common task for every operator of machinery in the modern industry. Especially those who are operating machinery such as 30 years old or more have to determine a well balanced way between maximisation of production and cost efficient maintenance. Determining the best solutions in terms of materials of the 21<sup>st</sup> century for a machine designed three decades ago can be a challenging process which sometimes can provide undesired setbacks. As the lifetime of many components is increasing driven by the technological progress, the maximum operating time between planned maintenance shutdowns has to be determined new. One of the key objectives is to find the right balance between condition-based (predictive) maintenance and time-based (preventive) maintenance. Such a procedure requires a good evaluation of the existing experiences in operation and maintenance and excellent knowledge of each individual machine. The user companies can request support in this matter from the experts of component suppliers and also by applying automatic monitoring and diagnosis systems.

Machinery monitoring systems can take over a major role in the process of developing and applying the best suitable maintenance strategy for a given population of machines. They provide valuable and objective information on the true “bad actors” of the machines, which limit the maximum achievable running time of a machine. Furthermore they support decisions to focus maintenance activities by detecting component failures at an early stage minimising consequential damage and enabling a combination of preventive and predictive measures.

The paper describes how effective concealed damages can be detected using modern monitoring technology by presenting case studies of different kinds of machines.

## 2 Early detection of a failed piston rod

Since spring 2004 two 4-throw reciprocating compressors of a LDPE plant are equipped with an online condition monitoring and protection system. Apart from the machinery vibration on the 5 cylinders and 4 crosshead slides also the p-V diagrams and vertical piston rod vibration are monitored. The operator company decided to equip these 30 year old machines with an advanced monitoring system as they had experienced unplanned shutdowns caused by unexpected mechanical failures of various components of the machine. Apart from the negative consequences to the reliability and the production of the plant the

troubleshooting and repair of the machine was time consuming due to a lack of information on the root causes. Consequentially with the installation of a condition monitoring system it was intended to limit the extend of possible damages by an efficient early failure detection enabling a fast and focused reaction of maintenance.

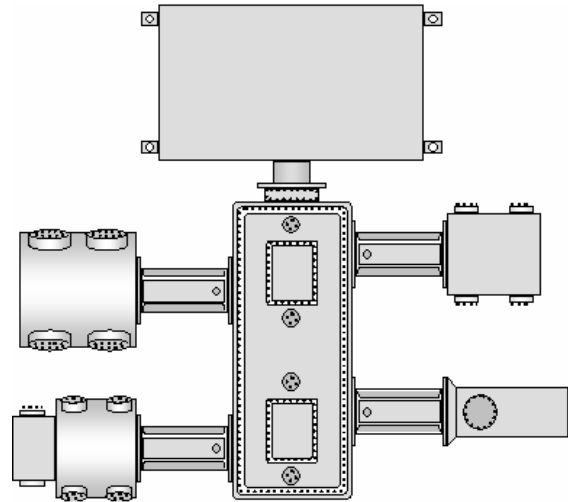


**Figure 1:** Top view of the 4 throw compressor

Within the first 6 months of operation with the monitoring systems installed one of the compressors was stopped due to high vibrations at the crankcase. A first inspection of the machine did not reveal any visible evidence of a mechanical problem or serious component failure. Instead of opening the crankcase and searching for the root cause of the high vibration by visual inspection the historic trend data of the early failure detection of the monitoring system were analysed. Additional information was retrieved by the so called ringbuffer of the monitoring system which provides transient signals of all connected sensors for all revolutions within the last 10 minutes before the shutdown.

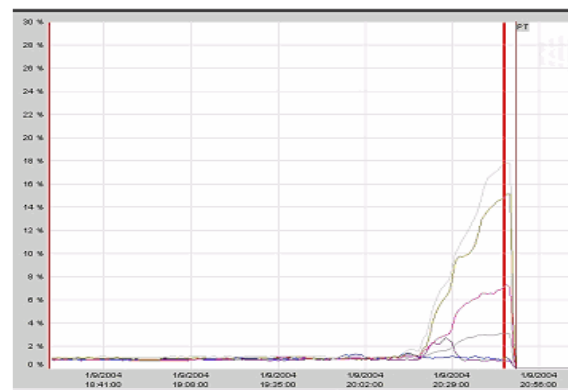


**Figure 2:** Trended crosshead slide vibration for a period of app. 2 hours prior to the shutdown

First indication of a change in the machines vibration was recorded well before the shutdown. Fig. 2 shows the trended vibration measured on the top outside of the crosshead slide for a crank angle of 210 to 270 degree crank angle after TDC app. 2 hours before the shutdown. The vibration monitoring applies a segmented analysis of the vibration in 36 segments of each 10 degree crank angle. Within the displayed period a strong increase of the vibration for the segments 23, 24 and 25 (220 to 250 deg. crank angle after TDC) is noted, while the rest of the revolution shows no significant change in the vibration.

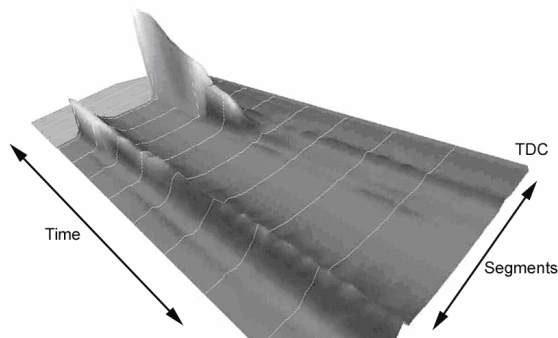


**Figure 3:** RMS crosshead vibration in 3-D trend view for a period of 1h prior to shutdown

Fig. 3 shows the measured RMS vibration of all 36 segments in a coloured 3-D landscape trend for a period of app. 1 hour prior to the shutdown. The rise of the vibration in only 5 of the 36 segments which would increase the total vibration of the full revolution only by app. 5% can be clearly seen.

The monitoring data revealed that the vibration peaks in the segments 23 to 25 were located at the rod load reversal. This is one of the two moments during a revolution when the piston rod load changes from tension to compression load. Vibration peaks measured at one or both of this positions can be seen as a characteristic indication of loose piston rod connections or cracked piston rods.

Additional evidence of the true root cause was provided by the analysis of the vertical piston rod position. Especially the measured peak-to-peak value of the rod position - the piston rod run out - showed a persistent rise of app. 100  $\mu\text{m}$  for more than 6 hours. Within the last 30 minutes prior to the shutdown a significant and sudden rise by additional 150  $\mu\text{m}$  peak-to-peak to a total of more than 250  $\mu\text{m}$  is recorded (Fig. 2).

The combination of the above described information is a typical indicator for a piston rod crack prior to a failure. When opening the cylinder of the fourth stage and pulling out the piston rod nothing special was recognized at first. The piston rod was still connected to the piston and the crosshead and the overall impression was safe. Only the data from the monitoring system which was recognised “objective” urged to continue their search for a possible failure. When opening the supernut connection between the piston rod and the crosshead it became evident that the piston rod in fact was broken within the thread region of the piston rod. The supernut itself covered the failure and surprisingly provided sufficient support to keep both pieces together.

After opening the supernut connection several fragments of the piston rod were found in between the two main pieces showing a conical surface of the fracture. Figures 4 to 6 show some pictures of the failed piston rod.

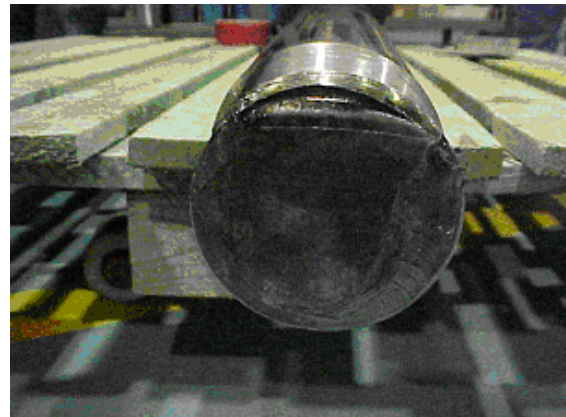


**Figure 4:** Surface of the failed piston rod



**Figure 5:** Fragments of the piston rod thread region

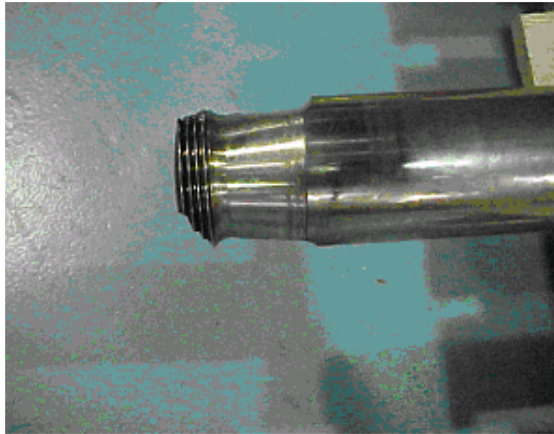


**Figure 6:** Top view of the failed piston thread region

A detailed analysis of the cracked surface of the piston rod determined a higher cycle fatigue mechanism as the root cause for the failure.

The above described case illustrates the possibilities of specialised monitoring systems. Such a case of a concealed piston rod failure would be undetectable from the outside e.g. by inspection tours in the plant. The monitoring system in this case did not only detect the failure and release an alarm, it also provided sufficient and credible information on the possible root cause. This was responsible to let the maintenance team continue their search even after the first check did not reveal the expected failure.

### 3 Detection of broken cylinder bolts

Another example for the successful detection of a concealed damage occurred on an integral compressor running in a natural gas production in Germany. The decision to install online condition monitoring was made by the company with the intention to improve safety protection for their 20-year old machine and to identify mechanical failures. The machine is located in a compressor station which is operated mostly unmanned and is equipped with an online condition monitoring and protection system using one accelerometer per compressor cylinder installed on the crosshead slide. The engine part of the machine is not equipped with vibration measurements, however, a total of 21 instruments such as piston rod temperatures, suction and discharge gas temperatures of the engine and compressor are additionally included into the monitoring system. Fig. 7 shows a sectional drawing of the machine.

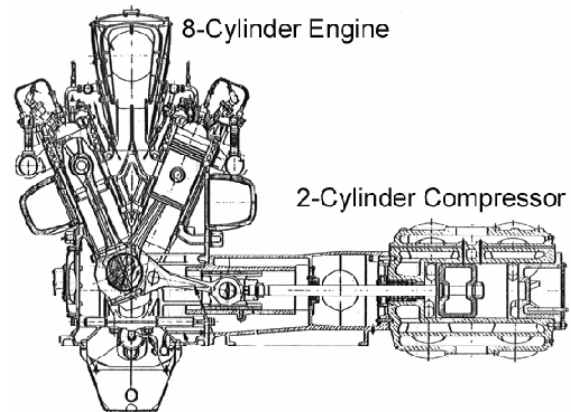


**Figure 7:** Schematic drawing of the monitored integral compressor

After a 3-week routine maintenance revision in July 2004 the machine was re-started. At first it appeared to run smoothly, but after a few minutes the monitoring system released vibration warnings resulting from crosshead slide vibrations. The segmented vibration analysis was pointing to high vibrations in the area of 20 to 50 degree crank angle after TDC. This was the only obvious change in the vibration of the whole machine and such warnings started to come up right after the restart. Fig. 8 and 9 show the vibration signals of the crosshead slide mounted accelerometer for one crankshaft revolution with the segmented analysis.

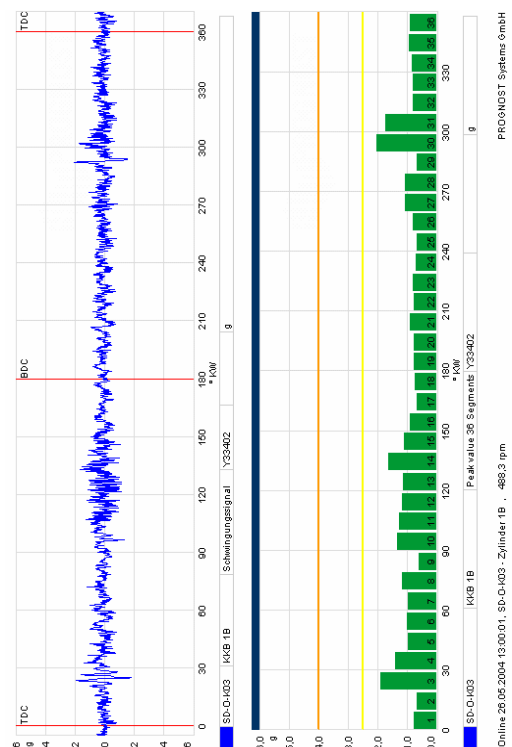


**Figure 8:** Crosshead vibration signal and 36 segment analysis for one revolution prior to overhaul



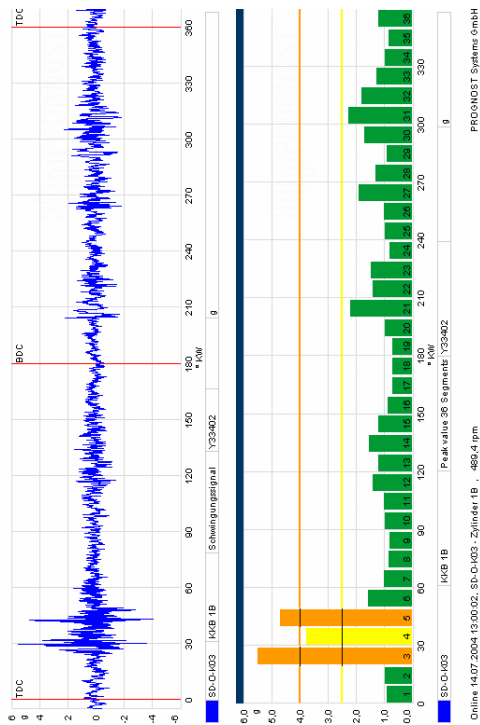


**Figure 9:** Crosshead vibration signal and 36 segment analysis for one revolution showing vibration peaks

Fig. 10 shows a 3-D view of the historic trend of the crosshead slide vibration for a period of one month before the shutdown and two weeks after the shutdown. It clearly shows the development of the increase in vibration and the limited area of the revolution which was affected.

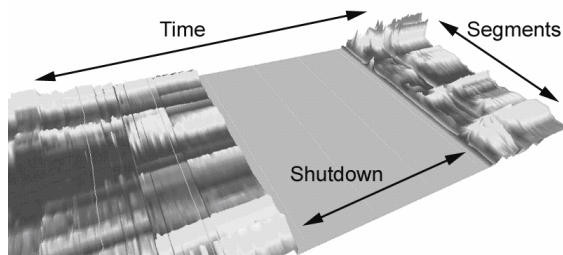


**Figure 10 :** 3-D trend view showing increased vibration after maintenance shutdown

The operating conditions of the machine were also analysed in order to eliminate any possible influence between machine load and the increased vibration. After such a correlation was ruled out it was decided to stop the machine and to inspect the crosshead slide area. It was suggested that there were loose components at the crosshead slide area or distance piece. However, as there were no further transient signals such as dynamic pressure and vertical piston rod position a more detailed analysis for example including dynamic piston rod load was not possible.

The machine was stopped and the maintenance team initially inspected the crosshead slide by opening the side cover. Nothing special was found and the tolerance of the connections near the crosshead were all found within specifications. A closer look at the casing showed that in fact 4 of the bolts which tie the crosshead slide to the main crankcase were broken. Fig. 11 shows a sectional drawing of the crosshead slide area of the cylinder with the position of the accelerometer and the broken bolts marked.

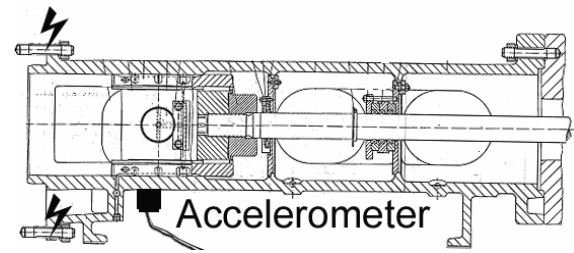


**Figure 11 :** Sectional drawing of the crosshead slide area of the compressor cylinder

This failed bolts had not been touched by the maintenance team during the recent shutdown activities. Metallurgic analysis provided evidence that the bolt had failed by fatigue due to increased stress – possibly caused by thermal stress - during shutdown and start of the machine.

## 4 Conclusion

The above mentioned case studies illustrate the improvements in protection and reliability of two users of reciprocating machinery. In both cases modern monitoring technology detected component failures at an early stage and enabled the maintenance team to take the required action. Each machine was individually equipped with protection and condition monitoring instrumentation to comply with the major objectives of the applied maintenance strategy.

The continuous online monitoring released alarms and provided root cause information pinpointing the damage. Both damages were not discovered during first inspections even after opening the machine and only the objective information from the monitoring initiated further inspections which finally revealed the failure. The early detection of the failures prevented catastrophic failures and minimized the damage and shutdown time to repair.

In both cases the users received the proof that their investment in monitoring equipment increased the efficiency of maintenance significantly by improving the early failure detection.



# **Solutions Developed to Meet Very Stringent Requirements for an Offshore Application of a Reciprocating Compressor System**

by:

**Hans Elferink**  
**Compressor Technology**  
**Thomassen Compression Systems**  
**Rheden**  
**The Netherlands**  
**elf@thomassen.com**

**André Eijk**  
**Flow and Structural Dynamics**  
**TNO Science and Industry**  
**Delft**  
**The Netherlands**  
**andre.eijk@tno.nl**

**4<sup>th</sup> Conference of the EFRC**  
**June 9<sup>th</sup> / 10<sup>th</sup>, 2005, Antwerp**

## **Abstract:**

During the lifetime of an existing gas well, located in the D15FA/FB field in the North Sea, the pressure has dropped and consequently production is reduced.

A depletion compressor must be added therefore to this existing platform to increase the production. This sounds easy but has been very challenging due to physical and other restrictions.

For this platform it appeared that a reciprocating compressor was the best choice based on its flexibility with respect to the specified operating conditions, available power, and efficiency. However, a reciprocating compressor generates additional vibrations and noise in the living quarters, which are located close to the compressor system.

The specified requirements, to meet the allowable noise and vibration limits in the living quarters could, in this specific case, not be met with straightforward solutions.

This presentation will explain the background that has led to the very stringent requirements and the efforts taken in compressor, skid, motor, piping and deck design to meet the specified requirements.

Special attention will be given to the measures taken to reduce the excitations acting on the platform, and the mechanical and acoustical analysis that have led to the final design of this reciprocating compressor system.

The solutions that have been developed can be regarded as non-standard and have resulted in new directions in solving very demanding system requirements.

## 1 Introduction



*Figure 1: Photo of the D15 offshore platform*

During the lifetime of a well the gas pressure diminishes and production resultantly reduced. On the existing D15 platform, owned at this moment by Gaz de France and located in the D15FA/FB field, 195 km NW of Den Helder (The Netherlands), a depletion compressor must be installed because the capacity has declined more steeply than anticipated, indicating limited reservoir connectivity and requiring acceleration of the field performance review and likely further development activities.

This sounds an easy solution but on an existing platform it may become a real challenge due to physical and other restrictions.

Several types of compressors can be selected for this purpose e.g. screw, turbo and reciprocating. A centrifugal compressor was unsuitable due to the wide range in suction and discharge pressures and in addition its rather low efficiency. A screw compressor is unable to handle the high pressure levels.

The result of a feasibility study, made by the operator, concluded that the solution for handling the required conditions could only be solved by the use of a single stage reciprocating compressor, which was the best choice concerning flexibility, available power, and efficiency.

One of the major disadvantages of the reciprocating compressor is its inherent generation of noise and vibrations mainly caused by mechanical loads of the compressor due to oscillating masses and torque variations, pulsation-induced forces and structure-borne sound (vibrations in the audible frequency

range) transmitted via the compressor skid and pipe supports to the steel structure of the main deck. As the living quarters are in close vicinity of the compressor (approximately 25 meters) the noise and vibration levels will there increase.

The first main question was whether the sound and vibration levels in the living quarters would exceed the allowable limits after installation of the reciprocating compressor system.

At first a feasibility study was carried out by TNO to investigate the possibility of mounting a reciprocating compressor on rubber anti vibration mounts (AVM's) on the main deck in such a way that the increase in noise in the living quarters would be less than 2 dB(A). From this study it was concluded that it is indeed possible to mount a reciprocating compressor system on the existing D15 platform without exceeding the allowable noise levels in the living quarters.

This project has shown that the acceptable solution could only be realized by close cooperation between the compressor manufacturer, end user, engineering contractor and vibration specialists. In this specific case of the D15 platform, Thomassen Compression Systems, TNO Science and Industry, NAM and Fluor. The final solution as developed can be regarded as unique for an offshore platform. The requirements and limitations, which have been faced with, are:

- a very low noise level as compressors had to be located near living quarters;
- limited power and starting current;
- smooth start up at high settling-out pressure;
- variable compressor process conditions;
- limited space (in area and height);
- limited crane capacity;
- unattended operation.

This paper will explain the efforts taken in compressor, skid, motor, pulsation dampers, piping and deck design to meet the specified stringent requirements.

## 2 Sound and vibration requirements

On the D15 platform there is an existing gas motor driven generator set which is located on the main deck. The generator set is mounted on rubber anti vibration mounts (AVM's) and produces via the platform construction the major structure-borne sound and vibration levels in the living quarters. By

adding a reciprocating compressor in close vicinity of the living quarters (approximately at 25 meters distance), additional noise will be generated in the living quarters. This additional noise is caused by the mechanical loads of the compressor, pulsation-induced forces on the dampers and piping and by structure-borne sound (vibrations in the audible frequency range) transmitted via cables and pipe supports.

As indicated in the introduction the first main question was if the noise vibration levels in the living quarters would exceed the allowable limits after the installation of the reciprocating compressor system.

The noise and vibration transfer, caused by mechanical forces and moments of the compressor, can be reduced by mounting the compressor on rubber mounts.

In this case the connected pipe system had to be flexible enough to withstand the dynamic movements of the compressor.

The transfer of noise and vibration, caused by pulsation-induced forces, can be minimised by the installation of large volume pulsation dampers, additional (acoustical) damping and avoiding coincidence of acoustical and mechanical natural frequencies. Mechanical separation of the pipe system from the platform construction should be achieved as much as possible.

The optimum design of the pipe system and support layout has been calculated with a pulsation and mechanical response analysis according to API Standard 618<sup>1</sup> of which the results have been presented in chapter 4 and 6.1.

In an earlier stage, vibration measurements under the gas motor skid have been carried out. An acoustic engineering office has determined the effect of the vibrations of the gas motor in the living quarters.

The generator set is under normal operational conditions the major structure-borne noise source at the main deck and from acoustic point of view, more or less positioned in the same way to the living quarters as the future compressor.

The results of these measurements have been used to calculate the expected noise level in the living quarters after the addition of the reciprocating compressor and its auxiliaries like cooling water system, pumps etc. The allowable increase was limited to 2 dB(A).

The allowable vibration levels in the vertical direction of the main deck have been calculated as a function of frequency to be able to realize a noise level below 45 dB(A) in the living quarters. The results are shown in table 1.

From the results listed in table 1 it can be concluded that for frequencies above 37.5 Hz, which is above 2 times compressor speed, the maximum vibration level of approximately 1 mm/s peak-to-peak should not be exceeded. For a frequency close to 4 times the compressor speed the acceptable level is higher.

The acceptable vibration levels above 25 Hz are all very low in comparison with the general accepted criteria for vibration level of approximately 6 mm/s peak-to-peak normally applied for foundations of reciprocating compressor installations.

To stay within these criteria on the main deck, a non-traditional and unique solution has been developed as explained in the next chapters.

**Table 1:** Allowable vibration levels in mm/s peak-to-peak at the main deck as a function of frequency

Frequency [Hz]	12.5	25	37.5	50	62.5	75
Vibration [mm/s pp]	12.5	3.2	1.2	0.7	1.8	1.1

## 3 Process, compressor and driver specification

### 3.1 Process specification

- Molecular weight: 19.6 g/mol.
- Suction pressure: 35 ÷ 76 bara
- Discharge pressures: 100 ÷ 121 bara
- System design pressure: 156 bar(a)
- Settling-out pressure: 121 bar(a)
- Flow control (by means of valve lifters) from 100%, 75%, 50% to 25%.
- Operation loads cases: see table 2

**Table 2:** Operation loads cases (\*Design condition)

	Case A	Case B*	Case C	Case D	Case E	Case F
P <sub>suc</sub> bar (a)	70.2	46.1	37.3	75.8	53.6	43.5
P <sub>dis</sub> bar (a)	101	101	101	121	121	121



## 3.2 Other System and Utility requirements and restrictions

- Driver electric power: 400 Volt AC
- Maximum starting power: 600 kW
- Maximum allowable voltage drop during start-up: <10 %.
- Package unit shall be designed for unattended operation;
- Excitation in the frequency range of 28÷40 Hz and above 50 Hz shall be minimized or avoided;
- Design area was very restricted in space;
- Design had to take care for escape routes;
- Maximum capacity existing crane is 18 tons.

To meet all the specifications and requirements, taking into account the restricted space available, a high speed reciprocating compressor (990 rpm) has been selected. From the feasibility study, carried out by TNO, it was shown that excitations in the range of frequencies from roughly 28 ÷ 40 Hz and above 50 Hz had to be kept to a minimum to avoid excitation of the mechanical natural frequencies of the platform structure.

These stringent requirements on noise and vibrations excluded use of a single stage 1 cylinder compressor.

In addition to above mentioned process specification, there was a requirement that the compressor had to be designed for future change to 2-stage operation. These requirements automatically lead to a 2-cylinder compressor configuration with horizontally opposed and balanced cylinders.

To avoid coincidence of platform resonances and compressor excitation, frequencies of 2<sup>nd</sup> order forces and moments of the compressor (around 33 Hz) had to be kept to a minimum.

As the compressor should be able to run from full flow until free flow conditions, also part load conditions had to be incorporated in these analyses (due to well characteristics the suction pressure of the compressor varies with the flow rate i.e. suction pressure increases if flow rate decreases).

The 2-cylinder compressor has a high 2<sup>nd</sup> order excitation component. To reduce this 2<sup>nd</sup> order component, Thomassen has designed a 4-cylinder high speed compressor with both compression cylinders at one side of the compressor and 2 dummy's on the opposite side. This configuration

yields very low 2<sup>nd</sup> order forces and moments, and additionally, it has the advantage of having all piping on one side of the compressor.

The suction and discharge cylinder nozzles were located at the sides instead of on top and bottom. This resulted in a more compact design and further reductions in weight, overall dimensions and moving masses.

For further optimisation 180 and 90 degree crankshafts were compared to find the lowest excitation forces, low start-up torque, and minimum torque fluctuations at full load and reduced capacity.

A 180 degree crankshaft would have been better with respect to starting torque, but a 90 degree crankshaft results in lowest 2<sup>nd</sup> order forces and moments and therefore avoiding 2<sup>nd</sup> order excitations. An overview of the free forces and moments are shown in figure 2.

It was finally decided to proceed with the 90-degree crankshaft. In addition, all rotating and moving parts have been weight balanced to avoid any unbalanced forces, other than those taken into account. The optimum crankshaft configuration has also been investigated in the entire platform finite element model as discussed in chapter 5.1.

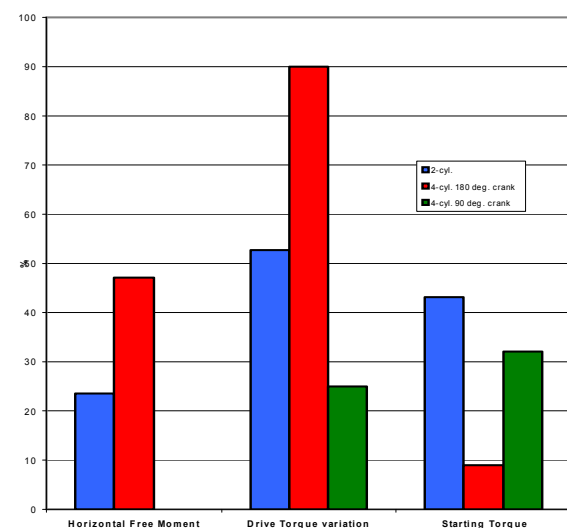


**Figure 2:** Overview with the 2<sup>nd</sup> order free moments and 2<sup>nd</sup> order drive torque variations and starting torque for three different compressor configurations

The entire range of process conditions, including part load conditions, has been analysed to develop a range of the expected loads, the resulting free forces and moments, drive torque variations, the

H. Elferink, A. Eijk: Solutions Developed to Meet Very Stringent Requirements for an Offshore Application of a Reciprocating Compressor System

conditions to start, and the resulting pulsations in the system.

The required capacity control is realized by valve unloading as specified by the end user.

It should be noted that the compressor optimisation was an iterative process together with the optimisation of the anti vibration mounts, the concrete filled skid, and the pulsation bottle design as described in the following chapters.

A photo of the final compressor is shown in figure 3.



*Figure 3: Compressor*

### 3.3 E-motor design

The options for VSDS (Variable Speed Drive System) and induction motors with soft starter were investigated. A VSDS system would have required too much space and was therefore no longer considered as an option.

The compression unit is required to provide the flow on demand and the compressor will remain under pressure when it is on stand by. This had been specified to minimize the emission. As a result the unit must be able to start-up under free flow condition where the suction pressure is slightly above discharge pressure. With a specially designed squirrel cage induction motor and a low voltage soft starter the starting current at maximum settling out pressure could be limited to 3.5 times nominal current with a maximum voltage drop of less than 10 %. A photo of the final motor frame is shown in figure 4.



*Figure 4: Motor on skid*

## 4 Optimisation in the on-skid compressor piping

### 4.1 Pulsation damper design

Besides mechanical loads, reciprocating compressors also generate pulsation-induced forces with frequencies of multiples of the compressor speed. As indicated earlier the amplitudes of the pulsation-induced forces should be kept to a minimum, especially in the vertical direction, to avoid an excitation of main deck resonances.

For a typical compressor installation, the pulsation level at the line connection, assuming an endless line, is limited to 80% of the API Standard 618 recommended limits. This is the so-called “damper check”<sup>2</sup>. The limit to 80 % is made to be able to optimise the system after the design of the piping is completed and finally to meet the API criteria.

However, for this system a further reduction to 50% of the API 618 limits has been applied to be able to meet the stringent vibration and noise criteria.

To keep the pulsation-induced forces across the dampers to a minimum, so-called baffle plates had to be installed together with a symmetric installation of the cylinder nozzles.

The size of the dampers had to be minimized because of the restriction in area and height.

A relatively large nozzle diameter between the cylinder and the pulsation dampers, necessary to achieve acceptable pulsations levels at the compressor valves, would result in too high shaking forces on the nozzles and in addition, potential thermal problems.

This has been avoided by the use of smaller and more flexible piping and by adding a secondary pulsation damper.

This has finally resulted in a construction with a large cylindrical, two-chamber pulsation dampers with a baffle plate, which are positioned aside and above the cylinders.

Additionally, secondary small spherical dampers between the cylinder and the cylindrical dampers have been installed. A picture of the pulsation dampers is shown in figure 5.

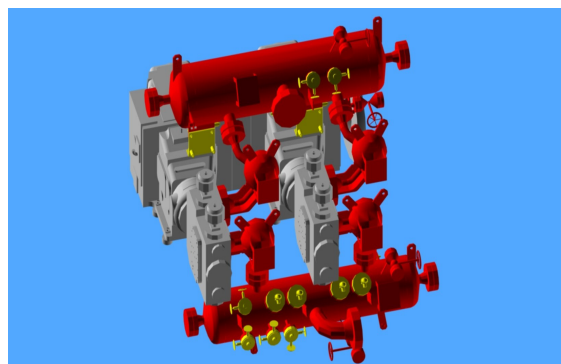


**Figure 5:** CAD model with the optimised pulsation damper configuration

## 4.2 Orifice plates

Besides an optimisation of the pulsation dampers, several orifice plates had to be installed to dampen acoustic resonances to meet the pulsation level criteria and to keep the pulsation-induced forces to a minimum.

For each investigated duty, a certain minimum pressure loss is necessary to dampen the pulsation-induced forces. For some duties and some part load conditions, especially duty D, E and F at 50% and 25% load, the required pressure loss to create sufficient damping, would lead to unacceptable high pressure losses for the other duties.

In discussions with the end user it appeared however, that the part load conditions of 50% and 25% occur only during start-up and for a limited time and duties D, E and F are less frequent running conditions.

Therefore it was decided to keep the vibration levels of the skid, deck and main piping and cyclic stress levels within the levels agreed upon for the 100% and 75% load condition of duty A, B and C. For the other duties and load conditions it was agreed upon to accept higher vibrations levels. However the cyclic stress levels of the piping had to be within the allowable level as given in API 618 to avoid fatigue failures.

In addition to some fixed orifice plates some replaceable orifice plates have been selected to

limit the pressure loss for each duty. Single bore orifice plates are effective for frequencies up to approximately 50-80 Hz. To dampen the high frequency components between 50-150 Hz, it is more effective to use the so-called multiple bore orifice plates<sup>4</sup>.

Calculations of this system show some frequencies of the pulsation-induced forces to be above 50 Hz. Therefore it was recommended to install some multiple bore orifice plates.

## 5 Mechanical analysis of the compressor and concrete-filled skid

### 5.1 Optimisation of the AVM's (Anti Vibration Mounts)

The noise and vibration transfer, caused by mechanical loads of the compressor, can be reduced by installing the compressor on rubber mounts. The foundation structure below and above the mounts must be sufficiently stiff and parallel noise transmission paths (pipes, cables etc.) must be avoided. In this case the connected pipe system had to be flexible enough to withstand the dynamic movements of the compressor.

From the feasibility analysis, carried out by TNO, it appeared that an additional mass (inertia) of approximately 40.000 kg was necessary to keep the compressor skid vibrations within acceptable levels.

It was therefore decided to mount the compressor, e-motor and auxiliary skid on an additional concrete-filled skid with sufficient mass and inertia. This concrete-filled skid has been designed, in close cooperation between Fluor and TNO, and will be mounted to the main deck with AVM's. The total weight of the compressor, driver, skid, pulsation dampers and concrete block is approximately 72.000 kg. This is a considerable high additional mass for a rather small offshore platform.

To achieve enough separation (which means lower vibrations on the main deck) between the 1<sup>st</sup> mechanical natural frequency of the compressor skid (including all equipment on the skid on AVM's) and the 1<sup>st</sup> excitation frequency of the compressor of 16.6 Hz, the 1<sup>st</sup> mechanical natural frequency had to be around 5 Hz. The final dimensions of the concrete filled skid are: width 3 meter, length 7 meters and a height of 1 meter. Further on, the existing platform beams have been



used to mount the skid to minimize the shut down time of the platform.

To optimise the AVM's type, a detailed FE (Finite Element) model of the compressor, driver, pulsation dampers, compressor skid, concrete-filled skid and a part of the main deck has been generated of which a picture is shown in figure 6. The compressor-motor skid is designed by Thomassen by FEM, and is designed for high stiffness. In figure 7 a picture is shown with the lowest rigid body mode shape at 4.33 Hz, which is close to the required value of 5 Hz.

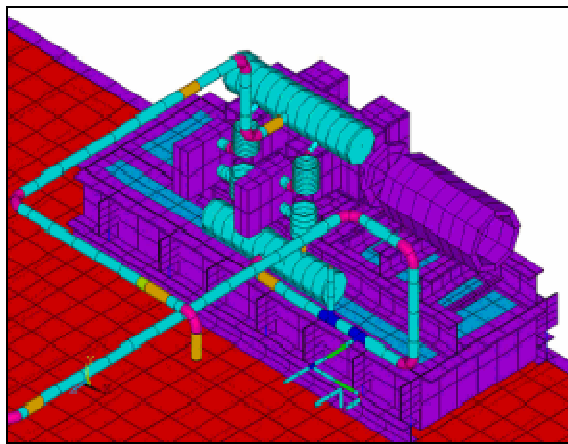


**Figure 6:** FE model

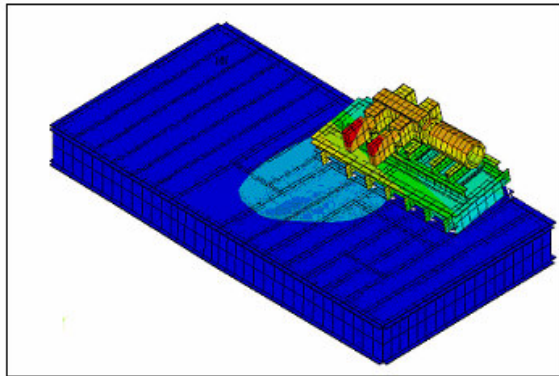


**Figure 7:** Lowest rigid body mode shape at 4.33 Hz

This FE model has also been used to further optimise the compressor configuration with respect to the calculated vibration levels as discussed in chapter 3. The compressor generates free forces, free moments and variation in drive torque loads. Thomassen provided different options for the crankshaft counterweights allowing tuning of the model for minimum vibration loads.

Based on the results of the detailed calculations performed by TNO, the optimum configuration, yielding the lowest (and allowable) main deck vibrations, has been selected.

To determine the maximum vibrations the vibrations, initiated by the pulsation-induced forces, have to be added to the vibrations initiated by the mechanical loads of the compressor. The results are discussed in chapter 6.

Finally, AVM's, make Rubber Design type RD 215 Shore 60 have been chosen as the best possible solution.

It should be noted further that all calculations have been carried out only for quasi-stationary loads of the compressor. To avoid that the pipe system will be damaged due to transient loads (start-up and shut-down) of the compressor, provisions have been made to avoid that the compressor skid will undergo unallowable deflections during the transient phenomena. Therefore, limiters have been chosen. A picture of the concrete-filled skid is shown in figure 8.



**Figure 8:** Concrete filled skid, mounted on AVM's

## 6 Acoustical and mechanical analysis of the pipe system

### 6.1 Acoustical analysis

As indicated in chapter 5, the vibration levels initiated by the pulsation-induced forces, must be added to the vibration levels, initiated by the mechanical loads of the compressor.



H. Elferink, A. Eijk: Solutions Developed to Meet Very Stringent Requirements for an Offshore Application of a Reciprocating Compressor System

To calculate the pulsation-induced forces, detailed acoustical models have been made of the piping with the PULSIM<sup>3</sup> program. The models start at the compressor cylinder up to suitable boundary conditions e.g. large vessels, closed valves, relief valves, main headers etc.

Despite the fact that the pulsation dampers were designed for pulsation levels of 50% of the API 618 criteria assuming an endless line, the pulsation levels in both the original suction and discharge pipe system did exceed the API 618 levels.

This was caused by acoustical resonances in the pipe system. To decrease the pulsation levels, (replaceable) orifice plates have been recommended to be installed at the line side nozzles (see chapter 4.2).

To reduce the pulsations at the suction side the pipe diameter has been increased between the separator and the suction damper. With these recommended modifications the pulsation levels have become within allowable levels for the 100% and 75% load conditions of duty A, B and C. For the other duties and load conditions the vibration levels exceed the normally accepted levels but fatigue failure of the piping will not occur since stress levels are below the fatigue limit.

## 6.2 Mechanical response analysis

To calculate the main deck vibrations resulting from both the mechanical loads and pulsation-induced forces, a mechanical FE model has been made of the compressor, e-motor, pulsation dampers, compressor skid, concrete-filled skid, AVM's, main deck and the piping. The simulation model is shown in figure 9 and the actual situation at site is shown in figure 10.

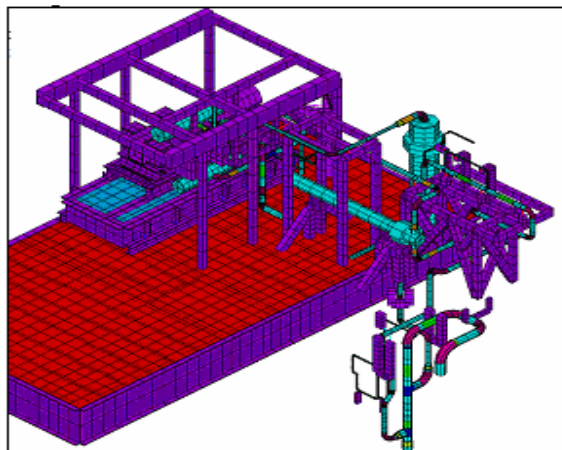


**Figure 9:** FE model of the complete system



**Figure 10:** System at side

At first the mechanical natural frequencies have been calculated, followed by a harmonic response analysis to calculate the vibration levels of all parts and finally the cyclic stress levels in the piping.

From the results of the original layout it was concluded that unallowable vibration levels occur at the main deck at frequencies of 1 and 4 times compressor speed. This was caused by an excitation of a mechanical natural frequency of a part of the main deck, which was too flexible to restrain the dynamic forces.

A further reduction of the pulsation-induced forces was not an option and therefore a recommendation was given to stiffen the flexible part of the main deck by means of an additional column, which connects the main deck with a stiff part of the deck below the main deck.

The simulations made, showed that the maximum vibration level of the compressor cylinders was rather high. This was caused by an excitation of a mechanical natural frequency of 79.16 Hz of which the mode shape is shown in figure 11.

A simple way to decrease the vibration levels was to place additional outboard cylinder supports for which Thomassen already made provisions on the cylinder.

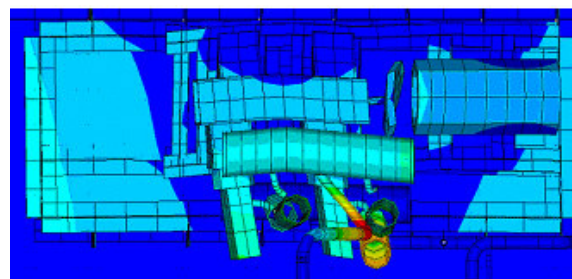


**Figure 11:** Top view of the mode shape at 79.16 Hz

H. Elferink, A. Eijk: Solutions Developed to Meet Very Stringent Requirements for an Offshore Application of a Reciprocating Compressor System

Finally, several additional pipe supports and stiffening of several beam structures was advised to keep the calculated vibration and cyclic stress levels of the piping and main deck vibrations within the levels agreed upon and without exceeding the noise level in the living quarters.

The calculated cyclic stress levels in the piping are within the allowable level which means that fatigue failure of the piping, caused by mechanical loads of the compressor and pulsation-induced forces, will not occur.

### 7 Summary

The requirements to add a reciprocating compressor on an existing platform, with the limitation that the increase of noise in the living quarters should be less than 2 dB(A), have been met. Non-standard solutions have been developed to meet this criterion.

This project has created a new direction in handling very demanding system requirements with variable process conditions for offshore compressor installations.

To achieve this acceptable and feasible solution close corporation was necessary between all parties involved to come up with the best approach to tackle this complex issue.

The extensive analyses have finally led to the following unique design of the installation of which a CAD model is shown in figure 12.

- High speed reciprocating compressor with a 4 cylinder frame with 2 cylinders and 2 dummy's;
- A crankshaft design with 90 degree cranks;
- Capacity control by suction valve unloading;
- Separate rigid skids for motor, compressor and auxiliaries;
- An induction motor with special windings and soft starter;
- An elastic coupling to reduce/separate the mechanical torque fluctuations from the motor;
- A torsional resonance frequency far below operating speed;
- A suction manifold damper equipped with baffle plate and a secondary spherical vessel;

- A discharge manifold damper equipped with baffle plate and a secondary spherical vessel;
- A system with a number of fixed and replaceable orifices to reduce pulsations in the piping and near compressor valves.
- Several orifice plates are of the multi bore design to reduce high frequency pulsations;
- A complete compressor package mounted on a stiff, concrete filled 40 tons skid with the required inertia. The concrete filled skid is mounted on the deck with 18 AVM's (Anti Vibration Mounts);
- Stiffening of the main deck structure;
- Special pipe supports to reduce the structure-borne sound (vibrations in the audible frequency range) transmitted to the steel structure of the main deck.
- Outboard cylinder supports;
- Several additional pipe supports and stiffening of existing steel structures

The compressor skid, mounted offshore, (before the pipe system was build around the compressor) is shown in figure 12. The final situation is shown in picture 13.

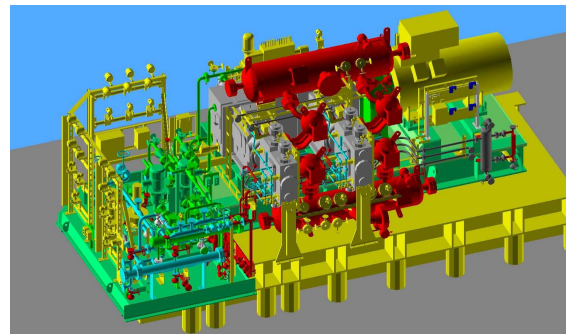


**Figure 12:** Compressor Package as designed



**Figure 13:** Compressor package on site

### 8 Acknowledgements

We like to thank NAM and FLUOR in the confidence they had in the know how and the flexibility of Thomassen and TNO Science and Industry to create a solution for this complex problem.

---

### References

- <sup>1</sup> API Standard 618, 4<sup>th</sup> Edition, June 1995.
- <sup>2</sup> A. Pyle (Shell Chemicals Houston), A. Eijk (TNO-TPD) and H. Elferink (Thomassen Compression Systems B.V.), “Coming 5<sup>th</sup> Edition of the API Standard 618”, 3<sup>rd</sup> EFRC-Conference, March 27-28, 2003, Vienna, Austria, pp 25-33.
- <sup>3</sup> Egas, G., “Building Acoustical Models and Simulation of Pulsations in Pipe Systems with PULSIM3”, Workshop Kolbenverdichter, 27-28 October 1999, Rheine, pp 82-108.
- <sup>4</sup> M.C.A.M. Peters, “Evaluation of damping devices”. EFRC report 2004.



GE Energy  
Oil & Gas

# **Advanced Monitoring and Diagnostic System for Reciprocating Compressors**

by:

**Enzo Giacomelli**  
GE Energy, Oil & Gas- Global  
Services  
Nuovo Pignone, Florence  
Italy  
[enzo.giacomelli@np.ge.com](mailto:enzo.giacomelli@np.ge.com)

**Enrico Calamai**  
GE Energy, Oil & Gas- Global  
Services  
Nuovo Pignone, Florence  
Italy  
[enrico.calamai@np.ge.com](mailto:enrico.calamai@np.ge.com)

**Daniele Martinelli**  
GE Energy, Oil & Gas- Global  
Services  
Nuovo Pignone, Florence  
Italy  
[daniele.martinelli@np.ge.com](mailto:daniele.martinelli@np.ge.com)

**Natascia Monachino**  
GE Energy, Oil & Gas- Global  
Services  
Nuovo Pignone, Florence  
Italy  
[natascia.monachino@np.ge.com](mailto:natascia.monachino@np.ge.com)

**4<sup>th</sup> Conference of the EFRC  
June 9<sup>th</sup> / 10<sup>th</sup>, 2005, Antwerp**

## **Abstract:**

Monitoring and diagnostics are leading to higher levels of safety and availability for reciprocating gas compressors. Timely and accurate detection of incipient failures reduces plant operation and maintenance costs with great benefits to the owners.

An advanced modular diagnostic system has proven to be advantageous for analysing and resolving potential faults such as the deterioration of valves, seals, bearings and other critical components.

By continuously monitoring the mechanical and thermodynamic behaviour of the compressor, the diagnostic system analyzes the performance, and displays a list of probable causes of deviations from normal operation and recommended corrective actions.

The ability to continuously monitor and evaluate rod drop, run-out, vibrations and P-V cycles for every cylinder has become a reality, giving a complete, real time assessment of the behaviour of the machine.

The modular advanced diagnostic system is based on the continuous comparison of measured or calculated values and those expected or allowed, taking into consideration the current operating conditions. The diagnostic system contains a mathematical compressor model that continuously calculates the expected values.

The flexibility of this approach makes it suitable for use with all kinds of reciprocating compressors.



## 1 Introduction

In Europe, most of petrochemical plants were built many years ago. Nevertheless, through the ongoing Reciprocating compressors are very important for compression of light gases and essential for high-pressure processes. They are very flexible and can work under highly variable operating conditions while continuing to maintain high efficiency. But they can have high maintenance costs and low reliability when the machines are not properly operated, controlled and maintained.

While high efficiency and performance of the compressor and short plant downtime are required to achieve higher levels of availability and plant profitability, the failures that can occur in compressor subsystems or components can compromise these objectives. As a consequence, availability and safety may suffer and it is possible to incur significant damage to the plant and to the environment.

In order to retain high efficiency (e.g., high thermodynamic performance) economically, the traditional preventive maintenance approach should be enhanced by or replaced with a predictive or more advance proactive methodology. This can be achieved with the installation of a diagnostic system that allows the detection of malfunctions or the increased likelihood of abnormal compressor behaviour.

Automated monitoring and diagnostics is an approach that can reduce operating and maintenance costs by facilitating the early identification of faults that may lead to deterioration of performance, efficiency and production, and to failures that potentially pose safety issues and may cause lengthy unplanned maintenance outages.

A fault is considered to be the consequence of a protracted anomaly causing an undesired deviation of the compressor parameters with respect to the expected running conditions. Fault detection is the process of identifying the presence of a fault in a machine, while fault isolation is related to the determination of the kind, location and time of detection of the fault. The term fault diagnosis encompasses both fault detection and isolation.

The system uses a model-based approach that relies on the use of an explicit mathematical simulation model of the compressor. A fault is diagnosed through the comparison of measured values and expected values. The measured values are given by the instrumentation installed on the compressor. The expected values are computed by the model using the same field measurements as inputs in order to dynamically determine the behaviour of the machine.

This approach relies on the principle of “consistency-based diagnosis” in which a fault is declared when an inconsistency of the measured

values with respect to the expected values continuously calculated by the mathematical model is evidenced.

Recent experience on the application of a diagnostic system for the improvement of compressor performance and availability will be discussed. The system is installed on a standard horizontal compressor of the balanced opposed type, equipped with two opposing double acting cylinders running at 590 RPM. The machine has two stages compressing a hydrocarbon gas. The operating pressures range is from 6 bar to a final discharge pressure of 55 bar. The operating temperatures are from 40°C to a final discharge temperature of 140 °C. The machine is installed outdoors.

The compressor and associated equipment were fitted with instrumentation to provide the signals and measured values necessary for the evaluation and assessment of the diagnostic system.

## 2 Reciprocating Compressor Analysis

### 2.1 Capacity control and automation

A gas compression system may consists of various machines including reciprocating compressors, related equipment, auxiliaries and drive systems.

Reciprocating compressors have an advantage of high efficiency and flexibility of service. They can run efficiently at partial capacity conditions using specialized devices; for example, step control can be integrated with variable clearance pockets or other systems to achieve a step-less capacity control capable of operating over a wide range of pressures, temperatures and capacity conditions.

In order for the machine, drivers and related auxiliaries to perform well, it is necessary to consider:

- Start-up and shutdown sequences
- Protection of the system with alarms and trips
- Capacity control and adjustment to the process variability
- Simultaneous control of multiple machines or a complete station

Control philosophies deal with optimization of the compressor’s specific consumption, which can be calculated from the quantity of fuel or electric power used by the drive system [9].

Automatic control of an installation requires:

- Suitable local instrumentation
- Measurement and transmission of variables
- Conversion of the data for computer processing
- A data processing system

- A function control system (pneumatic, hydraulic or electric) acting in accordance with the requirements of clearance pockets, valve un-loaders, speed, control, and on-off valves
- Protection instrumentation

It is always recommended that the systems be fail-safe and this is particularly important when handling hydrogen or other hazardous gases [4].

### 2.2 Instrumentation and control systems

Proper functioning of compression systems is dependent on essential instrumentation, and the skill and experience of the operators. The trend is toward centralizing the monitoring by equipping compressors and auxiliaries with remote control systems.

Traditional instruments (pressure gauges, temperature sensors and pressure switches) are today integrated with sophisticated transducers. Electronic instruments are greatly improving the accuracy, repeatability and reliability of readings. Microprocessor technology is also extending the performance of these instruments.

Remote monitoring allows for closer supervision of many areas such as the main driver, gear reducers, the lubrication system (with main bearing temperatures) and casing vibrations. In electric motors, windings, main-bearing temperatures and vibrations of the stator casing are monitored better now than ever before.

The functions related to start-up and shutdown sequences are carried out by the Unit Control Panel (UCP) located either in a control room or adjacent to the compressor. Start-up and shutdown sequences are executed by a Programmable Logic Controller (PLC) located inside the UCP cabinet. The PLC is provided with a Human Machine Interface (HMI), giving the operator easy control of the compressor. The monitoring and diagnostic system can be used solely for diagnostic functions but can also be integrated in a Distributed Control System (DCS) or Panel Control.

A DCS includes [4] robust and secure distributed control capabilities, advanced applications (multi-variable and batch control, optimization), plant-wide history, and information management capabilities, all in one unified system.

The modular design of the data acquisition system provides the opportunity to extend monitoring, troubleshooting and diagnostic functions to multiple compressors simultaneously.

### 3 Monitoring and Predictive Maintenance Integration

Process variables (pressures, temperatures, levels, capacities) and other important parameters are monitored in order to optimize operation. Monitoring and diagnostic systems also address safety aspects of compressor operation.

For example, vibration information that can identify problems in individual stages can be acquired by accelerometers. They are installed vertically on the transition sections, which connect the cylinders to the crosshead slipper guides. The broad frequency response (10Hz to 20Hz) is perfect for measuring the high frequency signals generated by impacts associated with piston rod loosening and knocking.

As another example, in polyethylene compressors using special cylinders with tungsten carbide plungers in contact with bronze elements, a combination of instruments including proximity probes and special thermocouples measure the relevant temperatures. Monitoring of plungers can prevent elevated temperature phenomena and abnormal conditions inside this complex system that are influenced by the quantity of oil, by the type of seals, and by the kind of cooling employed. Avoiding seizure problems enhances the life of seals and reduces the risk of reaction of the gas.

Remote monitoring allows the operator to periodically or continuously evaluate a compressor's mechanical behavior and performance, thus providing several advantages over the older manual methods, including: elimination or reduction of the risk of failures, increased equipment availability, maintenance cost reduction, optimization of spare parts, and energy savings. These new diagnostic approaches (periodic, mixed or constant) are useful, advisable or necessary depending on the criticality level of the machine in the plant.

The best results are obtained when control and diagnostic systems are specified during the design phase, and when the opportunity for remote monitoring by transmitting all data via modem is employed. Field data can be periodically transmitted to the manufacturer to obtain expert and timely evaluation of the equipment's performance including the ability to remotely access additional data to support analysis and diagnostics. With remote monitoring, the client can obtain complete support from the manufacturer, as the data can be analyzed by their team of specialists and the reliability group and with the support of engineering and designers when needed. The automated diagnostic system is able to perform all these activities without any on site human support.

Reduction of maintenance costs can be realized in two ways. The equipment reliability and Mean Time Between Failure (MTBF) of the overall system can be improved by using advanced

technology components. Another way to reduce maintenance costs is through a strategy of predictive or on-condition maintenance defined during the design phase. For example, machines can be designed with diagnostic systems that are capable of anticipating faults such as the deterioration of valves and seals. The possibility of continuously monitoring the cycle of every cylinder is becoming a reality. The ability of this technology and related solutions to anticipate failures and recommend corrective actions is advancing rapidly.

## 4 Diagnostic System Overview

The modular advanced diagnostic system performs predictive real time diagnostics to detect faults or anomalies without human intervention.

The measured values (field data) are inputs for the thermodynamic simulation algorithm that generates the expected values (Fig.1). Deviations between computed expected values and those measured point to a corresponding fault and its causes.

The system manages approximately 10,000 associations of deviations and causes using a fault matrix (Fig.2).

All the signals that identify the operating conditions of the compressor are collected using a dedicated acquisition system or DCS. The diagnostic system displays all the acquired values, their trends and the historical values.

The diagnostic system architecture (Fig.3) is highly modular and allows integration of multiple software levels (basic, advanced) and hardware components as required to achieve the objectives. In the configuration phase, the modules necessary to properly customize the system for the type of compressor and the installed instrumentation and related auxiliaries are defined. All the systems can be integrated in a Control Panel such as SCENETRON™.

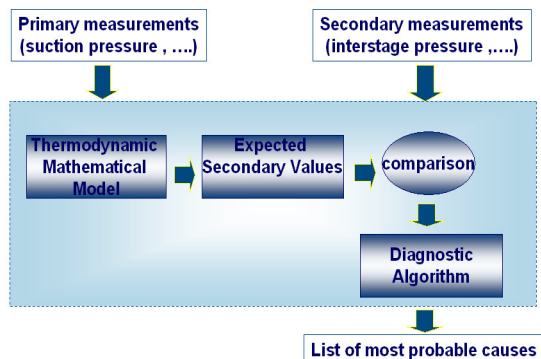


**Figure 1:** Diagnostic System for Dynamical elaboration of thermo-dynamical parameters

CAUSE	DEVIATION (referred to the expected value)	Suction Interstage Pressure : lower		
		Piston Rod drop: higher	Vertical Run-out: higher	
Piston Rider Bands in Cylinder N°...of ...stage N°...				
Cylinder Liner/Cylinder N°...of ...Stage N°...				
Piston Rod in Cilinder N°...of Stage N°...				
Carry-over of strange particles in Cylinder N°...of Stage N°...				
Improper tightening of Cylinder N°...of Stage N°...				
Cylinders Lubrication System				
Contamination in in the process gas				
Separators or Suction filters				

**Figure 2:** Extract of the matrix deviation/cause

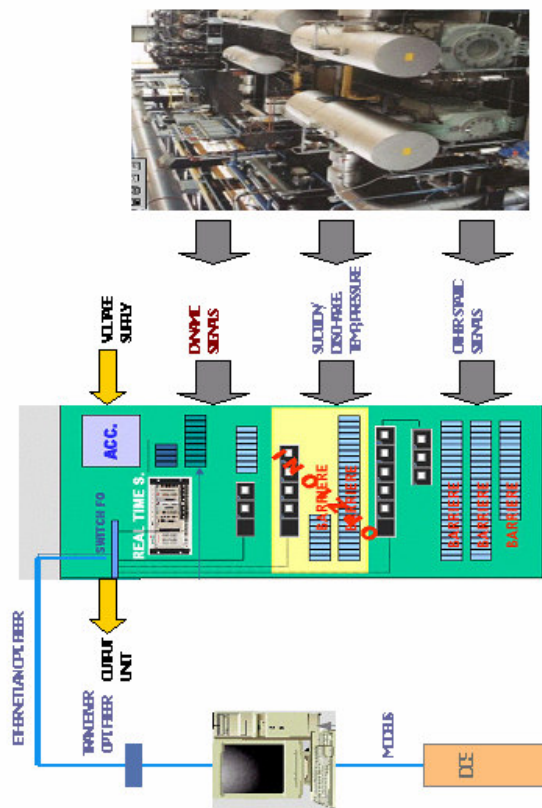


**Figure 3:** Diagnostic system architecture

## 5 Analysis and Evaluation of Data

### 5.1 Dynamic data

All dynamic data are acquired by a dedicated fast acquisition system, not by a standard DCS or acquisition modules. These parameters are acquired continuously and the results are compared using the same process flow indicated in (Fig.1).

Relevant examples of dynamic parameters include rod-drop, run-out, vibrations and P-V Cycles. Piston rider band wear can be indicated by excessive rod drop (Fig.4) and can be caused by gas contamination or failure of the oil cylinder



lubrication system. The diagnostic system also displays all the other parameters correlated to this failure. In addition, it can continuously detect the state of the piston rod, reporting the current drop and the estimated residual life.

By monitoring the run-out (Fig.5), it is possible to detect various anomalies such as improper tightening of the cylinder, carry-over of particles into the cylinder, cylinder liner wear, or piston rod wear. It can also continuously detect the piston orbit by giving the current position correlated to the rotation angle.

Detection of vibrations (Fig.7) at frequencies at the upper range of the vibration limit curve (red line) provides the ability to detect various anomalies such as: improper tightening of the cylinder, carry-over of particles in the cylinder, loss of efficiency in pulsation dampers or orifices, damage of the compressor foundations, or improper tightening of the frame.

The P-V cycles (Fig.8) describe the thermodynamic behaviour of the compressor. They are measured continuously for each compression chamber by dedicated dynamic pressure transducers and triggered by a key phasor installed on the flywheel. The actual P-V cycles (white line) are compared with the theoretical cycles (red line) that are generated continuously by the mathematical model. Deviations may be indicative of failures such as cylinder piston ring wear or suction and discharge valve failure. The diagnostic system gives the option to display single or overlapped cycles in closed or opened shape.

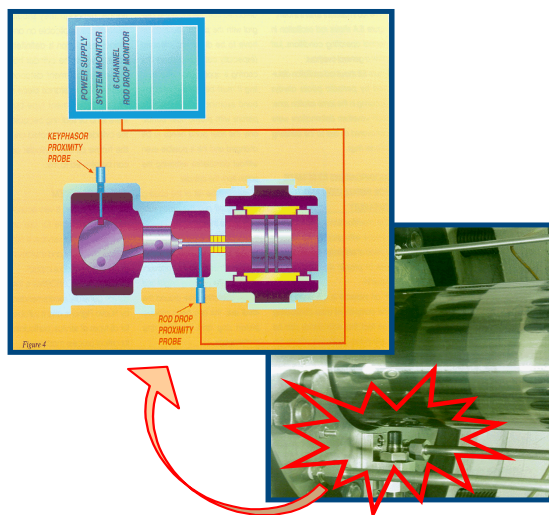


Figure 4: Rod drop monitoring

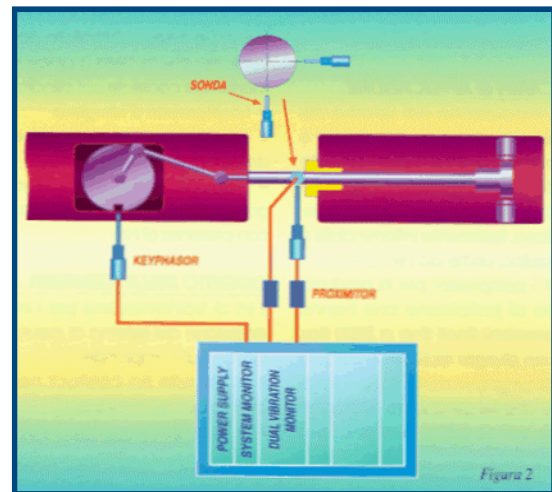


Figure 5: Run out monitoring

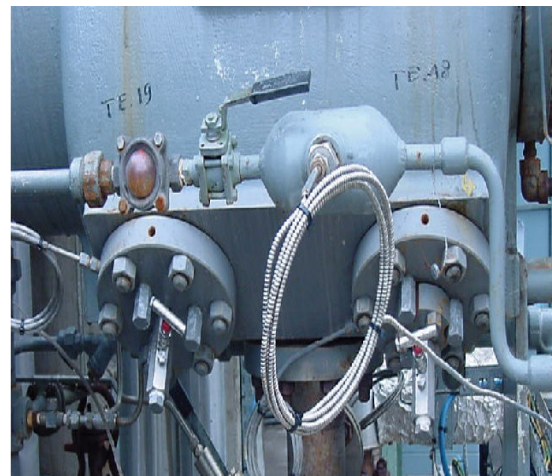


Figure 6: Valve cover temperature monitoring

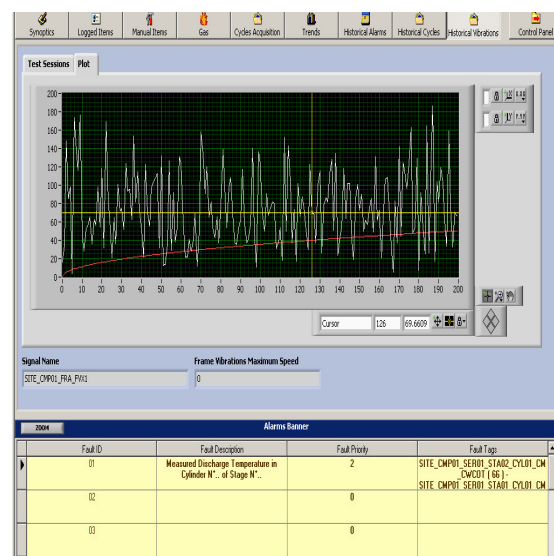


Figure 7: Frame Vibrations monitoring



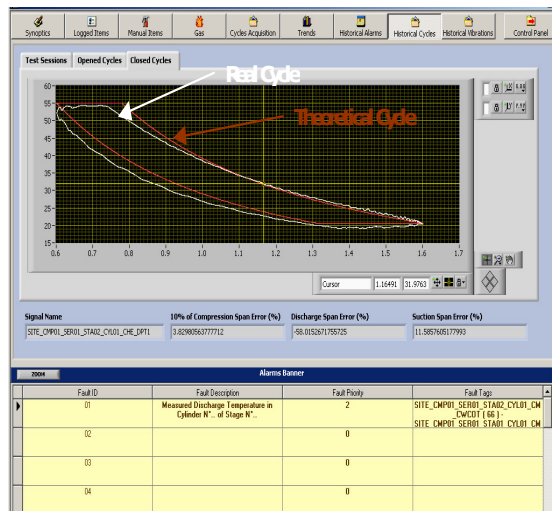


Figure 8: P-V Cycles

## 5.2 Static data

The data acquired by standard DCS or acquisition modules are generally static parameters. They are classified in two different categories: process data and other parameters. The former are necessary for the mathematical model; the latter are necessary to discern further details of anomalies.

Examples of process data parameters are suction or discharge pressure or temperature, gas composition, oil pressure, oil temperature, suction filter differential pressure, coolant fluid pressure and temperature.

The most frequent anomalies detected from the deviation of process data affect the following components: separators or suction filters, cylinder valve un-loaders, crosshead shoes, capacity control system and water cooling system.

Other parameters include the main bearing temperature, valve cover temperature, crosshead temperature and connecting rod big-end bearing temperature.

By monitoring the main bearing temperature (Fig.9) it is possible to detect various anomalies such as: oil cooler failures, main bearing wear or contamination in the crank-mechanism oil.

Monitoring the valve cover temperature (Fig.6) gives the ability to assess various anomalies such as: wear of cylinder piston rings, suction and/or discharge valve failure or capacity control system failure.

A new crosshead pin and connecting rod big end bearing temperature system (based on radar technology) allows continuous acquisition of the temperature of these moving components (Fig.10) through a 4-20 mA signal. An anomalous increase of this parameter can be attributed to various malfunctions such as a leak on load reversal of the crosshead pin or contamination in the crank-mechanism oil.

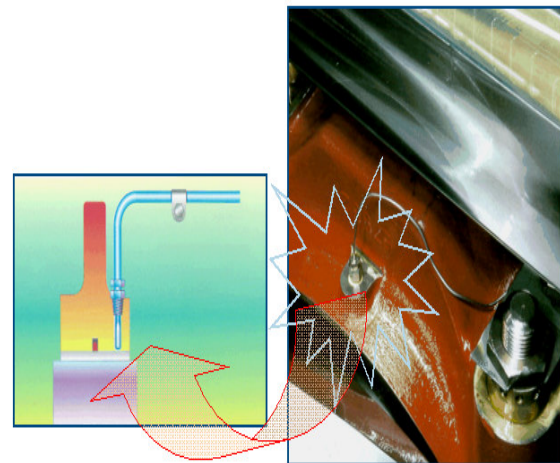


Figure 9: Bearing temperature monitoring

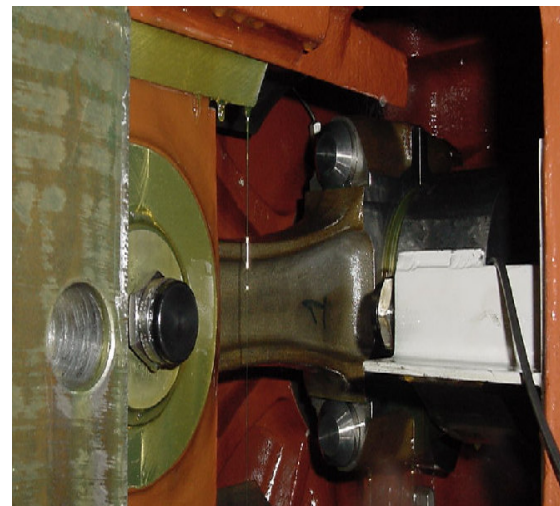


Figure 10: Crosshead pin and connecting rod big-end bearing temperature monitoring

## 5.3 Trends and history log

The measured static parameters are acquired using two different sampling times: the slower rate allows storage of data for a period of 3 months; the faster, storage for 24 hours.

The dynamic parameters are acquired, processed and stored using a dedicated system.

Old data are updated in the history log every 3 months.

## 5.4 System protection

The diagnostic system allows comparison of the measured values with the expected values generated by the model. The software processing unit analyzes all changes in the thermodynamic conditions of the compressor and updates the expected values in real time.

E. Giacomelli, E. Calamai, D. Martinelli, N. Monachino:  
Advanced Monitoring and Diagnostic System for Reciprocating Compressors

Every displayed parameter has three different associated states indicating its condition: green, yellow and red. The green state indicates that the value of the measured parameter is good; the yellow state indicates that the value is at the upper or lower limit of a predefined low-criticality range; the red state indicates that the value is at the upper or lower limit of the predefined a high-criticality range.

In case of a failure, the diagnostic system shows all the deviations of parameters and a detailed list of associated anomalies using special synoptic diagrams for each subsystem (gas (Fig.11a), oil (Fig.11b), cooling (Fig.11c), main driver, etc.).

The system can be configured to send to designed personnel the last occurring failure or the complete list via email, LAN or telephone messages.

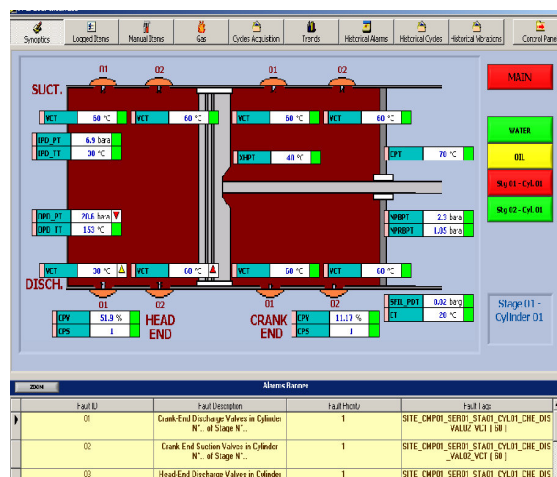


Figure 11a: Gas System synoptic

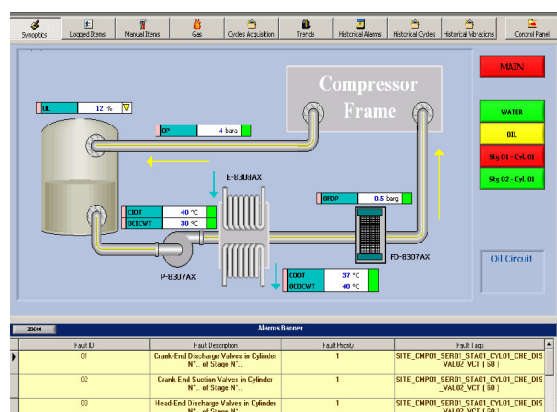


Figure 11b: Oil System synoptic

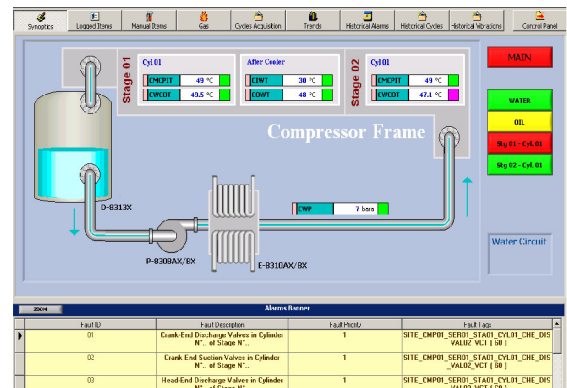


Figure 11c: Cooling System synoptic

## 6 Optimizing the Performance of Machines

Optimizing performance is a priority for the engineers involved initially in the design and later in the operation of the compressor. Reengineering activities, conducted in association with proactive service programs, include consideration of technologies and support systems to influence the performance of the machine, with the objective of updating the design or adapting it to new plant operating conditions.

Opportunities exist to exploit RAM (Reliability Availability Maintainability) engineering to enhance new units and existing fleets alike. Some of the RAM activities for supporting products include Reliability Block Diagram (RBD) simulation and Reliability Centered Maintenance (RCM) studies.

RBD is used during the design stage to evaluate the most critical components and to define necessary actions to improve the equipment's reliability. The evaluation of the design reliability and the potential availability of the machine and its auxiliaries is carried out utilizing special RBD software. The RBD is a graphical representation of the components/subsystems of the machine and their influence on reliability.

The analysis considers the system design and operating characteristics and determines failure modes, the affected components, items to be included in a maintenance plan; and finally it recommends the maintenance strategy and a list of high-level maintenance actions.

These various diagnostic systems are crucial for enhancing efficiency, cost savings and safety in the operation of reciprocating compressors and their auxiliaries. Through accurate and methodical monitoring of operations and process parameters, such systems make it possible to optimize the efficiencies gained through predictive maintenance.

### 7 Conclusions

Reciprocating compressors are continually becoming more efficient, thanks to advanced materials, engineering methods, automation systems and plant maintenance.

The safety of new installations and modernized facilities equipped with the latest generation of compressors (featuring remote monitoring systems and diagnostics system on site) is improved particularly in plants operating on hazardous fluids, or high operating pressures or temperatures. This technology simplifies operation by offering centralized control and monitoring systems and can enhance production.

Plant activities are constantly being enhanced through automation, reducing the cost of manual operations and improving reliability and efficiency. In addition, benefits from the latest compressor developments, such as automatic monitoring systems, permit predictive rather than preventive maintenance policies.

These improvements result in reduced operation and maintenance costs, and safer and improved working conditions.

### 8 Acknowledgements

The authors wish to thank GE Energy Oil & Gas Nuovo Pignone for the permission to publish the information reported in this paper.

---

### References

- [1] Chellini R., 1997, "Upgrading of Reciprocating Compressors Prove Economical Solution to Increased Plant Capacity" - Diesel & Gas Turbine Publications – Compressor Tech, Sept/Oct.
- [2] Generosi S., Passeri M., 1995, "The Control of Vibrations Induced by Reciprocating Compressors on Plant Piping: New Developments in Calculation Methods", Quaderni Pignone N. 56.
- [3] Giacomelli E., Agostini M., Cappelli M., 1986, "Availability and reliability in Reciprocating Compressors Evaluated According to Modern Criteria", Quaderni Pignone N. 42.
- [4] Giacomelli E., Montelatici A., Agostini M., Minardi M., 1991, "Automation and Diagnostic in Operation and Predictive Maintenance of Reciprocating Compressors", Quaderni Pignone N. 50.
- [5] Giacomelli E., Agostini M., 1992, "Safety, Operation and Maintenance of LDPE Secondary Compressors, PVP, Vol. 238, Codes and Standards and Applications for High Pressure Equipment, ASME 1992.
- [6] Giacomelli E., Falciani F., Dini R., Giusti A. 2001, "Design and Service Engineering to Improve Reliability of Reciprocating Compressors", NPRA 2001, Clean Fuels Challenge, Aug.28-29, Houston TX, USA, National Petrochemical & Refiners Association, CFC-01-211.
- [7] Giacomelli E., Fani R., Pratesi S., Gimignani L. 2002, "Improving Availability of Hyper-compressors" ASME-PVP- 2002 Vol. 436, Vancouver, Aug 2002.
- [8] Giacomelli E., Traversari A., 2001, "Very high pressure compressors (over 100 Mpa [14.500 psi])", Compressors Handbook, P.C.Hanlon ed., Mc-Graw-Hill, NY.
- [9] Giacomelli E., Giusti S., Lumachi F., Savelli F., 2004, "Control and diagnostic of reciprocating Compressors", Hydrocarbon Engineering,, October.



# **Analysis of Torsional Vibrations in Reciprocating Compressors driven by Electric Motors and Gas Engines**

by:

**Dr.-Ing. Andreas Laschet**  
**ARLA Maschinentechnik GmbH**  
**Hansestr. 2**  
**D-51688 Wipperfürth**  
**Germany**  
**E-mail: [a.laschet@arla.de](mailto:a.laschet@arla.de)**  
**Internet: [www.arla.de](http://www.arla.de)**

**4<sup>th</sup> Conference of the EFRC**  
**June 9<sup>th</sup> / 10<sup>th</sup>, 2005, Antwerp**

## **Abstract:**

Torsional vibrations usually occur in rotating machinery due to the dynamic behavior of motors (electric motors or gas engines) and driven machines like reciprocating compressors. It is necessary to detect critical speed ranges in advance by using suitable calculation methods. On the one hand standards and rules are applied, on the other hand advanced simulation tools are helpful to find the optimum driveline configuration considering nonlinear or transient effects and extended model structures. Simulation technologies can be used to determine the system sensitivity for an optimum rating of the dynamic system behavior.



## 1 Introduction

The analysis of torsional vibrations (TVA) in drivelines with reciprocating compressors is one of the major CAE tasks in the R&D domain. In order to determine the vibrations a priori – that means before the rotating machinery has been built – it is necessary to use industry proven simulation methods for the analysis<sup>1,2</sup>. API standards and publications (like: API 618<sup>3</sup>, tutorial according to API 684<sup>4</sup>) are important to notice, but can only cover a part of the whole analysis. Further literature describes the typical torsional vibration problems and how to solve them in more detail<sup>5,6</sup>. Due to the complex superimposition of dynamic effects allocated to the driving machine (electric motors or gas engines) and to the reciprocating compressor it is necessary to analyze the driveline as a whole.

Advanced simulation tools are used to analyze the dynamic behavior in the time or frequency domain, and also to investigate nonlinear effects<sup>7</sup>. Further studies are important to check the system sensitivity in terms of the variation of specific drive elements (like couplings, flywheels) and also the sensitivity with reference to the overall system configuration. Thus, it is the target to find out the best "rating" concerning the sensitivity of the system behavior and the parameter range in correlation with specific speed margins.

The typical procedure how to do a TVA of a complete drive system<sup>8</sup> is described in Fig. 1.

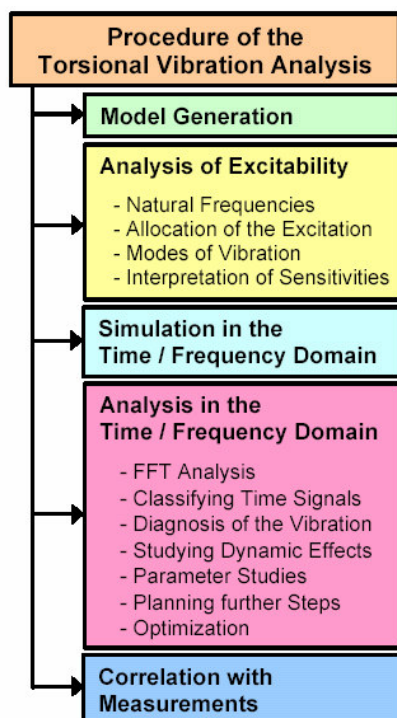


Figure 1: TVA procedure

## 2 Model Generation

### 2.1 Basics on Modelling

The first step of a torsional vibration analysis is to create a practice-oriented simulation model, which is not too complex but straightforward with reference to the engineering task, the reasonable model size, and the computation time (Fig. 2). Sometimes a target conflict occurs between the model size and the model quality.

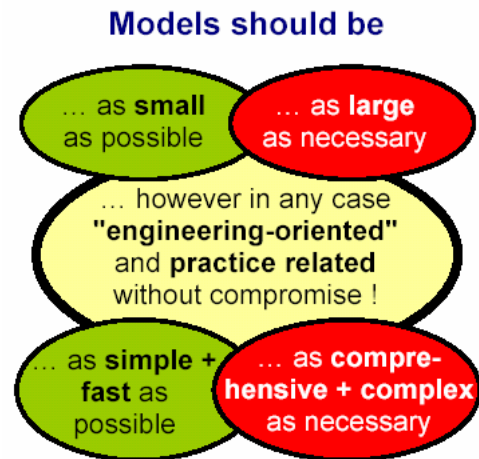


Figure 2: Model complexity

The following model building rules are to be respected<sup>1,8</sup>:

- formulation with respect to the planned model
- determination of the model limits
- model generation using reduction rules
- analysis of the linear model (natural behavior)
- "analysis of excitability" (i.e. interpretation of all natural frequencies and the corresponding modes)
- 1<sup>st</sup> model validation
- model extension (excitations, nonlinearities)
- test calculations, qualitative evaluations (concerning comprehensibility of the model)
- model reduction or extension, 2<sup>nd</sup> validation
- model refinement, quantitative evaluation
- discussing the model sensitivity (concerning data uncertainties or variations)

The discrete torsional vibration model consists of lumped inertias connected by stiffness elements (flexible, elastic connection). The inertias (i.e.: moments of inertia) are modelled as rigid masses, the stiffnesses (shafts, gear stages, connections between two coupling halves, etc.) have no masses.

Dimensions of the dampings are not necessary for the calculation of the natural frequencies and modes of vibration; in other words: we consider an undamped system first. See Fig. 3 for a typical torsional vibration model of a reciprocating compressor system driven by an electric motor (machinery "A"), and Fig. 4 showing a driveline with a gas engine (machinery "B").

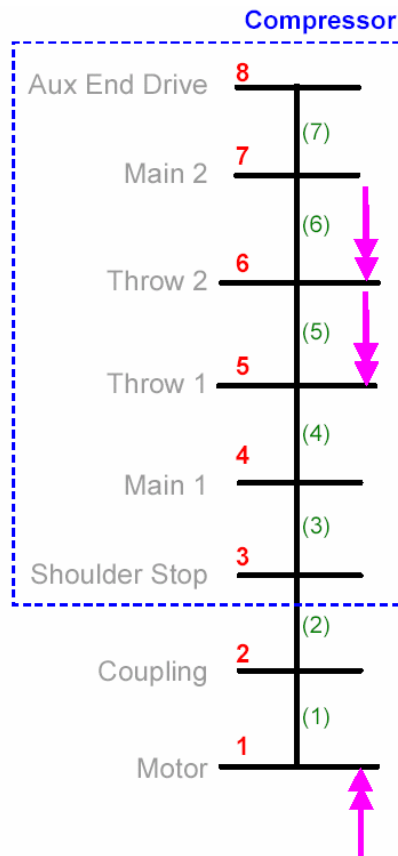


**Figure 3:** Driveline "A" with an electric motor

The main difference between the two systems is the modification of the model accuracy in terms of the inertia-stiffness-distribution on the driving side: Whereas an electric motor is – from the mechanical point of view – a single inertia, the gas engine has to be considered as a flexible subsystem with a flexible crankshaft system. On the other hand, it is also possible to distinguish between three different model strategies in case of engine driven systems. As shown in Fig. 5 the crankshaft may be a flexible, or rigid subsystem, or even neglected if a ground induced excitation is considered. For the model generation of a reciprocating compressor driveline the crankshaft of both engine and compressor should be taken as a flexible system (see Fig. 5a). The structure of a ground induced vibration model has significant disadvantages because the influence of the flywheel is neglected.

## 2.2 Determination of the Parameters

The system parameters, such as mass moments of inertia and torsional stiffnesses (elasticities), are derived from drawings. The base elements are

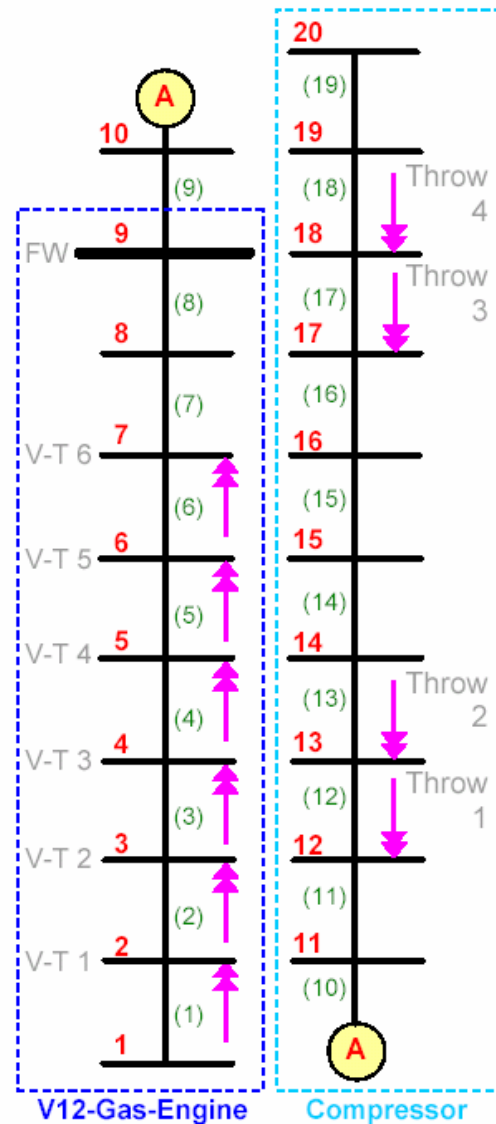


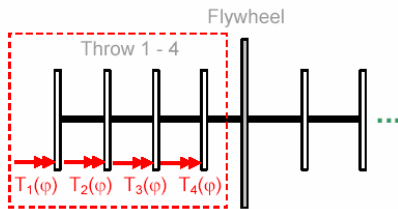
**Figure 4:** Driveline "B" with a gas engine  
V-T = throws of the Vee shape engine  
FW = flywheel

cones or cylinders. Thus, the geometrically generated model data usually are of high accuracy. A problem arises in case of the compressor or gas engine crankshaft. If there is no FEM model available to calculate the stiffness distribution of a crankshaft from throw to throw, we may use empirical formulae which are described in more detail in the literature<sup>9,10,5</sup>.

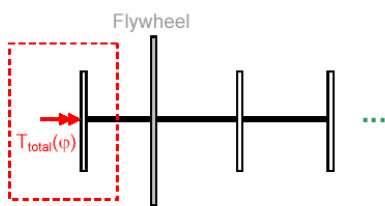
The important damping coefficients are determined later having finished the analysis of excitability. The subsequent model generation step will require

the input of all necessary excitation data corresponding to the compressor type, the load and speed situation, and the motor or gas engine excitation.

a) Flexible Crankshaft Model



b) Rigid Crankshaft Model



c) "Ground Induced" System

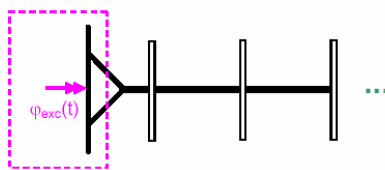


Figure 5: Crankshaft models

### 3 Analysis of Excitability

The first step of the analysis of the dynamic behavior of a drive system comprises the analysis of the natural behavior in terms of natural frequencies (eigenvalues) and the corresponding modes (vibration modes, eigenmodes) of the torsional vibration system. For this particular analysis we assume a linear torsional vibration system and disregard the damping influence, because damping does not influence the natural behavior considerably in the application which we discuss in this paper.

Usually, an  $n$ -mass system has  $n$  eigenvalues. The very first eigenvalue is always zero; this eigenvalue represents the rigid motion of a rotating drive system. Thus, the first significant natural frequency, which has to be considered as critical frequency, mathematically spoken is the second eigenvalue.

The modes are visualized as normalized values in three different ways:

- "Angular Displacement PHI" relating to every inertia station

- "Kinetic Energy EKIN" relating to every inertia station
- "Potential Energy EPOT" relating to every stiffness station

The energy visualization, which is an industry-proven method and first introduced by the author in 1988<sup>1</sup>, has typical advantages. The EKIN amplitudes represent the most important stations (inertias) which might be sensitive to external excitations as they occur in reciprocating machinery (like gas engines, reciprocating compressors). This method can also be applied to parametrical excitations due to the gear mesh in case of toothed gear stages. The mode visualization as EPOT amplitudes represents the most important elasticities (stiffnesses) which might indicate a critical element (like motor shaft, coupling, sections of the crankshaft) in resonance, if an excitation does really exist with the corresponding excitation frequency and a (considerable) dynamic amplitude. Therefore, the analysis of excitability supported by the energy analysis method is rather useful to understand the natural behavior on the one hand, and to find the most sensitive elements of a total drive system on the other hand. The knowledge of the sensitivity of drive elements with respect to torsional vibrations is important for the uncertainties of data<sup>11</sup> and also for the possibility to modify parameters in an acceptable range.

Fig. 6 shows a typical mode distribution of a discrete torsional vibration system for a specific natural frequency splitted in the three presentations of PHI, EKIN, and EPOT.

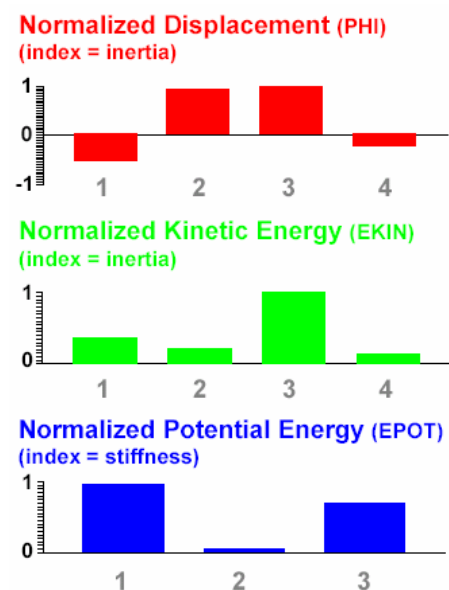
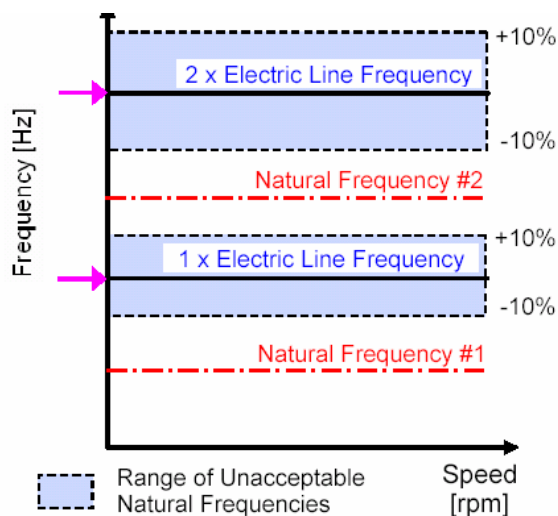


Figure 6: Vibration modes for a specific torsional natural frequency, visualized as PHI, EKIN, EPOT

The "Analysis of Excitability" also covers the visualization of possible resonance domains. Usually these resonances are graphically presented in the so-called CAMPBELL diagram (resonance diagram). This diagram shows the frequencies (=speed dependent excitation frequencies of every order and also the speed independent natural frequencies) vs speed (=operating shaft speed). The order lines refer to the excitations (1<sup>st</sup>, 2<sup>nd</sup>, and following orders). Higher orders greater than the 10<sup>th</sup> are also considered in the calculations, but usually they are not significant with respect to the maximum peaks in the signal responses. Due to the assumed linear system behavior during the analysis of excitability we just have to consider constant, load independent natural frequencies.

The interpretation of resonance domains in drivelines with reciprocating compressors is described in more detail in API 618<sup>3</sup> and API 684<sup>4</sup>. Fig. 7 shows the unacceptable frequency ranges in case of an excitation induced by the electric motor. It is obvious that there is no dangerous speed domain to be monitored but the speed independent single and double line frequencies (50 / 100 Hz or 60 / 120 Hz). Any torsional (and also flexural and lateral) natural frequencies  $\pm 10\%$  should be avoided. The 1<sup>st</sup> and 2<sup>nd</sup> motor speed order is also of importance, because resonance problems could also occur due to imbalances.

In Fig. 8 we study possible resonance domains in case of the excitations induced by reciprocating machinery like gas engines and reciprocating compressors. We observe the excitations with  $1x_n$ ,  $2x_n$  and multiple orders of the shaft speeds for a 2-stroke system (compressor), and with  $0.5x_n$ ,  $1x_n$ ,  $1.5x_n$  and multiple orders for a 4-stroke engine.



**Figure 7:** Visualization of unacceptable frequency ranges (excitations induced by an electric motor)

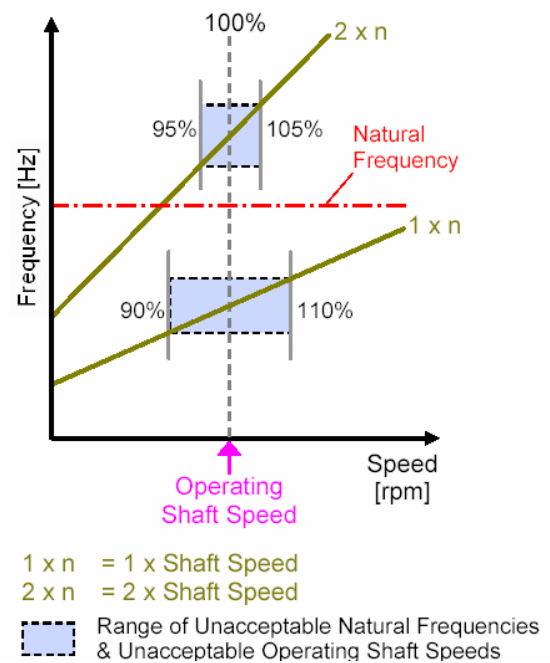


**Figure 8:** Visualization of unacceptable frequency and speed ranges (external excitations induced by the reciprocating machinery)

According to the type of the reciprocating machinery we consider the relevant excitation orders. Although API standards consider orders up to 10 as maximum, we should keep in mind that a V12 gas engine goes up to the 12<sup>th</sup> order (in steps of 0.5 due to the 4-stroke engine concept), and even the reciprocating compressor shows magnitudes with the orders of 11 and 12.

Before the dangerous and unacceptable range of operating speeds and frequencies is analyzed in detail, we should study the external excitations first. In this paper the TVA is presented for two different types of machinery: one machinery driven by an electric motor (designated as machinery "A", see Fig. 9 for the compressor excitation), and a second machinery driven by a gas engine (designated as machinery "B", see Fig. 10 for the gas engine excitation, and Fig. 11 for the compressor excitation). The different magnitudes and order characteristics between the single throw (single cylinder) excitation and the superimposed torque curve is obvious. The excitation does depend on both speed and the corresponding load situation.



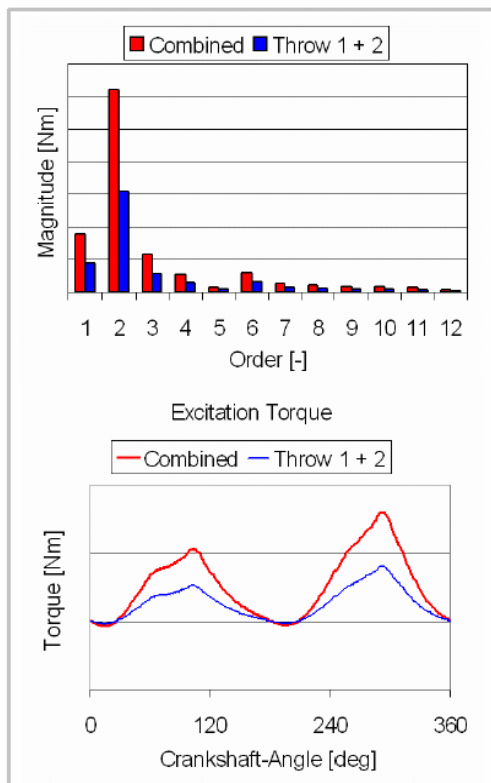


**Figure 9:** Machinery "A" – compressor excitation (2-throw compressor)

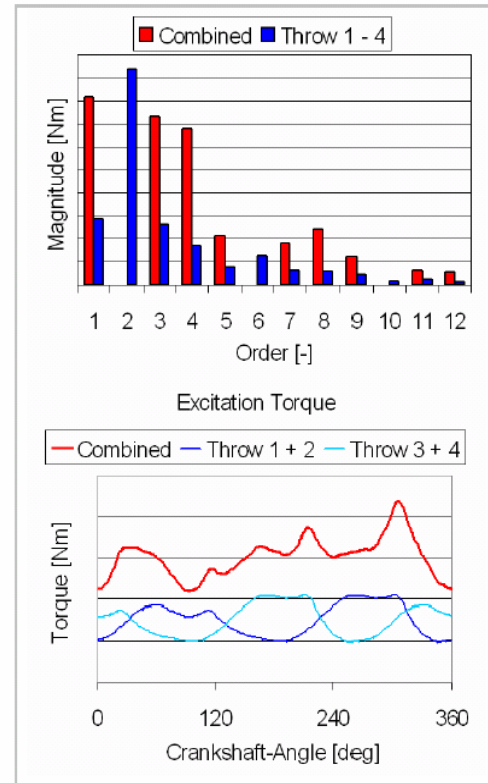


**Figure 11:** Machinery "B" – compressor excitation (4-throw compressor)

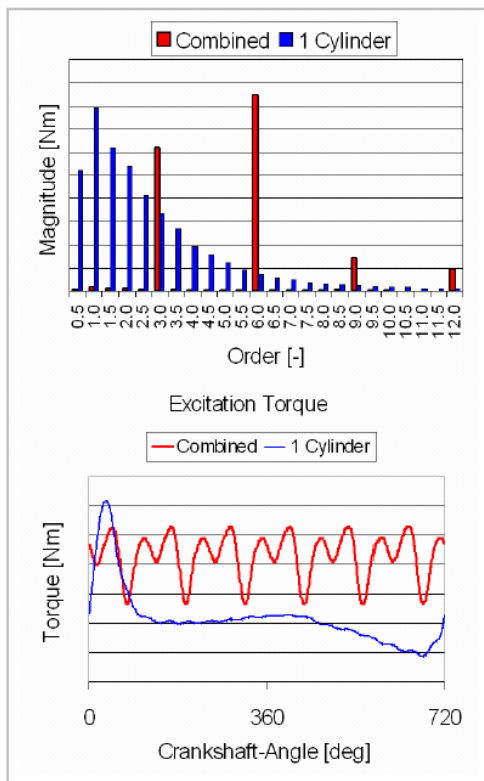


**Figure 10:** Machinery "B" – gas engine excitation (V12 engine)

According to API 618<sup>3</sup> (Ch. 2.5.2) the "torsional natural frequencies of the driver-compressor system (including couplings and any gear unit) shall be avoided within 10 % of any operating shaft speed and within 5 % of any multiple of operating shaft speed in the rotating system up to and including the tenth multiple". However, as the load situation varies, it is recommendable to use modern simulation technologies<sup>7</sup> in order to calculate the actual torques (including the maximum torsional stresses) for the operating speeds or the required speed range. The margins  $\pm 10\%$  or  $\pm 5\%$  are only approximate figures or reference values and may vary due to the real operating conditions.

## 4 Simulation of Torsional Vibrations

### 4.1 Machinery "A" (Electric Motor)

The TVA<sup>12</sup> includes the calculation of the real torques and torsional stresses in all drive elements considering the operating load and excitation conditions. Therefore, it is necessary to use the model as presented in Fig. 3 in order to calculate the torque response for every speed (and even for every time step). The applied simulation method does consider time dependent and nonlinear effects as well and is a suitable computation tool in order to verify the exact margins concerning permissible operating speeds. See Fig. 12 for more details with

reference to possible resonance speeds. The correlation between the CAMPBELL diagram and the torque signal is very good. It is obvious that the higher excitation orders (8, 9, 10) due to the compressor dynamics intersect a torsional natural frequency and cause higher magnitudes within the speed range from 750 to 990 rpm. A stress analysis has been carried out to show that safety and service factors are within acceptable margins. In order to carry out the simulation we need the knowledge of real damping coefficients which can be derived from the analysis of excitability by allocating stiffness elements to the most efficient modes EPOT modes<sup>1,8</sup>.

Similar calculations have been done to optimize the driveline of a CNG compressor station<sup>13</sup>. In this case a special flywheel configuration could improve the dynamic behavior significantly leading to a real advantage for the design of the total system including the control characteristics.

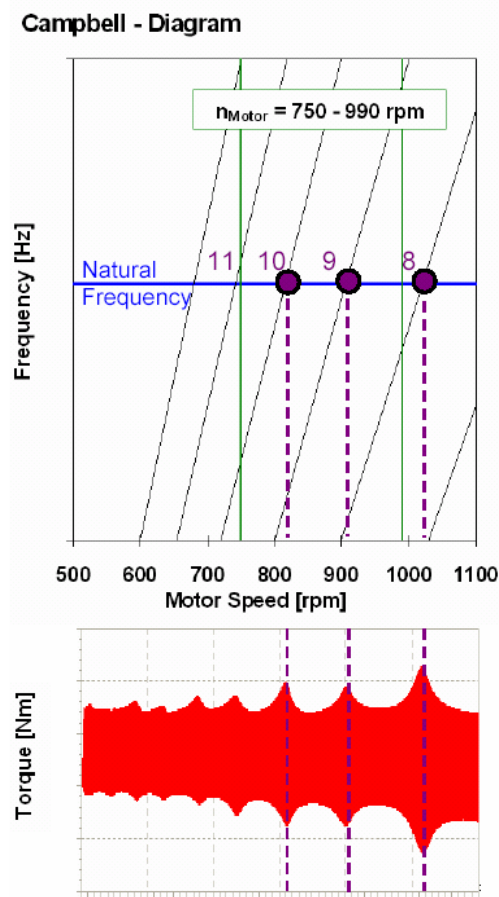


**Figure 12:** Machinery "A" – simulation results and correlation with the CAMPBELL diagram

## 4.2 Machinery "B" (Gas Engine)

A compressor machinery driven by a gas engine (see Fig. 4) must be analyzed in two directions: considering the excitation due to the reciprocating engine on the one hand and due to the reciprocating compressor on the other hand. The simulation should consider the speed dependent load. Furthermore there are typical dynamic effects which could cause problems in the driveline<sup>5</sup>:

- a) Gas Engine:  
engine misfire conditions, pressure imbalances, ignition problems, leaks
- b) Compressor:  
valve failure, gas pulsation, load steps

The applied simulation method in the time domain does also cover nonlinear effects as they may occur in rubber elements. Furthermore it is recommended to distinguish between the gas pressure effects and the inertia effects which are typical of any reciprocating process. The gas engine excitation primarily runs with the 3<sup>rd</sup>, 6<sup>th</sup>, and 9<sup>th</sup> order, whereas the compressor excitation is characterized by the 1<sup>st</sup>, 3<sup>rd</sup>, and 4<sup>th</sup> order.

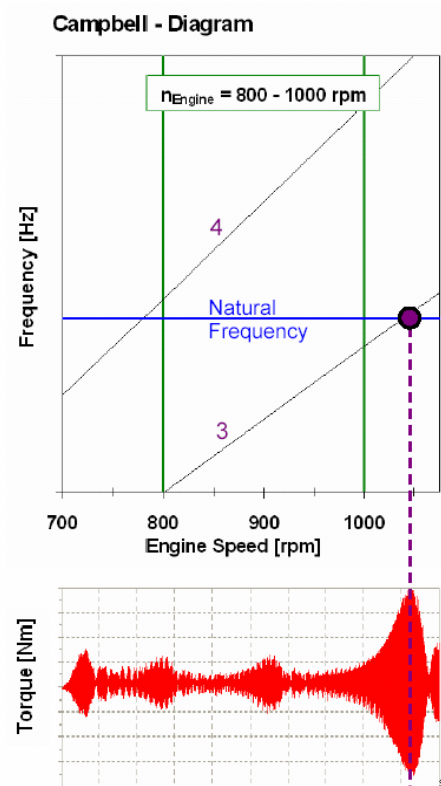


**Figure 13:** Machinery "B" – simulation results and correlation with the CAMPBELL diagram

Fig. 13 shows the 1<sup>st</sup> torsional natural frequency of this drive system together with the required operating speed range. No severe problem is detected, because the major order 3 is outside of the speed range.

Special rating functions are used to detect unallowed speed ranges. Such rating functions depend on the torque and stress peaks which occur in the operational speed range.

## 5 Conclusion

Computer simulation is a useful tool to analyze torsional vibrations in rotating machinery. The specific dynamic effects, which occur in reciprocating compressor drivelines, are analyzed in the time domain and presented in both time and speed domain. The influence of electric motors on the one hand and reciprocating gas engines on the other hand can be considered. As the state-of-the-art simulation software packages are very powerful, accurate and fast in terms of the computation time, it is recommendable to use such methods instead of relying on standard rules only.

The simulation methods as presented in this paper can also be used, if the requirements concerning the calculation exceed the requirements according to the API standards.

## 6 Acknowledgments

The author wishes to thank Dr.-Ing. Siegmund Cierniak from HGC Hamburg Gas Consult GmbH, Hamburg, Germany for his kind support concerning the projects which are the basis for the presented torsional vibration studies. Furthermore the author likes to thank Dipl.-Ing. (FH) Andreas Stöcker from ARLA Maschinentechnik GmbH for his assistance doing the calculations, the detailed analyses, and preparing the graphical presentations for this paper.

## References

<sup>1</sup> Laschet, A.: Simulation von Antriebssystemen, Fachberichte Simulation Vol. 9. Berlin, Heidelberg, New York: Springer-Verlag 1988

<sup>2</sup> Laschet, A.: Computer Simulation of Vibration in Rotating Machinery. Machine Vibration (1992) 1, pp. 42-51. London: Springer-Verlag 1992

<sup>3</sup> API Standard 618: Reciprocating Compressors for Petroleum, Chemical, and Gas Industry Services, 4<sup>th</sup> Ed., American Petroleum Institute, June 1995

<sup>4</sup> API Publication 684: Tutorial on the API Standard Paragraphs Covering Rotor Dynamics and Balancing: An Introduction to Lateral Critical and Train Torsional Analysis and Rotor Balancing, 1<sup>st</sup> Ed., American Petroleum Institute, Febr. 1996

<sup>5</sup> Feese, T.; Hill, Ch.: Guidelines for Preventing Torsional Vibration Problems in Reciprocating Machinery. Gas Machinery Conference, Nashville, Tennessee, 2002

<sup>6</sup> Wachel, J.C.; Szenasi, F.R.: Analysis of Torsional Vibrations in Rotating Machinery.

Proceedings of 22<sup>nd</sup> Turbomachinery Symposium, pp. 127-151, Texas A&M University 2003

<sup>7</sup> Various Software Packages: ITI-SIM, ITI-STAT, ARMD, ARLA-SIMUL, ARLA-SIMSTAT, special ARLA model building tools

<sup>8</sup> Laschet, A.: Torsional Vibration Analysis (TVA), Internal Report "ARLA Service for Engineers", No. R-TVA / 3.0, 2004 (<http://www.arla.de>)

<sup>9</sup> Harris, C.M.; Piersol, A.G.: Harris' Shock and Vibration Handbook, 5<sup>th</sup> Ed., New York: McGraw-Hill, 2001

<sup>10</sup> Rangwala, A.S.: Reciprocating Machinery Dynamics. New York: Marcel Dekker 2001

<sup>11</sup> Murray, B.D.; Howes, B.C.; Chui, J.C.; Zacharias, V.: Sensitivity of Torsional Analyses to Uncertainty in System Mass-Elastic Properties. 1<sup>st</sup> International Pipeline Conference, Vol. 2, pp. 975-982. New York: ASME 1996

<sup>12</sup> Stoecker, A.; Laschet, A.: ARLA Reports, Hamburg: HGC 2002-2005

<sup>13</sup> Laschet, A.; Cierniak, S.: Drehschwingungen in einer CNG-Tankstellen-Verdichteranlage. GWF Gas-Erdgas 146 (2005) No. 2, pp. 112-119

# **Increased Reliability and Extended Service Intervals in an Ethylene Oxide Plant**

by:

**Dr. Seedorf, Michael and Bartsch, Ulrich**  
**Technical Services Marl**  
**Sasol Germany GmbH**  
**45764 Marl**  
**Germany**  
**michael.seedorf@de.sasol.com**

**4<sup>th</sup> Conference of the EFRC**  
**June 9<sup>th</sup> / 10<sup>th</sup>, 2005, Antwerp**

## **Abstract:**

Sasol Germany, the German subsidiary of the South-African Sasol Ltd., operates – besides other production plants – an Ethylene Oxide plant in the Chemical Park at Marl, West of Germany. Two 2-stage piston compressors are in service to recompress residual gas to process pressure level. Efficiency was increased with optimisation and maximum utilisation of wear parts. Consequently, the service intervals of these critical reciprocating parts were extended significantly. Secondly, operation is more reliable since the implementation of safety-oriented monitoring methods. This paper describes how the implementation of a monitoring strategy leads to a more efficient and reliable machine operation and is split into the following parts: Description of plant and process; Operating conditions of the residual gas compressors; Objectives and optimisation activities; Achievement of objectives.



### 1 Introduction

Sasol Germany is a subsidiary of the South African Sasol Ltd., a global operating company in the oil, gas and chemical business. Sasol Germany belongs to the chemical part of the Sasol Group, mainly producing solvents, olefins and surfactants at five production sites. The headquarter is located in Hamburg. At the Marl site at the northern border of the Ruhr-Valley-Region in Northrhine-Westfalia Sasol Germany operates several production plants, one of them is an Ethylene Oxide plant (Fig. 1).



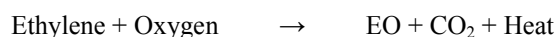
**Figure 1:** Ethylene Oxide Plant of Sasol Germany in Marl

### 2 Description of Plant and Process

Ethylene Oxide (EO) is one of the most versatile intermediates. Annual worldwide production exceeds 11 million tons, making it an important industrial chemical for a variety of everyday's applications like detergents & surfactants, cosmetics & bodycare products, antifreeze & solvents, etc.

The Ethylene Oxide (EO) plant is a typical interlinked production plant. The rawmaterials Ethylene and Oxygen are delivered via pipelines and converted in tubular reactors at a Silver catalyst under a pressure of about 20 bars.

Silver Catalyst



The heat of the exothermic reaction can be used for steam production. The formed EO Gas is then washed out in an absorption column with water, decompressed, condensed, and distilled. Then it is stored in a tank farm before it is sent either to the derivative plants on the site via pipelines or loaded into railcars and containers to be shipped to the customers.

The Ethylene Oxide plant consists of several hundreds of machines and apparatuses, i.e. columns, absorbers, heat exchangers, pumps, and compressors, etc. in different sizes and designs.

For the recompression of a number of residual gases to process pressure level two 2-stage piston compressors are in operation.

### 3 Description and Operation Conditions of the Residual Gas Compressors

The two identical 2-stage compressors were built in 1976 by Linde Type 2LX 220-2P, Mig (Fig. 2). The pistons are double-acting, dry-running in horizontal and opposed (boxing) position.



**Figure 2:** First stage (Ø 620 mm) of the Linde 2-stage piston compressor

In the first stage the gas is compressed from 1.4 bars(abs) and 29°C to 6.0 bar(abs) and 174°C, piston diameter is 620 mm. The second stage compresses from 5.1 bar(abs) and 38°C to 23 bar(abs) and 165°C, piston diameter is 320 mm. The flow rate is 3,000 Nm<sup>3</sup>/h at 585 rev/min and an electrical power of 520 kW. The gas mainly consists of Methane, Ethylene, and Carbon Dioxide with a content of ca. 30 % each, the rest consists of Nitrogen, Oxygen, Argon, Water, and other hydrocarbons (Fig. 3).

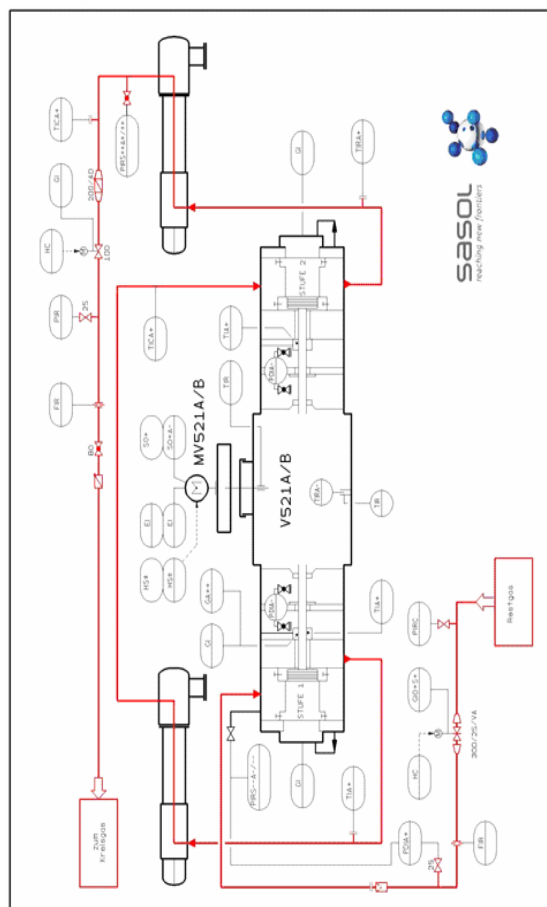


**Figure 3:** Flow sheet of the compressors

## 4 Objectives and Optimising Activities

Since commissioning both compressors had been running with a MTBR (mean time between repair) of 4,000 hours. After this time expensive inspections and repairing had to be executed. Especially all worn parts were exchanged periodically: Two rider rings and three piston rings of the first stage; two rider rings and five piston rings of the second stage; the inner parts of the main packing gland (Fig. 4); the oil wiper rings. Both piston rods had to be coated regularly with a chromium layer because of corrugations.

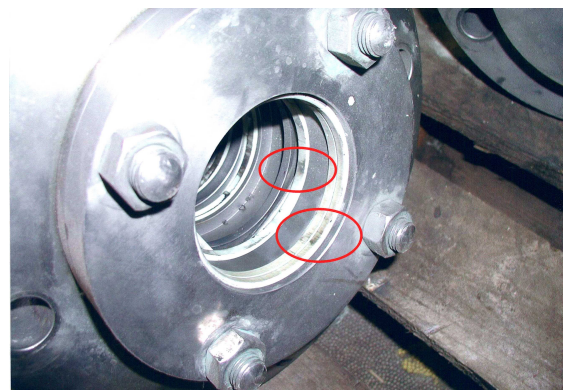


**Figure 4:** Main packing gland (PTFE) of piston rod with black spots caused by increased friction

The main objective of the optimisation activities was the extension of the MTBR from 4,000 hours up to 8 to 10,000 hours. This was done in several steps: Firstly the friction surfaces of the piston rods were coated with a material containing mainly tungsten, cobalt, and chromium using a kerosene-hypersonic technology. This formed a layer of 0.15 mm thickness and a surface hardness of 75 to 80 HRC. Secondly the cylinder liners were coated with a chromium material using the same technology which led to a surface hardness of 50 to 54 HRC.

The used kerosene-hypersonic technology is a so called continuous detonation coating system. The extremely high particle velocity leads to a strong adhesion on the basic material and to a high density of the sintered particles.

In a third step the main packing boxes of first and second stage were connected to the water cooling system.

The forth step consisted of a systematic search of suitable materials especially for the wear parts like rider and piston rings as well as for the packing glands and the oil wiper rings. The objective was to get an optimal PTFE transfer-layer between the friction surfaces and the wear parts.

For these action steps it was necessary to get reliable information about the conditions of the wear parts, what means early information about success or failure. Therefore an online monitoring system was installed at each compressor with the following features: Two vibration sensors were fixed on the cross head guides; two position sensors were fixed at the main packing boxes for the rod drop monitoring (Fig. 5).

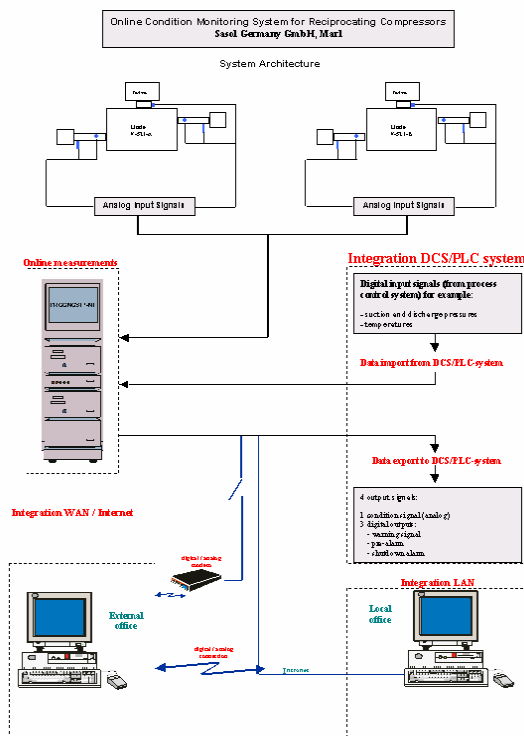


**Figure 5:** Architecture of the Online Monitoring System

The safety protection and condition monitoring system provides data logging, analysis, monitoring and diagnosis. The analogue sensor signals are digitised with a sampling rate of 25 kHz. The safety protection system ensures the analysis of each crankshaft revolution. It generates an alarm signal for the DCS system immediately, if a safety issue comes up. The condition monitoring system averages the analyses over several shaft revolutions and performs a separate threshold monitoring each minute.

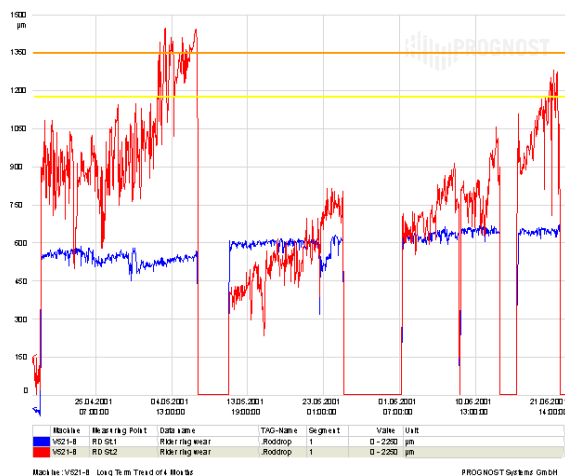


**Figure 6:** Rod drop analysis with increased wear

This monitoring system helped tremendously to recognise increased wear because of a bad choice of material combinations so that the compressor had to be taken out of service. The comparison of the indicated wear and actual wear showed extremely good correspondence. The difference was only 0.1 mm (Fig. 6).

## 5 Achievement of Objectives

On the other hand the monitoring signals were used to find the right material combinations for the aimed elongated service intervals. It took a few months of try and error till the best material was found which was indicated by a relatively smooth graph (Fig. 7). The chosen materials for the rider and piston rings as well as for the packing glands depend on the process conditions like pressure and temperature and on the components of the compressed gas. As a result the MTBR now amounts to more than 8,000 hours which means an improvement of 100 %.

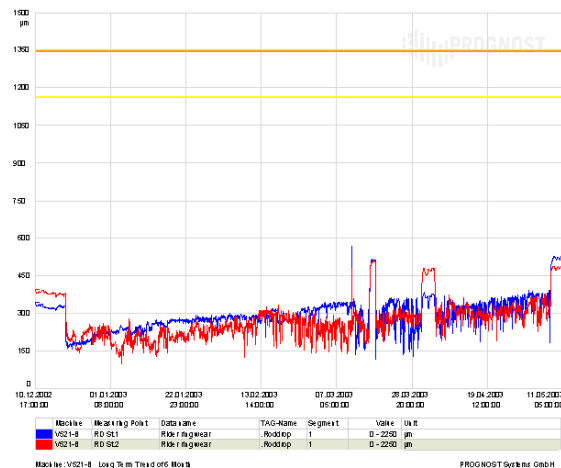


**Figure 7:** Relatively smooth signals for reduced wear

But the continuous online monitoring system shows a lot more important advantages than wear just monitoring. The early detection of pending mechanical damages by trend analysis leads to cost reduction and enhances availability. Furthermore the automatic alarm indication, in case of exceeded warning thresholds and the possible automatic shutdown of the compressors at critical operation conditions give significant safety improvements. In addition the integration and analysis of anyway available process data (DCS/PLC system) is helpful for fault analysis and cause study.

### 6 Conclusion

This paper shows how MTBR of a piston compressor was enlarged from 4,000 hours to more than 8,000 hours. That means an increase of more than 100 %. This result was reached by two main effects: The first is a systematic search of suitable material combinations for friction surfaces like piston rods or cylinder liners and the appropriate piston and rider rings as well as packing glands.

The second point is the installation of an online monitoring system which is a reliable instrument for the early detection of pending damages. Because of the doubling of the MTBR it is necessary to get an early indication of the state of these parts of the compressors which have been changed but also of those which haven't caused much trouble up to then.

As a result all described action steps led to a more reliable operation of the two compressors with an extension of the service intervals of 100 % combined with a significant reduction of maintenance costs. The supplier of the monitoring system is directly connected to the two compressors and keeps an eye on the signals 24 hours a day. Any untypical signals or the violation of limiting values are immediately analysed with the professional experience of the supplier. So it is possible to keep the almost 30 years old compressors in a good shape.

### 7 Acknowledgement

The authors would like to thank Christian Koers and Thorsten Bickmann, both Prognost Systems GmbH, for fruitful discussions, suggestions and support for the preparation of this paper.





## **Noise Reduction at a NAM-compressor Station**

**Harry Korst**

**Flow and Structural Dynamics  
(PULSIM)**

**TNO Science and Industry  
Delft**

**The Netherlands**

**harry.korst@tno.nl**

**Willem Brocatus**

**NAM-EPE-T-PC**

**Nederlandse Aardolie Maatschappij  
Assen**

**The Netherlands**

**willem.brocatus@shell.com**

**4<sup>th</sup> Conference of the EFRC  
June 9<sup>th</sup> / 10<sup>th</sup>, 2005, Antwerp**

### **Abstract:**

The introduction of a converted depletion compressor at the NAM-Grootegeest location resulted into excessive airborne noise levels that were clearly violating the permitted noise levels. Pulsation and noise measurements revealed that –high amplitude- pulsation levels at the higher compressor speed harmonics ( $> 300$  Hz) were the main cause of the problem. To investigate the attenuation of these pulsation levels a High-Frequency pulsation analysis was carried out, during which the effect of the installation of Multi-Bore Restriction Orifices (MBROs) at well-chosen locations was investigated. The analysis resulted in the recommendation to replace the existing single bore ROs with 15 MBROs. Pulsation measurements after the installation of the MBROs, confirmed a noise reduction of 7dBA. Together with other noise reducing measures like the application of pipe insulation and the sand filling of most supporting structures a total reduction of 15 dBA was achieved, clearly reducing the noise levels to within the permitted levels.

Final analysis shows that in this particular case the combination of a high-speed machine, the reverse flow capacity control system and a sub-optimal design of a re-used compressor was the main cause of the problem. To detect and solve these problems during the design stage, we therefore recommend carrying out a High Frequency pulsation analysis in those cases where a high-speed machines and/or a reverse flow capacity control system is used.

## 1 Introduction

To enable gas compression at the NAM-Grootegast location, the reciprocating compressor of the NAM-Suawoude location, was converted to a two-stage mode and reinstalled at Grootegast. The originally one-stage compressor made by Dresser Rand was equipped with two new larger cylinders to service the 1<sup>st</sup> stage. Also new 1<sup>st</sup> stage suction and discharge dampers were designed and installed. For the 2<sup>nd</sup> stage, two of the original cylinders and dampers were used. The compressor runs at a fixed speed of 985 rpm and can be operated at a variable suction pressure from 70 till 10 bar(a), while the discharge pressure varies between 96 and 66 bar(a). The process gas consists of natural gas, which has an average molecular weight of 18.9 g/mol.

In Suawoude the capacity of the compressor was step-controlled by the use of suction valve unloaders on the Head End of each of the four cylinders. To increase capacity flexibility, a stepless reverse flow capacity control system was installed on the Head and Crank End on each cylinder (Figure 1). The re-used original electromotor could not supply the power needed to operate the compressor at Grootegast at full load at high suction pressures. During these conditions the reverse flow system enables to operate the compressor at maximum power (maximum part loads). Capacity of the compressor can be controlled between 100 and 15% by the use of the reverse flow system.

When the compressor came into service at its new location, high airborne noise levels were encountered. Measurements of these noise levels revealed that levels were in excess of the allowable levels as laid down in Laws on Environment Control ('Wet Milieu Beheer'). Complaining neighbors further confirmed the excessive noise levels (Figure 2).

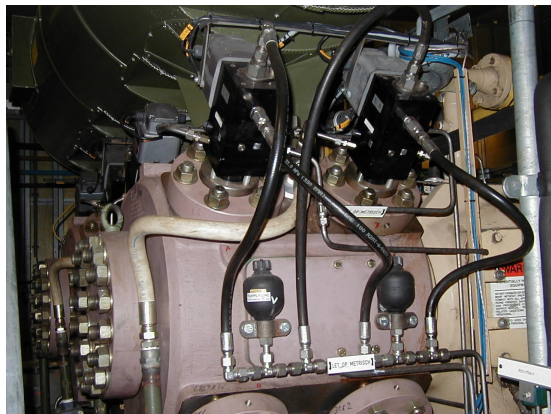


**Figure 1:** The suction side Head and Crank end of the compressor are equipped with reverse flow capacity controllers



**Figure 2:** Original noise contour as determined by an independent acoustic consultancy firm [1]; the dotted line indicates the permitted 50dBA noise contour

To secure production on the short term, a 10-metre high noise barrier was temporarily installed (Figure 3). This noise barrier that covered 3 of the 4 sides of the compressor installation is normally used during drilling activities. Meanwhile the search for a final solution was started, as it was not permitted to use the barrier as a permanent option.



**Figure 3:** In the background of this picture the temporary noise barrier is shown

Noise measurements further revealed that the process gas piping and its supporting outside the noise enclosure were the major sources of the encountered airborne noise levels. This means that a large number of secondary sources are present outside the compressor noise enclosure.

## 2 Field measurements

### 2.1 Pulsation and noise measurements

To further investigate the root cause(s) of this problem pulsation, vibration and noise levels have been measured by TNO. These measurements showed that in the process gas piping, large unexpected pulsation levels occurred at higher compressor speed harmonics ( $> 300$  Hz).

To investigate the possible relation between the encountered airborne noise levels and the pressure pulsations caused by the compressor, pulsation and noise levels have been synchronously measured at a large number of operating conditions. During some of the measurements the reverse flow control system was turned off. Pulsation levels have been measured in the 1<sup>st</sup> and 2<sup>nd</sup> stage suction and discharge pipelines. These four lines are the main process gas pipelines that feed and export gas to and from the compressor.

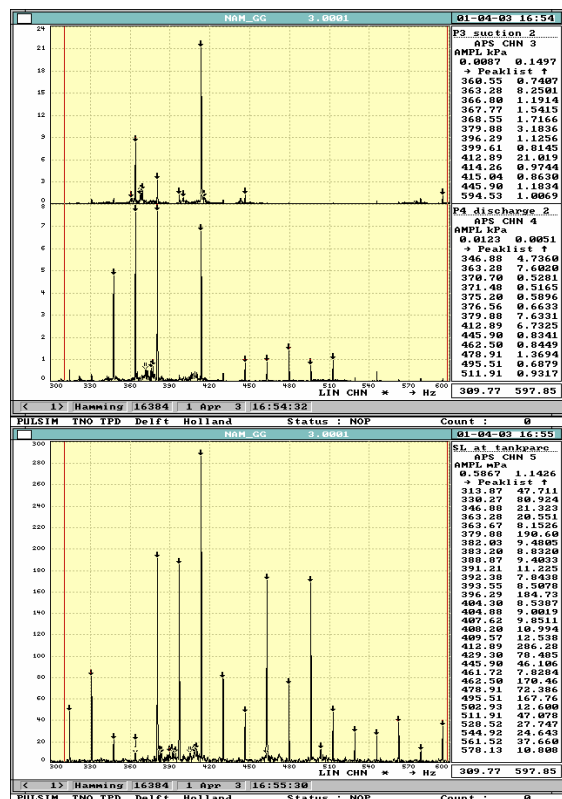


**Figure 4:** Example of measured pulsation (top) and noise levels (bottom); high-amplitude pulsation and noise levels between 300 and 600 Hz

In Figure 4 an example is given of the measured pulsation levels in the 1<sup>st</sup> stage suction and discharge piping. The FFT-analysis shows high-amplitude pulsation (top) and noise levels (bottom) between 300 and 600Hz. Vibration measurements showed that no excessive vibration levels occurred at the frequencies below 200 Hz. The mechanical integrity of the installation that had been analyzed in a 'standard' pulsation and mechanical response analyses (acc. API-Standard 618, design approach 3 [2], [3]), was not at stake here.

### 2.2 Barrier mass test

To investigate the effectiveness of possible noise reducing measures, a further test was carried out in which the effect of a temporary barrier mass was measured. The objective of this test was to investigate in which way energy from the compressor was transferred to the locations of the secondary sources of noise [4]. During this test two 12" 1500# horseshoe shaped flanges were mounted on an existing pair of 8" flanges in the suction 2<sup>nd</sup> stage piping (see Figure 5). In this way the test could be carried out without loss of production. The test showed that most of the energy was following the acoustical path. Here, pulsation levels in the process gas carry the energy of the compressor. The mechanical path, in which the pipe wall transfers the energy, appeared less important.



**Figure 5:** Barrier mass test

### 2.3 Effect of compressor load

Analyses of the measured pulsation and noise levels showed a clear relation between the occurring amplitudes and the compressor load. By making use of the reverse flow capacity control system we could continuously vary the compressor load. In Figure 6 audible noise levels [dBA] are printed as function of compressor load. In Figure 7 the synchronously measured pulsation levels in the 1<sup>st</sup> and 2<sup>nd</sup> stage suction line are presented. Note that also pulsation levels have been A-weighted and therefore are presented in a dBA-level.



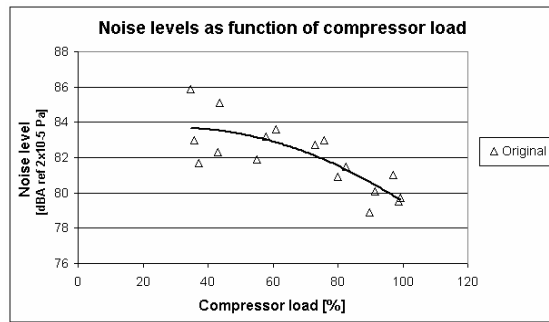


**Figure 6:** Measured noise levels as function of compressor load

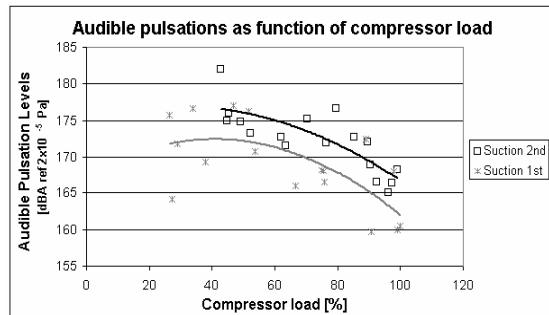


**Figure 7:** Measured pulsation levels in the suction 1<sup>st</sup> and 2<sup>nd</sup> st. piping as function of compressor load

Figures 6 and 7 indicate that both the measured noise and pulsation levels are depending on the compressor load. Both quantities show a tendency to higher amplitudes at a decreasing compressor load.

## 2.4 Conclusions of the measurements

The main conclusions of the field measurements are:

- The structural integrity of the installation is not at stake. Low-frequency (<200 Hz) pulsation levels and vibration levels are acceptable.
- The compressor is the cause of the excessive noise levels.
- The reverse flow capacity control system has an increasing effect on the occurring noise and pulsation levels.
- The compressor noise enclosure causes the expected amount of noise reduction. Secondary sources outside the noise enclosure are the main cause of the encountered excessive noise levels.
- The energy of these sources is transferred from the compressor by means of the pulsations in the process gas piping. Pulsation level amplitudes at frequencies above 300Hz are considerable.

## 3 High-Frequency Pulsation analysis

### 3.1 Introduction

As the high-frequency (HF) pulsation levels in the process gas piping are the main cause of the excessive noise levels, it is only logical that (part of) the solution has to be found in reducing these pulsation levels. For this purpose a high-frequency pulsation analysis was carried out by TNO. This High-Frequency pulsation analysis is executed as an extension of the normal low frequency analysis. The objective of the low-frequency analysis is to safeguard the mechanical integrity of the system. In this 'normal' analysis pulsation levels, vibration and cyclic stress levels are considered up to 200 Hz. Due to this low frequency range, radiated noise levels due to pulsations are not addressed in the API-Standard 618.

### 3.2 Model description

To be able to execute the analysis, the three acoustical models (suction, interstage and discharge piping) have been updated to accommodate resonance conditions at higher frequencies (smaller wavelengths). In practice this means that for instance parts of the cylinder passage volumes that originally were been modeled as volumes, are now modeled with their actual dimensions (lengths and diameters). To enable a direct comparison with the measured pulsation levels, simulations have been executed at the identical operating conditions that occurred during the measurements.

In this particular case the pulsation analysis has been expanded towards the 63<sup>rd</sup> harmonic frequency of compressor speed ( $\approx 1000$  Hz). The maximum frequency limit is dictated by the fundamental assumption of a 1 dimensional (1D) approach of the acoustical solution within the PULSIM software. This assumption imposes a maximum frequency where the so-called plane wave approximation is valid and can accurately be simulated according the following equation:

$$f_{\max} = 0.586 * \frac{c}{d_i} \text{ [Hz]} \quad [5]$$

in which:  $c$  is the speed of sound [m/s]  
 $d_i$  is the inner pipe diameter [m]

At a speed of sound of 400m/s and an inner diameter of an 8" Sch120 pipe, this results in a maximum frequency of 1280 Hz. Simulated pulsation levels have been compared to the allowable levels according API-Standard 618. Although this API-Standard is only intended for frequencies up to 200Hz (mechanical integrity), there are presently no known better alternatives.



## 3.3 Results of the analysis

During the HF-pulsation analysis the effects of installing restriction orifices (ROs) has been investigated. The objective of these orifices was to achieve acceptable HF (and LF) pulsation levels at the lowest possible pressure drop. Beside the pressure drop, also the location of the orifices and the effect of Multi-bore restriction orifices (MBROs) have been optimized. Due to the reduced wavelengths MBROs are usually most effective close to large volumes like dampers and separators.

Main conclusion of the acoustic analysis is that installing sleeve-mounted MBROs causes a significant reduction of the HF-pulsation levels. For most investigated operating conditions the HF-frequency pulsations are even reduced to levels below API-standard 618. The analysis therefore resulted in the recommendation to replace the existing single bore ROs by 15 sleeve-mounted MBROs. Most of the recommended MBROs are installed in the line and cylinder nozzles of the pulsation dampers. The chosen design of the MBROs deviates considerable from the standard ROs (see Figure 8).

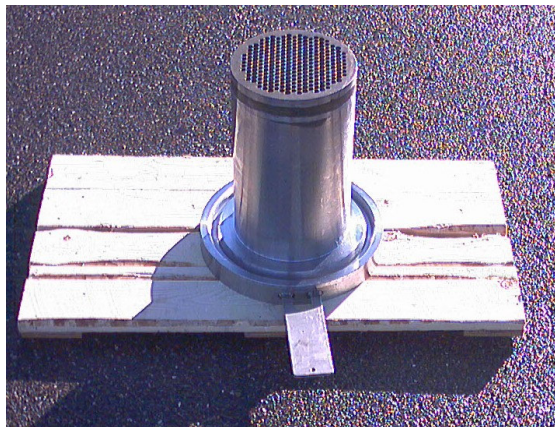


**Figure 8:** Multibore restriction orifice (MBRO), mounted at the end of a sleeve

The total additional pressure drop across these orifices is approx. 1.25% at 100% compressor load. So the average effect of each individual MBRO is limited to 0.1% additional pressure drop.

## 3.4 Other noise reducing measures

Beside the installation of the MBROs, also a number of other noise reducing measures have been discussed and implemented. The operator preferred to implement all noise reducing measures during one single shutdown of limited duration. A major advantage of this approach is that it has the maximum chance of achieving acceptable noise levels on the shortest possible term.

During a shutdown the MBROs were installed together with the following noise reducing measures:

- Application of acoustic insulation on all major process gas piping
- Application of sand-filling in most supporting structures
- Application of acoustic insulation on the supporting structures that could not be sand-filled

## 4 Effect of reverse flow capacity control system on pulsation levels

### 4.1 Introduction

From the noise and pulsation measurements in section 2 and the HF-pulsation analysis in the previous section it is clear that the reverse flow capacity control system has an effect on the occurring pulsation levels. In this chapter some background information on this phenomenon is given.

### 4.2 Reverse flow principle

The explanation of the reverse flow principle can best be given when looking at a PV-diagram. In Figure 9 a PV-diagram is given in which at point C (bottom dead center, BDC) the compression cycle starts.

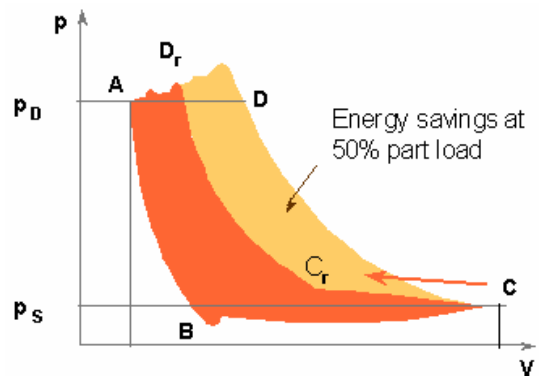


**Figure 9:** PV-diagram of a compressor

Under full load operation, the gas is compressed immediately after passing BDC. When the cylinder pressure reaches D the discharge valve opens. The gas is pushed out of the cylinder. When the piston reaches A (top dead center, TDC) the re-expansion begins. The gas, which is still present in the cylinder due to the cylinder clearance, re-expands. When the cylinder pressure reaches the suction pressure (B) the suction valve opens and gas is taken into the cylinder.

The power necessary for the operation of the compressor is proportional to the area enclosed by the indicator pressure curve.

To achieve capacity control the reverse flow regulation delays the closing of the suction valve. Thus cylinder pressure follows from C to Cr instead of from C to D. The required power consumption is therefore much lower than at full load. The slight pressure increase (C - Cr) is due to pressure losses in the suction valve. As the gas flows back from the cylinder chamber into the suction line, the quantity of gas in the cylinder available for compression is reduced. At Cr the suction valve is closed and the compression follows the line from Cr to Dr. As shown in the diagram the indicated power for approximately 50% load is only about half of the power required for full load. Thus the principle of reverse flow regulation saves energy compared to bypass control.

## 4.3 Effect on compressor flow pulses

This reverse flow capacity control affect the mass flow pulses that are generated at each of the cylinder sides of a reciprocating compressor. In Figures 10 and 11 this effect is explained by comparing the flow pulses at:

- 50% capacity controlled by unloading of the Crank End (step-control – Figure 10).
- 50% capacity controlled by reverse flow on both Head and Crank End (Figure 11)

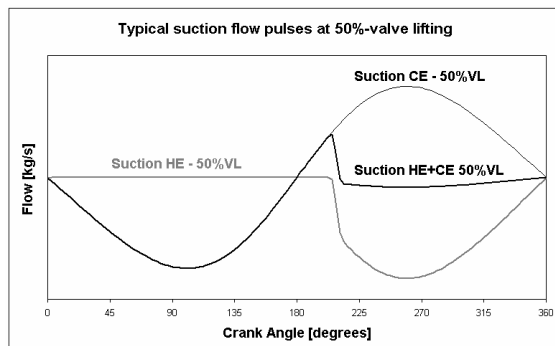


**Figure 10:** Flow pulse at the suction flange of a Single Acting Head End (SAHE) cylinder

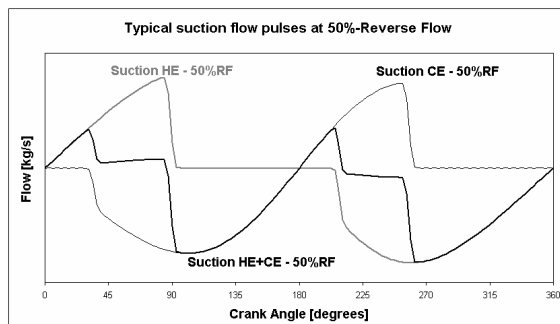


**Figure 11:** Flow pulse at the suction flange of a 50% loaded cylinder with reverse flow capacity control on Head and Crank end

The effect that these different flow pulses has on the frequency spectrum of the source levels of the pressure pulsations in given in Figure 12. It is clear that especially the amplitudes of the higher (better audible) frequencies are considerably larger in the reverse flow pulses.

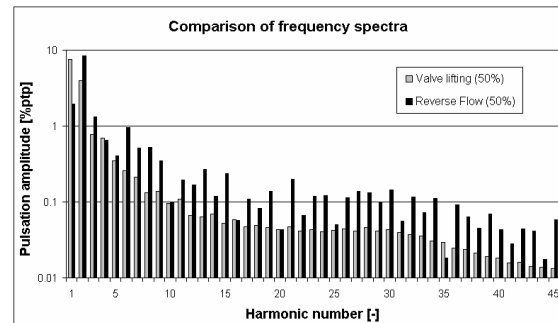


**Figure 12:** Frequency spectra of the simulated suction pulses in case of CE valve lifting (gray) and reverse flow capacity control at 50% load (black)

It is obvious that these larger amplitudes at higher frequencies also lead to a higher noise level. In Figure 13 these same results are presented once more, but in this case pulsation levels are A-weighted, so only the audible part of the pulsations is presented (dBA). When looking at the frequency spectrum, one can see that a considerable increase occurs in the 125, till 1000Hz octave bands.

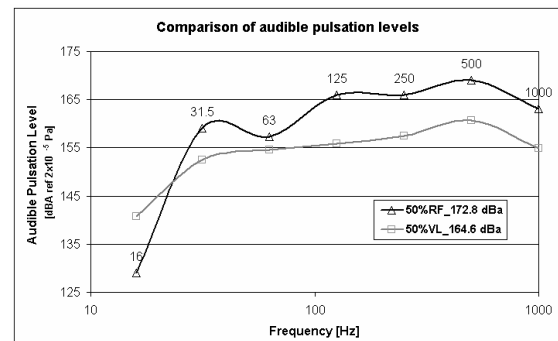


**Figure 13:** Comparison of simulated pulsation levels in case of CE valve lifting (gray) and reverse flow capacity control at 50% load (black)

## 5 Validation measurements

### 5.1 Comparison pulsation levels

Shortly after the shutdown during which all noise reducing measures were implemented, NAM granted TNO the possibility to carry out additional pulsation level measurements. In this way the net contribution of the MBROs on the total noise reduction could be established. In Figure 14 the pulsation levels at the suction 2<sup>nd</sup> stage are

presented as function of compressor load, before and after the installation of MBROs. A comparison of measured pulsation levels shows an average reduction of the audible part of the pulsation levels of 7 dBA.

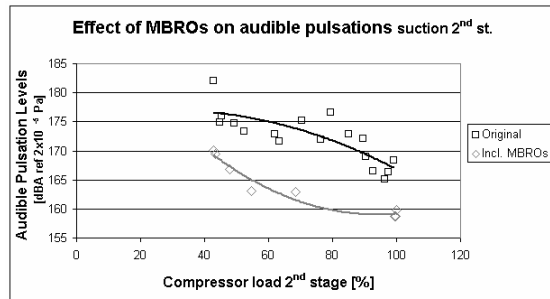


**Figure 14:** Effect of MBROs on measured audible pulsation levels at the suction 2<sup>nd</sup> stage as function of compressor load

## 5.2 Noise levels

The combined effect of all noise reducing measures on the occurring noise levels is presented in Figure 15. It is clear that a considerable noise reduction has been achieved and that also the dependency on compressor load has been reduced.

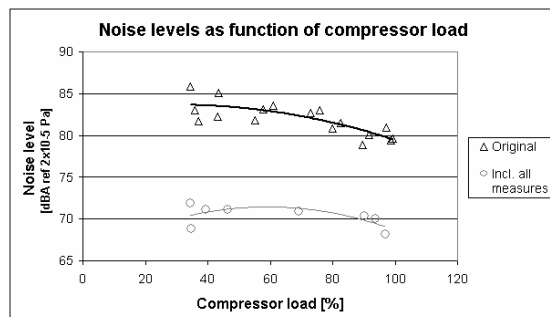


**Figure 15:** Effect of all noise reducing measures on the measured noise levels before (black) and after the modifications (gray)

When looking at the frequency spectrum of original and the reduced noise levels, one can see that the most important part of the reduction is achieved in the 1/2, 1 and 2 kHz octave band. These frequencies are far above the effective frequency limit of normal single-hole restriction orifices.

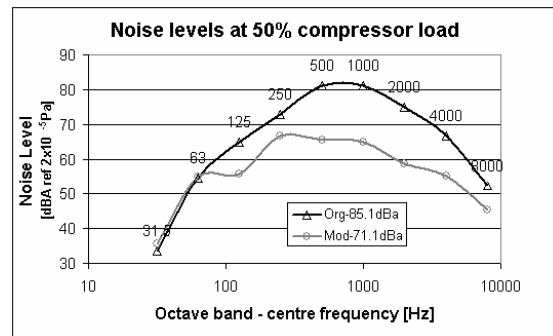


**Figure 16:** Frequency spectrum of measured noise levels at 50% compressor load before (black) and after the modifications (gray)

## 5.3 Noise contour

After all noise-reducing measures were implemented the temporary noise barrier was removed and the new noise contour of the total installation was determined once again by an independent acoustic consultancy firm. Noise measurements showed that the noise levels of the compressor installation were reduced by approximately 15dBA. In Figure 17 the modified noise contour plot is given. It can be seen that occurring noise levels are well within the permitted noise levels.

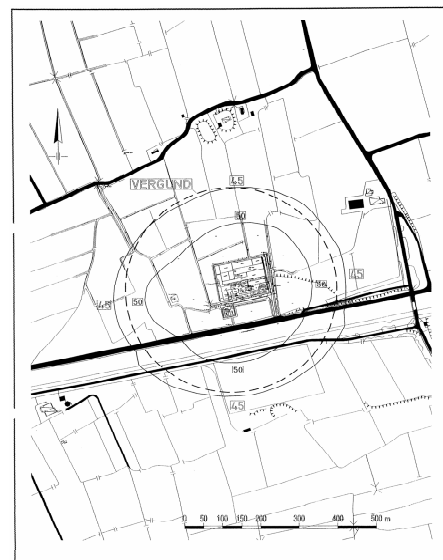


**Figure 17:** Modified noise contour (NAA - [6])

## 6 Conclusions and Recommendations

### 6.1 Conclusions

It is clear that the compressor caused high-frequency (> 300 Hz) pulsation levels at considerable amplitudes and that these pulsation levels could be directly related to the encountered excessive noise levels. Analysis of the

measurements and simulations show that a combination of the following three characteristics is the cause of the encountered problem:

- 1) High-speed compressor, therefore causing better audible pulsation levels at lower compressor harmonics.
- 2) Presence of the reverse flow capacity control. This system influences the shape of the compressor pulses. This inevitably leads to a shift towards higher (better audible) harmonics in the excitation source strength of the compressor.
- 3) The sub-optimal design of a re-used compressor.

In conjunction with these three points, it is clear that during the design phase insufficient attention has been paid to the effect of the compressor changes on the possible noise emission levels. The major four changes between the Suawoude (old) and Grootegast (new) operation modes are the different operating conditions, two-stage instead of one-stage operation, larger 1<sup>st</sup> stage cylinders, and reverse flow capacity control instead of valve lifting.

### 6.2 Recommendations

To prevent the unexpected occurrence of the high noise levels in compressor systems a number of measures are advised:

- First of all more attention should be paid to the specification (technical requisition) in respect to allowable noise levels. In this case only very limited information was available up front. More attention in the technical requisition will increase the awareness of the various suppliers.
- To detect and solve this kind of problem during the design stage, we recommend carrying out a High Frequency pulsation analysis in those cases where a high-speed machines and/or a reverse flow capacity control system is used. The standard pulsation analysis in the design phase according API-Standard 618 should be extended towards higher frequencies. In our opinion an analysis up to the 63<sup>rd</sup> harmonic should be specified. In this way it will be easier (and less expensive) to incorporate remedial measures for high frequency noise such as MBROs during the design phase of dampers and separators.
- In case an existing reciprocating compressor is equipped with a reverse flow capacity control system (retrofit), the existing pulsation analysis should be upgraded to include the difference due to the control system. In essence the way in which the compressor excites the various pipe systems becomes completely different. Also in

this case a pulsation analysis up to the 63<sup>rd</sup> harmonic of compressor speed should be specified.

As single bore restricting orifices are effective up to certain frequency (depending on size and flow rate), pulsation levels above this frequency can only effectively be damped by MBROs. The Flow and Structural department (PULSIM) of TNO has developed a selection and sizing program for MBROs, which can be used during the design stage for compressor installations.

Nevertheless it should be clear that MBROs are only recommended and should only be used when necessary. In many cases the normal single-hole restriction orifice (RO) will be sufficient to achieve an acceptable dynamic behavior.

### 7 Acknowledgements

First of all we wish to thank NAM for giving us the opportunity to carry out the validation measurements and to present the results in this paper. Without the information of the validation measurements it would have been impossible to determine the net contribution of the MBROs. We further hope that this paper helps avoiding or solving future problems during the design phase. Finally we wish to thank all the involved people from NAM, GSV and NAA in bringing this project to a successful conclusion.

### References

1. Memorandum 2422/jv/11130 on measured sound levels, NAA, March 10, 2003 'Resultaten geluidsmetingen 19-02-2003'.
2. API Standard 618, 4<sup>th</sup> edition, June 1995 Reciprocating Compressors for Petroleum, Chemical and Gas Industry Services.
3. G. Egas (TNO Science and Industry) "PULSIM a powerful tool for the control of vibrations in pipe systems, CETIM conference, July 2001, Sanlis, France
4. VDI 3733 "Geräusche bei Rohrleitungen, Noise at pipes", July 1996
5. A.D. Pierce, "Acoustics, an introduction to its physical principles and applications", 1989 edition
6. GSV Minutes of meeting: "Noise reduction compressor K-170", dated January 21, 2004. Results of noise measurements NAA.





# **Educating Reciprocating Compressor Engineers at the EFRC**

by:

**Dr.-Ing. Siegmund V. Cierniak**  
**HGC Hamburg Gas Consult GmbH**  
**Hamburg**  
**Germany**  
**S.Cierniak@HGC-Hamburg.de**

**Chairman of the EFRC Educating Committee**

**4<sup>th</sup> Conference of the EFRC**  
**June 9<sup>th</sup> / 10<sup>th</sup>, 2005, Antwerp**

## **Abstract:**

Why educate reciprocating compressor engineers?

The design, selection, operation and maintenance reciprocating compressors makes the education and training of different types of engineers a must. Due to these facts all compressor manufacturers, packagers and end users have a need for highly qualified, educated and skilled engineers. Our branch need snow and in the future, well educated and highly motivated graduates from the best universities and colleges.

The EUROPEAN FORUM for RECIPROCATING COMPRESSORS- EFRC is creating co-operation between the members of EFRC, other compressor makers, packagers, subsuppliers users and the well known universities, colleges, institutes and their students.

## 1 Some examples of these co-operative efforts:

- common supported theses
- presentations - made by people from companies at the universities
- excursions to workshops and facilities in our branch
- practical work of students in firms
- information about jobs for graduates
- sponsoring of first class results of student's (thesis', etc.)
- realisation of workshops as platform for recent students and graduates
- publication of studies, theses, research work

## 2 What EFRC members are already doing:

- participating in EFRC promotion committee
- hosting of excursions
- organizing of internships
- sponsoring of events
- subsidizing highly qualified students and graduates

## 3 Advantages for EFRC members:

- access to qualified engineers
- influence on the education of students
- part time jobs of students

## 4 Important results of the EFRC activity „Educating reciprocating compressor engineers”

### 4.1 Autumn 2000: Students' excursion to Germany, the Netherland and Belgium

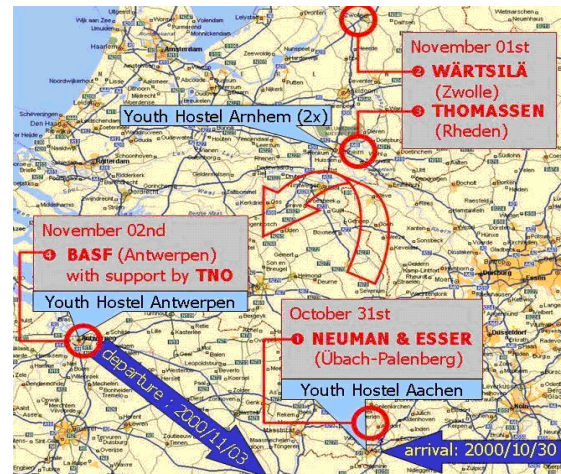


Figure 1: Students' excursion 2000

Tour on the facilities of :

- NEUMAN & ESSER GmbH, Übach-Palenberg / Germany
- WÄRTSILÄ Nederland BV, Zwolle / The Netherlands
- THOMASSEN Intern. BV, Rheden / The Netherlands
- BASF AG, Antwerp / Belgium
- TNO Inst. of Applied Physics, Delft / The Netherlands

### 4.2 Spring 2001: Workshop “Reciprocating compressors in Natural Gas Underground storages”

- Natural Gas Underground Storage Kraak (near Schwerin / Germany) “HEINGAS Hamburger Gaswerke GmbH” / compressors “ARIEL / HGC”
- Natural Gas Underground Storage Hamburg-Reitbrook "HEINGAS Hamburger Gaswerke GmbH" / compressors “ARIEL / HGC”



**Figure 2:** Workshop participants at the Natural Gas underground storage Kraak

### Seminar program (presentations)

- Dr. Ralf Luy, Heingas „Underground Storage technology“
- Dr. Andreas Laschet, ARLA „Torsional analysis“,
- Bernd Schmidt, Prognost „Condition Monitoring“
- Andre Eijk, TNO Delft „Pulsations“
- Dr. Klaus Hoff, Neuman & Esser “The product line of Neuman & Esser”
- Dr. Siegmund Cierniak, HGC-Hamburg “The range of Ariel’s compressor line”
- Prof. Dr. Gotthard Will, University of Dresden „Reciprocating Compressors in Natural Gas Underground Storages“.

### Workshop’s tasks

A computerized simulation program „Reciprocating Compressors in Natural Gas Underground Storages“ > “Selection and sizing”

### Prize winners

- Karsten Starke Bergakademie Freiberg / TU
- Uwe Seiffert David Bolz
- Ulrich Klapp
- Jan Leilich
- Ronald Schmidt
- Friedrich-Alexander-Universität Erlangen Nürnberg
- Georg Flade
- Matthias Huschenbett TU Dresden

## 5.2 Spring 2004: EFRC Workshop “POLAND”

Beginning of June 2004 (June 1 to June 05) the EFRC organized an event which was once again very successful.



**Figure 3:** Students in front of the lab of the Wroclaw University

App. 30 students from Austria, Czechia, Germany, Poland and the Netherlands travelled to Poland and visited the universities of Wroclaw and Krakow and its laboratories and also the compressor plants at the natural gas pipeline station of Tarnow and at the natural gas gathering station of Zanok. The participants had a very interesting training course reg. reciprocating compressor technology.

### Seminar program (presentations)

- Prof. Dr. Cyclis, University of Krakow/PL
- Prof. Dr. Pietrowicz, University of Wroclaw/PL
- Darek Rajtak, Ariel Corp., Katowice/PL
- Remco Habing, University of Twente/NL
- Andre Eijk, TNO Delft/NL
- Dr. Peter Steinrueck, Hoerbiger Vienna/A
- Matthias Huschenbett, University of Dresden/D
- Dr. Siegmund Cierniak, HGC Hamburg /D

The whole trip was for pre-qualified students absolutely free of charge due to the fact that the members of the EFRC sponsored this workshop.



**Figure 4:** The group of students in front of the Krakow University

THE GOLE for the participating students was to present a report (home work) reg. special tasks (presented by Matthias Huschenbett) within a certain time to a committee of EFRC members and getting an award and very attractive prizes for the 3 best students:

- |                       |  |
|-----------------------|--|
| 1 <sup>st</sup> grade | A free of charge compressor training course at Ariel's in Mount Vernon /Ohio/USA<br>+<br>a free of charge participating at 2005's EFRC conference in Antwerp/Belgium |
| 2 <sup>nd</sup> grade | 500,00 € cash<br>+<br>a free of charge participating at 2005's EFRC conference in Antwerp/Belgium  |
| 3 <sup>rd</sup> grade | a free of charge participating at 2005's EFRC conference in Antwerp/Belgium  |

The idea was to have this workshop in a county of one of the new EU member country (Poland).

EFRC gives all Europeans a clear signal:

**The recip-people are ready!**

**Workshop's tasks:**

Diagnostics of leaking valves in reciprocating compressors

Given data:

- Some Workshop objectives
- Some compressor data
- Installed sensors on the compressor
- The observed changes

- Some helping notes
- Due date:

Please send your report (incl. results) to Dresden University Sept. 30, 2004



**Figure 5:** Tour on the facilities of the Tarnow site

## Prize winners

### 1<sup>st</sup> grade

**Remco Habing**

University of Mechanical Engineering  
Fluid Dynamics  
P.O. Box 217  
7500 AE Enschede  
The Netherlands

### 2<sup>nd</sup> grade

**Torsten Kirchhoff**

University of Dresden  
Professur für Pumpen, Verdichter  
und Apparate  
01062 Dresden  
Germany

### 3<sup>rd</sup> grade

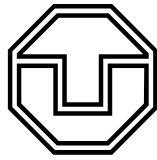
**Stefan Blendinger**

Friedrich-Alexander-Universität  
Erlangen-Nürnberg  
Lehrstuhl für Prozessmaschinen  
und Anlagentechnik  
Cauerstr. 4  
91058 Erlangen  
Germany

## 5 Next EFRC Workshop 2006

- Spring 2006
- Italy or France
- For students: free of charge
- Details will be published in Fall 2005





**TECHNISCHE  
UNIVERSITÄT  
DRESDEN**

# **Thermodynamic Simulation of Reciprocating Compressors to enable Diagnostics based on Measured Temperatures and Pressures**

**by:**

**Matthias Huschenbett / Prof. Gotthard Will**  
**Professorship of Pumps, Compressors and Apparatuses**  
**Technische Universität Dresden**  
**Dresden**  
**Germany**  
**matthias@memkn.mw.tu-dresden.de**

**4<sup>th</sup> Conference of the EFRC**  
**June 9<sup>th</sup> / 10<sup>th</sup>, 2005, Antwerp**

## **Abstract:**

Monitoring and diagnostic systems enable reduction of maintenance costs as well as improvement of efficiency of reciprocating compressors. To detect damage and wear at an early stage is one of the main tasks. Valves and gaskets are the most common reasons for unscheduled shutdowns. These defects have a significant influence on the thermodynamic process. Therefore it is possible to detect these failures by measured temperatures and pressures by means of a thermodynamic simulation of reciprocating compressors.

Opposite challenges to the simulation model are sufficient accuracy and real-time computation. Variable simulation architecture to enable applicability to various reciprocating compressors is demanded, too. This paper presents a simulation system which was designed for the purpose of online diagnostics.

## 1 Introduction

An economic operation of reciprocating compressors has high demands on availability, reliability and safety. In many cases the compressors are running at full capacity without having a second compressor in reserve. The operating companies claim longer maintenance intervals without unscheduled shutdowns and a less maintenance at all.

Despite improved materials and production technologies, a comparatively high effort caused by wear has to be expected in future, too. These costs can be reduced with modern monitoring and diagnostic systems.

Valves and gaskets are the most common reasons for unscheduled shutdowns. These defects have a significant influence on the thermodynamic process. Therefore, it is obvious to detect this damage by measured temperatures and pressures. This enables several advantages, too. On the one hand, these measurements have already been recorded or can be realized easy. On the other hand, these states follow thermodynamic laws which are equally valid to all reciprocating compressors. So, such a diagnostic system allows a versatile application to various compressors.

Therefore an EFRC research project has been carried out by the TU Dresden. The objective is a feasibility study exploring the potential of an approach based on the thermodynamic behaviour of the compressor. The measured values are restricted to temperatures, pressures and if available capacity.

## 2 Characterization of the diagnostics task

Experiences and experimental investigations with defect valves and gaskets show unambiguous characteristics of thermodynamic quantities and their changes. To conclude from altered temperatures and pressures to the state of the compressor is the task of a diagnostic system.

The development of such a diagnostic system has to be leaded by the following thoughts:

- The approaches for the formulation of diagnostic model can be based either on measured data or on theoretical system description.
- Validity and applicability for various reciprocating compressors
- Expected accuracy of the state analysis
- Expenditure for adaptation to a specific compressors

The science of technical diagnostics provides different approaches to the formulation of diagnostic models. Traditional techniques from the perspective of statistics and cybernetics are based on measured data. The quantitative correlation between the technical state and extracted diagnostic symptoms has to be determined by experimental investigations. But this method is not practicable for various applications because a large number of measurements under undamaged and defect conditions are necessary. Additionally, experimentally determined symptoms can not be generalized beyond any doubt. Many compressors have been running for a long time before a diagnostic system may be installed. Therefore a "good" condition can not be assumed in any cases.

A diagnostic system based on a theoretical description is more suitable for the utilization on different kinds of reciprocating compressors. Initial state of the compressor can be taken into account as well. The theoretical model is defined by the equations of the thermodynamic process and parameters taken from experiences or expertise. Linear model architecture is advantageous for the identification. However, the structure of the theoretical model is determined by the required quality for a reliable analysis. The less various measurements are available, the higher demands on quality. In this way, the restriction on measured temperatures and pressures leads unavoidably to an extensive theoretical model.

The challenge to the accuracy which has to be ensured by the theoretical description can be explained with a simple single stage compressor as example. This small air compressor was experimentally investigated for the evaluation of the thermodynamic behaviour. Figure 1 displays the gas temperature measured in the suction chamber as a function of rotational speed. The measurements have been executed with the same pressure in the suction and discharge pipe.

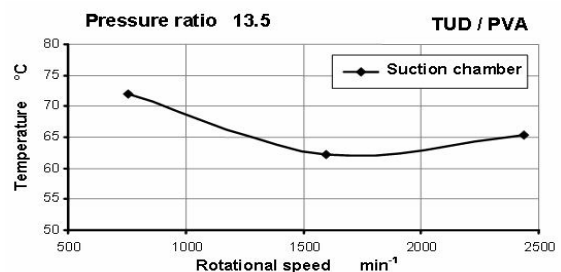


**Figure 1:** Measured gas temperature inside suction Chamber

The temperature decreases with a higher rotational speed in the range of 750 to 1600 rpm. This effect is caused by the lower heat quantity exchanged between gas and chamber wall within a revolution. However, a higher rotational speed than 1600 rpm leads to an increased temperature. This reaction can be explained by enlarged pressure loss in the discharge valve with an increased rotational speed. The higher pressure ratio within the cylinder chamber causes a rise of the cylinder temperature. Consequently, the heat flow to the gas in the suction chamber goes up as well. At larger speed this effect becomes dominant.

In this case, temperature in the suction chamber was measured at constant suction and discharge pressure and the state of the compressor has been always the same. The values changed nonlinear as a function of rotational speed. Accordingly, such thermodynamic behaviour has to be considered. Even this comparatively simple single stage compressor demands a high quality of the theoretical model as base for diagnostics.

Obviously, a suitable theoretical description of the compressor consists of an extensive and nonlinear system of differential equations. The unknown parameters which consider damage respectively leakage are included. However, an inverse formulation for the determination of these parameters is a hardly solvable task.

These difficulties can be avoided by a simulation of the special compressor. The simulation model can calculate the thermodynamic states dependent on the damage parameters in advance. Therefore, an utilization of diagnostic methods becomes possible with the help of the simulation, which is defined by balance, phenomenological and mechanical equations and can be adapted to the actual compressor state with measured data (Figure 2).

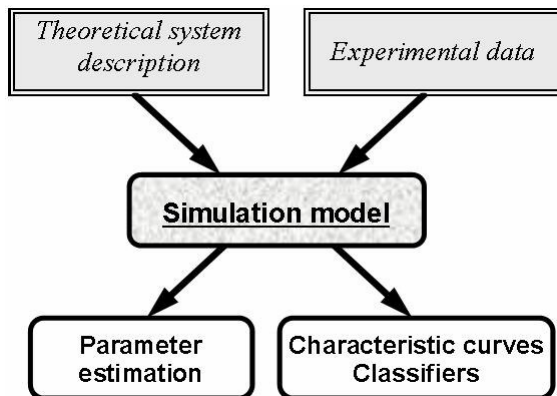


**Figure 2:** approaches for formulation of diagnostic model

Next chapter introduces the simulation model created for diagnostic purpose.

### 3 Simulation model

Following demands on a suitable simulation model can be inferred by the mentioned thoughts as well as by tasks of the diagnostic system which bases on this simulation:

I. A sufficient precision dependent on available measured values has to be ensured by the simulation. Valve and packing leakages should be taken into account by the theoretical model in a parametric way.

II. A transient system description is mainly required by two facts. On the one hand, the behaviour of temporal changes provides useful symptoms for diagnostics. On the other hand, such diagnostic system has to offer the possibility to cause an emergency shutdown to avoid further damage and danger.

III. Development of a precise theoretical model means high effort and costs, too. However, variable simulation architecture can compensate for this disadvantage. Therefore, a creation of a specific compressor model should be simply possible in a short time.

IV. Beside visualisation and diagnostic tasks regarding damage and wear a modern monitoring system should enable a better understanding of the compressor behaviour for the customer. A simulation simultaneously running to the real compressor can provide more precisely analyses concerning losses and efficiency. This purpose demands an optimized fast simulation.

V. The simulation model has to be suitable for the utilization within a diagnostic system. This fact pertains to quality of simulation as well as evaluation of the state parameters.

For the purpose of variable simulation architecture, the components of reciprocating compressor have been described numerically in individual modules. These modules are available in a library "Recip Toolbox" which can be used within the software environment Matlab/Simulink. The creation of a specific compressor model is simply done by "drag and drop" of required modules (Figure 3). The known element parameters can be set in the module dialog.

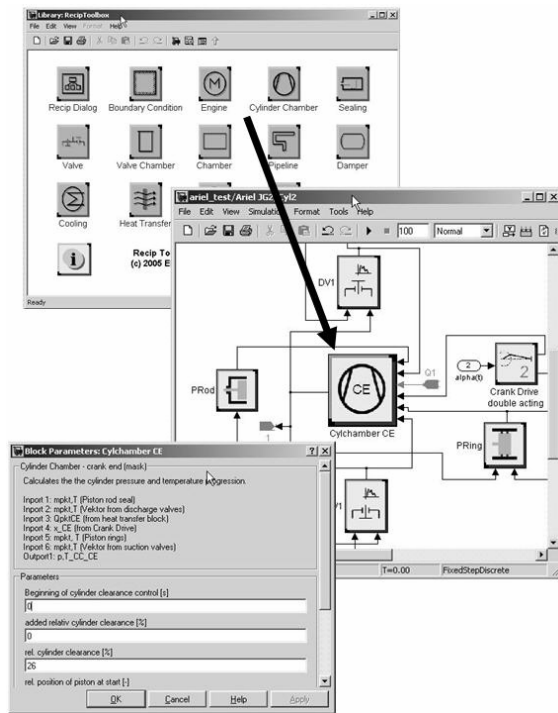


Figure 3: Creation of a specific simulation model

Various modules with different simplified assumptions (compressibility, dynamic etc) are available for every compressor component. So, the selection of specific module enables the possibility to influence accuracy as well as simulation time. An optimization of these opposite effects can be done easy.

### 3.1 Numerical design of the simulation

The theoretical imitation of reciprocating compressor is based on thermodynamic equations as well as dynamic of moved parts.

To reach a high simulation speed, the equation system is preferentially solved with fast numerical methods. Additionally, boundary conditions are assumed constant within a time step. The general design of a module is shown in figure 4.

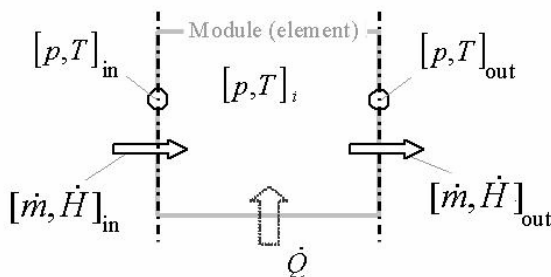


Figure 4: common design of a module (element)

Interfaces are defined by a state vector, a flow vector and heat transfer. The states within a module are calculated with explicit or implicit numerical methods according to the required precision. With this proceeding simultaneously simulation could be achieved by several test models (compiled mode).

### 3.2 Elements of the Recip Toolbox

Currently the library "Recip Toolbox" applicable in the software environment Matlab/Simulink contains following modules:

#### 3.2.1 Driving mechanism Cylinder

Modules of this category enable the calculation of the movement of engine and pistons. Several kinds of driving mechanism as well as different cylinder types (e.g. single- or double acting, differential piston etc) can be modeled. The angular velocity is assumed as constant. An extension for determination of loads and speed droop is presently worked on.

#### 3.2.2 Cylinder

The cylinder model can be built appropriately to the real construction with several sub elements.

*Cylinder chamber:*

Beside the movement of piston and the mass flow through valves, the computation of the state within the cylinder chamber takes into account the heat transfer as well as the leakages through valves, piston rings and packing. The transient mass and energy balance are numerically solved with a zero-dimensional model.

*Valves:*

The theoretical description of the valve considers a steady and compressible flow. Friction loss is included with the flow digit as function of valve plate motion. The dynamic of valve plate forced by pressure gradient can be calculated as spring-mass system. Reverse flow control due to keeping open the suction valve for a precisely defined time range is supported by the simulation, too.

*Valve cage:*

Measurements of temperature near valves, i.e. inside the valve cage, are absolutely required for the current diagnostic approach. Usually, more than one valve is placed in a chamber and therefore the state in the valve cage has to be computed separately. The transient balance equations are solved in these modules.



### Suction and discharge chambers:

The theoretical description is identical to the valve cage modules with additional consideration of heat transfer between gas and cylinder.

### Heat transfer:

To ensure a sufficiently precise determination of temperatures, the transfer and storage of heat in the complete cylinder cover are calculated within one module. Beside heat exchange between gas and cylinder, a possibly present cooling can be taken into account, as well. For this purpose, a discrete three dimensional cylinder model is computed with a numerical method (Euler method, first order).

### Piston rings and packing:

Piston rings and packing are modelled in independent modules. The consideration of damage or wear is included by parameters. Therefore, a precalculation of leakage effects is simply possible.

### 3.2.3 Damper and piping

In some cases, the effect of pulsation can't be neglected for the precisely computation of pressures and temperatures. Fast methods with sufficiently accuracy are required to realize a simultaneous online application. In this context, the assumption of quasi-compressible flow has been proven as a practicable way. Within a time step, the flow between two adjoined discrete volume elements is considered incompressible, however, the calculation of state values in these elements take into account compressibility.

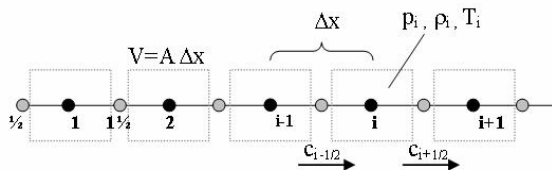


**Figure 5:** theoretical model for the calculation of the pipe flow

Computation of dampers by means of transient mass and energy balance is based on a zero dimensional model.

### 3.2.4 Cooler

The library "Recip Toolbox" provides several cooler modules, e.g. tube bundle heat exchanger. Effects of pulsations are regarded in the theoretical description, too.

## 3.3 Verification of the simulation

Various experimental investigations on reciprocating compressors have been carried out for the evaluation of simulation quality regarding capability for diagnostics based on measured temperatures and pressures. The validation and variable applicability of the simulation model will be demonstrated by measurements of two different compressors, a small single stage and a two stage compressor.

### 3.3.1 Small single stage air compressor

A single stage compressor used for boosting compressed air in large vehicle has been examined in the laboratory of the TU Dresden. The experiments have been carried out with a rotational speed range of 500 to 3000 rpm and pressure ratios of 11.5 and 13.5. Beside gas temperatures and pressures, the temperatures on different positions of the cylinder have been measured as well as the delivered flow rate.

The thermal balance of the water and air cooled cylinder was calculated with a three dimensional model. This computation considers the movement of piston and flow of cooling water, too. Figure 6 displays the comparison of the measured temperatures and the results of the simulation model.

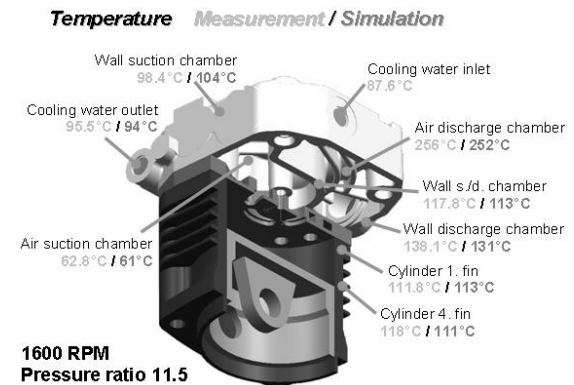


**Figure 6:** measured / simulated temperatures

A general approximation for Nusselt number  $Nu = C_1 \cdot Re^{C_2} \cdot Pr^{C_3}$  as function of Reynolds and Prandtl number is assumed for the ascertainment of heat-transfer coefficient  $\alpha = f(Nu)$ . At first, constants  $C_{1,2,3}$  are predefined by expert knowledge and later they will be corrected by an initial state identification within the diagnostic model.

M. Huschenbett, G. Will: Thermodynamic Simulation of Reciprocating Compressors to enable Diagnostics based on Measured Temperatures and Pressures

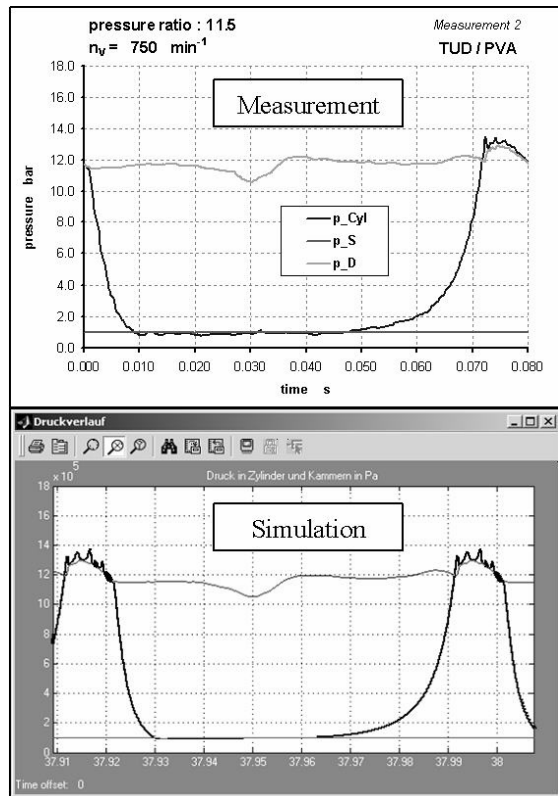


**Figure 7:** Comparison measurement – simulation pressure ratio 11.5 / 750 RPM

Investigations on this compressor indicate that consideration of pulsation and valve dynamic in the simulation model is required for a sufficient precise prediction of thermodynamic states. Measured and simulated pressure curves are shown in figure 7, whereas rotational speed amounts to 750 rpm and pressure ratio to 11.5. The simulation proves a well conformity with measurements. In this case, an acceptable accuracy may be achieved by a simulation with neglected pulsation, as well.

However, at a rotational speed of 1600 rpm the pulsations affect the thermodynamic states in a substantial manner. The discharge valve already opens at a pressure ratio of 10.5 (figure 8). Neglect of these dynamic effects leads to incorrect simulated pressures and temperatures. With the presented “Recip Toolbox” these thermodynamic values can be accurately calculated as required for diagnostic tasks.

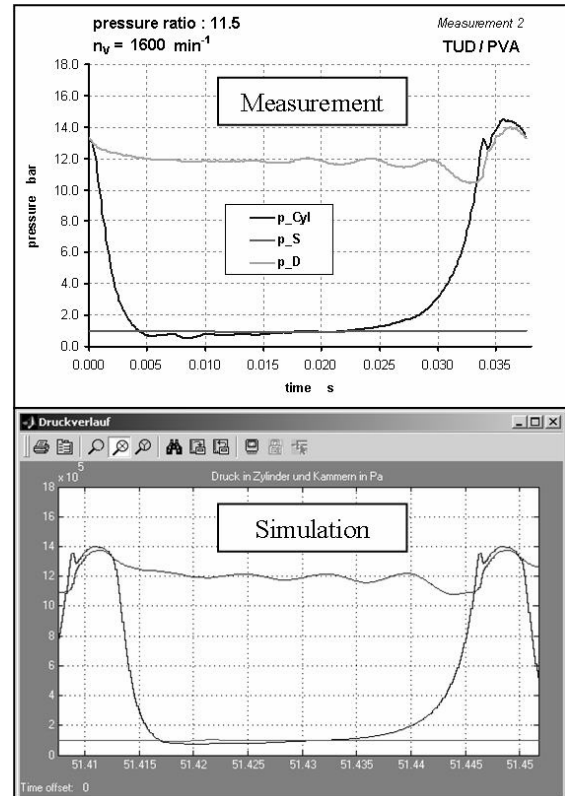


**Figure 8:** Comparison measurement – simulation pressure ratio 11.5 / 1600 RPM

### 3.3.2 Double stage air compressor

In the course of this EFRC research project experimental investigations were carried out at a test compressor Ariel JG2, too. This compressor is boosting environment air to a discharge pressure in the range of 5 to 9 bar and a rotational speed of 750 rpm.

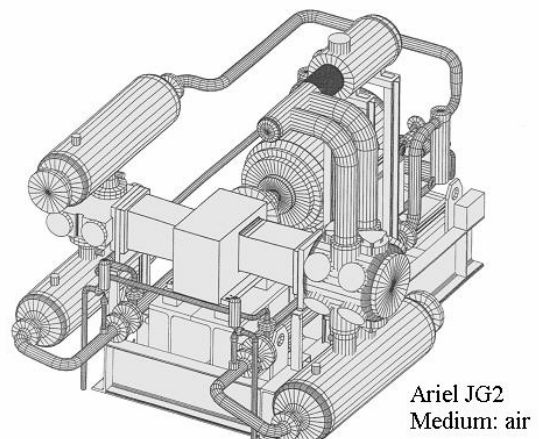


**Figure 9:** Compressor Ariel JG2

At multistage compressors the influence of gas dynamics causes a different intermediate pressure as expected by a steady flow simulation in many cases. This results from the pulsation effect on the pressure ratio within cylinder chamber. However, pressure values are characteristic signals for diagnostics. Also for this reason, the simulation model has to consider dynamic effects.

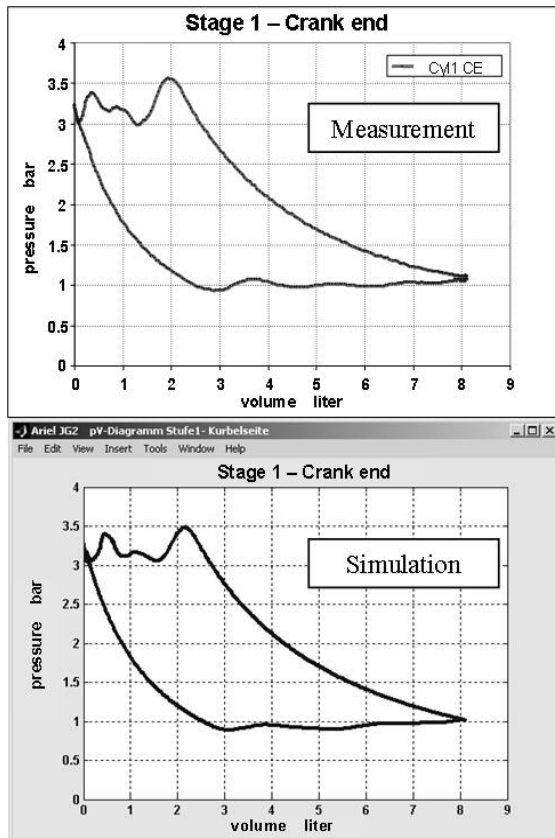


**Figure 10:** Comparison measurement – simulation Ariel JG2 / Stage 1 (crank end)

In figure 10 is displayed the measured and simulated indicator diagram (first stage, head end). A correct calculation of intermediate pressure was done by the simulation model in contrast to first attempts with steady flow models.

The reverse flow control can be computed by the simulation, as well. Figure 11 shows the measurement and computation results of the pressure curve of head end cylinder chamber of the second stage. The capacity control was set to 51%.

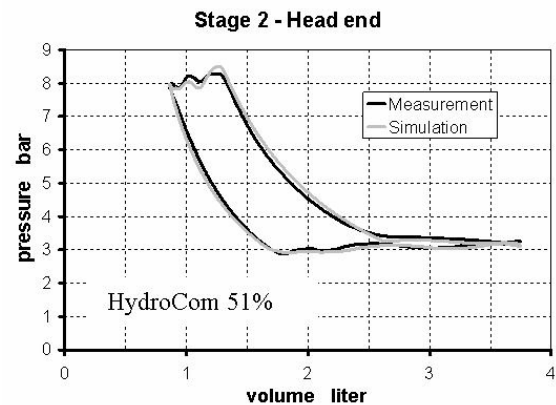


**Figure 11:** Comparison measurement – simulation Ariel JG2 / Stage 2 (head end)

Also for this compressor, a simplified 3D model has been used for computing thermal balance. Figure 12 displays the comparison of calculated and measured values recorded by a thermocouple placed on cylinder surface.

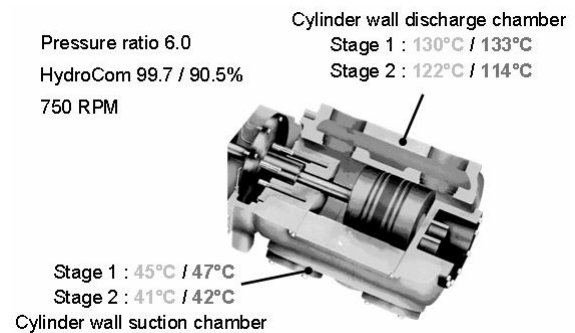


**Figure 12:** measured / simulated temperatures of the Cylinder wall

The demonstrated conformities of simulation and measurement presuppose well determined thermodynamic parameters. At first, these unknown parameters of a specific simulation model were set by values obtained from experiences or expert knowledge. The correction of these values can be done by a diagnostic approach (described in chapter 4). For this purpose, measurements are required at various operation conditions, e.g. different rotational speed or capacity control.

	Pressure ratio 7.0 HydroCom 99.6/99.7%		Pressure ratio 7.3 HydroCom 99.7/90.5%		Pressure ratio 6.0 HydroCom 77.7/70.7%	
	measured	simulated	measured	simulated	measured	simulated
Intermediate pressure	2.96 bar	2.97 bar	3.09 bar	3.11 bar	2.80 bar	2.80 bar
Discharge valve temperature stage 1	166°C	165°C	173°C	172°C	153°C	154°C
Temperature outlet intercooler	39°C	38°C	34°C	34°C	38°C	38°C
Discharge valve temperature stage 2	153°C	151°C	153°C	152°C	140°C	140°C
Temperature outlet aftercooler	40°C	39°C	33°C	33°C	36°C	37°C

**Figure 13:** Measurements and simulation results at various operating conditions



M. Huschenbett, G. Will: Thermodynamic Simulation of Reciprocating Compressors to enable Diagnostics based on Measured Temperatures and Pressures

Results of the trained simulation in comparison with measurements are listed in figure 13. Obviously, the simulation model replicates the initial state of this compressor in a sufficiently precise way.

#### Leakage through valves, piston rings and packing

Implementation of experiments with defect valves can be realized comparatively easy. In contrast, installation of leaky gaskets is associated with technical and economical difficulties. Furthermore, a controllable activation should be possible at a specific point of time. Therefore additional devices have been installed, which actually do not correspond to the real damages. However, the thermodynamic behaviour is approximately imitated.

A leakage through a discharge valve of the second stage was accomplished by means of a drilling through the valve body. The gap for leakage flow can be controlled by an adjusting screw (Figure 14).

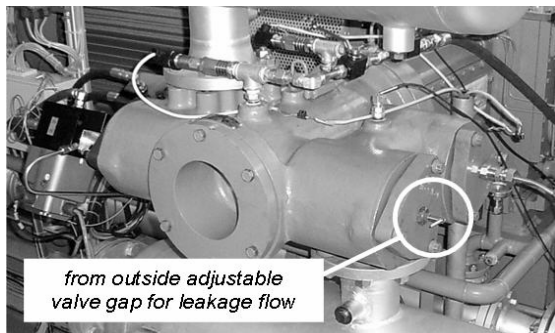


**Figure 14:** Installation for adjustable valve leakage at cylinder stage 2

The experiments have been carried out with several sizes of gap for leakage flow at various operation conditions. Figure 15 displays the measured pressure curves. The indicator diagram corresponding to the leaky valve shows expected differences during compression and expansion.

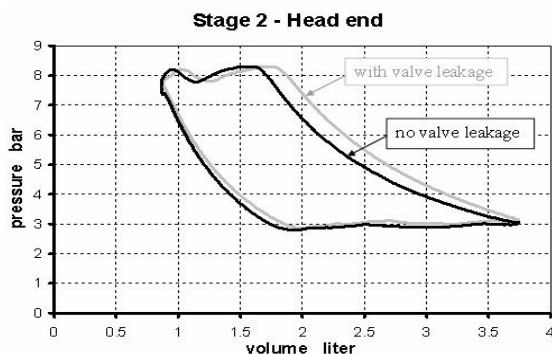


**Figure 15:** Measurement with and without valve leakage flow, stage 2 (head end)

The behaviour of the pressure caused by valve leakage can be calculated by the simulation model, as well (Figure 16).

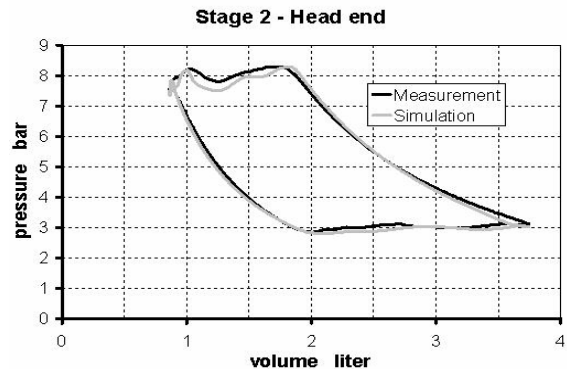


**Figure 16:** Comparison measurement – simulation discharge valve leakage Stage 2 (HE)

Leakage through piston rings and packing were imitated by bypass lines connected to the head and crank end cylinder chambers (Figure 17). The gap for leakage flow can be controlled by adjustment valves.

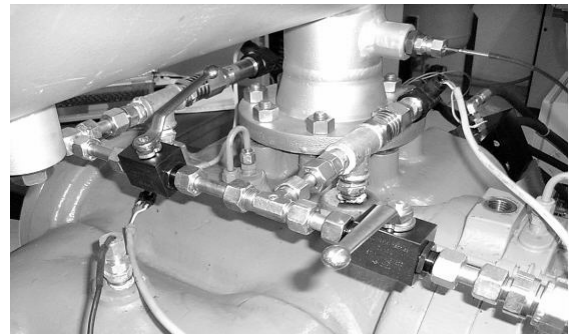


**Figure 17:** Installation for adjustable piston ring and packing leakage at cylinder stage 2

The measured pressure curves show typical changes corresponding to experiences with those damages, although the measured data are not identical to real behaviour caused by damage or wear. The validation of the simulation model is credible because the theoretical description of leakage flow within simulation model was adapted to the behaviour of bypass line. Figure 18 displays measured and calculated indicator diagrams. The upper diagram represents the state with a closed adjustment valve, i.e. no leakage flow, and the lower one was measured and simulated with a leakage from crank end cylinder chamber to the environment.



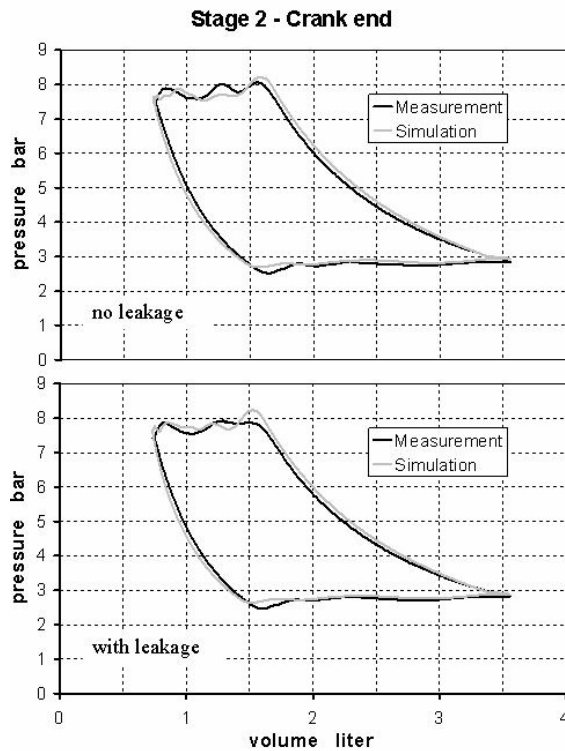


**Figure 18:** Comparison measurement – simulation imitated leakage through packing

The pressure curves show small but ascertainable differences during compression and expansion which are reproduced by simulation, too. This conformity is also achieved for temperatures.

To ensure this sufficient accuracy of the simulation model the unknown parameters are determined by means of diagnostics. The general approach is described in the following chapter.

#### 4 Diagnostic evaluation

The science of technical diagnostics provides different approaches to the formulation of diagnostic models. Traditional techniques from the perspective of statistics and cybernetics are based on measured data. However, this method is not practicable for various applications as explained in chapter 2. The general proceeding with a model based on theoretical description is displayed in figure 19.

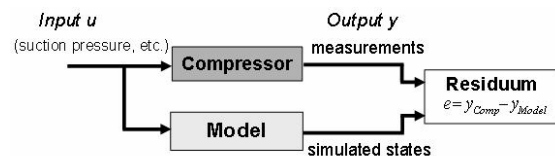


**Figure 19:** Diagnostic task for the parameter determination

Parameters of the model have to be determined with the constraint of a minimal value of the residuum. This residuum represents the differences of measured and simulated states. For this purpose, the thermodynamic states are predicted by the explained simulation model with variation of the parameters in a reasonable range. The results of the simulation model are analysed like measured data with diagnostic method of classification, i.e. classifiers are trained with the simulation results. Evaluation of measurements with these classifiers enables the determination of the unknown parameters, which represent the real state of the compressor.

To extract diagnostic symptoms by measured and simulated signals is advantageous in many cases. For example, such a diagnostic symptom was used in the course of a thermodynamic estimation of a small non-lubricated compressor. This symptom corresponds to the tightness of the compressor. Figure 20 displays measured and simulation results of the diagnostic symptom as a function of measured volume rate. The computation has been done with various assumptions of leaky state.

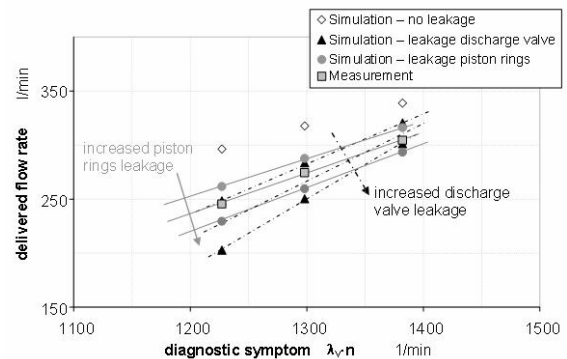


**Figure 20:** determination of the state of a non-lubricated compressor

The state of the compressor can be achieved by minimal difference of simulation and measurement (residuum). Figure 20 shows a good similarity of measurements and simulation with leakage flow through piston rings. Therefore, the state of the compressor is most likely characterized by leaky piston rings.

The several examined leaky states of the double stage compressor (Ariel) are evaluated with this proceeding, as well. A selection of simulation results and one measurement are displayed in figure 21. In this case, the ratios of pressure and temperature of suction and discharge side are used as diagnostic symptoms.

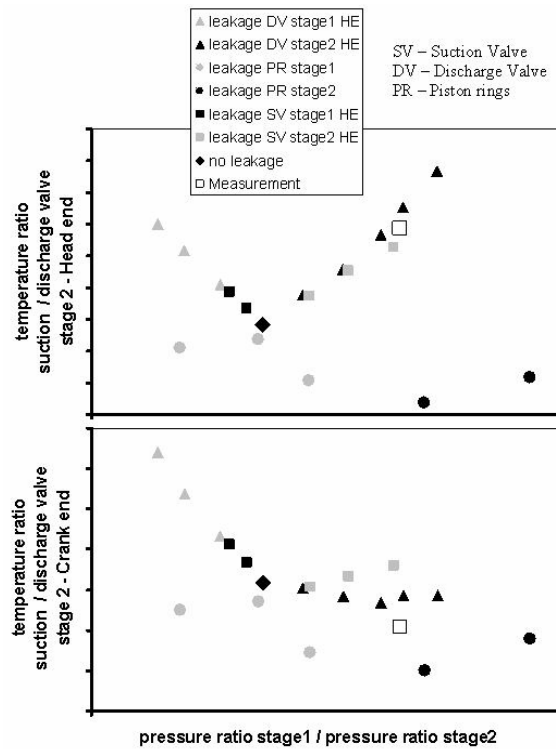


**Figure 21:** determination of the state of a double stage compressor

In the upper diagram the measurement indicates a similarity to the state classes “leaky discharge valve” as well as “leaky suction valve” (both second stage). In the lower the distance to the state class “leaky discharge valve” represents the minimal residuum. Obviously, a defect discharge valve situated at second stage (head end). Actually, this measurement was examined with a controlled leakage through this valve described in chapter 3.3.2.

The figures 20 and 21 are useful for illustration, however, the compressor state is determined by a mathematical approach for the evaluation of multi dimensional classifiers.

Alternatively, the simulation of a special compressor enables a mathematically solvable parametric model. The thermodynamic correlations are included in this diagnostic system by simplified approximation functions whose coefficients are calculated by the simulation model. Therefore, the state of the compressor can be evaluated with methods of parametric estimation.

The effort for the simulated combinations of the parameters to determine coefficients of approximation function is equal to teach the model of classification. Therefore this method offers no significant benefit. The first tests show more exact diagnostics gained by classification.

## 5 Conclusion

The explained simulation model enables diagnostics of leaky valves and gaskets by measured temperatures and pressures. A sufficient accuracy is ensured by the consideration of dynamic effects. The efficiently simplified theoretical description of the modules realized a fast simulation speed.

The variable applicability to various reciprocating compressors is demonstrated by two different compressors. Both examples show a sufficient conformity of measured and simulated states. This conformity is also achieved for measurements and simulation with leaky valves and gaskets.

Diagnostic evaluation by means of classifiers enables the determination of initial state as well as leakage flow through valves, piston rings and packing.

# **Valve Dynamics and Internal Waves in a Reciprocating Compressor**

by:

**Roland Aigner, Georg Meyer and Herbert Steinrück**  
**Institute of Fluid Mechanics and Heat Transfer**  
**Vienna University of Technology**  
**Vienna**  
**Austria**  
**roland.aigner@tuwien.ac.at**

**4<sup>th</sup> Conference of the EFRC**  
**June 9<sup>th</sup> / 10<sup>th</sup>, 2005, Antwerp**

## **Abstract:**

Internal pressure waves influence the performance of reciprocating compressors in two ways: Firstly they interact with the valve dynamics and secondly they excite an oscillating moment onto the piston. On the basis of 2-D and 3-D simulations using a commercial CFD code and the experiences of compressor manufacturers a 1-D flow model is introduced. Valve dynamics are described by a modified Costagliola-model which takes pressure waves in the cylinder into account. Comparison with experiments shows that this 1-D model is sufficient to predict accurately not only gas flow and pressure distribution inside the cylinder but also important design criteria of the valves such as impact velocity of the valve plate and valve losses.

## 1 Introduction

In the present study we investigate pressure waves in a reciprocating compressor of barrel design. The motivation of this study is twofold. Firstly, during the compression of heavy gases in fast running compressors oscillations of the piston rod have been observed which have been attributed to pressure waves in the cylinder. Secondly, and even more important for the design of compressor valves, it has been observed that the prediction of the impact velocity of the valve plate onto the valve seat is overestimated by conventional methods which do not take the waves in the compressor into account.

At first glance describing the wave systems in a compressor seems to be a complicated task. However, it turns out that a quasi one-dimensional model for the gas flow in the compressor coupled to a simple valve model is sufficient to describe the main effects. Thus an easy to handle design tool based on the above mentioned quasi 1-d model is within reach.

First we review preliminary studies and the state of the art. Then we introduce the quasi 1-d model, compare its solution with a full 2-d, and 3-d solution. But even more important we compare the results with measurements at a test compressor.

### 1.1 State of the art and preliminary studies

Conventional theories are based on the work done by Costagliola<sup>1</sup>. The change of state inside the cylinder is assumed to be quasi stationary and isentropic. Thus the thermodynamic state (pressure, temperature, density) is taken to be uniform within the cylinder. It is only a function of time. The motion of the valve plate is then determined by the pressure difference across the valve. Since wave phenomena within the cylinder are neglected this leads to considerable deviations of the calculated from the measured valve motion. In particular the impact velocity of the valve plate onto the valve seat differs markedly from measured values.

Studies of E. Machu<sup>2</sup> give a first insight of the effect of waves and unsteady flow inside the cylinder. Simple waves are calculated by the method of characteristics. It is shown that the calculated impact speed is considerably reduced by taking the waves into account. However, the reflections of waves have been neglected and thus the interaction of waves and valve dynamics cannot be described. Moreover this model does not account for geometry effects.

Based on the one dimensional Euler equations G. Machu<sup>3</sup> introduced a model which is capable to describe laterally running waves in the compressor and their interaction with the valve dynamics. This model has been extended by the authors and its results will be compared to full 3d and 2d numerical solutions on the one hand, and more important with measurements on the other hand.

## 2 Mathematical Model

### 2.1 Geometry

#### 2.1.1 3-d Simulation

The interior of a reciprocating compressor can be found in figure 1. Valve pockets are located at both sides of the cylinder. The piston is shown in an intermediate position, where it does not mask the valve pockets. The valves are adjacent to the circular lateral surfaces of the valve pockets. Prescribing the motion of the piston and valve boundary conditions, which are described later, this 3-d geometry has been used for a full CFD-simulation. However, computation times which are of the order of several days are too large for every day use.

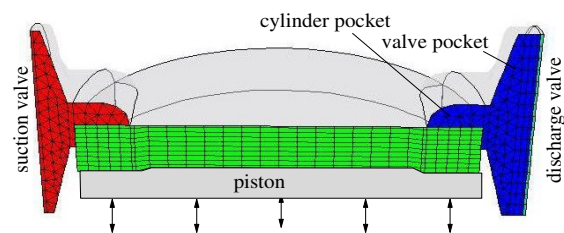


**Figure 1:** Geometry for 3-d simulation

#### 2.1.2. 2-d Simulation

A remarkable reduction of computation time can be obtained by using a 2-dimensional geometry. However, mapping the original 3-d problem onto a 2-d problem is not trivial at all. Care has to be taken that the volumes and of the 3-d model and the 2-d model are the same. Thus the 2-d domain of computation is a distortion of the cross section of the original geometry. In particular the cylinder is replaced by a cuboid with its length equal to the bore of the cylinder, the same height and same volume. Thus the all length scales in the main direction of the wave propagation and the volumes in the compressor are the same as in the original 3-d geometry. A detailed description can be found in G. Meyer<sup>5</sup>.



### 2.1.3 1-d simulation

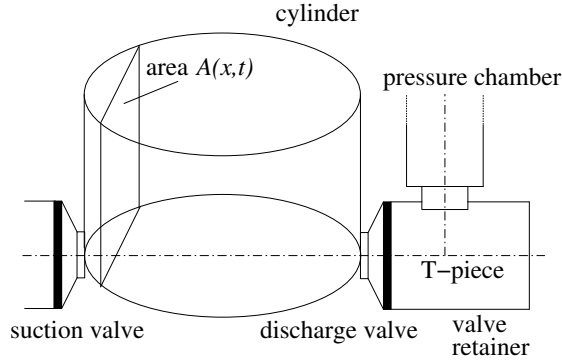


**Figure 2:** Schema of one dimensional model

In the quasi 1-d model the wave propagation along the diameter ( $x$ -axis) of the cylinder from the suction to the pressure valve is considered. The equations of motion (Euler equations) are integrated over a cross section  $A(x,t)$  perpendicular to the  $x$ -axis. The effective cross sections of the quasi one-dimensional model are displayed schematically in figure 2. From left to right we have the suction valve, suction valve pocket, cylinder, discharge valve pocket, discharge valve, valve retainer and the pressure chamber, which is connected to the valve retainer by a T-piece.

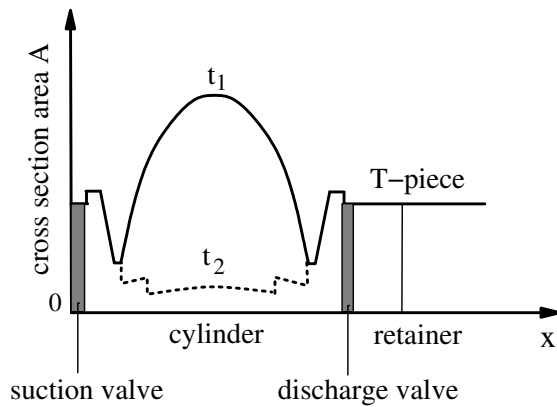


**Figure 3:** Cross section area  $A$  along space coordinate  $x$  at time  $t_1$  and time  $t_2$

Complicated geometries are replaced by simple forms. For instance truncated cones and cylinders represent the valve pockets. If CAD-data of the geometry is available, the cross-section areas along the  $x$ -axis can be determined directly. Due to the piston motion the cross-section  $A(x,t)$  inside the cylinder varies with time. Figure 3 shows appropriate area functions depending on  $x$  at different times  $t_1$  and  $t_2$ . At  $t_2$  the piston masks the valve pocket such that the effective cross section area  $A(x,t)$  is discontinuous there.

## 2.2 Governing Equations

### 2.2.1 Piston Motion

The distance between piston and top of cylinder  $h$  depending on time  $t$  can be determined using the properties of the crank mechanism. We use the length of the crank lever  $r$ , the length of the piston rod  $l$ , the smallest distance between piston and cylinder top  $h_0$  and the present angle of the crankshaft  $\varphi$  to obtain

$$h = r + l + h_0 - r \cos \varphi - l \sqrt{1 - \left(\frac{r}{l}\right)^2 \sin^2 \varphi}, \quad (1)$$

where  $\varphi = 2\pi n t$ . Here,  $n$  denotes the speed of the crankshaft.

### 2.2.2 Flow Field

The governing equations for the flow of gas are obtained by taking the mass and momentum balance over a cross section. The variables  $\rho$ ,  $u$ ,  $p$  have their usual meaning, density, velocity and pressure, respectively.

$$\frac{\partial \rho A}{\partial t} + \frac{\partial (\rho u A)}{\partial x} = 0, \quad (2)$$

$$\frac{\partial \rho u A}{\partial t} + \frac{\partial (\rho u^2 A + p A)}{\partial x} = p \frac{\partial A}{\partial x}. \quad (3)$$

Assuming isentropic flow conditions we have

$$p \rho^{-\kappa} = \text{const}, \quad (4)$$

where,  $\kappa$  denotes the ratio of specific heats. Note that eq. (3) is not of conservation form. The right hand side of equation (3) constitutes a momentum source of the flow due to a variation of the cross section. Since the cross section  $A$  may vary rapidly at the transition from the cylinder to the valve pocket, the derivative  $dA/dx$  may become large causing numerical problems. Using the isentropy condition (4) for smooth solutions the momentum equation becomes

$$\frac{\partial u}{\partial t} + \frac{\partial}{\partial x} \left( \frac{1}{2} u^2 + \frac{\kappa}{\kappa - 1} \frac{p}{\rho} \right) = 0 \quad (5)$$

We remark that equation (5) is equivalent to equation (3) for smooth solutions only. Discontinuous solutions corresponding to shocks or to sudden changes of the flow cross section are associated with an increase of entropy and thus are

not described correctly by (5). However, it turns out that the increase of entropy in the considered cases is small and thus has been neglected.

### 2.2.3 Valve Dynamics

The state of a valve is specified by the distance between valve plate and seating (valve lift)  $x_v$ . The motion of the valve plate is determined by the forces acting on it. We consider the following three contributions to the resulting force: the pressure difference across the valve acting on an effective force area  $A_v$  of the valve plate, the springing and thirdly a contribution due to viscous forces in the initial stages of valve opening. Denoting the pressure in front of the valve  $p_1$  and behind the valve  $p_2$  we obtain the equation of motion for the valve plate

$$m_v \ddot{x}_v = (p_1 - p_2) A_v - k(x_v + l_1) - F_{adh}. \quad (6)$$

Here  $m_v$  stands for the mass of the valve plate. The constants  $k$  and  $l_1$  denote stiffness of springing and initial deflection of the springs. An initial sticking effect is modelled by the force  $F_{adh}$ . It is caused by the viscosity of the gas in the valve gap resulting in a small time delay when the valve is opening. It reads as follows (Flade<sup>4</sup>)

$$F_{adh} = f_1 \frac{\dot{x}_v}{x_v^3}. \quad (7)$$

The factor  $f_1$  depends on geometric features of the valve and properties of the gas. It also takes lubrication oil at the valve plate into account.

### 2.2.4 Flow through the valve

The flow through the valve is considered as the (stationary) outflow of a gas from a pressurized container through a convergent nozzle. Thus this model takes the pressure loss due to separation into account. The mass flow through the valves is given by St.Venant and Wantzell<sup>6</sup>,

$$\dot{m} = \phi \rho_1^0 \left( \frac{p_2}{p_1^0} \right)^{\frac{1}{\kappa}} \sqrt{\frac{2\kappa}{\kappa-1} \frac{p_1^0}{\rho_1^0} \left( 1 - \left( \frac{p_2}{p_1^0} \right)^{\frac{\kappa-1}{\kappa}} \right)}. \quad (8)$$

where  $p_1^0$  is the total pressure before and  $p_2$  is the pressures after the valve, respectively. The effective flow cross section  $\phi$  of the valve is assumed to be a function of the position of the valve plate  $x_v$  only. It has to be determined empirically.

### 2.2.5 T-Piece

It turns out that it is not sufficient to consider pressure waves in the cylinder to describe the valve dynamics. The waves in the valve retainer and pressure chamber have to be taken into account also (see figure 2). In the quasi 1-d model it is described by two pipes connected at a junction or T-piece. We require that a junction itself has no volume and that the mass and energy balances are satisfied.

## 3 Numerical Solution

### 3.1 Finite Volume Method

For the numerical analysis it is useful to write the continuity equation (2) and the equation of motion (5) in conservation form:

$$\frac{\partial \mathbf{u}}{\partial t} + \frac{\partial \mathbf{f}(\mathbf{u}, x)}{\partial x} = 0, \quad (9)$$

where the state vector  $\mathbf{u} = (\rho A, u)^T$ , and  $f(u, x)$  is the so called flux function.

The computational domain consists of the interior of the compressor, including the cylinder and the valve pockets, the valve retainer and the pressure chamber. The equations of motion (9) are solved by a finite volume scheme. Since the cross section of the flow domain is not constant special care has to be taken. The f-wave algorithm by LeVeque<sup>4</sup> can handle even discontinuous cross sections of the flow domain.

### 3.2 Boundary and Interface Conditions

The finite volume scheme has to be supplied with appropriate boundary conditions. If the valves are closed, they are described as a fixed wall, by setting  $u=0$ . If the valve is open the mass flow is prescribed. It is obtained by equation (8) as a function of the total pressures before and after the valve and the valve plate position. The pressure outside the suction valve is kept constant. To determine the pressure after the discharge valve wave propagation in the valve retainer and the pressure chamber is computed using the finite volume scheme. At the end of the pressure chamber the pressure is prescribed. The equation of motion (6) of the valve plate is solved simultaneously by an explicit second order scheme.

### 3.3 Time step

The time step  $\Delta t$  of the numerical integration has to be chosen such that the stability conditions of the numerical schemes are satisfied. On one hand the CFL condition  $\Delta t < \Delta x / (c + |u|)$ , where  $\Delta x$  is the interval length of the spatial discretization and  $c$  is the velocity of sound and on the other hand  $\Delta t < m_v/k$  have to hold.

## 4 Comparison of the numerical solutions with measured data

### 4.1 Experimental setup

A double acting, 2 cylinders, barrel design reciprocating compressor was tested at Burckhardt Compression, Switzerland. The main specifications of the compressor can be found in table 1.

**Table 1:** Main specifications of the experimental compressor

Type of compressor	Burckhardt Compression 2K90-1A: 2 cylinders, double acting
Bore diameter	0.22 m
Stroke	0.09 m
Speed of Crankshaft	980 ÷ 990 rpm
Clearance	1.5 mm
Type of valve	110K12
Gas	Air
Ambient pressure	0.97 bar
Discharge pressure	1 ÷ 5 bar

Pressure sensors inside the cylinder and valve retainer (see figure 4) record the pressure at different locations.

In order to ensure a fair comparison of measured data with numerical simulations three of four working chambers have been sealed off during measurements by covering the valve pockets of these chambers.

The relative pressures in the diagrams are referred to an ambient pressure of 0.97 bar (at the day of measurements).

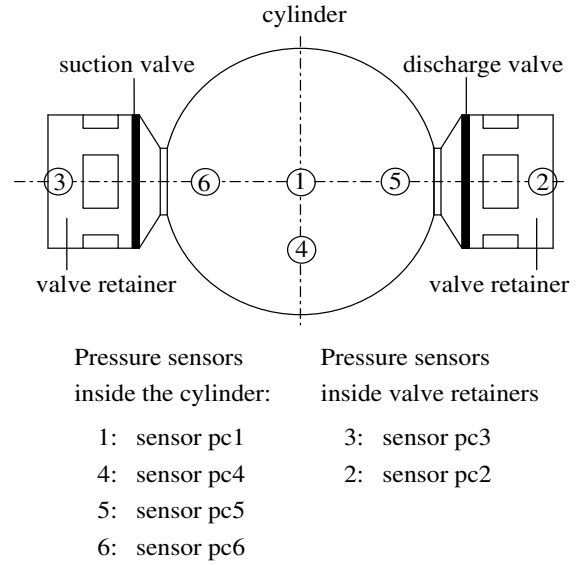


**Figure 4:** Position of pressure sensors

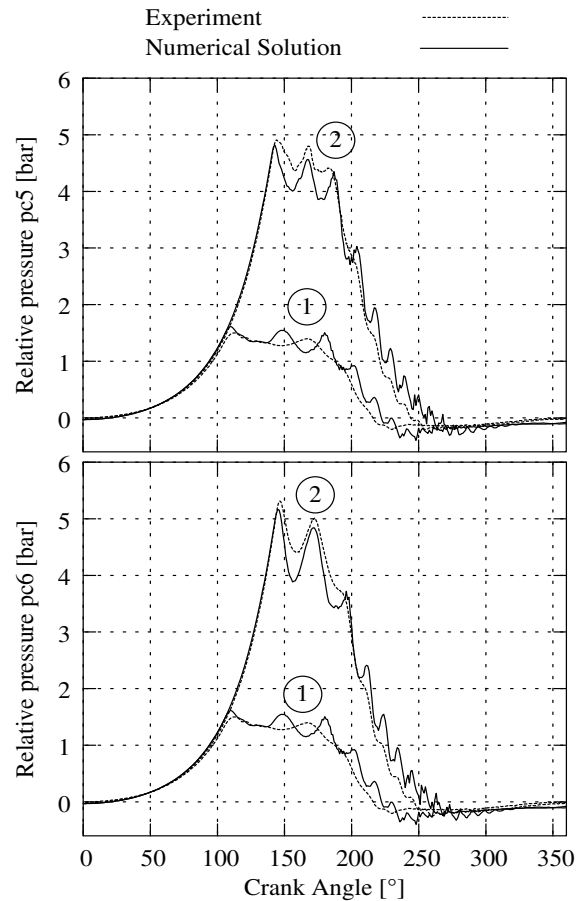


**Figure 5:** Comparison of numerical solution of quasi 1-d model and experiment, a) pressure at discharge valve, b) pressure at suction valve for discharge pressures of 2 bar (curves 1) and 5 bar (curves 2)

In figure 5 a comparison of the measured pressures at pc5 and pc6 with the numerical solution of the quasi one dimensional model for discharge pressures of 5 bar and 2 bar are given. In figure 6 a comparison of the pressure at pc2 in the valve retainer is given. In the following we will discuss the solutions in detail. Here and in the following we will focus on the case with discharge pressure 5 bar only.

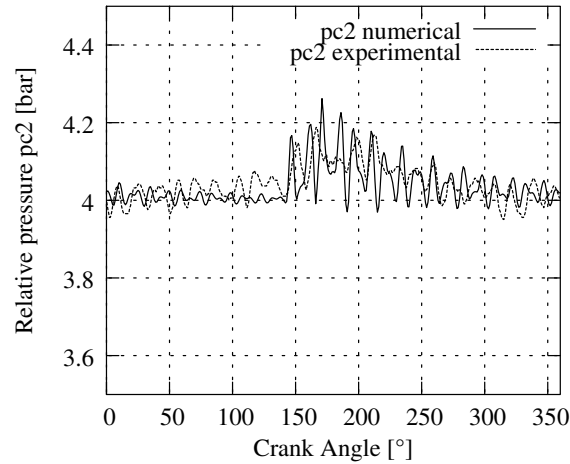


**Figure 6:** Pressure in the valve retainer at pc2

## 4.2 Initiation of waves

In figure 7 the pressure readings at pc5 and pc6 close to the discharge valve and the suction valve, respectively, and the position of the valve plate as a function of the crank angle are shown.

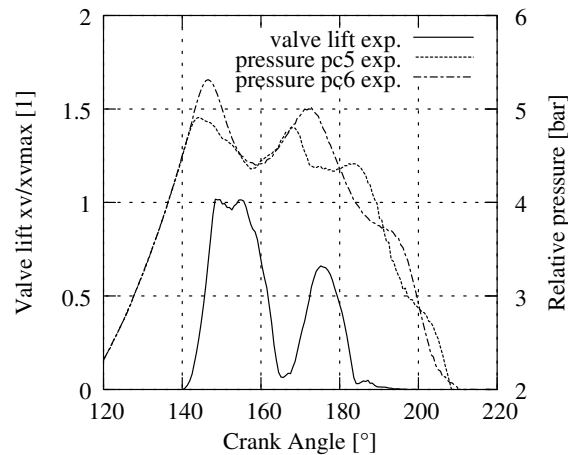


**Figure 7:** Initiation of waves by the opening of the discharge valve: pressure close to discharge valve dotted line, pressure at suction valve dashed line, position of valve plate solid line

The pressure distribution inside the compressor is shown in figure 8. During compression when both valves are closed the pressure is uniform in the

cylinder ( $CA=140^\circ$ ). When the pressure in the cylinder exceeds the pressure in the valve retainer plus the springing the valve starts to open. The pressure near the outflow valve ceases to increase and reaches a maximum, while the pressure close to the suction valve still increases. The opening of the valve has initiated a wave which reaches the opposite side of the cylinder at a crank angle  $CA=146^\circ$ , just before the valve has completely opened. Then the rarefaction wave is reflected at the suction side. Thus the pressure at pc6 attains also a maximum. But it is markedly larger than that on the pressure side (sensor pc5).

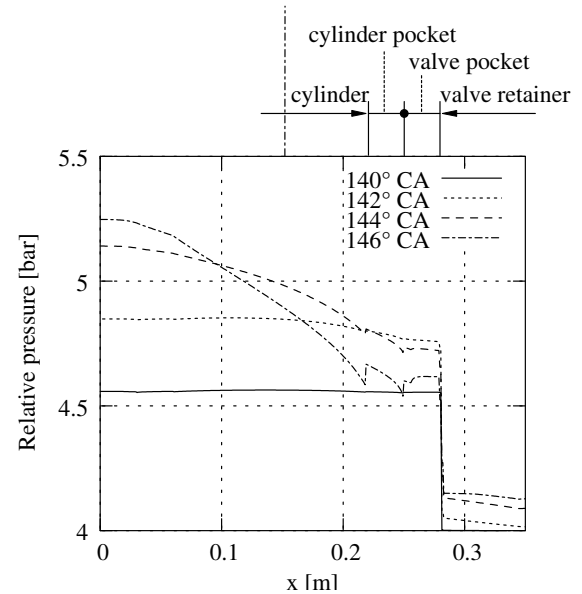


**Figure 8:** Pressure distribution in the cylinder and valve retainer at wave initiation  $CA=140^\circ$  discharge valve still, closed,  $CA=142^\circ$  valve opens, at suction side still isentropic compression,  $CA=146^\circ$  rarefaction wave has reached suction side

When the valve plate hits the valve seat the pressure in front of the pressure valve is large enough to keep the valve open until  $CA=155^\circ$ . Then the pressure has dropped such that the valve begins to close again reducing the mass outflow. This tends to increase the pressure again. The increase of pressure forces the valve to open and a complicated interaction of the valve motion with the pressure waves in the cylinder takes place. Shortly after the piston has passed the lowest volume dead centre the valve closes finally. At that time a complicated system of waves travelling back and forth is left in the cylinder. In figure 9 the difference of the pressure readings at pc5 and pc1 is shown and compared with the numerical solution. We observe that during expansion the waves are damped and their period tends to the travelling time of waves across the cylinder,  $2d/c$ , corresponding to



the lowest eigen mode in lateral direction. We want to point out that at the beginning of the expansion phase a mix of modes with several eigen frequencies have been present. These modes have been all initiated by the valve motion. As said above the zeroth eigen mode has the smallest damping and remains visible until the suction phase starts.

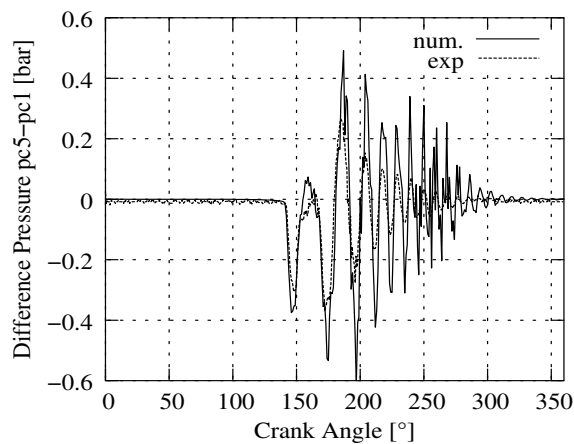


**Figure 9:** Difference of pressures at discharge valve and cylinder centre ( $pc5-pc1$ )

#### 4.3 Super elevation of the pressure due to initial sticking

Comparing the pressure reading  $pc5$  close to the discharge valve with the corresponding numerical solution shows that opening of the valve is predicted to early (see figure 10).

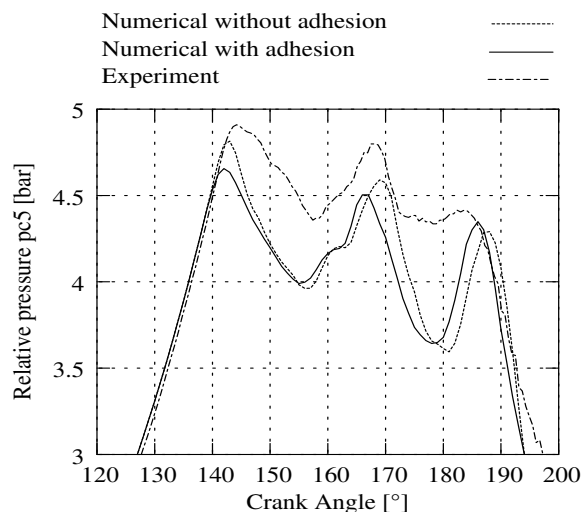


**Figure 10:** Delay of valve opening due to viscosity in valve gap

As a consequence the pressure maximum at  $pc5$  is about 0.2 bar to small. With other words in reality the opening of the valve does not start when the

pressure in the cylinder balances the pressure in the retainer and the springing. An additional delay occurs. In Flade<sup>4</sup> the dynamic behaviour of a valve plate is analyzed. If the initial gap is very small, say in the range from  $1\mu m$  to  $5\mu m$  viscosity hinders the gas to flow into the valve gap resulting in a local pressure drop in the valve gap. Applying asymptotic methods an additional force holding back the valve plate can be identified (7). It turns out that the result depends on the initial gap width, which cannot be measured easily. Here the initial gap width  $1.5\mu m$  has been chosen to fit the data.

#### 4.4 Pressure loss at sudden change of cross section.

In Figure 11 the pressure at  $pc5$  computed with the method where the pressure loss is taken into account is compared with the measurements and the numerical solution without this correction.

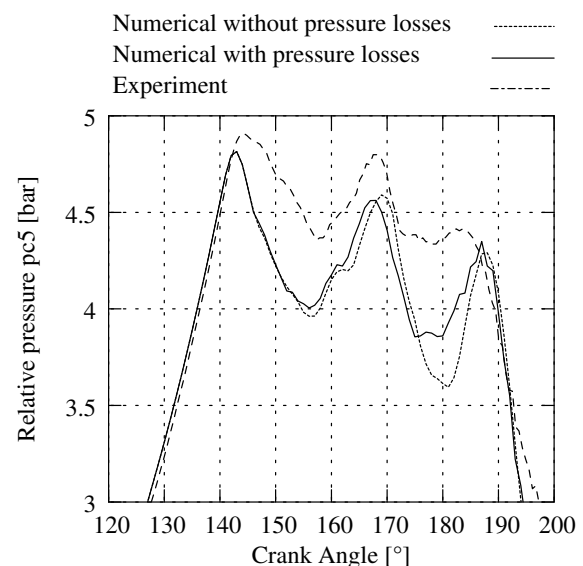


**Figure 11:** Effect of pressure loss at entrance to cylinder pocket: Solution without pressure loss (dotted line), with pressure loss (solid line) and measure data (dashed line)

The pressure at  $pc5$  predicted by the numerical solution where the sticking effect has not been taken into account drops after the first maximum at an crank angle of  $144^\circ$  to a minimum at CA  $156^\circ$ . This minimum is about 0.4 bar smaller than that of the measured data. At the second minimum at a crank angle of 180 degrees (dead centre) the difference is even worse (0.8 bar). A possible explanation for this difference may be the following. During outflow the gas is compressed under the piston. There it flows through a narrow channel towards the valve pocket. At the entrance of the cylinder pocket the gas faces a sudden increase of the effective cross section of the flow

channel. This sudden increase of the cross section is physically associated with a pressure loss which is not accounted for in the present model. We impose at the sudden change of cross section continuity of the mass flow and pressure. This procedure is applied only if the discharge valve is open and the ratio of effective cross section after and before is larger than an arbitrary value, say 3. Otherwise equation (5) is used.

The deviation of the simulation from the measurement is decreased, but still considerable. It is believed that the flow at the entrance of the cylinder pocket is two- or three dimensional.

#### 4.5 Influence of the waves in the retainer

Considering the motion of the valve plate we observe that the first opening of the discharge valve agrees more or less with the measured data. But there are remarkable differences in the second opening. The numerical solution predicts that the valve opens again completely, but measurements show that it opens only to 65%. This is attributed to the fact that waves are neglected in the valve retainer. Taking the valve retainer and its connection to the pressure chamber modelled as a T-piece into account good agreement for the valve motion is obtained (see figure 12).

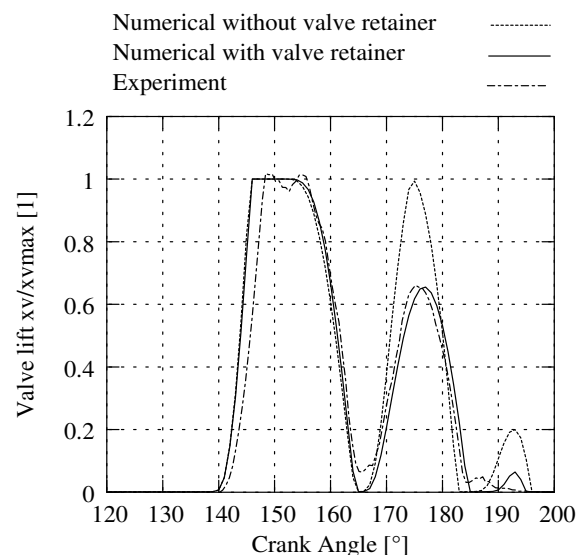


**Figure 12:** Influence of pressure waves in the valve retainer

#### 4.6 Damping of waves during expansion

In figure 13 the difference between the pressures at the discharge valve and the centre of the cylinder  $p_{c5}-p_{c1}$  as a function of the crank angle is shown

after the discharge valve is closed. This pressure difference represents the waves in the cylinder.

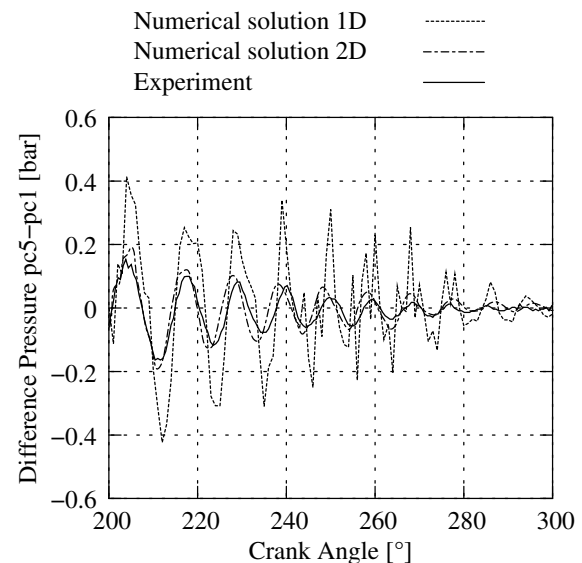


**Figure 13:** Damping of the waves during expansion: Numerical solution of 1-d model compared with numerical solution of 2-d model and measured data

During expansion the waves in the compressor are damped. The numerical solution of the quasi 1-d model, the numerical solution of a 2-d model and the measured data are compared. The damping rate of the solution of the 2-d model agrees well with the observed one. The damping predicted by the quasi one-dimensional is slightly too small.

The excitation of waves is overestimated by the 1-d model resulting large amplitudes. It has to be noted that the numerical solution of the 2-d dimensional model has been obtained for a relatively fine grid. 3198 cells in the upper dead centre and 15978 cells at the lower dead centre. For coarser grids the damping phase has been dominated by numeric dissipation giving unrealistic strong damping. However, 3d simulation using a sufficient fine grid to resolve the damping of the waves would take a couple of weeks and thus has not been performed. The high numerical dissipation of the used Solver FLUENT 6.1.22 is caused by the first order accuracy of time integration when using dynamic meshing. There is hope that using a second order time integration coarser meshes can be used such that a 3d-simulation becomes reasonable.

#### 4.7 The impact velocity

The impact velocity of the valve plate onto the valve seat can be extracted from the valve motion. In figure 14 the calculated and measured impact

velocities for different discharge pressures are compared and are in good agreement.

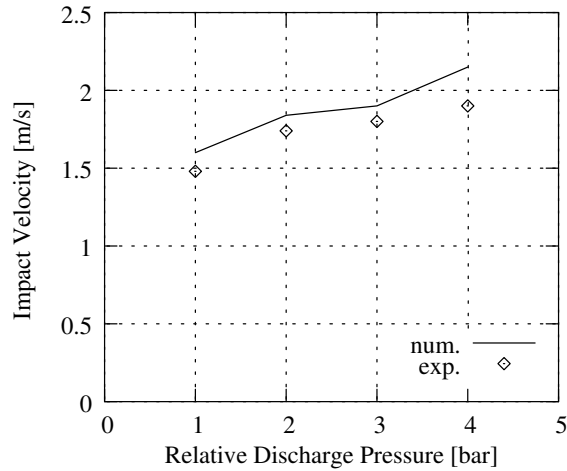


Figure 14: Impact velocities

#### 4.8 Valve losses

In figure 15 the computed mean pressure  $p$  is shown in the  $p,V$ -diagram. The shaded area corresponds to losses at the discharge valve.

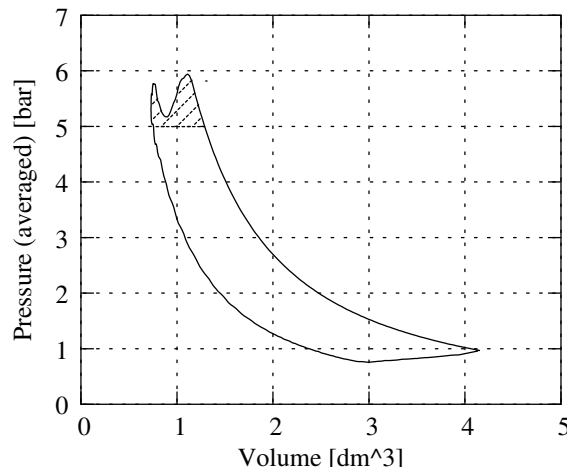


Figure 15:  $p,V$ -diagram, valve losses

#### 5 Comparison with 2-d and 3-d CFD simulations

To verify the assumptions of the quasi 1-d model CFD simulations using FLUENT 6.2  $\beta$ -release have been performed. The valve dynamics are implemented by user defined functions. The mass flow through the valve is calculated using the St. Vernant Wanzell formula (8) and is distributed evenly as mass sinks (or sources) over the first cell row adjacent to the valves. A detailed description can be found in G. Meyer<sup>5</sup>.

Here we show the pressure distribution at the cylinder cap (figure 16a) and in the (vertical) plane of symmetry of a compressor (figure 16b). Near the centre line the curvature of the pressure surfaces is small. Thus we expect that the internal flow is well approximated by the quasi 1-d model. The interaction between the valve dynamics and the waves in the compressor turns out to be similar. The advantages of the CFD simulation are that regions where the flow is two or three dimensional are well represented, for instance the flow in the valve pockets. The main disadvantage is the large computation time which is due to the fine mesh needed to resolve the waves properly. Otherwise the waves are unrealistically damped by numerical dissipation.

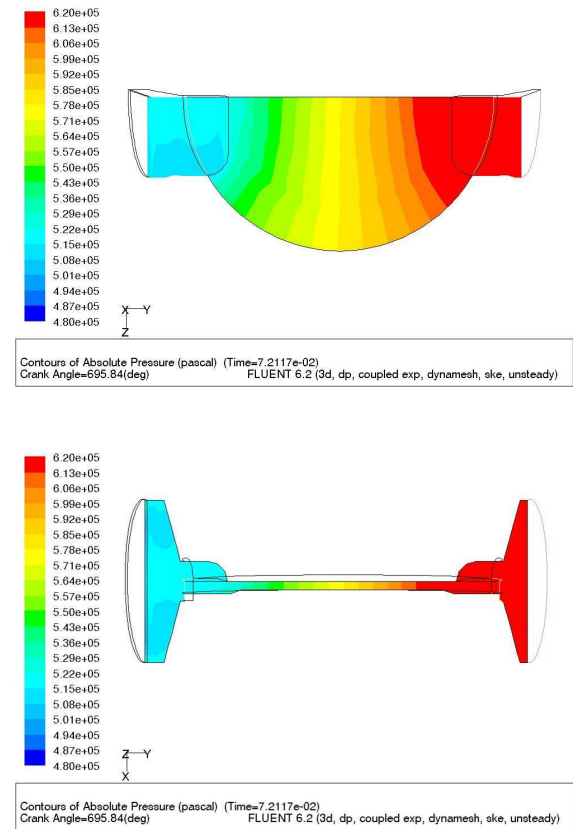


Figure 16: Pressure distribution at the cylinder cap (a) and in the symmetry plane (result of 3d simulation)

#### 6 Conclusion

In the project ‘The flow in a reciprocating compressor’ sponsored by the EFRC different models predicting the pressure waves in the cylinder and their interaction with the valve dynamics are investigated. Following an idea of G.Machu<sup>3</sup> it turns out that a quasi 1-d model is sufficient. In particular the impact velocity of the

valve plate onto the valve seat can be predicted well. Thus the quasi 1-d model will be used as the basis of design tool.

Future research will include the investigation of fast running compressor for heavy gases. The moment onto the piston will be of special interest and how it can be influenced by a special shape of the piston. In a parallel project the heat transfer from the cylinder wall and piston rod onto the gas will be investigated.

## 7 Acknowledgements

The research is financed by the European Forum for Reciprocating Compressors. The authors want to thank G. Machu and P. Steinrück (Hoerbiger) and G. Samland and D. Sauter (Burckhardt Compression) for many fruitful discussions.

---

## References

- <sup>1</sup> Costagliola, M. (1950): The Theory for Spring Loaded Valves for Reciprocating Compressors. J. Appl. Mech, 415-420.
- <sup>2</sup> Machu, E. (1998): Problems with modern high speed short stroke reciprocating compressors: Increased power requirement due to pocket losses, piston masking and gas inertia, eccentric gas load on the piston. Gas machinery conference USA.
- <sup>3</sup> Machu, G. (2004): Calculating reliable impact valve velocity by mapping instantaneous flow in a reciprocating compressor. Gas machinery conference USA.
- <sup>4</sup> Flade, G., Steinrück, H. (2004): Anfängliches Öffnungsverhalten von Kompressorventilen. PAMM Proceedings in Applied Mathematics and Mechanics, 4, 450-451.
- <sup>5</sup> Meyer, G. (2004): Simulation der Strömung in einem Kolbenverdichter. Diplomarbeit, TU-Wien.
- <sup>6</sup> Zierep, J. (1997): Grundzüge der Strömungslehre. Springer Berlin Heidelberg.





# **Effect of Pulsations on Separator Efficiency**

by:

**S.P.C. Belfroid, G. Alberts**

**Department Flow and Structural Dynamics**

**TNO Science and industry**

**Delft**

**The Netherlands**

**stefan.belfroid@tno.nl**

**4<sup>th</sup> Conference of the EFRC**  
**June 9<sup>th</sup> / 10<sup>th</sup>, 2005, Antwerp**

## **Abstract:**

To test the hypothesis that pulsations affect the separation efficiency of gas liquid separators, the efficiency as a function of pulsation frequency and amplitude has been investigated experimentally. During the investigation, separation efficiency measurements have been carried out on different types of separators. The frequencies were varied up to 100Hz and the amplitudes up to 6% peak-to-peak. Efficiency decreases were measured up to 60% of the efficiency without pulsations.

## 1 Introduction

Numerous failures of compressor valves and piston rods have been reported caused by liquids in the compressor, despite the presence of a liquid separator located upstream of the compressor. In reciprocating compressor applications the separator acts in a strongly pulsating flow. Besides a non optimal design of the separator vessel, several mechanisms have been investigated to explain this regular occurrence of liquid carry over.

The first mechanism is the phase behaviour in the system between the separator and the compressor. The gas exits the separator at saturation conditions. Due to a pressure loss or due to pulsations, condensation might occur. The formed liquids can often easily accumulate and carry over into the compressor on a regular basis. The second mechanism is the disturbance of the droplet or liquid film behaviour in the separator itself. The design of gas-liquid separators is based on average flows. The effect of pulsations on the separation efficiency is never taken into account in the design of separators.

To verify this last mechanism, the separation efficiency as a function of pulsation frequency and amplitude has been investigated experimentally. During the investigation, separation efficiency measurements have been carried out on a vertical knock-out vessel with and without a vanepack and an axial cyclone. The aim of the experiments was to measure the effect of pulsation frequency and amplitude on this efficiency.

This research has been done in commission by the EFRC R&D working group.

## 2 Experimental set-up

In Figure 1, a schematic is plotted of the separator test set-up. The liquid, which is in all experiments water, is injected in the (pulsating) gas flow by using a spray nozzle<sup>1</sup> in order to create a mist flow. By varying the injection pressure on the spray nozzle, the injected liquid rate can be varied. The injection point position was varied from approximately 2.0m upstream from the vessel inlet, close to the vessel, approximately 0.2m from the vessel, and in the vessel.

The separators used are a large knock-out vessel<sup>2</sup>, which could be used with and without a vane pack<sup>3</sup> and an axial cyclone<sup>4</sup>. The knock-out vessel used is a large diameter ( $\varnothing 300\text{mm}$ ) vessel with a total height of 1400mm. The vanepack can be inserted in the vessel. The vessel was kept as simple as possible. This means that no specific inlet devices, such as half open pipes, were used. The inlet tubing

has either an internal diameter of 67mm or 79mm. The inlet tubing was made of Perspex so visually the spray formed could be observed. All experiments with the axial cyclone are done with the  $\varnothing 67\text{mm}$  tubes. The volume of the vessel of the axial cyclone is with a volume of 15liter much smaller than the vessel used as a knock-out drum, which has a volume of nearly 100liter.

After injection, the fluid is separated from the gas flow by the separators. The amount of liquid that is injected and the amount of liquid that is separated are measured, by weight, in order to calculate the separation efficiency. The pump delivers a constant flow with a pressure up to 100 bar. By means of a bypass the injection pressure can be controlled. The injected liquid rate is determined by measuring the water rate pumped.

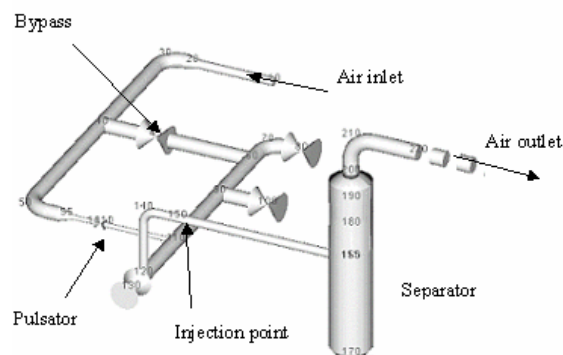


**Figure 1:** Experimental set-up

Pulsations are generated by means of a 'pulsator'. That is, a rotating cylinder with a number of bores. By varying the frequency of rotation of the cylinder, the frequency of the pulsations is varied. The pulsations generated in the experiments are in the range of 0 to 100Hz. By means of the bypass valve part of the flow can be diverted from passing through the pulsator. This results in a variation of the amplitude of the generated pulsations. In the case of the reference measurements without pulsations, the complete gas flow is passed through the bypass and the pulsator is closed off. Only large amplitude pulsations could be generated if an acoustic resonance could be excited in the system. This means that the experiments are performed only at specific frequencies. All the frequencies were well below the internal resonance frequencies of both vessels so no internal acoustic resonance could be excited in the separators.

Online measurements were performed of the static injection pressure and the gas flow. The pulsations are measured by means of the pressure measurements at several locations in the inlet tubing and in the vessel. By means of a two microphone method<sup>5</sup> the standing and travelling

waves can be re-constructed from the pressure measurements in the tubing. From this re-construction the velocity amplitudes are determined at the various points in the inlet tube.

In the experiments, the frequency, the gas and liquid flows are varied over a wide range (Table 1). At each setting of process conditions, nominally four experiments are done to measure the reproducibility.

**Table 1:** Process variations

Parameter	Range
Pulsation frequency [Hz]	20 – 100
Gas flow [m <sup>3</sup> /hr]	100 - 600
Liquid flow [l/m]	0.4 – 0.75

### 3 Results

#### 3.1 Knock-out vessel

In the experiments with the knock-out vessel, efficiency experiments are carried out with varying frequency, gas rate and liquid rate. At first experiments are carried out without the vanepack in place. In Figure 2 the separation efficiency of the knock-out vessel is presented as function of inlet velocity, with and without pulsations. All the experiments plotted in Figure 2 are for pulsations at a frequency if  $f \approx 84$  Hz. In case of multiple points at the same inlet velocity, the liquid injection rate was varied. The reproducibility of the efficiency measurements is shown by error bars. The measurements normally have an accuracy of less then  $\pm 5\%$ . The variations measured could in most cases be attributed to instabilities of the liquid pump. In case of low inlet velocities ( $u < 20$  m/s), no difference without or with pulsations could be measured. However, for the higher inlet velocities ( $u > 20$  m/s), the difference measured was between 5 and 10%. In terms of absolute amounts of liquid that are not separated this corresponds to large liquid rates.

The reduction in separation efficiency showed no relation with the frequency (see Figure 3). However, a trend with the pulsation amplitude in the vessel is clearly. In Figure 3 the separation efficiency is plotted as function of pulsation amplitude for different frequencies. The trend is that for pulsations amplitudes larger than 200 Pa the separation efficiency drops. This trend is visible for all frequencies. This would confirm the idea that the droplet motion is affected by the pulsations. To distinguish between effects in the vessel and upstream of the vessel, the position of the injection nozzle was varied from upstream to in the vessel.

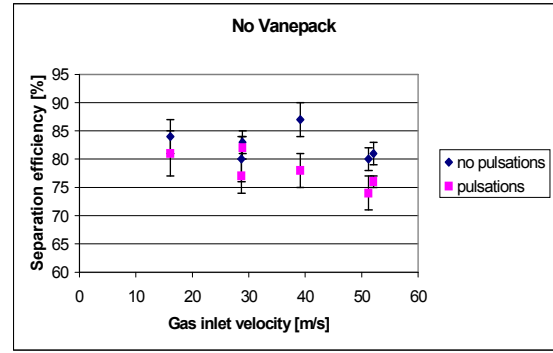


**Figure 2:** Separation efficiency of the knock-out vessel without and with pulsations (84Hz)

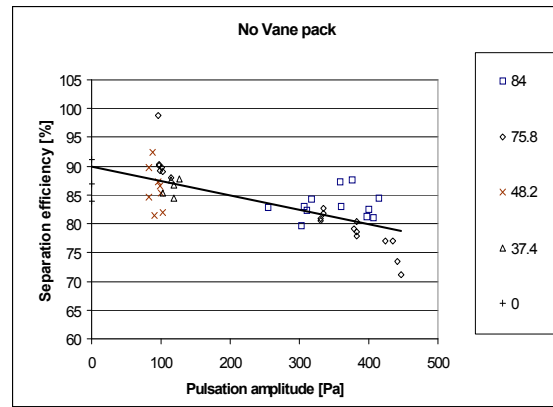


**Figure 3:** Separation efficiency as function of pulsation amplitude in the vessel (no vanepack) for different frequencies

The nozzle was set in the vessel at the height of the inlet nozzle and directed upwards. In this method no homogeneous liquid load is obtained. However, if the pulsations in the vessel are the cause of the decrease in efficiency, this should be detected in this way. In Table 2 the efficiency with and without pulsations is given. For all experiments the frequency was  $f \approx 84$  Hz and the amplitude of the pressure pulsations in the vessel  $p \approx 225$  Pa. The liquid injection rate was set at  $q_l = 0.7$  l/min. In these case of the liquid injection upstream of the inlet, an efficiency decrease was measured of approximately 5%. In the case of the injection in the vessel no efficiency decrease was measured. This means that the mechanism for the separation efficiency decrease must be sought outside the vessel i.e. in the inlet section.

**Table 2:** Effect of the position of the liquid injection nozzle on the separation efficiency without and with pulsations. The main frequency of the pulsations is for all cases  $f \approx 84$  Hz and the amplitude of the pressure in the vessel  $p \approx 225$  Pa

Liquid Injection position	Separation efficiency [%]	
	No pulsations	Pulsations (84 Hz, 225 Pa)
Position 1 (2.0m upstream)	$81 \pm 2$	$76 \pm 1$
Position 2 (0.2m upstream)	$80 \pm 2$	$74 \pm 3$
Position 3 (in vessel)	$64 \pm 3$	$63 \pm 2$

### 3.2 Knock-out vessel with vanepack

The same trend of an efficiency decrease as function of pulsation amplitude is measured in case a vanepack internal was used in combination with the knock-out vessel. In Figure 4 the separation efficiency is plotted as function of the pulsation frequency for the experiments with and without vanepack. The total reduction of separation efficiency is less for the vanepack, but the same trend is measured.

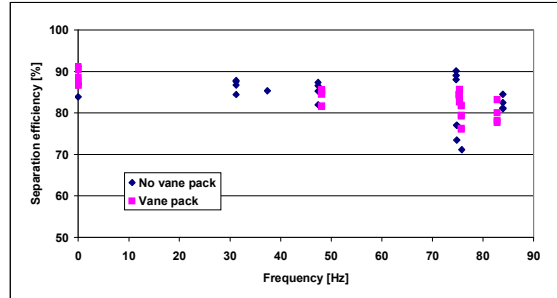


**Figure 4:** Separation efficiency as function of pulsation frequency for an knock-out drum with and without vanepack

### 3.3 Axial Cyclone

The third type of separator tested is the axial cyclone. The vessel itself was much smaller than the vessel used for the knock-out vessel experiments. The change in vessel volume enabled us to generate higher pulsations in the vessel itself as the reflection between inlet piping and the vessel was reduced. A liquid injection directly in the knock-out vessel showed no effect of pulsations in the case of the axial cyclone, therefore, the liquid injection nozzle was always positioned approximately 0.2m from the vessel inlet (position 2). For all the experiments with the axial cyclone the liquid injection rate was set at  $q_l = 0.7$  l/min.

In Figure 5 the effect of pulsations are plotted for different inlet velocities. In the case of no pulsations the efficiency drops for increasing inlet velocity similar to the knock-out vessel but more severe (Figure 2). The design velocity of this type of separator is in the order of  $u = 15$  m/s. A decrease in efficiency for higher gas throughputs is caused by the transport of the liquid film in the cyclone<sup>6</sup>. With respect to the experiments with pulsations, for inlet velocities larger than 10 m/s, the pulsations have a large effect on the separation efficiency. For the case of  $u = 17$  m/s the efficiency drops below 50%, while the efficiency without pulsations almost was 90%. The decrease has been measured for different frequencies.

No clear relation was found between the pressure amplitude in the vessel, which was measured at the top, and the separation efficiency (Figure 6).

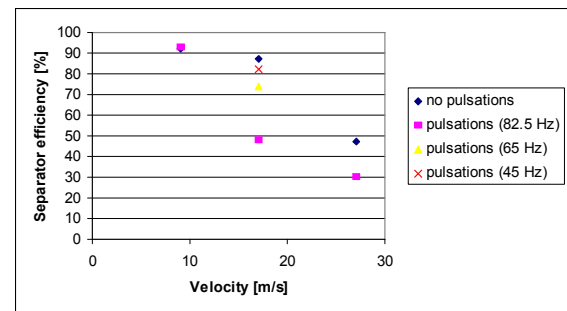


**Figure 5:** Separation efficiency as function of inlet velocity

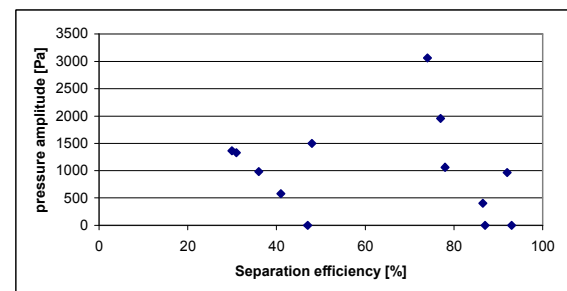


**Figure 6:** Separation efficiency as function of pulsation amplitude

## 4 Discussion

Based on the experiments with the knock-out vessel and the axial cyclone, a clear efficiency decrease is measured in the case of a pulsating flow. From the experiments with the direct injection in the knock-out vessel it can be concluded that the cause of the efficiency decrease is at the inlet piping. The main disruption of both the liquid and the gas flow due to pulsations is at the vessel inlet. In the case of pulsations, the amplitude of the pressure is very



small, even in the case of a resonance. The pulsations are in the order of 1% peak-to-peak. However, the amplitude of the velocity fluctuations can be very large (up to 100% or higher).

The velocity fluctuations at the inlet of the vessel are reconstructed from the pressure measurements in the inlet tubing with a two-microphone method<sup>5</sup>. In Figure 7 a reconstructed velocity wave pattern is plotted for  $f=84$  Hz for a measurement with the knock-out vessel at an inlet velocity of  $u=50$  m/s. The vessel is at  $x=0$ . The velocity fluctuations at the inlet of the nozzle are 25 m/s, which is 50% of the mean velocity!

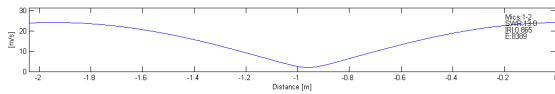


**Figure 7:** Reconstruction of the velocity by means of a two microphone method

With these velocities fluctuations, a maximum velocity amplitude at the inlet is obtained. In the figures Figure 8 and Figure 9 the separation efficiency, normalised with the efficiency measured with no pulsations, is plotted as function of the maximum velocity. The maximum velocity is defined as sum of the mean velocity and the amplitude of the velocity fluctuations at the vessel inlet. For both the knock-out vessel and the axial cyclone, the normalised efficiency drops for the larger velocities. In the case of the axial cyclone there is a threshold velocity. In the case of the knock-out vessel the threshold is less evident due to the limited number of measurement points. The threshold relates to a mechanism at the vessel inlet.

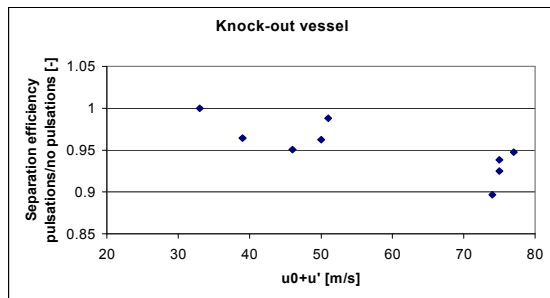


**Figure 8:** Normalised separation efficiency as function of maximum inlet velocity for the knock-out vessel

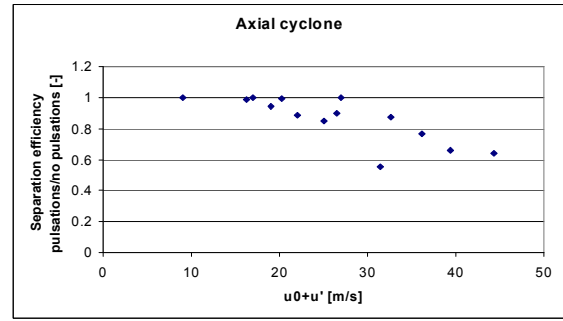


**Figure 9:** Normalised separation efficiency as function of maximum inlet velocity for the axial cyclone

The threshold velocity can be correlated to the behaviour of both the gas and the liquid phase. This threshold velocity can be described by a simple correlation<sup>7</sup>. This relation is propriety of the EFRC R&D working group.

In figure 10 the normalised efficiency is plotted as function of a normalised maximum velocity. In the case of the knock-out vessel the threshold is approximately one and a half times the critical velocity. In the case of the axial cyclone the threshold is very near the critical velocity. The difference between the two experiments may lie in a better separation efficiency for smaller droplets for the knock-out vessel compared to the axial cyclone.

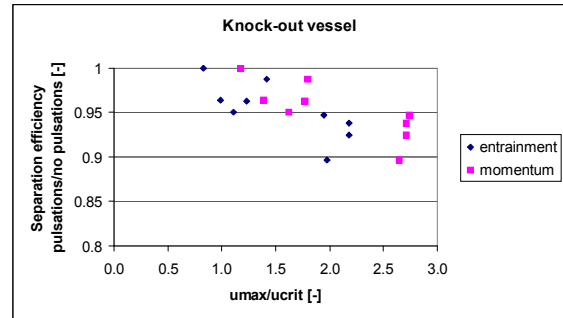


**Figure 10:** Normalised separation efficiency as function of normalised maximum inlet velocity for the knock-out vessel

## 5 High pressure natural gas case

The velocities in our experiments are higher than normal operating conditions. However, in field applications the critical velocities are also much lower. As an example a natural gas case is examined (Table 3). In this example case, the critical gas velocity  $u_{crit}=5.6$  m/s.

The gas velocity itself is  $u_g=4.3$  m/s just below this onset point. With pressure pulsations of 2% peak-to-peak the gas velocity fluctuations will be in the order of 3 m/s. The ratio of maximum velocity to critical velocity is in our base case nearly 1.3. This means that based on our experiments, there is change of a decreased separation efficiency.

This means that also in field applications the maximum velocity can exceed the critical velocity.

**Table 3:** Parameter values of example natural case

Parameter	Value
Pressure [bar]	50
Temperature [°C]	25
Density [kg/m <sup>3</sup> ]	40
Speed of sound [m/s]	430
Tubing diameter [mm]	254
Gas flow rate [c3 Nm <sup>3</sup> /h]	40
Liquid flow rate [mass %]	0.05

## 6 Conclusion

Experimentally, we have investigated the hypotheses that pulsations could be the cause of a decreased efficiency of gas/liquid separators. The separation efficiency of three types of separators, knock-out vessel with and without vanepack and an axial cyclone, has been measured with and without pulsations. The pulsation frequency has been varied between 0 and 100Hz with a maximum pulsation amplitude of 5% pp in the separation vessel.

The efficiency of all separators tested decreased in the case of high pulsations. The efficiency drop measured could be as large as 60% of the efficiency without a pulsating flow. From the experiments it can be concluded that the cause of the decrease is the inlet of the separator vessels. A correlation to determine a critical velocity is found. For maximum velocities below this critical velocity, no efficiency decrease was measured. For velocities higher than this critical velocity, the efficiency decreased almost linearly with the maximum velocity.

It has been made plausible that the same mechanism occurs not only in the experimental set-up, but also may occur in the case of high pressure applications.

It is therefore recommended that in the design of separators not only the average gas and liquid flows are taken into account, but also the maximum velocity including the pulsation velocity fluctuations.

## 7 Acknowledgements

The authors wish to thank Leobersdorfer Maschinenfabrik AG for supplying the axial cyclone for our experiments and the EFRC R&D working group to made this work possible.

## References

- <sup>1</sup> Type PJ15 from Bete via Spray Best which would generate droplets in the order of 50µm.
- <sup>2</sup> The vessel has an internal diameter of Ø300 mm with a total length of 1400mm. The inlet (Ø67 mm) was situated at a height of 750 mm from the bottom of the vessel. The vane pack could be installed at a height of 1100 mm. Based on these dimensions droplets smaller than 300 µm should be separated.
- <sup>3</sup> Mist Eliminator DV270 from Munters with the specs:  
Size : Ø290 mm x 193 mm  
Maximum air velocity : 4 m/s  
 $d_{100}=35$  µm  
The vanepack was set approximately 200 mm from the gas outlet. The vanepack used was installed with vertically oriented vanes.
- <sup>4</sup> Axial cyclone type SNH-7 (supplied by LMF)
- <sup>5</sup> H. Bodén, M. Åborn, Influence of errors on two-microphone method for measuring acoustics in ducts, J.Acoust. Soc. Am 79(2), February 1986
- <sup>6</sup> C.Verlaan, Performance of novel mist eliminators, PhD thesis TUDelft 1991.
- <sup>7</sup> For the details of the correlations the EFRC (Dr. P. Steinrück) can be contacted.

# **Modification of a Reciprocating Compressor due to process Changes in the TOTAL Refinery in Spergau/ Germany**

by:

**Steffen Gast**

**Sales Manager**

**BORSIG ZM Compression GmbH**

**Zwickau**

**Germany**

**s.gast@borsig-zm.com**

and

**Peter Michael Rainer**

**Rotating Equipment Manager**

**TOTAL Raffinerie Mitteldeutschland GmbH**

**Spergau**

**Germany**

**peter-michael.rainer@total.de**

**4<sup>th</sup> Conference of the EFRC  
June 9<sup>th</sup> / 10<sup>th</sup>, 2005, Antwerp**

## **Abstract:**

Process changes in refineries are a common practice nowadays. In many cases the capacity of the existing compressors can be increased such that the flow rate may be stabilized at a higher level for a further period of time. In some cases, however, these process changes are so extensive that the compressors have to be replaced.

## 1 Introduction

Process changes in refineries are normal due to the market's cost pressure, the constantly tightening laws for the minimization of CO<sub>2</sub> and the pressure to improve product quality. To meet the cost pressure existing systems are operated near to their limit of performance.

One result is that existing compressor systems have to be optimized within those changes.

The main objective is to reach better process parameters with the compressor unit. This may be achieved by increasing the speed on the one hand, and by reboring or replacing the cylinders on the other, taking into account the maximum permissible rod forces. However, using these measures an increase in the flow rates of not more than 20-30 % may be obtained, depending on the reserve capacity of each compressor.

If the changes required in the process parameters are not achieved through the measures described it might be necessary to replace the existing compressors with bigger units. Often the end user has to give in to the cost pressure and, together with the compressor manufacturer, has to look for possibilities which maintain as much as possible of the existing infrastructure of the original compressor unit.

This lecture describes one example of the replacement of a reciprocating compressor using the existing infrastructure along with the problems involved.

## 2 History and description of the modernization

The refinery on which this lecture focuses was built between 1994 and 1997 at the southern edge of the Leuna plant on behalf of the French Elf group. Since 2003 the refinery's name has been TOTAL Raffinerie Mitteldeutschland due to the groups' merger. The design and construction of the refinery was realized by a consortium of companies, Technip, Lurgi and Thyssen. The aerial picture shows a view of the process plants from the South and the adjoining parts of the Leuna plant.



Figure 1: Complete view of refinery

The refinery has a processing capacity of approx. 10.5 million tons of mineral oil annually.

The quality of the products complies with valid European norms. Quality assurance was one reason for the modification of the compressor unit presented in this lecture.

### 2.1 Necessity of visbreaker offgas application in vacuum gas oil hydrogenation

The original design of the refinery required that the visbreaker offgas (approx. 4.5 tons p.a.) accruing in the visbreaker had to be used for H<sub>2</sub>S removal and LPG extraction in the FCC. From 2003 this application was no longer possible because the sulphur content in the petrol was lowered. The alternative was to process this gas via the flare gas recovery system without modification of the plant. However, this alternative led to an overload of the flare gas compressor and did not comply with the regulations for the refinery's operational approval. As an answer to this problem, the recontacting of this gas by extension of the offgas processing in the vacuum gas oil desulphurization (VGO) was developed. This solution has following advantages:

- extraction of approx. 7.8 kt/a. propane
- extraction of approx. 7.2 kt/a. butane
- extraction of approx. 5.0 kt/a. naphta
- as well as a reduction of CO<sub>2</sub> emissions by 10 kt/a.

Figure 2 shows modifications to the existing offgas processing in the VGO plant which were necessary to achieve this application.

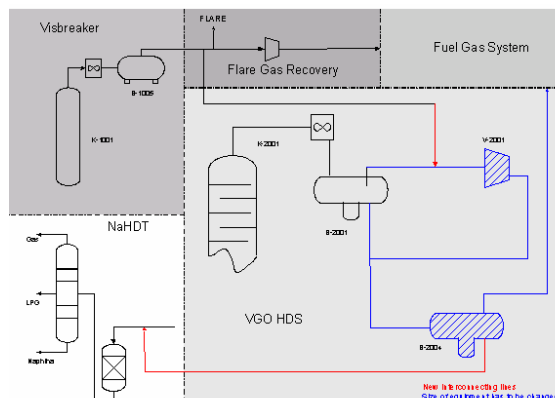


Figure 2: New offgas processing

- increase in the offgas compression capacity with all secondary units (by approx. 400 %)



S. Gast, P.M.Rainer:

Modification of a Reciprocating Compressor due to Process Changes in the TOTAL Refinery in Spergau/ Germany

- increase in the recontacting capacity (vessels, piping)
- increase in the cooling and pump capacity for naphta

## 2.2 Main requirements

The most fundamental conditions limiting the achievement of the modification included:

- integration of the modification into the existing VGO unit;
- installation of as many components as possible while the plant was in operation; and
- further use of the basic foundations of the compressor and the naphta pumps.

Due to the process change in the refinery a volume flow rate which was 4 times higher compared to the former process parameters was required. Suction pressure, intermediate pressure and discharge pressure were to remain at the same levels.

The existing control unit including the measuring system had to be adapted and used further. The most important task was to maintain the existing infrastructure, above all the compressor foundation (see Table 1 below).

The TOTAL refinery engaged a construction expert to establish whether it was possible to continue to use the compressor foundation taking into account the higher forces and momenta of the larger reciprocating compressor now necessary in this location. The specialist confirmed that the foundation could withstand the extra load the larger compressor would bring.

**Table 1:** Main requirements by the customer

- **increased capacity by 400 %**
- **suction pressure, intermediate pressure, discharge pressure remain at the same levels**
- **control concept almost unchanged**
- **existing measuring system has to be reused**
- **space for installation on foundation is not extendible**
- **existing steel structures are to be used**

### 2.2.1 Technical parameters

Table 2 shows the changes in the mass flows and compressor parameters.

**Table 2:** Technical parameters

Existing compressor	New compressor
Flow: 2085 kg/h	Flow: 8855 kg/h
Power: 160 kW	Power: 630 kW
Bore 405/270 mm	Bore 760/490 mm
490 rpm	490 rpm

### 2.2.2 Control concept

Figure 3 shows the control concepts of both the old and the new compressor. The new concept no longer needed the clearance pocket control of the 1<sup>st</sup> and 2<sup>nd</sup> stage so that the new compressor unit was equipped with a bypass between the 1<sup>st</sup> and 2<sup>nd</sup> stage as well as an overall bypass.

A continuously variable flow control achieved by temporarily opening the suction valves was no longer possible because the offgas would tend to polymerize at the higher compression temperatures resulting from this control.

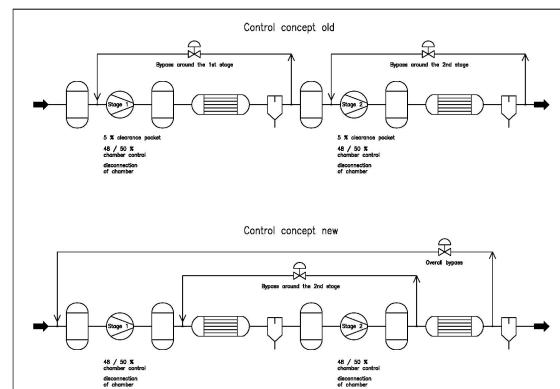


**Figure 3:** Control concept former and new compressor

### 2.2.3 Space and setting up conditions

The difficulties arising from the replacement of the old with the new compressor, using the existing infrastructure, can be seen by reference to Figure 4 where a size comparison can be made. The size and design of the foundation could not be changed for this modification so it was necessary to look for ways in which to fasten the new compressor, which was much bigger, on to the original foundation block without damaging the foundation reinforcement. Figure 5 shows how, together with the refinery management, a solution was achieved.

S. Gast, P.M.Rainer:

Modification of a Reciprocating Compressor due to Process Changes in the TOTAL Refinery in Spergau/ Germany

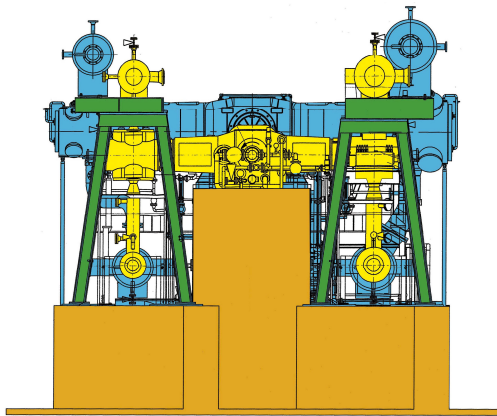


**Figure 4:** Comparison of the compressor sizes

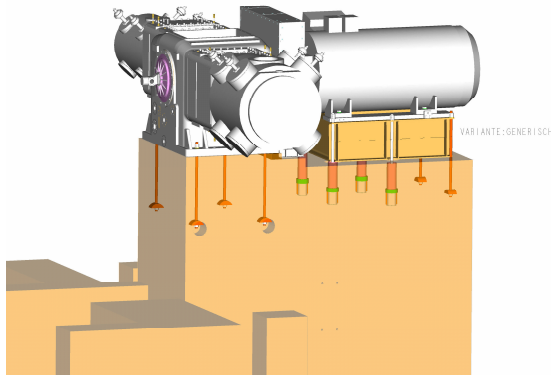


**Figure 5:** Fastening the compressor on the existing foundation

Special attention had to be given to the boreholes. To avoid cracking in the foundation these could not be located too close to its outer edges. The compressor and the two outer fixings of the motor, in particular, were fixed to the foundation by different means (Figure 6).

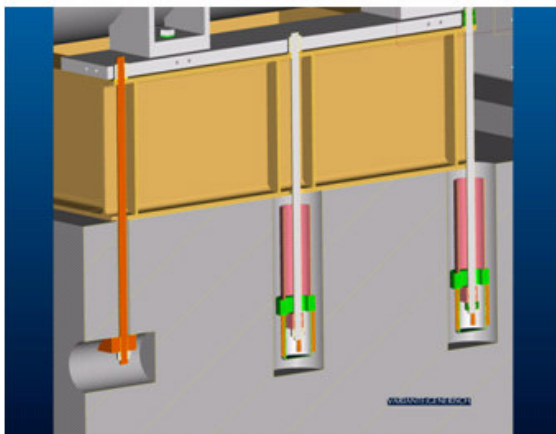


**Figure 6:** Special solution for fastening the compressor on the existing foundation

### 2.2.4 Measuring System

Since an increase in the flow rate had been realized whilst maintaining the number of stages and the levels of suction pressure, intermediate pressure and discharge pressure, the existing control system as well as the existing measuring equipment had also to be further utilised. The local panel as shown in Figure 7 was completely maintained. In addition, a rod drop control system was integrated into the new compressor.

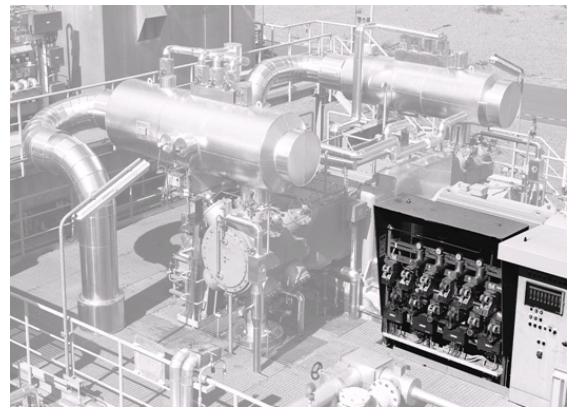


**Figure 7:** Local panel on 6-m-platform

## 3 Problems after start-up

During operation big vibrations occurred on the suction side piping although a pulsation analysis according to API 618 app. 3 had been made at the refinery's request. The measurements carried out by the customer demonstrated excessive vibration values. The vibrations measured on the suction lines amounted to values between 10 mm/s towards the motor axis and nearly 40 mm/s in the pistons' operating direction. It followed as a logical consequence that the vibration values of the compressor should be recorded. Figure 8 shows the oscillation amplitude at the 1st stage cylinder cover in the pistons' operating direction. The recorded measurements of the vibration values were unclear as to possible causes.

S. Gast, P.M.Rainer:

Modification of a Reciprocating Compressor due to Process Changes in the TOTAL Refinery in Spergau/ Germany

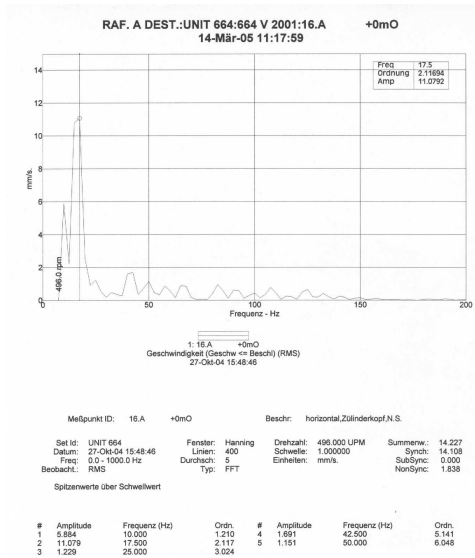


**Figure 8:** Vibration measurement of 1<sup>st</sup> stage cylinder cover in the pistons' operating direction

It was noticeable that the maximum oscillation amplitude of the piping arose when the compressor reached nearly double speed. As a consequence an additional support was installed to hold the piping in order to reduce the vibrations. With the help of this support vibrations on the suction line 1<sup>st</sup> stage were significantly reduced. However, the clamping of this line resulted in an overload of the inlet flange at the 1<sup>st</sup> stage pulsation damper. The compressor had to be stopped. Continuing operation was not feasible neither with vibrating piping without fixed point nor with an overloaded inlet flange. The risk of escaping gas containing H<sub>2</sub>S was too high and totally unacceptable.

## 4 Searching for causes

To determine the causes, the compressor was started up again for a short measuring run under strict safety precautions. Vibration measurements were carried out on the piping system and the foundation with the help of pipeline dynamics specialists, the designer of the piping as well as specialists for construction dynamics. The analysis of this measuring run as well as the investigations had the following results.

### 4.1 Piping

It was found that some of the solid bearings holding the pipeline had not been designed in accordance with the piping's isometry. However, in the mechanical response analysis these solid bearings had been the basis of the calculations. Simultaneously, the pulsation analysis had recommended orifices to reduce the gas pulsation, some of which had not been installed. Furthermore,

the installation of the piping did not exactly correspond to the as-built-drawing, which led overall to space problems during the installation of solid bearings in the suction side pulsation dampers area.

### 4.2 Vibration measurements at compressor and foundation

The vibration measurements, which were carried out at 50 % and at 100 % load of the compressor, revealed that very high vibration values were reached above all in the operating direction of the compressor (see Table 3 below).

The measuring points are shown in Figure 9.

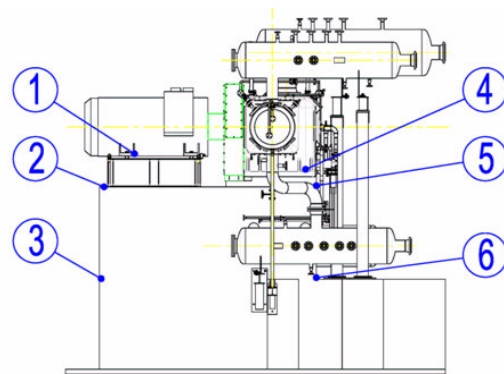


**Figure 9:** Measuring points for the vibration measurements as recorded in Table 4

**Table 3:** Cumulative values of the vibration velocities  $V_{eff}$  (mm/s)

Measuring Point	Measuring Direction	Load 0%	Load 50%	Load 100%
1	Motor Axis	0.6	2	1.2
Foot of Motor	Axis piston rod	9.7	10.1	11
	Vertical	1	1	1.2
2	Motor axis	1.4	3.1	2.3
Foundation on the motor + 6m	Axis piston rod	9.8	10.4	11.3
	Vertical	1.2	1.4	1.2
3	Motor axis	1	1.5	1.9
Foundation Wall + 3m	Axis piston rod	6.4	6	7.3
	vertical	1.2	1.6	1.7
4	Motor axis	0.7	2	1.5
Compressor frame	Axis piston rod	9.9	10.2	11.1
	vertical	1.9	2.3	2.1
5	Motor axis	0.6	1.8	1.3
Foundation Compressor frame	Axis piston rod	7.1	7.2	7.5
	vertical	2.3	2.6	2.5
6	Motor axis	0.4	1.2	0.9
Foundation Wall + 3m	Axis piston rod	4.5	6.5	6.8
	vertical	0.4	0.5	0.6

S. Gast, P.M.Rainer:

Modification of a Reciprocating Compressor due to Process Changes in the TOTAL Refinery in Spergau/ Germany

After that the natural frequency of the foundation was measured by an impact analysis. Amounting to approx. 17 Hz, the natural frequency of the foundation was very close to the 2<sup>nd</sup> harmonic natural frequency of the compressor, which comes up to 16.3 Hz. That is to say, the analysis revealed very clearly an undesirable resonance event.

This result was confirmed by vibration measurements carried out during the operation of the compressor (Figure 10).

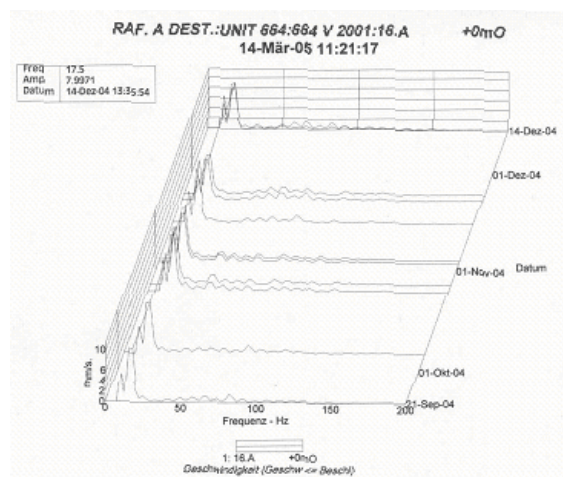


**Figure 10:** Waterfall diagram of the vibration measurement at the cover side of the 1<sup>st</sup> stage cylinder over a period of 3 months

### 4.3 Forces exciting the compressor

As result of the high vibrations measured at the foundation, the foundation's design was rechecked in detail. A serious defect was detected in the design which led to the loads on the foundation caused by the compressor being considerably reduced contrary to the requirements of the compressor's manufacturer.

Consequently, the existing foundation was overloaded contrary the original statement of the specialist engaged.

## 5 Elimination of causes

In order to be able to operate the compressor safely on a foundation whose size was very limited, essential improvements were necessary with respect to piping, foundation, free forces and momenta of the compressor.

### 5.1 Piping

In the beginning, the pulsation dampening orifices had been installed in the main pipings due only to lack of time and space. Later, a check was made to establish if orifices were also necessary in the safety and expansion pipings. As a result some pulsation dampening orifices were additionally installed.

The pipe support concept was optimized between the static and dynamic load of the pipings and on the basis of the vibrations measured additional or modified supporting joints were designed first and foremost on the suction side pipings at the pulsation damper (see Figure 11).



**Figure 11:** Support suction side 1<sup>st</sup> stage modified by TNO

### 5.2 Foundation

An FEM model of the foundation was drawn up.

The modelling of this model revealed important facts about the actual vibrations of the compressor components. Not only were the individual foundation units vibrating but also the whole foundation plate. The vibrations of the pulsation dampers, also that is to say of the piping, were accordingly high due to the movements in the resonance some of which were actually moving in opposite directions.

The increased vibrations corresponded with the measured values using the existing foundation's simulation model and the determined natural frequency. So this provided clear and definite proof of what was causing the excessive vibrations. The next task, then, was to look for an effective way of bringing the natural frequency out of the exciting area.



Modell V0 - Basismodell

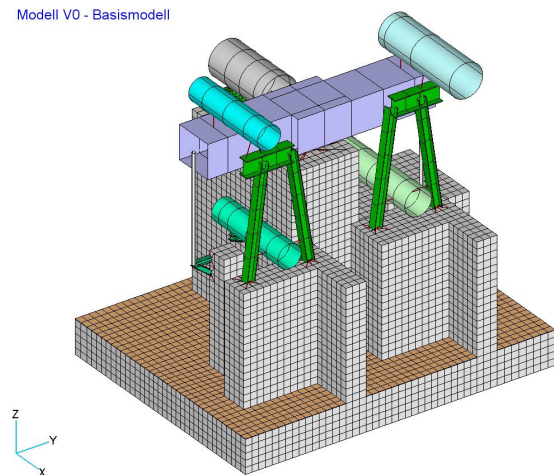


**Figure 12:** Original compressor foundation

Figure 13 shows the optimum result achievable from the calculation and simulation.

However, the simulation showed that with the help of the top concrete layer on the existing foundation, the natural frequency could not be moved by 20 % min. out of the measured resonance area as requested in literature. But the resonance movements of the individual foundation units could be significantly reduced or avoided altogether by the modification of the foundation.

Due to the limited space available a detuning of only approx. 10 % could be reached. The new optimized foundation was designed in a way that all piping and cylinder supports could be directly attached to the foundation.

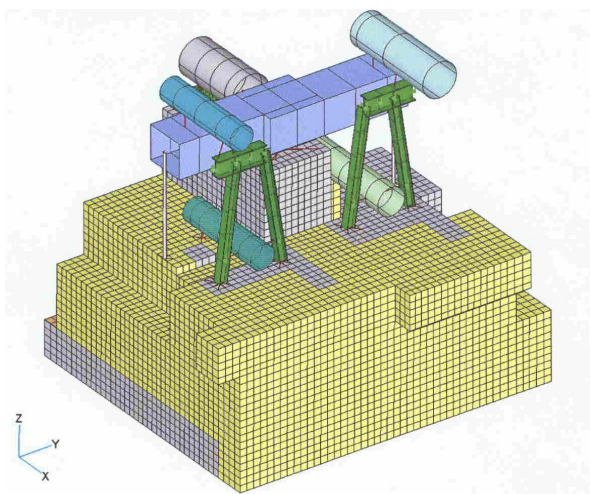


**Figure 13:** Optimum design of foundation model – Front view

## 5.2 Reduction of the free forces and momenta of the compressor

Since the optimization of the foundation resulted in detuning the natural frequency by only 10 %, the free forces and momenta of the compressor had also to be reduced.

The free forces and momenta of a horizontally balanced opposed “boxer” compressor are mainly determined by the different weights of the moving axes and by the angular misalignment of the cranks.

In this case the bigger 1<sup>st</sup> stage piston with a diameter of 760 mm was, of course, heavier than the small piston. With the help of suitably simulated optimization runs the optimum weight, stiffness and permissible deformation was sought, while at the same time making it possible to reduce the exciting forces. A reduction of the free forces by at least 10 % was aimed at.

Obviously, the mass balancing of the axes could not only be realized by reducing the weight of the 1<sup>st</sup> stage piston. The moving mass of the 2<sup>nd</sup> stage had to be increased as well. With this necessary optimization the actual rod load as a result of gas and inertia force had to be taken into account. In addition, attention had to be drawn to the fact that the existing suction valve unloading had a substantial influence on the rod load by shutting off compression chambers.

The original piston was welded, but now a cast piston was favoured in order to achieve maximum possible reduction in weight.

GGG40.3 was the chosen piston material since it is a two-piece braced piston which is subject to variable kinds of stress. The maximum stress was limited by the material. The calculated maximum permissible deformation of the piston amounted to 0.2 mm.

At first the optimization was simulated with an unribbed piston. By reducing the weight the stiffness of the piston was also reduced.

Figures 14 and 15 show the results of the optimization runs of an unribbed cast piston. As expected, the point of highest stress concentration was in the middle of the piston axis since there the momenta resulting from gas and inertia forces are at their highest levels. However, the deformations which were calculated were much higher than the maximum permissible values, so that this option had to be dropped.

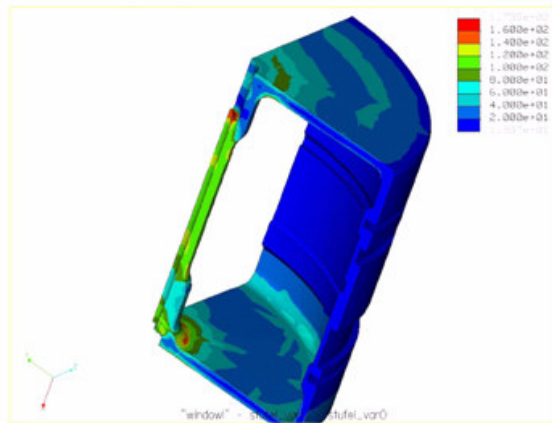


**Figure 14:** Flow of stress – piston without ribs

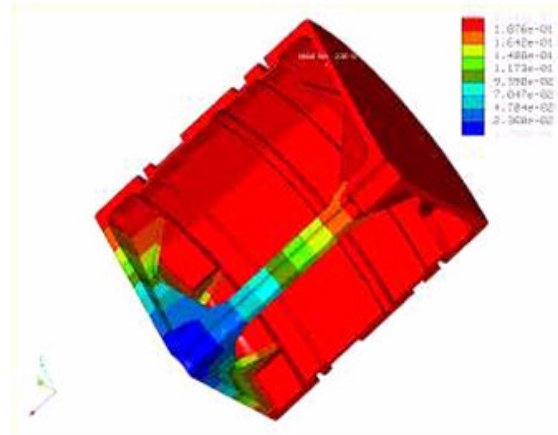


**Figure 17:** Deformation – ribbed piston

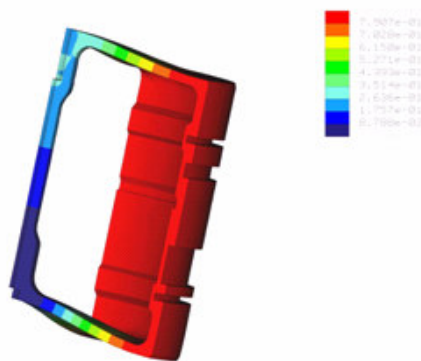


**Figure 15:** Deformation – piston without ribs

A slightly ribbed cast piston showed the best results with regard to stiffness, stress and reduction in weight. The calculated deformation did not exceed the required limits. The maximum permissible stress was not reached at a single point.

Figures 16 and 17 show the calculated stress flow of a ribbed piston and the determined maximum deformation of such a piston.

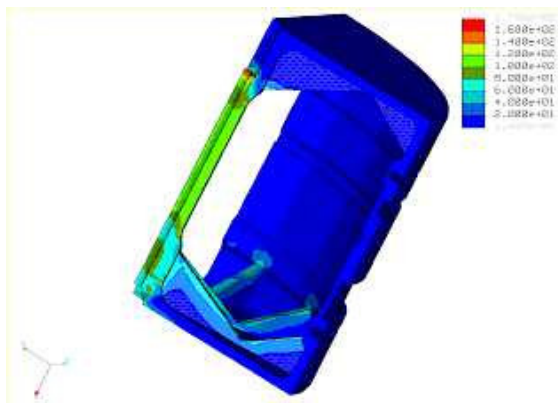


**Figure 16:** Flow of stress – ribbed piston

Figure 18 shows the original state of the forces. Figure 19 shows the reduction of the compressor's free forces which were eventually reached by optimizing the weight of the 1<sup>st</sup> stage piston and increasing the weight of the 2<sup>nd</sup> stage piston.

$F_{yges}$  is the graph of the resulting forces of the 1<sup>st</sup> and 2<sup>nd</sup> order, the y-axis being the operating direction of the pistons.  $F_{y1}$  represents the forces of the 1<sup>st</sup> order and  $F_{y2}$  the forces of the 2<sup>nd</sup> order.

**Forces y-Direction**

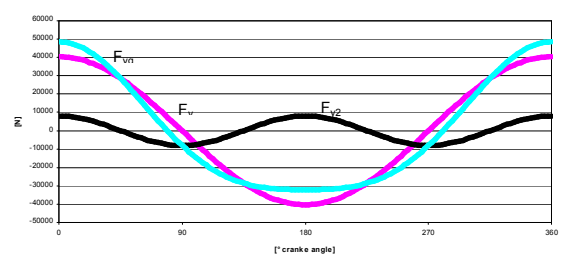


**Figure 18:** 1<sup>st</sup> and 2<sup>nd</sup> order forces in original state

**Forces y-Direction**

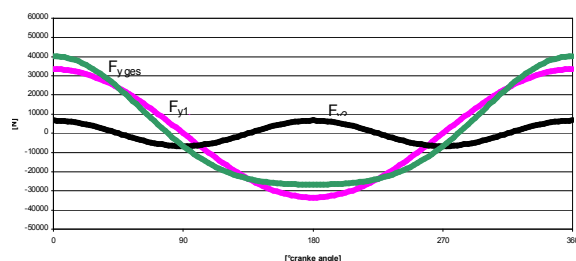


**Figure 19:** 1<sup>st</sup> and 2<sup>nd</sup> order forces after optimization

S. Gast, P.M.Rainer:

Modification of a Reciprocating Compressor due to Process Changes in the TOTAL Refinery in Spergau/ Germany

---

The difference in the vibrating masses of both axes was reduced by this design so that a 17% reduction of the free forces was achieved compared with the original design. The impact of the resulting small increase of the momenta on the foundation block was smaller than that of higher free forces.

Thanks to the reduction of the free forces and the modification of the foundation and the piping, an optimum overall result for the future operation of the compressor was eventually achieved. However, despite all realized measures it was not possible to keep the maximum permissible oscillation amplitude of 2.0 mm/s at the upper edge of the foundation.

## 6 Conclusion

Due to prevailing cost pressures on the market, it is a common practice for existing components to have to be used further when modifying an existing plant to increase performance and to increase the load. Great efforts will have to be made, though, to analyse the loading capacity of the component parts and to guarantee the reliability of the entire new plant.

In the case described here the following tasks were necessary:

- simulation of combining an existing foundation with a bigger, new compressor (FEM model)
- pulsation analysis of the piping system including check of as-built-status of existing components
- vibration measurements at the compressor to confirm the simulation results

The modernization process presented in this lecture was made more difficult, expensive and protracted by a serious mistake in the design of the original foundation. At this point there shall not be made an assessment as to the extent to which such mistakes in calculation may be ruled out by engineering companies in advance. The lecture demonstrates that later on the consequences of calculation mistakes were corrected to the greatest possible extent by taking appropriate measures. However, in most cases the result has to be a compromise between maximum requirements and achievable facts.

---

## References

- <sup>1</sup> Wölfel Beratende Ingenieure TOTAL Raffinerie Mitteldeutschland, Verdichter 664V-2001, Maschinengründung, Schwingungsprobleme 2. Bericht: Untersuchung und Bewertung von Sanierungsvarianten
- <sup>2</sup> Ingenieurgesellschaft Schwingungsmesstechnik Maschinendiagnose GbR Prüfbericht Nr.: 181/12/04, Leuna/Germany, 2004
- <sup>3</sup> A. Eijk, TNO Pulsation Analysis Visbreaker Offgas compressor V2001, Delft, 2004

# **Pulsation Study for two 2,250 bar Hyper Compressors – Measurement, Theory, Measures –**

by:

**Dr.-Ing. Brümmer, Andreas**  
**KÖTTER Consulting Engineers, Rheine, Germany**

**4<sup>th</sup> Conference of the EFRC**  
**June 9<sup>th</sup> / 10<sup>th</sup>, 2005, Antwerp**

## **Abstract:**

In a LDPE-plant two hyper compressors are operating in parallel. In order to improve the blend performance, it was planned to increase the static pressure on the discharge side of the compressors up to 2,400 bar. By means of suitable measures the release of the safety valves caused by pulsation related pressure peaks had to be prevented for the further operation. Additionally, a safe and reliable operation of the plant from vibration technical aspects had to be ensured. For processing a pulsation study in conjunction with pressure and pipe vibration measurements was conducted. It turned out that in order to avoid the release of the safety valves due to pulsations a synchronisation of both compressors at a fixed phase relationship is the favourable solution. Additionally, high pipe vibrations were reduced by installation of orifices and new pipe supports. Finally, after realisation of the measures the discharge pressure has been raised up to 2,400 bar without any pulsation or vibration problems.



### 1 Introduction

For the production of polyethylene (LDPE) two 2-stage, 4-crank, maximum pressure reciprocating compressors (hyper compressors) are applied, which produce in a present parallel operation a reactor mean pressure (discharge pressure 2<sup>nd</sup> stage) of 2,250 bar. In order to increase the blend performance, the reactor mean pressure of the plant has to be increased to 2,400 bar. The new static mean discharge pressure of the reciprocating compressors does not exceed the original design range of the plant. Therefore, no rebuilding measures are planned for the compressors and the piping system.

Based on previous examinations and the experience of the operator it is however known that maximum pressures in the piping system are temporary significantly above the static mean value. The pulsations excited by the reciprocating compressors are responsible for this. In case the temporary pressure peaks lie above the release pressure of the safety valves, a blow-off occurs and this leads to an immediate shut-down of the plant.

The first target of the in the following presented pulsation study therefore is to design measures, which reduce the maximum pressure peaks of the 2<sup>nd</sup> stage to a level possibly below 2,500 bar. Generally, two approaches are to be examined for this purpose. One possibility is the favourable synchronisation of both compressors (phase relationship). The other possibility is the installation of pulsation dampers (e.g.  $\lambda/4$ -resonators). The second target of the pulsation study is to ensure a safe and reliable operation of the plant from vibration technical aspects for the planned discharge pressure. In case of expected critical vibrations, effective measures have to be proposed.

### 2 General approach

The processing of the project is carried out in two phases.

In phase I the vibration technical actual-status-situation of the plant in the zone of the maximum pressure compressors is measurement-technically registered, proceeding from the suction side of the 1<sup>st</sup> stage to the interstage and then to the discharge side of the 2<sup>nd</sup> stage up to the beginning of the reactor. Here, the pressure pulsations of both compressors at various positions are recorded simultaneously together with the piping vibrations as well as the top dead center signals of the 8<sup>th</sup> cylinder of each compressor. The measurements are performed in the steady operation of the plant. In order to detect the influence, which the mean static pressure has on the pulsations and vibrations, the

discharge pressure is reduced for a brief period by approximately 150 bar and then raised again. The measured data are analysed with regard to conspicuous vibration levels and compared to the valid guideline values.

In phase II the two compressors as well as the piping system between the inlet flanges of the pulsation dampers, 1<sup>st</sup> stage, and the reactors are digitised. Subsequently, the unsteady viscous compressible flow in these sections is numerically calculated. The results are compared to the measurements and the numerical system as well as the acoustical characteristics of the reactor is adapted accordingly.

Using the verified numerical model the optimal phase relationship between both compressors with reference to the pulsations is calculated for the increased discharge pressure of 2,400 bar. Furthermore, various pulsation dampers are simulated and their effects are compared. Based on the changes in the pulsations – and therefore in the exciting shaking forces – the changes in the piping vibrations are forecasted. In case of expected critical pipe vibrations, effective measures are designed. Finally, the recommended phase relationship between both compressors as well as the necessary further measures and procedures for the assurance of a safe and reliable operation of the plant are submitted to the operator.

### 3 Basics of assessment and guideline values

As initial orientation values for the evaluation of stationary flexural vibrations on piping the vibrations [1] as shown in figure 1 are adopted and these were also incorporated into the VDI guideline 3842 [2]. These are experience values, which were determined statistically over a period of over 25 years by means of measurements taken on pipework with geometries and holder spacings as normally applied in petrochemical engineering. They are not suitable for the assessment of shell vibrations, brief-period vibrations or vibrations on short piping attachments (e.g. nozzles).

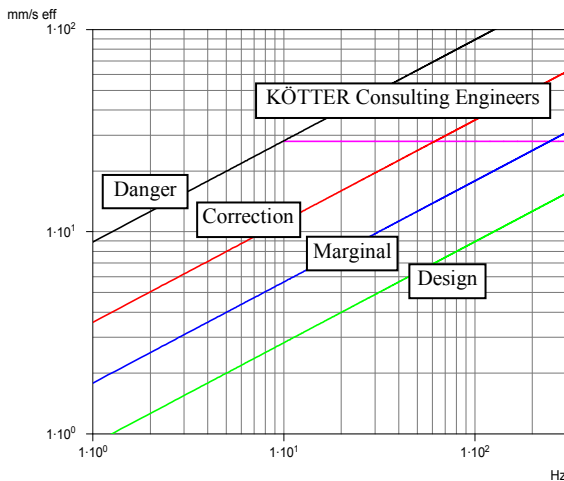


**Figure 1:** Orientation values of allowable piping vibrations with a stationary flexural stress and train

Determined vibration velocities above the line “danger” are normally regarded as being so dangerous that damage to the plant can occur. Additionally, the flexural vibrations of the piping above a frequency of 10 Hz, which exceed a value of 28 mm/s rms are subject to a closer analysis. This procedure is based on our own experience and the standard of Neuman & Esser [3], which envisages this limit value for flexural vibrations on piping and represents an extension of the former VDI guideline 2056 [4].

Generally, attention is drawn to the fact that the values stated are merely orientation values. The decisive factor for allowing vibrations is ultimately the material stress within the pipe wall, which is detected / recorded at critical locations by means of a mobile strain gauge measurement.

## 4 Basics of numerical calculations

### 4.1 Compressor data

Both hyper compressors are of the same type and manufactured by N.P.O. Frunze, Sumy, Ukraine in the year 1977.

Type: 4-crank, 2-stage ethylene hyper compressor

Cylinders: 8 single-acting (2/2 A-flow and 2/2 B-flow)

Speed: 250 1/min (fixed)

Suction pressure: 250 bar

Interstage pressure: approx. 1,100 bar

Discharge pressure: 2,250 bar (condition during measurements)

2,400 bar (aspired condition)

Driver: synchronous electric motor

Drive power: 5 MW

### 4.2 Numerical flow simulation

The process consists of two separate flows, the A-flow and B-flow. Both flows are established at the suction side, 1<sup>st</sup> stage, of both compressors and are merged together inside the reactor. The numerical flow simulation is carried out separately for the A-flow and B-flow. For example the piping sections of the interstage of compressor A and the discharge side of the 2<sup>nd</sup> stage of both compressors (B-flow) are shown in the figures 2 and 3. The digitised piping section starts at the inlet flange of the pulsation damper, 1<sup>st</sup> stage, suction side and ends at the beginning of the reactor. The acoustical model includes the relevant cylinders and valves of the compressors. Because there will be no pressure change at the suction side, 1<sup>st</sup> stage, it is not necessary to extend the flow simulation at this side.

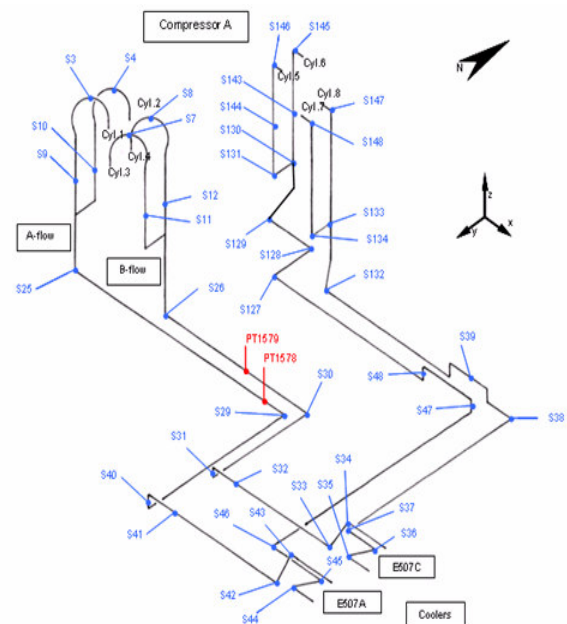


**Figure 2:** Sketch of the interstage of compressor A (A- and B-flow) and the pipe vibration (e.g. S48) and pressure pulsation (e.g. PT1578) measuring points

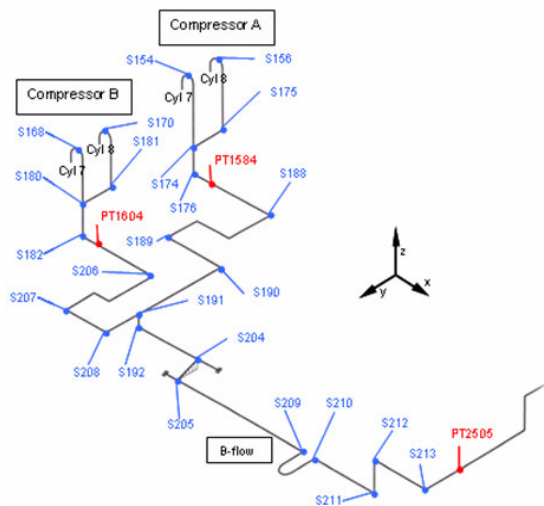


**Figure 3:** Sketch of the discharge piping, 2<sup>nd</sup> stage, (B-flow) of both compressors and the pipe vibrations (e.g. S170) and pressure pulsations (e.g. PT1604) measuring points

The physical boundary condition at the beginning of the digitised piping section is an anechoic end. At the end of the digitised piping section (reactor) the boundary condition is adapted to the measuring data. It turned out that an anechoic end is a good choice, too.

The calculation of the flows in the areas as mentioned is performed on the basis of one-dimensional, unsteady, viscous, compressible Navier-Stokes-equation, the continuity equation and the conservation of energy by means of the method of characteristics in the time domain. In this case, the plunger movement of each cylinder – and with this, the time-dependent volume in the cylinder area – is given full consideration by means of an adaptive network. The opening and closing of the suction and discharge valves is effected in accordance with the actual differential pressures over the individual valve. The state variables of the fluid in the cylinder area and the overall piping system are continually calculated using the dependencies  $\rho(p, T)$ ,  $c_p(p, T)$ ,  $c_v(p, T)$  [5] according to the actual pressures  $p$  and temperatures  $T$ . In this case, the real gas behaviour based on the equations of state mentioned above as well as the wall influence of the piping on the sound velocity of the fluid are taken into consideration.

As the result for any point of the truncated system, the calculation provides the time-dependent shape of the pressure, the density and the flow velocity. Based on this information the shaking forces acting on the piping induced by the pulsations are calculated.

## 4.3 Numerical flow simulation

Due to the unchanged exciting frequencies and unchanged piping resonance frequencies a numerical calculation of the mechanical pipe vibrations is not required for the entire pipe system. Whereas the changing shaking forces due to the changing pulsations caused by the increased static mean pressure are important in terms of the expected pipe vibrations.

In case of required modifications to the pipe support in areas of conspicuous structure vibrations the piping system with and without modifications is modelled using the program ANSYS.

## 5 Measured data and assessment (original situation)

From the signals of the proximity sensors for the top dead centers the phase relationship of  $\varphi = 285^\circ$  results between the compressors A and B during the entire examination of the pipe vibrations. Accordingly, cylinder no. 8 of compressor A is  $285^\circ$  (190 ms) earlier in the top dead center than cylinder no. 8 of compressor B. The cylinder sequence with reference to the top dead center is in timing sequence:

cyl. 1 + 6 – cyl. 4 + 7 – cyl. 2 + 5 – cyl. 3 + 8,

where the phase offset is  $90^\circ$  in each case. Therefore, even with single acting cylinders the main pulsation frequency (8.3 Hz) is twice the rotational speed of the compressor (250 1/min).

### 5.1 Mechanical vibrations

The vibration measurements have been carried out at more than 300 measuring points at the piping and the compressors. At each measuring point the vibrations have been measured in three directions:

- x... shaft direction of the compressor
- y... horizontal
- z... vertical.

It turned out that there are high vibration levels even in the unchanged system, which will be discussed in the following. For this purpose - as an extract out of the total system – the measured vibrations at the piping of the interstage of the compressor A (A- and B-flow) and at the discharge side, 2<sup>nd</sup> stage, of both compressors (B-flow) are shown in figures 4 and 5. The corresponding measuring points are described in figures 2 and 3.

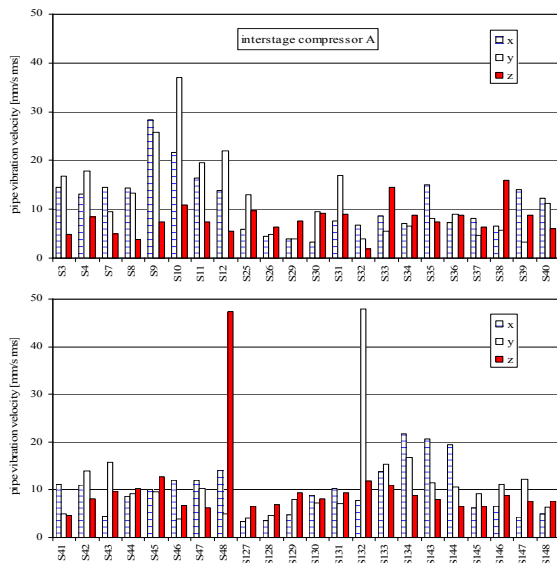


**Figure 4:** RMS vibration velocities (2 - 1,000 Hz) of the piping on the interstage of the compressor A

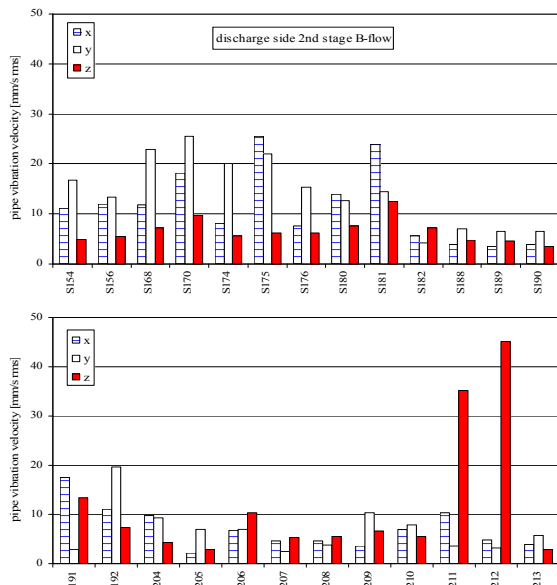


**Figure 5:** RMS vibration velocities (2 - 1,000 Hz) of the piping of the B-flow on the discharge side, 2<sup>nd</sup> stage

The measured vibration frequencies are generally above 20 Hz and therefore the orientation value of allowable pipe vibrations is 28 mm/s rms. The measured vibrations are in the range or above this value in several areas. High vibrations at the piping of figures 2 and 3 are measured:

- in the vicinity of the cylinders (e.g. S9, S10, S132, S170, S175, S181)
- at the A-flow of the interstage (e.g. S48)
- at the B-flow, 2<sup>nd</sup> stage, discharge side (e.g. S211, S212).

These areas are selected from the total system because of their typical excitation and amplification mechanisms subsequently discussed.

## 5.2 Pressure pulsations

The pressure pulsations have been measured synchronously at several points using the installed absolute pressure sensors of the process control system. Together with the installed carrier frequency amplifier these transducers are able to measure pulsations up to a frequency of about 200 Hz.

As an example the measured pulsations at the interstage of the compressor A and at the B-flow, 2<sup>nd</sup> stage, discharge side are shown in figures 6 and 7. It is obvious that the dominant pulsation frequency is twice of the rotational speed of the compressor.

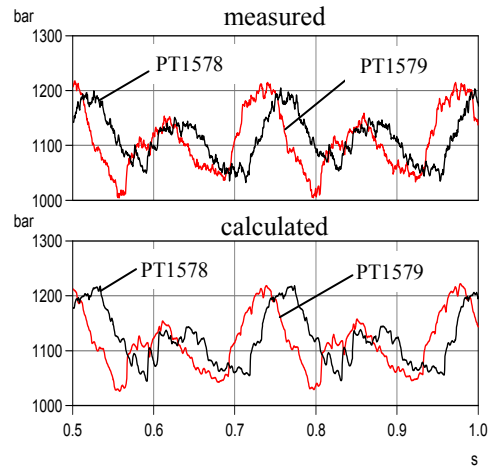


**Figure 6:** Measured and calculated pressure pulsations at the interstage of compressor A (original situation)

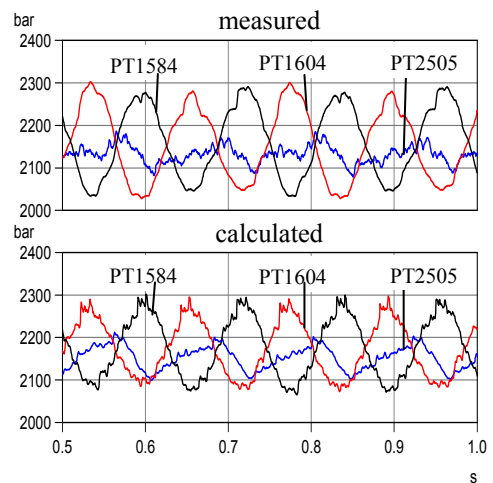


**Figure 7:** Measured and calculated pressure pulsations at the discharge side of the 2<sup>nd</sup> stage flow (original situation)



## 6 Prognosis and recommended remedial actions

### 6.1 Comparison between measured and calculated pulsations

Besides the measured the numerically calculated pressure pulsations are shown in figures 6 and 7. Generally, there is a good agreement between the measurement and the numerical simulation. The numerical model therefore can be regarded as being verified. In the following it will be used for:

- understanding the cause-and-effect chain for conspicuous pipe vibrations
- calculation of the optimal phase relationship between both compressors and the design of required pulsation dampers as necessary
- calculation of the pulsation induced shaking forces acting on the piping

for the planned operation condition (increased mean static pressure).

### 6.2 Variation of the phase relationship between both compressors

In the present case there is the possibility of reducing pressure pulsations at the 2<sup>nd</sup> stage, discharge side, by optimising the phase relationship  $\varphi$  between both compressors. The mean static pressure in the zone of the compressors for the following calculations is assumed to be 2,400 bar for the A-flow and 2,330 bar for the B-flow (future situation).

For the analysis the calculated amplitudes of the pressure pulsations at 8.3 Hz (twice the rotational speed of the compressors) are plotted versus the phase angle  $\varphi$  (figure 8). It is evident that the level of the pulsations depends on the phase relationship  $\varphi$ . The curves show a periodic behaviour with reference to a phase shifting of 180° (e.g.  $\varphi = 15^\circ$  corresponds to  $\varphi = 195^\circ$ ). The physical reason for this lies in the immediate join-up of the gas flows of the two cylinders of one compressor (e.g. cylinders 5 and 6) downstream the discharge valves. Concerning the pulsations it is irrelevant, whether for example the cylinder 5 of the compressor A runs with a phase shift of  $\varphi$  to the cylinder 5 of compressor B, or with the same phase shifting to cylinder 6 of the compressor B.

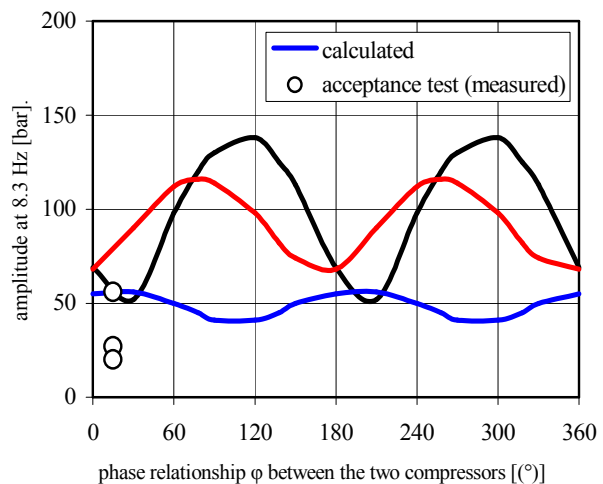


**Figure 8:** Pressure pulsation amplitudes of the B flow for the frequency of 8.3 Hz in the planned situation with increased mean static discharge pressure versus the phase relationship  $\varphi$  between the two compressors

It can be figured out that the phase relationship  $\varphi = 15^\circ$  is favourable, because in this situation the B-flow has relatively low pulsation amplitudes (A-flow too, but not presented). In order to verify that higher pressure fluctuations do not locally occur in the piping system, additionally the calculated pressure pulsations for a large number of points along the pipe axis have been checked. It appeared that at a mean static discharge pressure of 2,400 bar and a fixed phase relationship of  $\varphi = 15^\circ$  (between both compressors) the maximum temporary pressure peaks in the A-flow and B-flow at the discharge side, 2<sup>nd</sup> stage, are below the acceptable maximum pressure of 2,500 bar.

Instead of the described synchronisation of the two compressors (fixed phase shift) the pressure fluctuations in this case can also be reduced effectively with branch-off resonators (e.g.  $\lambda/4$ -resonator, Helmholtz-resonator). These resonators are piping pieces, which are closed at one end. The open side is coupled to the line containing the flow by a T-piece. Using this damping devices the numerical flow simulation shows residual pressure pulsations downstream the resonators – independently of the phase relationship  $\varphi$  – below 50 bar (0-peak). The effect of the resonators is therefore comparable to the synchronisation of the two compressors so that it was possible to make a selection from the view of operational and / or commercial aspects.

Finally, it was decided to realise the synchronisation of both compressors with the fixed phase relationship of  $\varphi = 15^\circ$ .

## 6.3 Reduction of conspicuous pipe vibrations

In order to reduce conspicuous pipe vibrations, it is important to understand the cause-and-effect chain of the vibrations. In the present case it turned out that there are two different amplification mechanisms. In the vicinity of the cylinders (e.g. S9, S10, S132, S170, S175, S181) the primary cause for high vibrations lies in a strong flow resonance between neighbouring cylinders (e.g. cyl. 1 + 2) and their junction. At locations more away from the cylinders (e.g. S48, S211, S212) the exciting pulsations in the frequency range above 20 Hz are pretty low. In this region it is more common that structural resonances are the main cause for high vibration.

In figure 9 is - as an example for pulsation induced pipe vibrations - the situation at the measuring point S10 (interstage) shown. The measured dominant vibration frequency is about 33 Hz. The calculated pressure pulsations at S10 - original situation - show this dominating frequency, too. Based on the knowledge of the physical dependencies the best opportunity to reduce the exciting pulsations and therefore the high pipe vibrations in this case is to install orifices at the junction of the separate cylinder flows. By this solution the flow resonance between neighbouring cylinders is almost vanished (figure 9).

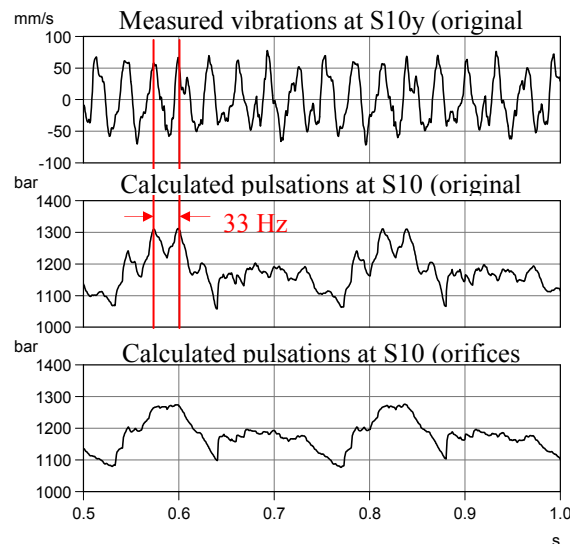


**Figure 9:** Measured pipe vibrations at the measuring point S10 (top) and calculated pressure pulsations (centre) in the original situation as well as calculated pressure pulsations (bottom) with installed orifices

In addition to a vibration reduction it is to note in particular that the orifices have a protective effect on the compressor valves as well as on the dynamic engine loads, because they also reduce the pressure fluctuations in the cylinder area and the compression zone. Furthermore, due to their installation positions these orifices are not comparable with orifices that are located in a uniform flow. In the case dealt with here, the orifices primarily lead to a reduction of the pulsations and not to a significant change of the static pressure upstream and downstream of the orifice. In this way for example the temporary maximum absolute pressure is reduced by the proposed orifices – also between cylinder and orifice – and is not raised – like in a steady flow (figure 9).

Concerning pipe vibrations due to mechanical resonances the piping section at measuring point S212 is analysed in the following. Based on a frequency response analysis the natural frequency and the mode shape of the piping at the area of this point (discharge side, 2<sup>nd</sup> stage) is calculated (figure 10). It turned out that the calculated natural frequency (36 Hz) and the corresponding mode shape correlates with the measured vibration frequency (33 Hz) and mode shape (dominant vibrations in the vertical direction). The best solution to avoid the high vibrations therefore is to install an additional support, which is stiff especially in the vertical direction. In order to avoid new resonance vibrations, the used piping clamp should contain damping material.

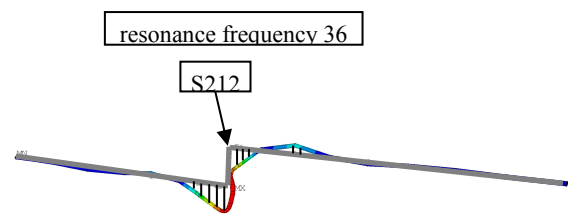


**Figure 10:** Calculated mode shape of the piping at the resonance frequency of 36 Hz in the area of measuring point S212

Altogether, with the objective to reduce and avoid conspicuous pipe vibrations at each cylinder at the suction side and at the discharge side an orifice has been installed. The additional power consumption because of these 16 orifices at each compressor is about 1.4 % of the drive power (5 MW). At locations of mechanical resonance vibrations additional supports have been installed.

## 7 Results of acceptance test

After realisation of the recommended measures

- fixed phase relationship between both compressors ( $\varphi = 15^\circ$ )
- installation of 16 orifices at each compressor
- installation of additional pipe supports at locations of structural resonance vibrations

the residual pressure pulsations and pipe vibrations have been checked. The measured amplitudes of the pressure pulsations are shown in figure 8. The pipe vibrations are presented in figure 11. It appears that all values are in an acceptable range.

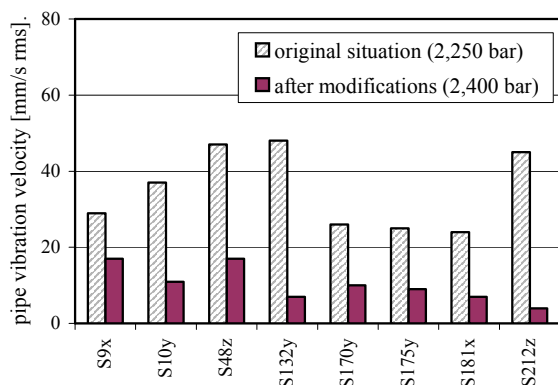


**Figure 11:** Measured pipe vibrations in the original situation and after realisation of measures for the increased discharge pressure of 2,400 bar

Altogether, the whole project of increasing the discharge pressure up to 2,400 bar could be realised without a release of the safety valves or vibration problems. Additionally, the operating company observed an improved behaviour of the compressors concerning the required maintenance, which might be an outcome of the reduced pressure pulsations in the area of the compressors. Ultimately, this presumption must still be confirmed, however, by time.

## 8 Conclusion

In a LDPE-plant two hyper compressors are operating in parallel. In order to improve the blend performance, it was planned to increase the static pressure on the discharge side from a level of 2,250 bar up to 2,400 bar. By means of suitable measures the release of the safety valves caused by pulsation related pressure peaks had to be prevented for the future operation. Additionally, a safe and reliable operation of the plant from the view of vibration technical aspects had to be ensured.

For processing a pulsation study was established with a numerical model of unsteady flows of both compressors. The model was verified using measured pressure signals. Subsequently, the optimal phase relationship between the running compressors with regard to the pressure pulsations was determined. It turned out that the residual pressure pulsations are below the acceptable limit of 2,500 bar in case of a fixed synchronisation of both compressors to a phase relationship of  $\varphi = 15^\circ$ .

The causes for conspicuous pipe vibrations were analysed based on flow and structural simulations as well as measurements. Close to the compressor high pipe vibrations were caused by acoustical resonances. In contrast to that primary mechanical natural frequencies were responsible for conspicuous vibrations of the piping system outside of the compressor environment. In order to avoid high pipe vibrations, the flow resonances were attenuated through orifices and the mechanical resonance vibrations were reduced through additional pipe supports.

After realisation of the recommended measures the mean static pressure on the discharge side of both compressors has been increased up to 2,400 bar without any pulsation or vibration problems as confirmed by an acceptance test.

## References

- [1] Wachel, J.C.: Martson, S.J., Atkins, K.E.: Piping vibration analysis. Proceedings of the 19th turbomachinery symposium 1990. The turbomachinery laboratory, Texas, A & M University System College station, pp 119 - 134.
- [2] N.N.: Schwingungen in Rohrleitungssystemen. VDI-Richtlinie 3842, (2004).
- [3] N.N.: Erweiterung der VDI-Richtlinie 2056. NEN 7-4-1 Werksnorm der Firma Neuman & Esser, (1984).
- [4] N.N.: Beurteilungsmaßstäbe für mechanische Schwingungen von Maschinen. VDI 2056. 2. Auflage, (1964) (in the meantime replaced by the DIN ISO 10816 - part 1 to 6).
- [5] Benzler, H.; Koch u. A.: Ein Zustandsdiagramm für Äthylen bis 10000 ata Druck. Chem.-Ing.-Technik 17 (1955) 2.



# **Automatic Strength Calculation of Pistons for Reciprocating Compressors**

**by:**

**Egidius Steinbusch**

**Gerhard Knop**

**Peter Houba**

**Frank Ohler**

**Dr. Klaus Hoff**

**Central Division of Technology  
Neuman & Esser GmbH & Co. KG  
Übach-Palenberg  
Germany**

**4<sup>th</sup> Conference of the EFRC  
June 9<sup>th</sup> / 10<sup>th</sup>, 2005, Antwerp**

## **Abstract:**

The individuality of process gas compressors requires flexibility regarding piston geometry. Therefore, usually each piston has to be evaluated as to its strength. With the help of a piston standard that leaves only a few individual parameters such as piston height and diameter, a finite element simulation (FEA) and a fatigue strength calculation can be performed in an almost fully automatic way. The result of this simulation is a piston design that meets the special requirements of the respective application. The output of the calculation is input for a parametric CAD model. In this way the design time for a process gas piston can be significantly reduced and the reliability concerning strength is always proved.

This report describes the newly introduced design sequence, a computer program that was developed especially for automatic strength calculations, the piston standard and its implementation in the computer program, the evaluation of critical piston locations and the use of a parametric CAD model.



## 1 Introduction

The continuous demand for higher component quality and cost reduction led to more and more numerical simulations at an early stage of product design.

In recent years an FE analysis of a compressor piston was carried out when the CAD model was sufficiently complete. The typical piston design verification process was iterative and multiple people were involved. The process starts with a CAD model that was designed with intuition and user accumulated experience. After finishing the CAD model the FE model could be generated. A well-known loop then began: Generating geometry, meshing, applying boundary conditions and loads, solving, post-processing and, finally, delivery of fatigue strength calculation results to validate or invalidate the design. If the design was not acceptable, then the analyst went back to the designer for redesign. After modifying the design the design/analysis iterative loop was done again. This iterative process worked well and served the piston design process for years. Nevertheless, it was an expensive and time-consuming process and there is no distinct competitive advantage in using it.

Summarized, this former functioning had a few major disadvantages:

- The manually carried out FE analysis and fatigue strength calculation was a time-consuming and costly process
- As a result of the FE analysis and fatigue strength calculation a major piston redesign could be necessary. The redesign meant scrapping the designer's work from the previous several days
- In most cases an optimized piston design concerning strength was not possible due to the huge simulation time
- Due to the time-consuming process not all pistons could be simulated and calculated with this deep approach

This report describes the newly introduced piston design sequence. To eliminate the disadvantages of this design sequence a special computer program (Pistonsim) was developed to create a seamless interface between analyst, FE and CAD environment based on the concept of automated FE analysis. The main goals were to reduce development time and costs as well as minimize piston failure risk for all manufactured pistons.

## 2 Developing a new piston design sequence

### 2.1 Different approaches

Generally, there are several possibilities to develop a new piston design sequence. Standard FE packages integrated in a CAD environment are available to provide the designer with FE simulation results. Integrating FE programs into CAD software makes transferring models into analysis a simple operation.

Nevertheless, this concept hides a few disadvantages. The geometry necessary for manufacturing turns into huge analysis models that can consume a tremendous part of development time by increasing analysis time. To run a FE simulation it is necessary to convert the CAD-specific geometry into a simulation-specific geometry for FE analysis. This means removing of all unimportant structural details. Simulation-specific geometry may also take advantage of symmetry and only take a portion of the analyzed structure. The major disadvantage is the inaccuracy in the simulation results due to inferior mesh quality. The FE packages integrated in a CAD program normally use a mesh generator capable to discretize complex CAD models into triangular or tetrahedral meshes. This triangular or tetrahedral meshes deliver, especially in areas with high stress gradients, inaccurate simulation results in comparison to a hexahedral mesh.

A completely different approach to develop a new piston design sequence is the methodology of automated FE. Using this approach, FE is customized for the piston development. A user who normally does not have any specific FE know how is capable to start a program, which performs a complete FE including pre-processing, solving of the equation system and post processing.

To enable the analyst engineer to use numerical tools and reduce design time, the automated FE approach was used. In contrast to the FE software packages offered by the CAD companies, this automated FE method is due to the programmable interfaces adaptive to almost any individual needs.

With the chosen method, the piston design and calculation is done before the CAD modeling. This is the main difference between the design method used before.

## 2.2 Preconditions for automated FE analysis

### 2.2.1 Standard piston design

The most important requirement to develop a full automatic FE simulation and fatigue strength calculation for pistons of reciprocating compressors is a standard piston design. The high number of piston design variants had to be reduced. The way to a standard piston design is described by Knop G., Houba P., Steinbusch E., Hoff K.<sup>1</sup>

After the calculation of many different piston designs – especially by means of the FE method – a lot of experience and findings could be gained which could be utilized to develop the best possible piston design. One of the remarkable features of this standard piston design is its simply build-up. The automated FE analysis of the piston is based on this simple standard design. The standard piston design is shown in figure 1.

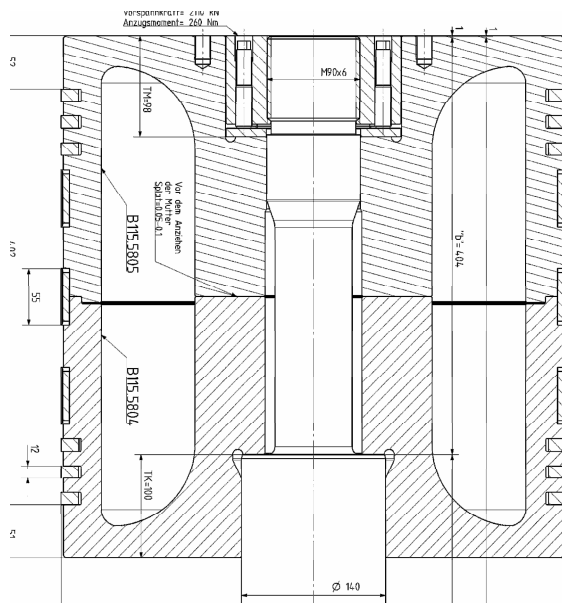


**Figure 1:** Example of a piston in accordance with the standard - design

The standard piston is built up out of two cast pieces which are clamped by means of an integral bolt (piston rod).

The small number of variable dimensions like piston bottom thickness, inner radii and ring positions makes it possible to run a fully automated FE modeling and strength calculation procedure. With the concept of automated FE, a piston can be simulated, calculated and dimensioned within the shortest possible time.

### 2.2.2 FE API

Second requirement to develop an automated FE simulation and calculation tool for pistons is a FE-API (Application Programming Interface). Pre- and post processor must have a programmable interface which can be used for the programming. This API contains hundreds of FE functions that can be called from a programming language. The API provides all the tools to develop entire applications on top of the FE environment<sup>2</sup>.

With the FE-API the possibility to create an automatic feed of input data from the piston program to the FE program as well as automatic access of output data from the FE program is available.

## 3 The piston calculation program Pistonsim

### 3.1 Introduction to Pistonsim

Pistonsim is a calculation software which enables the user to calculate, size and optimize pistons for reciprocating compressors based on the concept of the automated FE analysis.

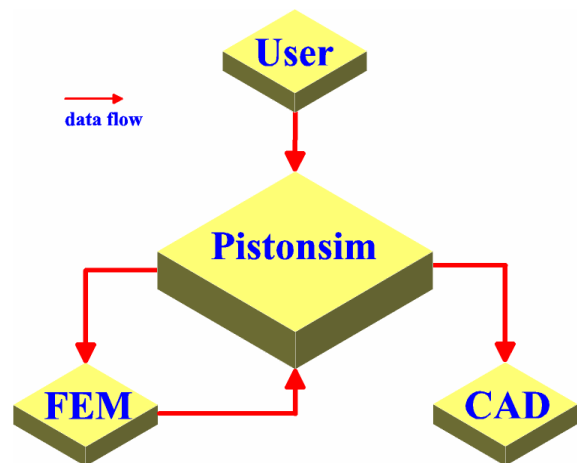


**Figure 2:** The new piston design sequence: data flow between Pistonsim, User, FE and CAD

The complete data flow between user, Pistonsim, FE and CAD is shown in figure 2. The analyst engineer provides Pistonsim with all necessary simulation data. Pistonsim converts this data into an input data flow for the FE program. After finishing the fully automated FE analysis all necessary output data are sent back to Pistonsim. In the software a CAD interface is integrated which allows an optimal linking between Pistonsim and the CAD system.

## 3.2 Data input / pre-design piston

There are two options to supply Pistonsim with the necessary input data. First of all it is possible to put in all data by hand in the program interface. Besides this option it is possible to load an input file with all necessary data from an external compressor calculation program.

For both options the simulation program has to be supplied with the following input data:

- Machine data (e.g. frame size, speed, stroke cylinder diameter etc.)
- Thermodynamics (e.g. pressures etc.)
- Piston / piston ring geometry (e.g. piston height, radii, number of piston rings etc.)
- Guide ring geometry (e.g. ring location)
- Piston material
- Data strength calculation (e.g. surface quality)

All standard data used in the software (e.g. material strength data, standard geometry) are saved in a data file which is adaptive to the user's specific needs.

Specific FE data like constraints, element concentration are implemented in the software.

Figure 3 shows the Pistonsim input data interface.

Figure 3: Input interface Pistonsim

Once all data are filled into the input surface it is only a single button-click to pre-design the piston in the FE environment. In a fraction of seconds the piston design is visible in a 3-D solid model. In no time the analyst engineer acquires information

about piston mass, locations of piston and guide rings as well as piston shape. The optimal positions of all piston and guide rings are calculated by the software.

The piston design can be easily changed until the design meets the user's requirements. Figure 4 shows the 3-D solid model which Pistonsim creates in the FE environment. This 3-D solid model is intended for visualization before starting the calculations. It is not used for the mesh generation.

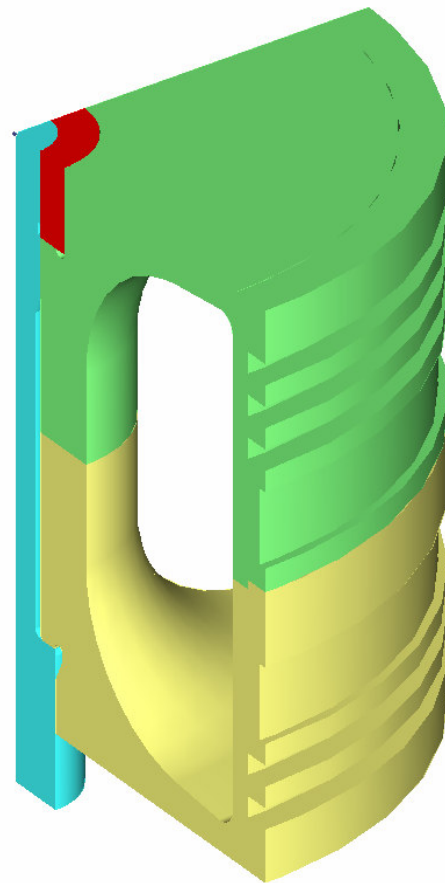


Figure 4: Automated generation Solid model

## 3.3 Automated generation FE model and starting simulation

Once the analyst engineer starts a FE simulation first the FE model is generated. Pistonsim provides the FE program with all necessary data to generate a hexahedral mesh.

The element size of the hexahedral mesh is calculated based on the main piston dimensions taking into account element quality at highly loaded piston areas. Critical areas e.g. at the seat between piston rod and piston parts are meshed with a ruled hexahedral mesh.

Pistonsim generates the finite element boundary conditions, applies loads and physical parameters. The loads are applied in several load sets. The meshed FE model with applied constraints and loads is shown in figure 5.

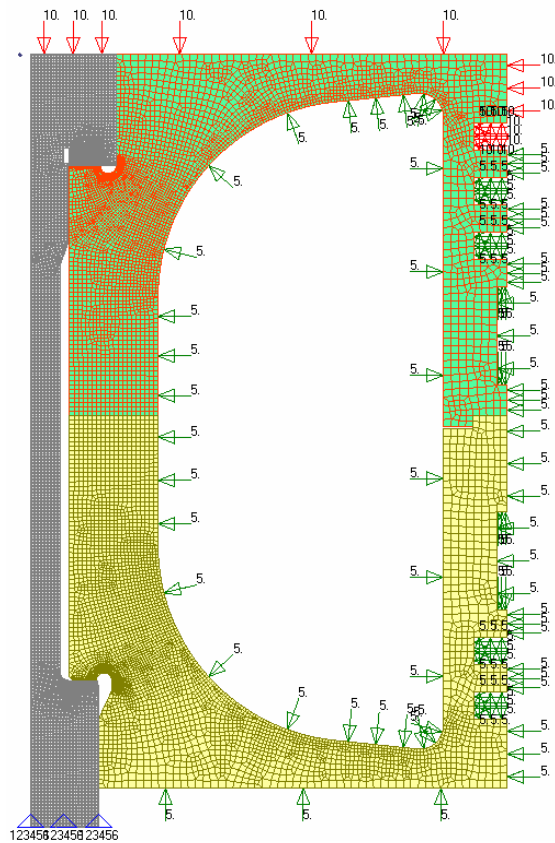


**Figure 5:** Automated mesh generation with constraints and loads

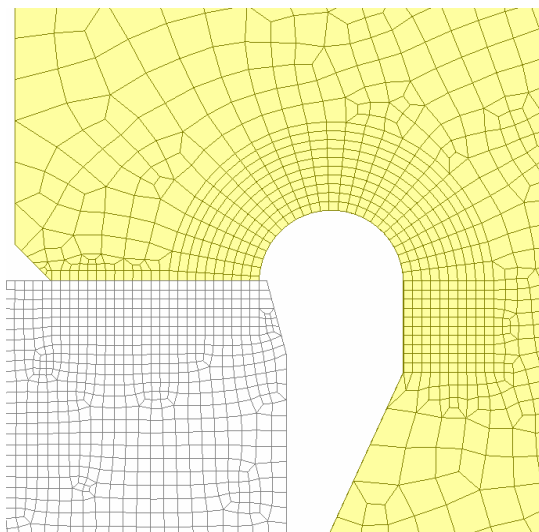


**Figure 6:** Automated mesh generation with ruled mesh at highly loaded areas

Figure 6 shows a detail of a highly loaded area with perfect mesh quality in order to provide most accurate stress values.

The program starts the FE analysis after completing the mesh, constraints and load generation. The applied load sets are analyzed and FE output sets are generated.

### 3.4 Calculation results

#### 3.4.1 Dynamic load piston rod

The two piston parts are connected by a pre-stressed bolt connection. The safety of this highly dynamically stressed connection is an essential part of the structural safety of the piston rod and piston.

Machinery bolt connections are verified by e.g. the VDI 2230 guideline. Since the results of this analytical approach are partly very rough or the input parameters are difficult to determine, the FE method is a state of the art method to calculate bolt loading accurately.

Pistonsim calculates a dynamic safety factor for the piston rod neck and thread. The piston rod neck elements are pre-stressed in the FE model by a negative temperature. The correct temperature is calculated in two steps. In a first step the piston rod is pre-stressed with a temperature of  $-100^{\circ}\text{C}$  in the FE model. After running this first load set a correction factor for the pre-stress temperature can be built from the FE derived pre-stress force. In this first load set only the pre-stress temperature is applied to the FE model. In all other load sets the corrected temperature and all external loads are applied to the FE model and full pre-stress is reached.

After the FE analysis is finished the dynamic stress (amplitude) in the piston rod neck and thread can be determined. The calculated dynamic stress values are compared with the fatigue endurance limit. VDI 2230 gives equations to calculate the fatigue endurance limit (amplitude) of bolts (nominal stress approach).

The dynamic safety factors can be calculated once the dynamic nominal stress in piston rod neck and thread are known.

#### 3.4.2 Angular ring deflection

The introduced standard piston designs are softer than a piston with e.g. ribs. As a result of this soft design the endplate deflections are larger and therefore the piston and guide ring grooves are loaded higher.

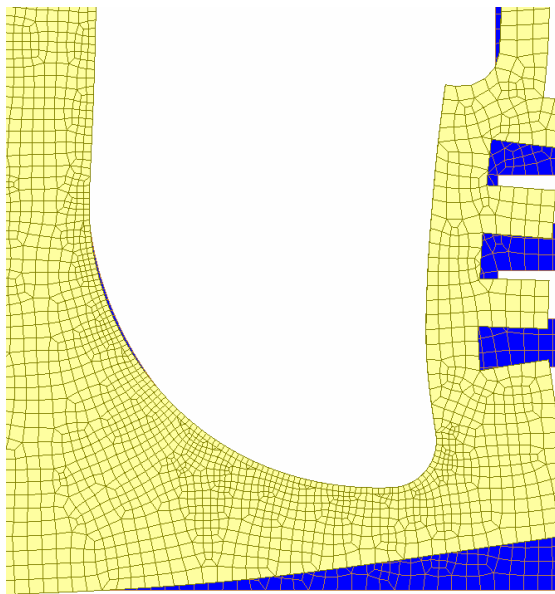


As the radii of the piston and guide ring grooves are very small, the local stress calculation and the fatigue strength verification is time consuming and difficult at these locations. For a simpler valuation, a unique reference calculation with exact stress determination was carried out. With these results, an admissible angular deflection was settled, depending on Young's Modulus, fatigue strength, and dynamic support factor for the given stress gradient.

Pistonsim calculates the angular ring groove deflection in every piston and guide ring groove. The maximum calculated angular ring groove deflection is compared with the admissible angular deflection.

Figure 7 shows the angular ring groove deflection of a piston.

**Figure 7:** angular ring groove deflection in the FE model



## 3.4.3 Fatigue strength calculation

The fatigue strength verification is based on the FKM code "Rechnerischer Festigkeitsnachweis für Maschinenbauteile", 3rd edition 1998<sup>3</sup>. The calculation is performed on the basis of local stress values. Pistonsim delivers a complete, well documented proof of integrity for fatigue strength in several critical piston points of proof.

The fatigue strength calculation sequence according to the FKM guideline is shown in figure 8.

The proof is delivered along the local stress concept as described in the FKM guideline "Rechnerischer

Festigkeitsnachweis für Maschinenbauteile", section 3. The basic principle is to estimate the fatigue based on the elastic, local stress in the critical points compared to strength values derived from an un-notched material probe under uniaxial load. In the course of the FKM-guideline, the local stress concept is modified to a purely elastic load situation. Precondition for the use is hence an elastic material state.

To calculate the fatigue strength of a piston according to FKM guideline stress values at a proof point (usually a surface node) and at a support point (usually a reference node below the surface) have to be known.

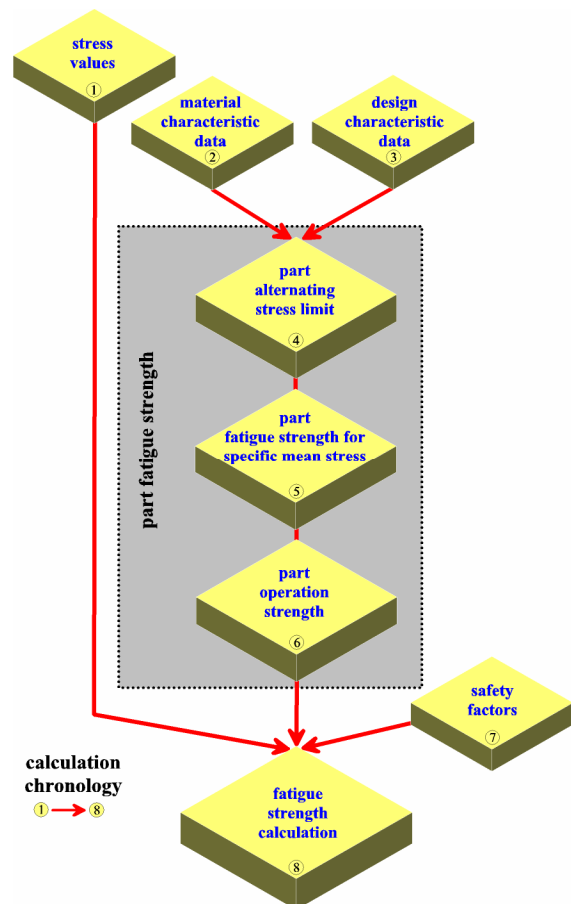


**Figure 8:** calculation fatigue strength: calculation sequence according to FKM guideline

The FE analysis provides the Principal stress values S1, S2 and S3 in the proof point as well as the Principal stress values S1 and S2 in the support point. S1 and S2 are in the direction of the surface and S3 is normal to the surface pointing inwards. In general, a stress gradient normal to the surface exists for all stress directions parallel to the surface. Only these directions provide a dynamic support of the stress at proof point.

The mean stress values and amplitudes in the proof point as well as the reference amplitudes in the support point can be calculated by the software now.

The material data necessary for the fatigue calculation (at reference diameter) are taken from an implemented database and multiplied with a technological size coefficient which is calculated by Pistonsim in dependency on piston dimensions and material.

Pistonsim automatically considers all relevant parameters that influence the fatigue strength like surface roughness, mean stress sensitivity, piston temperature etc.

The FKM guideline is one of the few codes giving specific, detailed guidelines for the definition of required safeties depending on damage, inspection and so on. Based on the material, damage in case of failure, probability of occurrence of peak load, inspection and testing, safety factors are defined.

Pistonsim calculates a fatigue utilisation according to the FKM guide line (inverse of a safety number) at four piston locations. These locations are shown in figure 9.

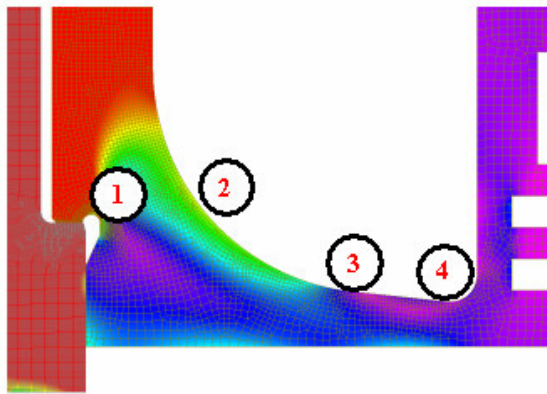


**Figure 9:** calculation fatigue strength: calculation locations at the piston

### 3.5 Pistonsim CAD Interface

Two different concepts for the implementation of a CAD interface in Pistonsim were considered. The first was to create a Parasolid in the FE environment. The CAD program can import the Parasolid and generate the piston drawings. The main disadvantage of this concept is the huge programming expense to create the CAD geometry because the FE analysis runs with a simulation piston geometry, which is not suitable to create drawings of raw and finished piston parts.

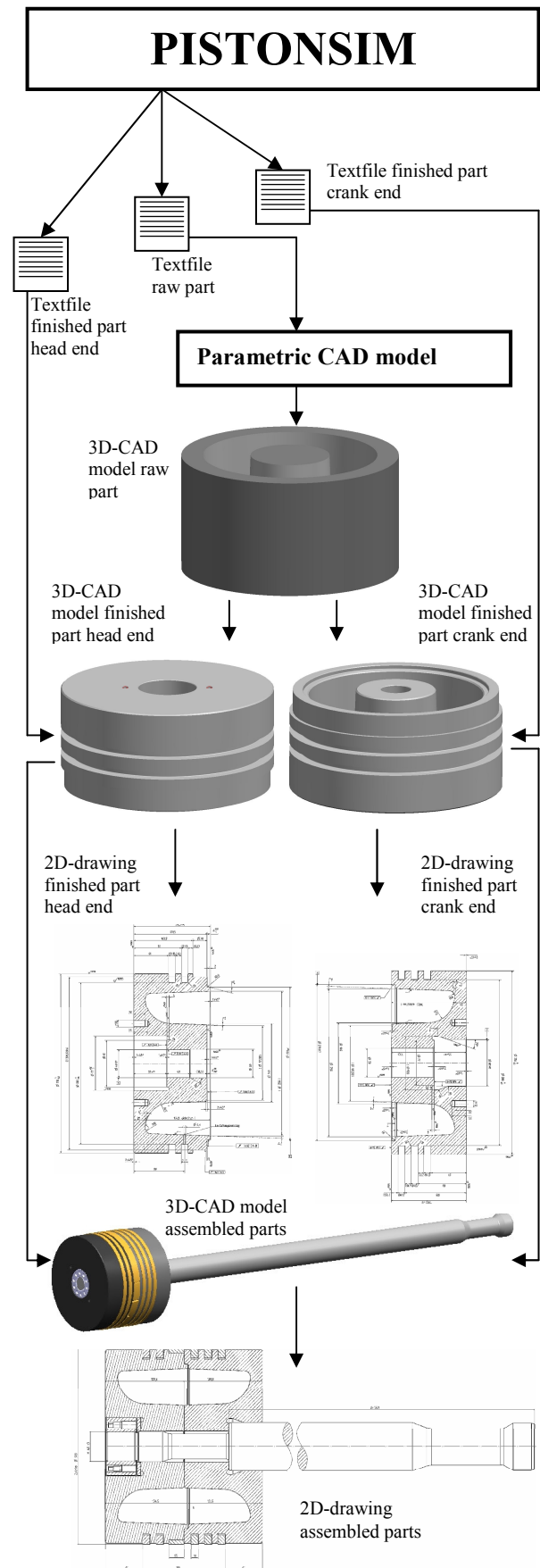


**Figure 10:** automated CAD sequence after FE analysis

J.E. Steinbusch, G. Knop, P. Houba, F. Ohler, K. Hoff:  
Automatic Strength Calculation of Pistons for Reciprocating Compressors

The alternative concept was to set up a parametric CAD model in the CAD environment. This model is used to generate the drawings of the raw and finished piston parts. The parametric CAD model has to be supplied with all parametric dimensions to generate the CAD geometry. This parametric model can read all input data from a simple text file. After the FE analysis is finished the piston drawings can be generated in no time.

Last mentioned concept was implemented in the developed software Pistonsim. Pistonsim provides the parametric CAD model with the necessary dimensions to generate the CAD geometry in the CAD environment. This parametric model reads all input data from a simple text file, which is generated after the FE analysis. The following procedure is applied after the FE analysis:

- Automated generation of text files in Pistonsim with all necessary data (dimensions) to generate the piston CAD geometry
- Generation of raw part drawings with a parametric CAD model for the raw parts
- Generation of finished part drawings with a parametric CAD model for the finished parts
- generation of assembly piston drawing

The CAD sequence after FE analysis is shown in figure 10.

## 4 Conclusion

In order to use all potentials to reduce development time and costs of pistons for reciprocating compressors and guarantee a high product safety it is necessary to integrate development tools as closely as possible into the development and design process.

The standard FE packages integrated into the CAD systems are not capable to give accurate simulation results due to their insufficient mesh quality. An excellent mesh quality in highly loaded piston areas is an important requirement to achieve accurate calculation results.

The calculation program Pistonsim has been developed to focus on the needs of analyst and design engineers. It provides a quick and easy way of calculating, optimizing and designing pistons for reciprocating compressors. The simulation and design process is significantly accelerated, especially by a tremendous reduction of simulation time in the FE environment. The developed program simplifies the entire design process and

guarantees that the necessary degree of safety is achieved for every manufactured piston.

The accurate stress analysis in the engineering process for parts of reciprocating compressors is a key requirement for minimizing development time and risk.

---

## References

<sup>1</sup> Knop G., Houba P., Steinbusch E., Hoff K.

The way to a piston standard for reciprocating compressors, Compressor User International Forum, Karlsruhe / Germany, 2004

<sup>2</sup> MSC.visualNastran for Windows 2002; API Reference, MSC Software Corporation

<sup>3</sup> FKM-Richtlinie (1998); Rechnerischer Festigkeitsnachweis für Maschinenbauteile. 3. Aufl., Forschungskuratorium Maschinenbau, Frankfurt

<sup>4</sup> VDI 2230, Systematische Berechnung hochbeanspruchter Schraubenverbindungen Zylindrische Einschraubenverbindungen, VDI Düsseldorf, 2003



# **Development of a New Gas Compressor - Design of a Crankshaft and Strength Test by Means of FEM**

by:

**Gerhard Braun  
Josef Mehrer GmbH & Co KG  
Balingen  
Germany  
g.braun@mehrer.de**

**4<sup>th</sup> Conference of the EFRC  
June 9<sup>th</sup> / 10<sup>th</sup>, 2005, Antwerp**

## **Abstract:**

The increasing design demands of machinery components since years further the quick spreading of the Finite-Elements-Method (FEM). Especially for complex components, such as a crankshaft, considerable advantages are resulting. Due to FEM the risk of over-dimensioning and under-dimensioning is decreased, thus saving material resp. expenses, without risking an increase of failure. Within the framework of a new development, a strength test of a crankshaft for a piston compressor was carried out in cooperation with the University of Dresden.



## 1 Introduction

Within the framework of a new development of a piston compressor, the crankshaft was to be newly designed and its load capacity to be proven. The water-cooled, 2-cylinder compressor was vertically designed, with crosshead. Calculation of strength was based on a max. RPM of 850/min and max. drive capacity of 75 kW (fig. 1).

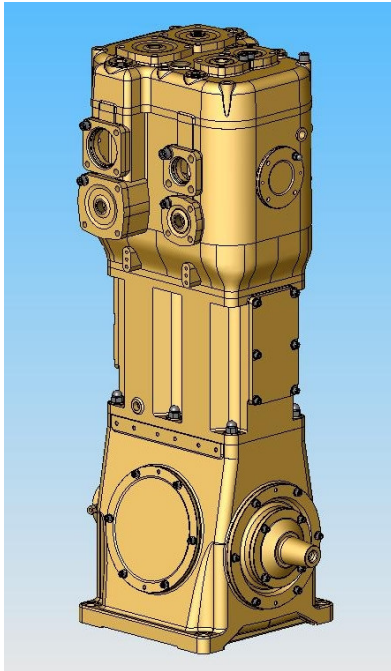


**Figure 1:** Two-cylinder compressor of vertical design

Calculation is done by means of the Finite-Elements-Method. The double stroke crankshaft (fig. 2) is a component of a slider-crank mechanism, which is force-analytically treated in well-known way.

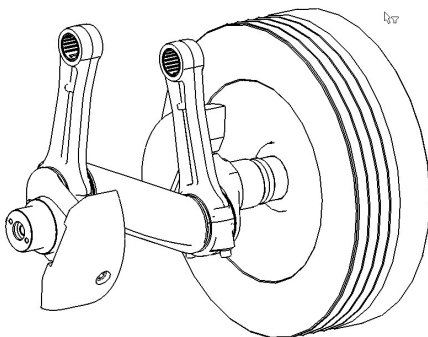


**Figure 2:** Crankshaft with connecting rod and flywheel

## 2 Calculation Model

### 2.1 Elements applied

For the calculation model (fig. 3) 80209 elements SOLID 187-elements with 124051 nodes have been used. The SOLID 187-element is a three-dimensional 10-node-element. SOLID 187 has quadratic displacement set-ups, and is especially suitable for 'irregular linkings', typically resulting from CAD/CAM-systems. 72640 elements are allotted to the crankshaft, the remaining elements to the bearing of the crankshaft.

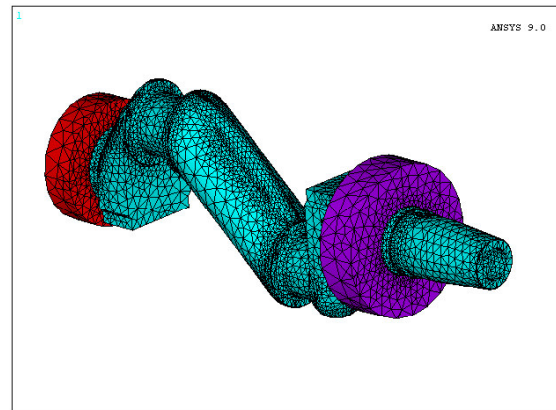


**Figure 3:** Calculation model

### 2.2 Boundary Conditions of Forces

The force diagram (fig. 4) of the compressor shows the course of forces T1, R1, T2, and R2, meaning:

- T Tangential force: being active at the crank pin and tangentially acting upon same.
- R Radial force: acting upon the crank pin and being active in direction to axis of rotation of the crankshaft.
- L Bearing force: acting upon the bearing
- $F_G$  Force of gravity of V-belt pulley
- $F_R$  Belt force: acting horizontally upon the crankshaft end

T1 and R1 are acting at crank 1, being positioned at drive side (drive side = V-belt side resp. pulley side).

T2 and R2 are acting at crank 2, being positioned at greasing side.

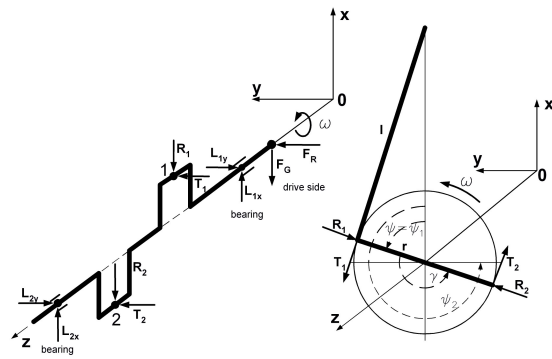


**Figure 4:** Course of forces at crankshaft

$T_1$ ,  $R_1$ , and  $T_2$ ,  $R_2$  are functions of the crank angle (fig. 5).

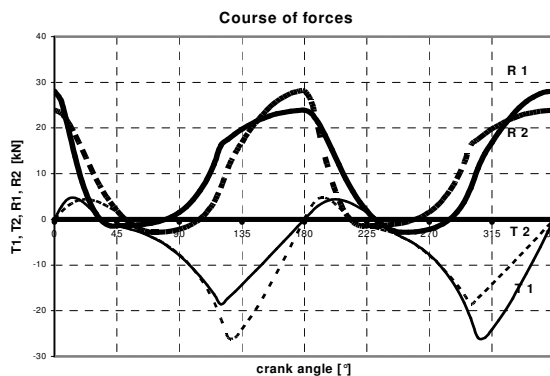


**Figure 5:** Course of forces at crankshaft

At both bearings all above mentioned forces ( $T_1$ ,  $R_1$ ,  $T_2$ ,  $R_2$ ,  $F_R$ , and  $F_G$ ) are causing force reactions, being responsible for the balance of forces (bearing forces:  $L_{1x}$ ,  $L_{1y}$  and  $L_{2x}$ ,  $L_{2y}$ ). These forces are calculated within the Finite-Elements-Analysis. When there is balance, this is a verification possibility of manifest of the calculation.

$T_1$ ,  $R_1$ ,  $T_2$ ,  $R_2$  are oscillating forces, individually fluctuating around their mean values. Forces  $T_i$  ( $i=1,2$ ) are producing a pulsatory moment of torsion, supporting at the flywheel. Same acts as blind moment memory, so that the belt force can (quasi) be considered to be constant.

Formation of model is made in a way, that the crankshaft is resting in the bearing, described in the next paragraph, and the forces are revolvingly applied.

Comments:

- Actually, there are further forces acting at the crankshaft which, however, as per agreement, are not to be considered in the calculation.

- All forces are applied in a way, that they are supported distributed onto several nodes, in order to avoid stress singularity as far as possible (fig. 6).

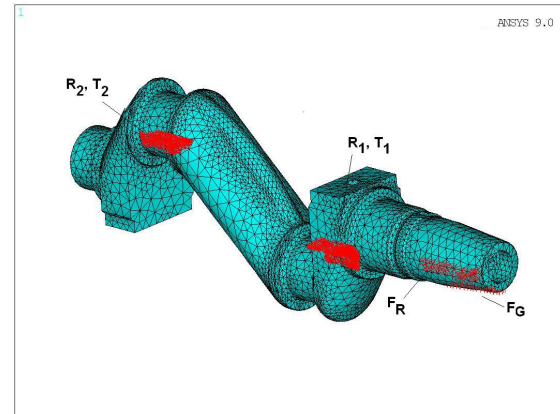


**Figure 6:** Distributed forces at crankshaft

## 2.3 Conditions of Displacement

The elasticity of the bearing influences the calculation by coarsely depicting the bearing's geometry, and converting same with an effective E-model and a transversal contraction number. The outer nodes of the bearing are clamped, the inner nodes are forming the plane of section to the crankshaft. The bearing rings with their relating displacements at the outer surfaces are shown in fig. 3.

## 3 Results

A stress evaluation as per FKM-recommendation was carried out, comprising the static and fatigue endurance test.

Besides the two different loads, referring to the change of operational signs of the belt force (see  $F_R$  in fig. 4), the following boundary conditions are – besides others - considered in the evaluation:

- Material
- Temperature: (-40 °C) -25 °C...80 °C
- Time: 100,000 h

The static stress test starts with determination of the total safety factor. Same depends on material, operational conditions, and damage results to be expected. Due to the low ductile yield of 3%, the material is to be classed as non-ductile. This fact and the damage results being classed as high – assuming a non-destructive material test – finally results in the relatively high total safety factor of 3.49, thus finally resulting in an admissible stress which, according to the individual hypothesis (normal stress hypothesis, shape changing energy

hypothesis, resp. strength hypothesis) renders rates of utilization of up to 33%.

While for the static strength test the max. load is entered, the deflection and average stress must be entered for the fatigue strength test. Same have also been determined at the most critical node. Analogously, a total safety factor of 2.16 results, thus for fatigue parameters resulting in rates of utilization of max. 40%, depending on hypothesis (see above).

The following pictures are showing the crankshaft and appearing stress at different turning angles. As easily visible, the critical areas are found at the shaft shoulders of both crank pins (fig. 7 + 8), resp. at flywheel side of the basic bearing (fig. 9).

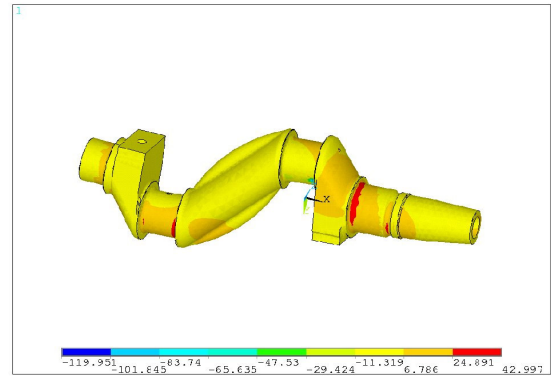


**Figure 9: Mai**

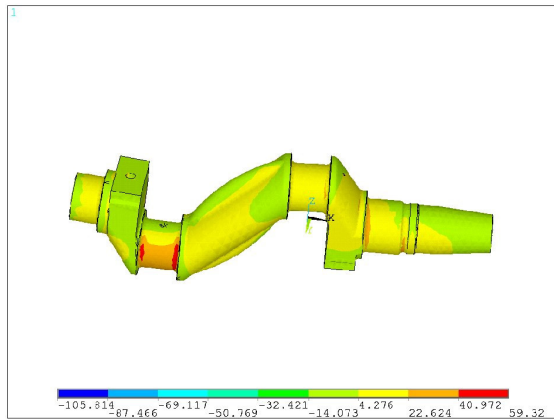


**Figure 7: Main stress (s1) at crank angle of 135°**

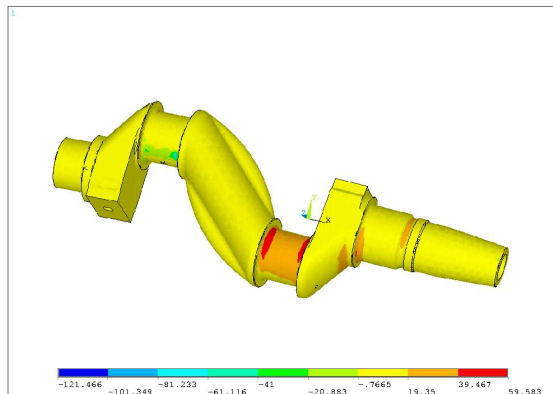


**Figure 8: Main stress (s1) at crank angle of 315°**



# **Operating History of Moderate-speed API-618 Compressors in Refinery Service**

**By:**  
**George M. Kopsick**  
**Director International Sales**  
**Ariel Corporation**  
**35 Blackjack Road**  
**Mount Vernon, Ohio 43035**  
**gkopsick@arielcorp.com**

**4<sup>th</sup> Conference of the EFRC**  
**June 9<sup>th</sup> / 10<sup>th</sup>, 2005, Antwerp**

## **Abstract:**

API Standard 618, Reciprocating Compressors for Petroleum, Chemical and Gas Industry Services, is written to cover both moderate-speed and low-speed reciprocating compressors for critical service applications but does not define the piston and rotating speed characteristics of each design. This paper looks at historic piston and rotating speed limits, what these limits are today and how these two design alternatives can be applied to achieve the reliability objectives set forth in API-618. The basic differences between the two alternative designs are reviewed in light of both physical characteristics of the designs and changes in materials and manufacturing technology. Finally, the design, applications and operating history of a number of moderate-speed units operating in refinery service are described and discussed.



### 1 Introduction

API Standard 618, Reciprocating Compressors for Petroleum, Chemical and Gas Industry Services provides design standards for “moderate-to-low speed” compressors for critical petrochemical, chemical and industrial gas services. The specification’s lack of a definition for moderate and low speed compressors, together with no quantitative limits on either piston or rotating speed, has led to confusion and misunderstanding as to what constitutes a moderate-speed compressor and its acceptability for critical service applications. Additionally the specification evolved from the initial edition published in 1964 which was written for low-speed designs to the current edition covering both low and moderate-speed units. The design standards provided in the document have been made equally applicable to both design alternatives which is not appropriate in all cases.

The objective of this paper is to provide a definition of low and moderate-speed compressors and the differences between the two designs. Additionally, piston and rotating speed limits for the refining industry are quantified. Design and application limits needed to insure reliable operation are discussed for both design alternatives. Operating history of various moderate-speed units is provided. API Standard 618, Reciprocating Compressors for Petroleum, Chemical and Gas Industry Services provides design standards for “moderate-to-low speed” compressors for critical petrochemical, chemical and industrial gas services. The specification’s lack of a definition for moderate and low speed compressors, together with no quantitative limits on either piston or rotating speed, has led to confusion and misunderstanding as to what constitutes a moderate-speed compressor and its acceptability for critical service applications. Additionally the specification evolved from the initial edition published in 1964 which was written for low-speed designs to the current edition covering both low and moderate-speed units. The design standards provided in the document have been made equally applicable to both design alternatives which is not appropriate in all cases.

The objective of this paper is to provide a definition of low and moderate-speed compressors and the differences between the two designs. Additionally, piston and rotating speed limits for the refining industry are quantified. Design and application limits needed to insure reliable operation are discussed for both design alternatives. Operating history of various moderate-speed units is provided.

### 2 API-618

The API-618 specification is an accumulation of design and application guidelines based on operating experience with reciprocating compressors. Its primary purpose is to provide minimum compressor design and application requirements to achieve safe, reliable compressor installations with long maintenance intervals. The first paragraph of Section 2, Basic Design, of API-618 states two general design objectives:

- Provide a minimum of 20-year service life
- Provide three (3) years of uninterrupted service

The specification is continually updated to incorporate new knowledge and experience. The benefits gained from the specification have led to an expansion of its application to new or alternative compressor designs and to additional industries. API-618 originally applied only to low-speed reciprocating compressors for refinery service. As new editions of the specification were written, the scope was expanded to include moderate-speed compressors as well as chemical and gas industry applications.

API-618 states that it is applicable to both low and moderate-speed compressor designs, but does not define these terms or designs. The primary reason for this is because a commonly accepted industry definition does not exist. To add to the confusion, the term ‘moderate-speed’ does not really exist in Europe. Most European companies refer to compressors as either low or high-speed designs.

Rotating and piston speed limits have never been defined in API-618. The specification includes the following qualitative limits in paragraph 2.2, “Allowable Speeds”:

- “Compressors shall be conservatively rated at a speed not in excess of that known by the manufacturer to result in low maintenance and trouble-free operation under the specified service conditions.”
- “The maximum acceptable average piston speed (in meters per second or feet per minute) and the maximum acceptable speed (in revolutions per minute) may be specified by the purchaser where experience indicates that specified limits should not be exceeded.”

Because no piston or rotating speed limits were established, many purchasers incorporated them into their company specifications. Most customer limits were established initially for the low-speed designs covered in the first edition of API-618. As technology changed and the moderate-speed design was added to API-618, many of these limits were never amended.

API-618's compressor design requirements are stated in Section 2, Basic Design. The first edition of the specification based these on experience and knowledge gained from low-speed reciprocating compressor installations designed and installed in the 1950's and early 1960's. As technology and the specification evolved to include both low and moderate-speed compressors the design requirements that did not apply to one of the designs were not segmented from those that applied to both. Rather, the paragraphs are made applicable to both designs with the proviso that the user has the option to accept alternative designs.

Moderate-speed compressors were developed after the low-speed designs and incorporated technology that was not available previously. This enabled them to accomplish the reliability and durability objectives of API-618 using different designs than those used in low-speed units. The differences result in some deviations to specific design paragraphs of API-618, but not the overall objectives. The main deviations will be defined and discussed later in this paper.

## Defenition of low and moderate-speed

No formal definitions of low and moderate-speed units exist in the compressor industry. Most people think of compressor speed as the rotating speed of the crankshaft.

Low and moderate-speed compressors are categorized by their rotating speed. The rotating speed range that identifies each type of equipment will always be a subject of debate, but a reasonably accepted definition based on the common designs available at the time the first edition of API-618 was issued, as low-speed, is provided in the following table.

**Table 1:** Low and Moderate Compressor Rotating Speeds

	Low-Speed	Moderate-Speed
RPM	200 – 600	600 - 1200

The rotating speed and the compressor's categorization as either a low or moderate-speed design does not determine or define the piston speed of the unit. Piston speeds are dependent on the rotating speed and the length of the piston stroke length. Because of this, application limits on rotating and piston speed must be independently reviewed.

## Relationship between Rotating and Piston Speed

Piston speed is an important design parameter because it is a significant factor in determining the life of compressor wear parts. The instantaneous piston speed varies from zero at the end of the stroke, to a maximum near the middle of the stroke, and back to zero. However, as a matter of practicality, "average" piston speed is used to establish limits, make comparisons between units and determine wear rates of wear components. Any desired piston speed can be achieved at any rotating speed by selecting the appropriate piston stroke length. Piston speed, stroke length and operating speed are related by the following formula:

$$\text{Average Piston Speed (m/s)} = \frac{\text{Stroke (mm)} \times \text{RPM} \times 2}{60 (\text{s/min.}) \times 1000 (\text{mm/meter})}$$

or

$$\text{Average Piston Speed (ft/min)} = \frac{\text{Stroke (inch)} \times \text{RPM} \times 2}{12 (\text{inch/ft})}$$

Depending on the stroke length of a compressor it can be applied at various synchronous speeds to achieve desired piston speed limits. The following graph illustrates how both low and moderate-speed units can achieve the same piston speed at different rotating speeds:

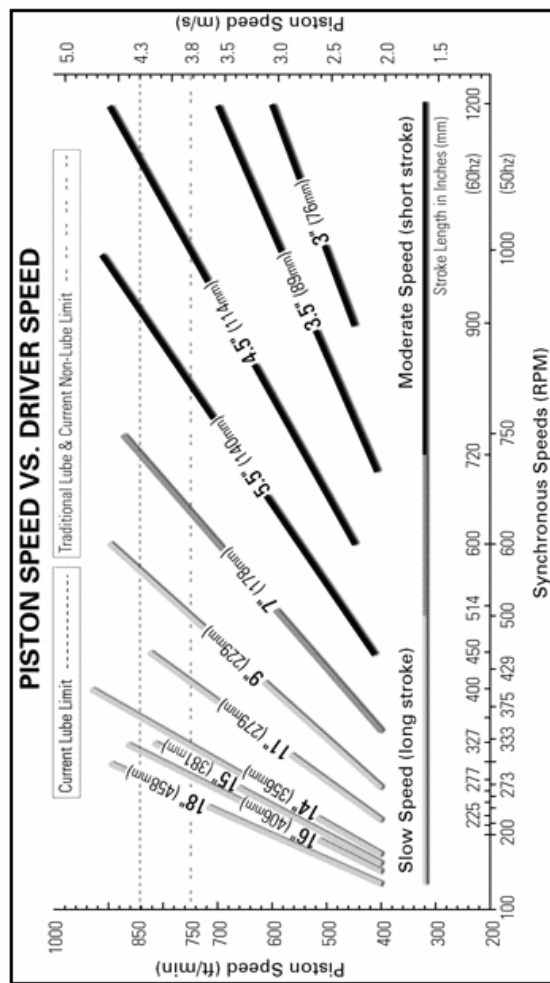


**Figure 1:** Piston Speed vs. Driver Speed

The exact rotating speed that separates low from moderate-speed compressors will always be a matter of discussion. The 600-RPM demarcation stated in this paper is based on the highest rotating speed that was commonly available when the first edition of API-618 was published in April 1964. Some users may select a lower speed than this based on their experience at the time they created their internal specifications.

## Historical Perspective of Compressor Design

### Low-speed Designs

API-618, First Edition published in April 1964 was based on compressor operating experience from the 1950s and early 1960s. These compressors had evolved from designs that operated at approximately 100 rpm in the early 1900s. The units were driven by steam or internal combustion cylinders mounted on the same crankshaft as the compressor cylinders or by an electric motor. Many of the electric drivers used support bearings

that were common to the compressor system. Improvements in design, materials and manufacturing technology resulted in operating at increased speeds and reliability throughout the first half of the 1900s. The increase in operating speeds was driven by the fact that higher speed units were smaller and therefore less costly.

Most reciprocating compressors installed in refineries during the 1950s and 1960s were integral-engine compressors or a stand-alone compressor driven by an electric motor or steam turbine. Many of the same components were used for both the integral engine/compressor and compressor frames. This was done for both practical and economic reasons. The compressor manufacturers had a large variety of existing designs for cylinders, running gear, distance pieces and other components that could be used as part of an integral engine unit or to create separate compressor frames. Doing anything else would increase costs, add risk associated with new designs and make supplying parts more difficult.

The speeds at which these designs could operate were limited by a number of factors. Piston speeds needed to be limited to about 3.8 m/s (750 ft/min) in order to achieve the desired three years of uninterrupted operation between required maintenance. This limit was arrived at empirically through operating experience. Non-lubricated compressors were typically applied with piston speed limits at or below 3.6 m/s (700 ft/min). Three years of operation between maintenance was not realistic for a non-lubricated compressor at that time.

Design and material technology available at that time determined the maximum rotating speeds at which engines and compressors could operate and achieve the desired operating time between required maintenance. Integral engines operating at up to 500 rpm were available, but those operating over approximately 300 rpm did not provide the uninterrupted service life desired. Because of this, operating at about 300-rpm became the standard at that time.

Compressor designs were based on piston stroke lengths that enabled the unit to operate within both piston and rotating speed limits. The most common designs in North America were based on 381 and 356 mm (15 and 14-inch) strokes that operated at 300 and 327 RPM respectively. The drive speed and stroke length of these compressors resulted in piston speeds of about 3.8 m/s (750 ft/min). Other designs were built for various synchronous drive speeds. These included 406 mm (16-inch) units running at about 277 RPM, 279 mm (11-inch) stroke at 400 RPM, 229 mm (9 inch) stroke at 514

RPM and 178 mm (7-inch) stroke at 600 RPM. Integral engine compressors that operated at 400 and 500 RPM utilized the 279 and 229 mm (11 and 9-inch) stroke components. The 178 mm (7-inch) and many of the 279 and 229 mm (9 and 11-inch) stroke units were driven primarily by electric motors. Older designs operating at lower speeds were available but were not as economic as the higher speed unit and had disappeared by this time.

The lack of any quantified piston and rotating speed limits in the First Edition of API-618 published in April 1964 resulted in many companies incorporating the limits into their company specifications. Companies that sold refinery process designs also incorporated them into equipment specifications that they required the customer's equipment meet in order to qualify for the process reliability guarantees. Many of these specifications have remained unchanged since they were originally issued. The maximum rotating speed of 400 RPM, or in few cases 600 RPM, seen in many current specifications can be related directly to compressor designs that were common in the 1950s and 1960s.

### *Moderate-speed designs*

Whereas the low-speed design was associated with an integral engine heritage, moderate-speed units descend from the high-speed compressors designed to be driven by gas engines operating at 1000 RPM and higher. These gas engines operated at significantly higher speeds than integral units. This enabled size and therefore cost of gas engine compressor packages for a specified power rating to be reduced. These 'high-speed' engines were not as reliable and did not have the ability to provide long periods of uninterrupted service compared to their integral alternatives. The market for which they were originally designed was oil and gas production, where the unit's reliability and length of uninterrupted service was not as critical as it was in a refinery application, but the reduced cost was a significant advantage to the user. The large number of compressor packages purchased by the oil and gas production companies provided the economic incentive to build and continuously improve both the reliability and length of uninterrupted service offered by high-speed compressor designs. This development started in the 1950s and continues today.

High-speed compressors differed from low-speed designs in both rotating and piston speeds. A conscious decision was made to reduce wear part life in order to achieve the greater oil and gas production output desired by the users. Piston speeds were increased to about 5.1 m/s (1000 ft/min.) to maximize the flow from the compressor

during the one-year period that the engine could be operated before maintenance was required. The economic benefit of the increased flow exceeded the cost of replacing compressor wear parts when the engine needed to be serviced.

Early high-speed compressor designs were not known for their reliability. During the ensuing years much was learned about how to design frame and bearings systems for higher rotating speeds, how to correctly balance a unit to reduce vibration, provide reliable cylinder lubrication and most importantly valve designs for operation at high cyclic rates. The large number of compressors sold provided the economic incentive to create the technology required for reliable operation. Improved valve design technology and the development of non-metallic materials for valve plates and compressor wear parts were key technical innovations. By the 1990s a high-speed compressor's design could be expected to provide 98% availability without changing any wear parts during the 18-month period gas engines are now operated between major maintenance requirements. A common 1100 KW (1500-horsepower) high-speed compressor design operates at 1400 rpm with a stroke length of 114 mm (4.5-inch) resulting in a piston speed of 5.3 m/s (1050 ft/min). While the majority of compressors used in the upstream industry in the early 1950s were low-speed designs, by the 1990s they were almost exclusively high-speed units.

Moderate-speed compressors suitable for critical service applications were developed by using design and materials technology advances developed to enable the creation of reliable high-speed units. These designs use the same piston speeds as equivalent low-speed designs. Valve and compressor design methods developed for high-speed units were then used to create a unit that met the selected piston speed limits while operating reliably at higher rotating speeds. Many high-speed frame and running gear components met the critical service design requirements. Many other items such as distance pieces had been designed in accordance with API-618 and could be used without modification. Other components such as pistons and cylinders for low molecular weight gas were specifically created for typical downstream applications. The result of these design efforts was a moderate-speed compressor with components that met API-618's requirements for uninterrupted operation periods at rotating speeds between 600 and 1200 rpm. As an example, the 114 mm (4.5 inch) stroke frame and running gear from a high speed compressor designed for 1500 rpm can be used in moderate-speed applications. When applied in critical service refinery application, it would be operated at rotating speeds of either 900 or 720



rpm. The resulting piston speeds are respectively 3.4 or 2.7 m/s (675 or 540 ft/min).

Moderate-speed compressors are now starting to be used in critical downstream applications. Components specifically designed for the applications, in conjunction with current engineering and material technology enable them to provide the reliability and uninterrupted service required for these applications. The moderate-speed design's inherently lower first and installed cost was one element that made companies look at using it in place of the proven low-speed compressors. The other reason was that insurance spares, such as crankshafts, connecting rods and other running gear components, were typically available from the manufacturer's factory stock or had very short lead times. This was because the parts or casting they were produced from were used in high-speed compressors, which are built in relatively high volumes. Their availability eliminated the user's need to purchase insurance spares to eliminate lengthy outages if an infrequently needed but long delivery part was required.

### Allowable Operating Speeds

Any discussion of allowable compressor speeds must be divided into two sections: piston and rotating speed. Piston speed affects the operating life of the piston rings, wear band and packings. Rotating speed affects the valve cyclic (fatigue) life and the forces and moments created by the compressor.

#### *Piston speed*

Piston speed limits are primarily defined by operating experience. As stated previously, when the first edition of API-618 was published in April of 1964, most refinery compressors were limited to a maximum piston speed of 3.8 m/s (750 ft/min) for lubricated and 3.6 m/s (700 ft/min) for non-lubricated services. Non-metallic materials and better lubrication designs have enabled piston speeds to be increased. Piston speed limits for the majority of lubricated applications are now commonly offered as high as 4.2 to 4.4 m/s (825 to 875 ft/min). Non-lubricated compressors are typically applied up to a piston speed limit of 3.8 m/s (750 ft/min). Though three years of uninterrupted operation is realistic for a lubricated compressor, it should not be assumed for non-lubricated applications. API-618 recognizes this, and it is one of the reasons that the statement "It is recognized that this is a system design criteria." is appended to the requirement for three years of uninterrupted operation.

Many factors such as process variables, operating temperature and pressure, and material selections can greatly affect component operating life. No definitive equation exists to calculate the expected life of wear components. A first order approximation of the main factors that affect wear rate can be expressed as:

$$\text{Wear depth} = (k) (P) (V) (t)$$

Where:

k = empirical wear factor

P = pressure loading per unit area of the wear component on the counterface (the surface against which the wear component is moving)

V = Sliding velocity (piston speed)

t = Running time

This relationship assumes that the wear material is applied within its temperature and other application limits, and that the chemical and mechanical characteristic of the counterface surface are correct.

The relationship indicates that the wear rate of the material is a function of piston speed and is independent of rotating speed or stroke length other than how they contribute to defining the piston speed. Within a reasonable variation around the point at which the empirical wear factor was determined, wear rate is linearly related to piston speed and the pressure loading of the wear component. Low and moderate-speed compressors operating at the same piston speeds and wear band loads can be expected to exhibit similar wear rates. Decreasing the piston speed and pressure loading on the components can extend wear component life.

The operating life of compressor wear components can be reduced by factors other than piston speed and the pressure loading of the components. Items that must be avoided if the desired service life is to be obtained include:

- Lack of particulate filtration or liquid separation from the process gas stream
- Lack of, or incorrect cylinder lubrication
- Incorrect non-metallic material selection for non-lubricated applications (This is primarily caused by improper process gas or dew point information.)
- Operating the compressor outside of the range for which it was designed (The normal problem is operating at a point or gas composition that results in discharge temperatures that exceed the application limits of the non-metallic materials.)

These items affect low and moderate-speed designs equally and reduce wear component life in a significant number of installations.

### *Rotating speed*

The rotating speeds at which a compressor can operate and meet the reliability objectives of API-618 have increased appreciably since the first edition of the specification came out in 1964. Compressors can now operate at speeds of up to 1200 RPM for three years before maintenance is required. The technological improvements that enable this include:

- Compressor design techniques created during the development of reliable high-speed reciprocating compressor and engine designs
- Non-metallic valve plate materials
- Improved valve designs
- Improved valve dynamic calculation capability
- The availability of valve design software as well as performance software to quickly calculate operating conditions and verify the suitability of the valve design

Valve design technology together with the advent of non-metallic materials is the primary reason compressor rotating speeds can be increased while still achieving the uninterrupted operating time goal set forth in API-618. The cyclic fatigue life of valve plate material is a major factor in determining the operating life of a valve. The stress created by the impact velocity of the valve plate on the seat normally is the most important limiting factor. When API-618 was first published the majority of valves utilized metal plates. These plates could theoretically operate for an infinite time at impact velocities of 3 m/s or lower. Above that, they were limited by the cyclic fatigue life of the material. Non-metallic materials had finite cyclic fatigue life for all stress levels but could operate at higher stress levels and provide reliable operation for the period between scheduled maintenance. The evolution of technology now enables moderate-speed compressor valves with non-metallic plates to operate for three years at impact velocities equivalent to those used in low-speed designs, typically seven (7) m/s. Non-metallic valve plates also provide better sealing and more tolerance to dirt and liquid in the process gas flow. They have now replaced metallic valve plate materials in most low and moderate-speed compressor valves.

The life expectancy of a moderate-speed compressor valve can be imputed from the operating history of high-speed compressors.

Properly applied valves in high-speed compressors operate reliably (98%+) at impact velocities of 10 m/s for a minimum of 18 months and longer. If the compressor operated at two-thirds its rated speed, the valve would take 2 ¼ years to open and close the same number of times. Because of this, the life of the valve would be expected to be a minimum of 2 ¼ years. All valve designs are a trade-off of flow efficiency vs. life. In oil and gas production operations customers want maximum flow and high valve reliability during the 18-month time between maintenance of the gas engine driver. Valves are rebuilt when engine maintenance is done. Because of this, valves are typically applied in high-speed compressors at higher valve lifts and impact velocities than in refineries where the requirement is for high reliability and three years' life. The normal impact velocity limit used for valves in oil and gas production service is 10 m/s. Moderate-speed units achieve the three-year uninterrupted run time by decreasing the valve impact velocity to 7 m/s. This reduces the impact stress and therefore increases the cyclic life of the non-metallic plate material. Since valve plate impact energy is related to the impact velocity squared, impact energy is cut in half. This in conjunction with the reduced cyclic rate of operation enables valves to operate for the three-year uninterrupted period specified in API-618. The moderate-speed compressor operating history that is provided later in this paper also verifies it.

If both low and moderate-speed valves are correctly designed, there are a number of other design requirements that have a larger impact on valve life than the cyclic life of the valve plate material. These include:

- Selecting the most reliable type of valve design for the application
- Eliminating particulate matter and liquid carry-over in the process gas through inlet filters or separation
- Defining all potential operating points and associated gas compositions
- Conducting a dynamic analysis to define the correct valve components and insure the valve plate impact velocities are within conservative limits that enable the 3-year operating life criteria to be met
- Selecting the correct valve sealing element (i.e. plate, ring or poppet) material for the application

One or more of the above factors are typically the reasons for a valve not achieving its expected operating life. Inlet filtration and separation increases the initial cost of an installation but can have dramatic effects on the reliability of the

compressor installation. New compressor performance calculation software that includes basic valve dynamic analysis is now available. Using it to verify the suitability of the valve design over a wide range of operating conditions and plot maps showing any areas that should be avoided helps eliminate problems.

### Forces and moments

The forces and moments created by reciprocating compressors affect both foundation design and mechanical vibration. Moderate-speed designs exploit both the geometric layout of the cylinders and balance methods to enable them to operate at higher rotating speeds. The inertial force of the reciprocating components generates most compressor forces. The gas loading on the piston normally acts in the opposite direction of the inertial force and acts to reduce the forces. The inertial force generated by one throw of a compressor can be calculated with the following formula:

$$F_{\text{inertial}} = (m) (\omega^2) (R) (\cos \theta + R/L \cos 2\theta)$$

where

$m$  = Mass of reciprocating components

$\omega$  = (RPM)  $2\pi / 60$

$R$  = Crank throw (Stroke / 2)

$L$  = Connecting rod center distance

$\theta$  = Crank angle in degrees

Low-speed units are built in horizontal, vertical and "Y-style" configurations.

Horizontal configurations included provisions for balancing, but not to the level of balance provided in moderate-speed compressors. Additionally, opposing throws of low-speed units typically were not component balanced during assembly to determine and correct for variations in the actual weights of component castings vs. that assumed in the engineering design. The forces created by the compressor were provided for by mounting the unit on a concrete foundation with sufficient mass to absorb them. A one (1) MW low-speed horizontally opposed compressor is typically balanced to about 50 pounds (23 kg). Units can easily be balanced to about half of this amount and less if required.

Moderate-speed compressor designs always utilize horizontally opposed cylinders. The inertial forces of the opposing cylinders act in opposite directions and, to the extent that the reciprocating masses of the opposing throws are equal, cancel each other out.

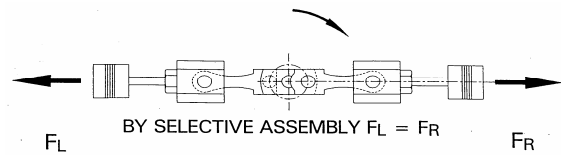


**Figure 2:** Equal masses result in equal but opposite inertial forces

Moderate-speed compressors component balance the reciprocating mass of opposing throws. A one MW high or moderate-speed compressor will typically have opposing throws balanced to within approximately one kilogram. Balance is achieved by selecting crossheads and piston rod nuts of the correct weight to accomplish this. Balance weights that bolt on are not used because of the risk of loosening and detachment.



**Figure 3:** Balance nuts and crossheads

The inertial force equation can be used to compare the forces created by low and moderate-speed compressors in similar applications. The following table compares the forces created by a 1 MW compressor in a typical refinery service. The stroke length of all three alternative is calculated to provide a piston speed of 750 ft/min (3.8 m/s) so that force created at each speed is directly comparable. The actual stroke of the unit would depend on the compressor manufacturer and would be selected to provide a piston speed equal to or less than the limit desired for the project.

## Selection & Sizing

G.M. Kopschick: Operating History of Moderate-speed API-618 Compressors in Refinery Service

**Table 2:** Comparison of forces generated by low and moderate-speed compressors in like services

Compressor Type	Low-Speed	Moderate-Speed	Moderate-Speed	Moderate-Speed
RPM	300	600	750	1000
Piston Speed m/s (ft/min)	3.8 (750)	3.8 (750)	3.8 (750)	3.8 (750)
Stroke mm (Inch)	381 (15)	191 (7.5)	152 (6.0)	114 (4.5)
Unbalance Lbs. (Kg)	10 (22)	10 (22)	10 (22)	10 (22)
%( $M \omega^2 R$ )	100%	23%	28%	38%

The above table shows that the forces created by moderate-speed units are actually less than for a comparable low-speed unit. Though the force increases with the square of the rotating speed, it decreases linearly with the stroke length reduction required for maintaining the specified piston speed. It also reduces linearly with unbalance mass.

The forces created by a reciprocating compressor are handled by transmitting them to a sufficiently large foundation through anchor bolts to prevent any relative motion between the compressor and the foundation. The larger the force, the larger the foundation needs to be and the more energy is transmitted through the anchor bolts. Reducing the forces and moments created by a compressor helps eliminate long-term foundation problems that occur as the concrete degrades over time due to age and the effects of a plant environment.

### Moderate Speed Compressor Designs

Moderate-speed compressors used in critical refinery service are designed and built in accordance with API-618. Component designs are equally robust in both low and moderate-speed units and equally compliant to API-618. The only exceptions to this are a few design requirements of low-speed designs such as cylinder water jackets and liners that are not required by moderate-speed compressors. The reasons for these deviations will be explained later in the paper.

Moderate-speed compressors are not just high-speed compressors slowed down to provide piston speeds acceptable to a refinery application. Not all component designs used in high-speed designs are appropriate for critical service applications. The following component designs will be part of a moderate-speed design but are not always be found in a high-speed unit:

#### Frame and running gear

- Forged steel crankshaft and connecting rods
- Precision fit, replaceable bearings on the crankshaft and big end of the connecting rod
- Conservative bearing and piston rod loads

#### Distance pieces and packing

- A variety of distance pieces designed in accordance with API-618 to select from
- Options for purged and water cooled pressure packing with a variety of material selections for both lubricated and non-lubricated applications
- Intermediate and wiper packing with designs and options such as purge capability and non-metallic materials suitable for the intended application.

#### Cylinder, piston and valves

- Piston designs that include non-pressure loaded wear bands designed in accordance with API-618 with material options for both lubricated and non-lubricated applications
- Piston designs with the additional piston rings required for low molecular weight gas
- Compressor valve design options appropriate to the intended application

Each manufacturer will have a unique list of comments and exceptions to API-618. Most of the items are for deviations when the supplier has a different design with proven operational reliability. Moderate-speed compressor designs will not comply with the requirement for cylinder water jackets and liners. This is because these designs are required for the majority of low-speed design applications but are not needed by the moderate-speed alternative.

### Compressor Cylinders

Low and moderate-speed compressor designs are equally compliant with the majority of the API-618's cylinder design requirements. The two areas where the low and moderate-speed cylinder designs deviate are the inclusion of water jackets and cylinder liners.

#### Water Jackets (Cylinder Cooling)

API-618 specifies that cylinders operating above stated discharge temperatures must have water jackets that are either static filled, have an atmospheric or pressurized thermosyphon or have forced liquid coolant depending on the discharge



temperature. Additionally, any cylinder operating fully unloaded for extended periods shall have a water jacket with a forced liquid coolant.

There are two reasons for this requirement. The first is that water jackets were needed when API-618 was first written for the dimensional stability of the cylinder bore of long-stroke, low-speed compressors. The length of the cylinder and the casting quality available at that time resulted in the cylinder bore deforming as cylinder temperature increased. Water jackets were required to insure the heat effect was evenly spread around the cylinder bore to increase dimensional stability. This was critical in view of the use of metallic rings, and the fact that the bore of the cylinder was soft (approximately 20 - 25 Rc). If the cylinder bore distorted dimensionally, the hard piston rings in use at the time the first edition of API-618 was issued would scrape the cylinder bore and damage it.

The second reason that water jackets were required was to carry away the heat generated by cylinders operating fully unloaded (both HE and CE) for extended lengths of time. A third reason was that it was thought that by having the jacket water temperature over the temperature of the inlet gas it would help eliminate condensation when the process gas was introduced to a cold cylinder during start-up.

API-618 uses the term cylinder cooling for the water jacket. Inlet water temperature is specified to be a minimum of 6 degrees C (10 degrees F) above the gas inlet temperature to eliminate gas condensation, primarily during shutdowns. The static and thermosyphon designs specified in API-618 will maintain bore stability but have no real mechanism to transport heat away from the cylinder. The inclusion of these designs reinforces the fact that water jackets are used to maintain bore stability rather than to transport heat away from the cylinder. The forced liquid cooled cylinder design specified in API-618 does transport heat away from the cylinder in the water. In operation, the majority of the heat is picked up in the discharge passage of the cylinder where the maximum gas to liquid temperature differential exists. The amount of heat transferred from the surface of the bore is small. If the cylinder is viewed as a single pass shell-and-tube heat exchanger with a 381 mm (15 inch) long 'tube' of 25 to 35 mm (1 to 1.4 inch) cast iron having a mean gas to water differential temperature of 60 degree C (108 degrees F), it is apparent that little heat can be transferred from the cylinder bore. A forced liquid cooled cylinder does provide enough heat transfer to reduce heating problems in extended periods of unloaded operation.

The benefit of heating a cylinder before start-up to prevent liquids for condensing from the process gas stream does not eliminate liquid problems on start-up. The volume of the piping and pulsation vessels upstream of the cylinder is much larger than the volume of the cylinder itself. Any liquid that may form in a horizontal cylinder before start-up will drain to the discharge valve located on the bottom of the vessel and be expelled on the first stroke. The real issue is the large quantity of liquid that can form in the volume upstream of the cylinder and be carried into the cylinder in one large mass. It is this liquid that causes the majority of valve and cylinder damage. Heating the cylinder will not eliminate this problem. The upstream piping must be designed as short as possible to reduce the volume of condensable gas. Secondly the piping must not have areas where liquid can be trapped and later carried into the cylinder. Pulsation vessels must also have provisions to drain any condensation rather than trap it. Finally the upstream piping and vessels can be heat traced to eliminate condensation that could be formed before start up. High-speed units in natural gas service typically are compressing gas that is at its dew point. The above design piping and vessel design philosophy is employed in the design of the package. The piping and vessels are rarely heat traced. The packages have a history of starting without liquid problems. Liquid damage typically occurs when the upstream piping has a leg where liquids can accumulate and are later carried through as a slug.

Moderate-speed compressor designs utilize cylinders with shorter stroke lengths. Current casting technology, the uses of non-metallic wear materials and the short bore length enable dimensional bore stability to be maintained without the need for water jackets. The reliability of these designs has been proven over the last thirty years in oil and gas production and gas transportation applications. Whereas previously water-jacketed cylinders were standard in these applications few if any are utilized now.

Cylinders that do not require water jackets have the benefit of eliminating the need for cylinder cooling water systems, the maintenance of those systems and the probability of bore distortion if cooling water flow is lost or the water jacket becomes plugged. Non-water jacketed cylinders do have the problem of not being suitable for operating totally unloaded for extended periods of time.

### *Cylinder Liners*

API-618 specifies that cylinder liners be provided. Low-speed compressor designs are typically supplied with liners, while moderate-speed designs may or may not.

Originally, long-stroke cylinders had problems with bore dimensional stability if the casting did not grow uniformly as the temperature increased. This in conjunction with the relatively hard rings used at the time API-618 was first published and the low bore hardness could result in damage to the bore's surface. Cylinder liners were included to help get a cylinder with bore damage back in service quickly and as cost effectively as possible. A cylinder could be taken to a repair facility for liner replacement, and the unit would be back in operation within 5 to 7 days.

API-618 requires that piston rods be surface hardened in the packing area to increase their service life and help protect against damage. The option of hardening the surface of the cylinder bore to obtain these same benefits was a technology that did not exist at the time low-speed units were designed. Piston rods could be heat treated to increase their surface hardness while retaining suitable base material physical characteristics. A cylinder could not be heat treated to harden the bore surface because the base material at that time would not provide suitable pressure vessel characteristics.

The development of technologies such as ion-nitriding enables manufacturers to harden the surface of cylinder bores to 58+Rc without changing the base material characteristics. The hard surface provides the increase in life and resistance to damage that a hardened piston rod provides.

Moderate-speed cylinders can be obtained with liners, without liners and with hardened unlined bores depending on the manufacturer. The short stroke of moderate-speed cylinder designs enables bore stability to be better maintained than on a long-stroke design. The use of non-metallic rings and the improvement in casting technology eliminates problems with thermal growth causing the piston to scrap the cylinder wall.

The inclusion of a liner in a moderate-speed cylinder degrades the performance of the compressor because of the increased fixed clearance added in the valve area. For this reason, most manufacturers do not include a liner unless the customer requests it.

A cylinder, either low or moderate speed, is still susceptible to bore damage due to particules in the

gas, lubrication problems or operating the unit with worn wear bands and/or piston rings. A hardened cylinder bore helps protect against bore damage and increases the life and reliability of the cylinder.

If damage does occur to the cylinder bore, a liner can be replaced or the entire cylinder body can be replaced. Moderate-speed compressor manufacturers normally make the cylinder from castings with relatively high production volumes. Thus, these castings are typically in stock. The cost of replacing a new moderate-speed cylinder body is about equal to the cost of taking a slow-speed cylinder to a machine shop, removing an interference-fit liner and replacing it with a new liner. This is possible because a moderate-speed cylinder is about half the size of the equivalent slow-speed cylinder and is produced with stock castings that are ordered in quantity. It takes about one week to replace a liner, the same time required to obtain a new moderate-speed cylinder from a manufacturer that has stock castings.

Low and moderate-speed cylinders can also be damaged due to liquid slugs carried into the compressor or by ingesting a foreign object such as a valve part. A cylinder liner does not help place the unit back in service in either of these cases because other areas of the cylinder are often damaged. A new or rebuilt cylinder is typically required to correct these problems. Being able to source a new moderate-speed cylinder in a week eliminates much of the downtime normally incurred in these situations.

### **Operating History**

The majority of reciprocating compressors operating in refineries and industrial gas applications are low-speed designs. Operating experience gained from these units has provided an understanding of the design and application limits needed to achieve three years of uninterrupted service. Much of this knowledge is directly applicable to moderate-speed compressors in similar applications. Similarly, the operating histories of high-speed compressor designs are useful in verifying the reliability and application limits applied in critical services. The longevity and bore stability of short-stroke, non-water jacketed cylinder designs has been verified by over 30 years of experience.

A number of high-speed units found their way into refinery service in the past. Some of these were operated at lower rotating and therefore piston speeds. Many were applied at the same speeds as in oil and gas production applications. The majority of these utilized pistons originally designed for natural gas applications, even in low molecular

## Selection & Sizing

G.M. Kopschick: Operating History of Moderate-speed API-618 Compressors in Refinery Service

weight gas service. If properly applied, they have operated reliably on refrigeration, acid gas, vapor recover and other services. When misapplied, especially on light molecular gas services, they do not operate reliably. Because of their low initial cost, there was a large incentive to attempt to use these for purposes for which they were never designed. Their poor reliability has hindered the introduction of moderate-speed units into the downstream industry.

A number of API-618 moderate-speed units have been installed in refinery applications and have been operating for a number of years. These units are configured with piston, distance pieces and other components correctly designed for the application. They operate at piston speeds needed for the desired long uninterrupted service but at higher rotating speeds typical of moderate-speed designs. The operating history of correctly configured moderate-speed units applied in refinery service verifies their ability to meet the reliability and operating time between required maintenance required by API-618. The following is the operating history of six units, built by three different manufacturers:

### Example 1

Service: Recycle gas compressor for a hydrogen desulfurization unit located in a German refinery

#### Compressor configuration:

- Two-throw, single stage
- Stroke: 108 mm (4.25 inch)
- API-618 Type C distance pieces
- Purge provisions were provided for the distance piece compartments, pressure packing and intermediate packing.
- Water cooled pressure packing
- Piston designs include non-pressure loaded wear bands sized for 5 psi loading and sufficient piston rings for low molecular gas applications
- Non-water jacketed nodular iron cylinders with bores hardened to approximately Rc 61
- Distribution block type cylinder lubrication system
- Hoerbiger HydroCom capacity control system
- Kotter on-line performance monitoring system

Driver: Variable speed induction motor

(Note: capacity control is normally accomplished using the Hoerbiger HydroCom capacity controllers on the suction valves of the compressor,

RPM: 742

Piston speed: 2.67 m/s (526 ft/min)

Lubricated / Non-lubricated: Lubricated

Power: 199 kW (267 Bhp)

Gas composition: (Gas composition varies over time)

C1	13.3
C2	4.7
C3	3.5
I-C4	3.4
N-C4	0.0
I-C5	1.4
N-C5	0.0
C6+	0.0
H2S	0.2
H2O	Saturated
H2	73.5

Flow (Min / normal / max): 2500 / 7000 / 9200 Nm<sup>3</sup>/hr

Suction pressure: 21 bara (304 psia)

Discharge pressure: 36 bara (507 psia)

Discharge temperature: 101 C (193 F)

Start-up date: December 10, 1999

#### Maintenance;

- 8000 hours: Replaced discharge valves with damaged plates. The root cause of the problem was that the discharge valves were incorrectly specified. The original valves were supplied with metal rather than non-metallic valve plates. The wide flow variance provided by the HydroCom system resulted in the discharge valve impact velocity during low flow operation exceeding the operating capability of the metal plates in the valve. The valve design was changed to incorporate non-metallic valve plates. Suitable valve springs were selected for the range over which the compressor was operated. The new valve design resulted in some initial problems because the stack clearance of the valve and valve cap were incorrect. This was identified and solved quickly by refinery personnel.
- 28,800 hours: All wear components were changed as part of a preventive maintenance program during a plant turnaround. The pressure packings and piston rod were worn to the point that they required replacement or rebuilding. All other components were in serviceable condition but were replaced as part of the preventive maintenance program. No components other than the discharge valve mentioned above were changed before this point.

## Selection & Sizing

G.M. Kopschick: Operating History of Moderate-speed API-618 Compressors in Refinery Service

- 32,484 hours: The unit has operated for 32,484 hours as of January 15, 2004. The unit was take out of service at this point due to changes in the process.

### Example 2

Service: Make-up gas compressor for a Hydrocracker in a refinery located in Oklahoma

- Compressor configuration:
- Four-throw, three stage with two cylinders on first stage service
- Stroke: 4.5inch (114 mm)
- API-618 Type C distance pieces
- Purge provisions were provided for the distance piece compartments, pressure packing and intermediate packing.
- Water cooled pressure packing
- Piston designs include non-pressure loaded wear bands sized for 5 psi loading and sufficient piston rings for low molecular gas applications
- Non-water jacketed nodular iron cylinders with bores hardened to approximately Rc 61
- Distribution block type cylinder lubrication system
- Variable volume clearance pockets on first stage cylinders
- Ring type valves

Driver: Single speed induction motor

RPM: 885

Piston speed: 664 ft/min (3.37 m/s)

Lubricated / Non-lubricated: Lubricated

Power: 1050 Bhp (782 kW)

Gas composition: (Gas composition varies over time, H<sub>2</sub> varies from about 80 to 90%)

C1	4.0
C2	4.0
C3	3.0
I-C4	0.0
N-C4	3.0
I-C5	0.0
N-C5	1.0
C6+	0
H <sub>2</sub> S	0.0
H <sub>2</sub> O	Saturated
H <sub>2</sub>	85.0

Flow (design): 5.5 MMSCFD

Suction pressure: 6.55 bara (95 psia)

Discharge pressure: 120 bara (1735 psia)

Discharge temperature: 107 C (225 F)

Start-up date: May 2002

Maintenance:

- 200 hours (approx.): Crankshaft detuner added and cylinder lubricator pump replaced. The root cause of the problem was an error in the torsional study. Lack of sufficient separation at higher order frequencies resulted in a fatigue failure of the cylinder lubricator drive shaft. Shaft end torsional readings were taken before and after the detuner was added to confirm both the problem and that the correct separation levels were obtained. The problem was resolved and the unit was operating within three days of the initial occurrence of the problem.
- 8,000 hours (approx.): A scheduled preventive maintenance check was performed. This check was part of an established refinery practice based on operating experience obtained from other units in similar service. Cylinder lubrication was checked to insure it was sufficient. The valves and forth stage cylinder bore were visually inspected. All components were in good condition and were put back in service.
- 14,300 hours (approx.): Three valves were replaced in the second stage cylinder. One valve had foreign material embedded in the non-metallic valve ring element. The other two rings showed some signs of heat cracking. Only the three valves that showed damage were replaced. All of the valves in the compressor at this time were original to the unit and had been used during start-up. The source of the foreign material was unknown. Since the valves had operated well to this point no further analysis was conducted.
- 22,200 hours (approx.): As of April 2005, the unit has operated without maintenance on the compressor. Maintenance has been required on the main motor starter and scrubber level switches. One significant difference has been noticed between this unit and other low-speed compressors in similar service. All other units in similar service were applied as three-stage units with discharge temperatures of slightly over 135 C (275 F). The shell and tube intercoolers on these units need to be rodded out every four months to eliminate scale buildup caused by the cooling water quality. The moderate-speed compressor was applied as a four-stage unit to reduce the operating discharge temperature to approximately 107 C (225 F). This was feasible because the installed cost of the four-stage moderate-speed unit was less than a comparable three-stage low-speed



## Selection & Sizing

G.M. Kopschick: Operating History of Moderate-speed API-618 Compressors in Refinery Service

unit. The original intention was to prolong the life of the Teflon based wear materials by running them cooler. The reduction in operating temperatures has eliminated the scale problems with the shell and tube heat exchangers, which have not required any maintenance since start-up.

### Example 3

Service: Hydrogen compressor for hydrogen production service located in a Gulf Coast refinery near Houston USA

Compressor configuration:

- Six-throw, two stage with three cylinders on each stage
- Stroke: 150 mm (5.9 inch)
- API-618 Type B distance pieces
- Purge provisions on distance piece and pressure packing
- Water cooled pressure packing
- Piston designs include non-pressure loaded wear bands sized for 5 psi loading and sufficient piston rings for low molecular gas applications
- Water-jacketed cylinders with liners. Bores are not hardened
- Plate valves

Driver: Single speed induction motor

RPM: 715

Piston speed: 3.56 m/s (704 ft/min)

Lubricated / Non-lubricated: Non-lubricated

Power: 2523 kW (3375 Bhp)

Gas composition:

C1	0.0
C2	0.0
C3	0.0
I-C4	0.0
N-C4	0.0
I-C5	0.0
N-C5	0.0
C6+	0.0
H2S	0.0
H2O	0.0
H2	100.0

Flow (design): 51.6 MMSCFD

Suction pressure: 21.7 bara (314 psia)

Discharge pressure: 60.3 bara (875 psia)

Discharge temperature: 93 C (200 F)

Start-up date: November 1, 2001 (full time operation)

Maintenance:

- 10,500 hours: Preventive maintenance was conducted on the compressor during a planned two-week shutdown.

The following parts were replaced:

- Piston rings and wear bands
- Pressure packings
- Wiper
- Valves

None of the parts showed any signs of undue wear.

- 26,700 hours: The unit was shut down to remove the motor for use in a service deemed more critical. A motor was fitted to the unit and the compressor was placed back in operation after two weeks. The compressor was in good operating condition at this point and had operated continuous since the preventive maintenance shutdown.
- 28,500 hours: Operating hours as of April 2005.

### Example 4

Service: Nitrogen compressor for nitrogen production service located in a Washington refinery USA

Compressor configuration:

- One-throw, single stage
- Stroke: 76 mm (3.0 inch)
- API-618 Type C distance pieces
- Water cooled pressure packing (water cooling provision not utilized in service)
- Piston designs include non-pressure loaded wear bands sized for 5 psi loading and sufficient piston rings for low molecular gas applications
- Non-water jacketed nodular iron cylinders with bores hardened to approximately Rc 61
- Fixed volume clearance pocket
- Plate valves

Driver: Single speed induction motor

RPM: 890

Piston speed: 2.25 m/s (445 ft/min)

Lubricated / Non-lubricated: Non-lubricated

Power: 19 kW (25 Bhp)

## Selection & Sizing

G.M. Kopschick: Operating History of Moderate-speed API-618 Compressors in Refinery Service

Gas composition:

C1	0.0
C2	0.0
C3	0.0
I-C4	0.0
N-C4	0.0
I-C5	0.0
N-C5	0.0
C6+	0.0
H2S	0.0
H2O	0.0
N2	100.0

Flow (design): 0.30 MMSCFD  
 Suction pressure: 7.2 bara (95 psia)  
 Discharge pressure (maximum): 21.7 bara (315 psia)  
 Discharge temperature (maximum): 165 C (330 F)  
 Start-up date: December 1997

Maintenance:

- 8,000 hours: The pressure packing was replaced as part of a preventive maintenance program. The original pressure packing was in serviceable condition when removed.
- 23,150 hours: Nitrogen plant contract ends and unit is shutdown. Other than the pressure packing no other parts or maintenance were performed.

### Example 5

Service: Nitrogen compressor for nitrogen production service located in a Washington refinery USA

Compressor configuration:

- Two-throw, three stage
- Stroke: 76 mm (3.0 inch)
- PI-618 Type C distance pieces
- Water cooled pressure packing (water cooling provision not utilized in service)
- Piston designs include non-pressure loaded wear bands sized for 5 psi loading and sufficient piston rings for low molecular gas applications
- Non-water jacketed nodular iron cylinders with bores hardened to approximately Rc 61
- Fixed volume clearance pocket
- Plate valves

Driver: Single speed induction motor  
 RPM: 890  
 Piston speed: 2.25 m/s (445 ft/min)  
 Lubricated / Non-lubricated: Non-lubricated  
 Power: 66 kW (89 Bhp)

Gas composition:

C1	0.0
C2	0.0
C3	0.0
I-C4	0.0
N-C4	0.0
I-C5	0.0
N-C5	0.0
C6+	0.0
H2S	0.0
H2O	0.0
N2	100.0

Flow (design): 0.30 MMSCFD  
 Suction pressure: 7.2 bara (95 psia)  
 Discharge pressure (maximum): 82.8 bara (1200 psia)  
 Start-up date: September 2003

Maintenance:

- 8,000 hours: The pressure packing, piston rings, wear bands and valves were replaced as part of a preventive maintenance program. The original pressure packing was in serviceable condition when removed. After a visual inspection they were determined to have estimated remaining life of 4 – 6 months. The piston rings and wear bands were within 0.51 mm (0.020 inches) of new dimensions. Valves are replaced and sent out to be rebuilt. The rebuilt valves are installed during the next scheduled preventive maintenance. All wear components were replaced by two people within eight (8) hours.
- 12,400 hours: As of April 2005 the unit has run continuously without shutdown.

The industrial company that owns and operates this unit and the one shown in Example 4 has 5 other compressors similar to the unit in Example 4. The initial units were supplied with single compartment distance pieces and required the pressure packings to be changed at approximately nine months due to oil ingress from the frame. Later units were supplied with API-618 Type C distance pieces. These units are operated on an 18-month preventive maintenance schedule. The operating histories of these units indicate a 99%+ on-line availability during this 18-month period. Their operating records show some of these non-lubricated units have operated for 90,000 hours with only scheduled maintenance at 99.9% operational availability.

### Example 6

Service: Hydrogen compressor for hydrogen production service located in the USA

Compressor configuration:

- Four-throw, one-stage Stroke: 150 mm (5.9 inch)
- API-618 Type B distance pieces
- Purge provisions on distance piece and pressure packing
- Non-water cooled pressure packing
- Piston designs include non-pressure loaded wear bands sized for 5 psi loading and sufficient piston rings for low molecular gas applications
- Water-jacketed cylinders with liners. Bores are not hardened
- Plate valves

Driver: Single speed induction motor

RPM: 710

Piston speed: 3.50 m/s (693 ft/min)

Lubricated / Non-lubricated: Non-lubricated

Power: 2980 kW (4000 Bhp)

Gas composition:

C1	0.0
C2	0.0
C3	0.0
I-C4	0.0
N-C4	0.0
I-C5	0.0
N-C5	0.0
C6+	0.0
H2S	0.0
H2O	0.0
H2	100.0

Flow (design): 46 MMSCFD

Suction pressure: 21.7 bara (315 psia)

Discharge pressure: 56.2 bara (815 psia)

Discharge temperature: 135 C (200 F)

Start-up date: May 2004 (full time operation)

Maintenance:

- 2,000 hours: Coupling disk pack was replaced due after finding cracks in the disc pack
- 6,000 hours: Upgraded coupling installed
- 13,400 hours: As of the first part of April 2005 the unit has operated continuously without shutdown since the coupling replacement. Preventive maintenance is scheduled for 18 months (or approximately 13,000 hours).

### Conclusion

Reciprocating compressors for critical downstream applications must provide reliable, long operating periods between required maintenance intervals. API-618 and other compressor specifications were written to capture and communicate good design practices to the industry.

API-618 was first published in 1964 and was based on the materials, technology and low-speed design experience available at that time. The specification evolved to apply to both moderate and low-speed designs. The lack of a definition of moderate and low speed compressors, together with no quantitative piston or rotating speed limits lead to confusion about what constitutes a moderate-speed compressor. Additionally, as the specification evolved the applicability of the various design paragraphs to either or both low and moderate-speed compressors was not included.

Additional specifications for reciprocating compressor have been written by users and engineering contractors to define their unique requirements. Many of these included piston and rotating speed limits based on the low-speed designs common at the time the first edition of API-618 was written. Many times, as these these specifications were updated piston and rotating speed limits remained unchanged. Additionally, low-speed compressor design requirements were applied to the moderate-speed alternate.

The use of low-speed experience and specifications to evaluate moderate-speed design alternatives lead to confusion as to the acceptability of the use of moderate-speed units in critical service applications. The lack of operating experience has also resulted in a selection of known low-speed designs because of the critical nature of many of the applications.

A definition of low and moderate-speed compressors and the piston speed limits currently used for refinery applications have been provided in this paper. Additionally, a description of important differences in the two designs is reviewed.

A number of customers have installed and operated moderate-speed compressors in critical services during the last few years. The operating history of some of these units is presented in this paper. This history illustrates that moderate-speed operate as reliably as the low-speed designs. Both designs achieve the operating periods between required maintenance and longevity as long as they are correctly applied.

A number of industrial gas companies are now using moderate-speed compressors where they had previously used low-speed designs while meeting the same high levels of reliability they have always had to guarantee. Another illustration of the acceptance of moderate-speed units for critical service application is that existing customers are purchasing them for their needs rather than going back to the traditional low-speed compressors they had used previously.





# **Experimental Study of a Resonating Ring Plate Valve**

by:

**Remco Habing, Rob Hagmeijer**  
**Mechanical Engineering**  
**(Engineering Fluid Dynamics)**  
**University of Twente**  
**Enschede**  
**The Netherlands**

**Jeroen Bolle, Jan Smeulers**  
**Flow and Structural Dynamics**  
**(PULSIM)**  
**TNO TPD**  
**Delft**  
**The Netherlands**

**4<sup>th</sup> Conference of the EFRC**  
**June 9<sup>th</sup> / 10<sup>th</sup>, 2005, Antwerp**

## **Abstract:**

For more than a century people have been modelling the fluid-structure interaction of automatic valves. The long-term objective of the research presented in this paper is to develop means to determine valve parameters from valve dimensions and flow conditions. In this paper the results are presented of the research on a simple ring plate valve. The objective is the experimental validation of traditional quasi-steady flow theories for unsteady flow conditions.

An experimental method has been designed to measure accurately the instantaneous valve opening, the instantaneous pressure difference across the valve, and the instantaneous volume-flow rate through the valve. Results are presented for: semi-empirical coefficients for both normal- and reverse flow, gas force and flow rate for unsteady flow, collision events for both the ring plate valve and a compressor valve.

## 1 Introduction

Although structural details may differ considerably, the principle of operation of all types of automatic valves is similar. It is possible to distinguish the same basic functional elements in valves of different design. See Fig. 1.

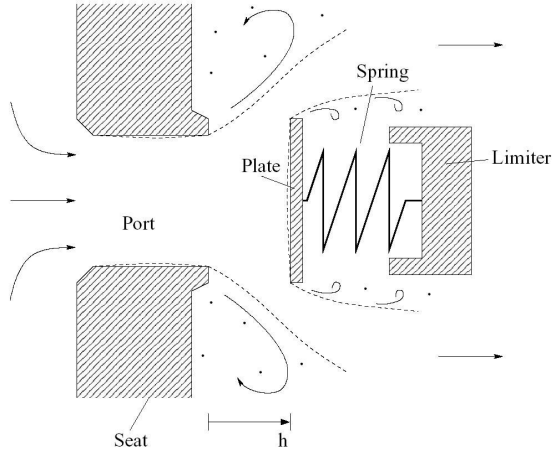


**Figure 1:** Sketch of various elements of a compressor valve ( $h$  is the opening)

The motion of the valve plate and the unsteady flow of gas through the valve is essentially a fluid-structure interaction phenomenon. Costagliola<sup>1</sup> performed pioneering work for the case of modelling compressor valve behaviour. All traditional valve theories are unified into a single theory, which we will refer to as the Basic Valve Theory. This theory considers the valve as a *black box* and provides a semi-empirical description of the valve state variables. The state variables are: the instantaneous pressure difference  $\Delta p$  across the valve, the instantaneous volume-flow rate  $\Phi_v$  through the valve, and the instantaneous valve opening  $h$ .

The *Basic Valve Theory* considers quasi-steady flow. The volume-flow rate is expressed as

$$\Phi_v = \alpha[h] L_g h \sqrt{\frac{2}{\rho} \Delta p} \quad (1)$$

where  $\alpha[h]$  is the vena contracta factor and  $L_g$  is the total edge length of the plate. We consider incompressible valve flow with mass density  $\rho$ . The effects of viscosity (e.g. vena contracta after flow separation and wall friction) are taken into account by the semi-empirical coefficient  $\alpha \sim O(1)$ . This coefficient is found to depend on Reynolds number and geometry. It is expressed as function of the

valve opening  $h$ . The structural dynamics is modelled as a mass-spring system with a single degree of freedom, i.e.

$$\begin{cases} m \frac{d^2 h}{dt^2} + \zeta \frac{dh}{dt} + k_s (h + h_{pl}) = F_g \cdots 0 < h < h_{\max} \\ \frac{dh}{dt}[t^+] = -e_{res} \frac{dh}{dt}[t^-] \cdots h[t^\pm] \in \{0, h_{\max}\} \end{cases} \quad (2)$$

where  $m$  is the effective plate mass,  $\zeta$  is the damping constant,  $k_s$  is the spring stiffness,  $h_{pl}$  is the preload distance,  $h_{\max}$  is the maximum valve opening,  $e_{res}$  is the restitution coefficient and  $t$  is the time. The instantaneous gas force  $F_g$  acting on the plate is modelled as the force exerted on the plate in a quasi-steady state, i.e.

$$F_g = c_g[h] A_p \Delta p \quad (3)$$

where  $A_p$  is the port area. The semi-empirical coefficient  $c_g \sim O(1)$  is determined by experiments considering a hovering valve plate. It is expressed as function of  $h$ .

In 1893 Westphal<sup>2</sup> already takes into account the ‘breathing’ of a valve when the plate speed is significant. St Hilaire *et al.*<sup>3</sup> show that the pressure forces developed in the unsteady potential flow past a harmonium reed excite the reed vibration. Flow visualization studies are performed which indicate that the jet instability is not important in exciting the reed vibration. This all suggests that both plate speed and fluid inertia should be accounted for to improve the Basic Valve Theory.

The *Extended Valve Theory* considers some unsteady flow effects. In the Basic Valve Theory only one flow rate is considered. However, even for incompressible flow the valve outlet flow rate  $\Phi_v^{out}$  (at outer edge of plate) is not identical to the valve inlet flow rate  $\Phi_v^{in}$  (at port inlet area) when the plate is in motion, i.e.

$$\Phi_v^{out} = \Phi_v^{in} - A_v \frac{dh}{dt} \quad (4)$$

where  $A_v$  is the valve plate area. The fact that usually the port length is considerably longer than the valve opening or sealing rim length, suggests that flow inertia effects could play a role in the valve dynamics. The pressure difference could have a phase-shift in time compared to the flow rate, i.e.

$$\Delta p = \frac{1}{2} \rho \left( \frac{\Phi_v}{\alpha L_g h} \right)^2 + \rho \frac{L_p}{A_p} \frac{d}{dt} \Phi_v \quad (5)$$

where  $L_p$  is the port length.

## 2 Experimental Method

### 2.1 Experimental Set-Up

Fig. 2 shows a photograph of the specially designed ring plate valve, which we will refer to as the model valve.

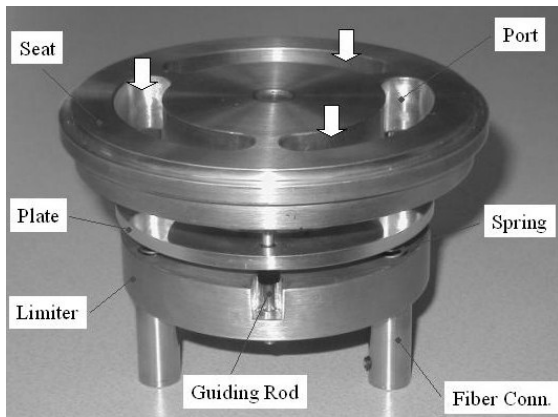


**Figure 2:** Photograph of partially dismantled ring plate valve. The flow direction is indicated with arrows

The seat is compatible with a flange, which can be connected to pipe segments. Rocking of the plate is prevented by means of three guiding rods. In the center of every coil spring a glasfiber bundle is positioned, mounted on the limiter, to measure the valve opening  $h$  by means of a light-intensity method.

In order to measure the valve state variables  $h$ ,  $\phi_v$  and  $\Delta p$  simultaneously, the following set-up has been realized (Fig. 3).

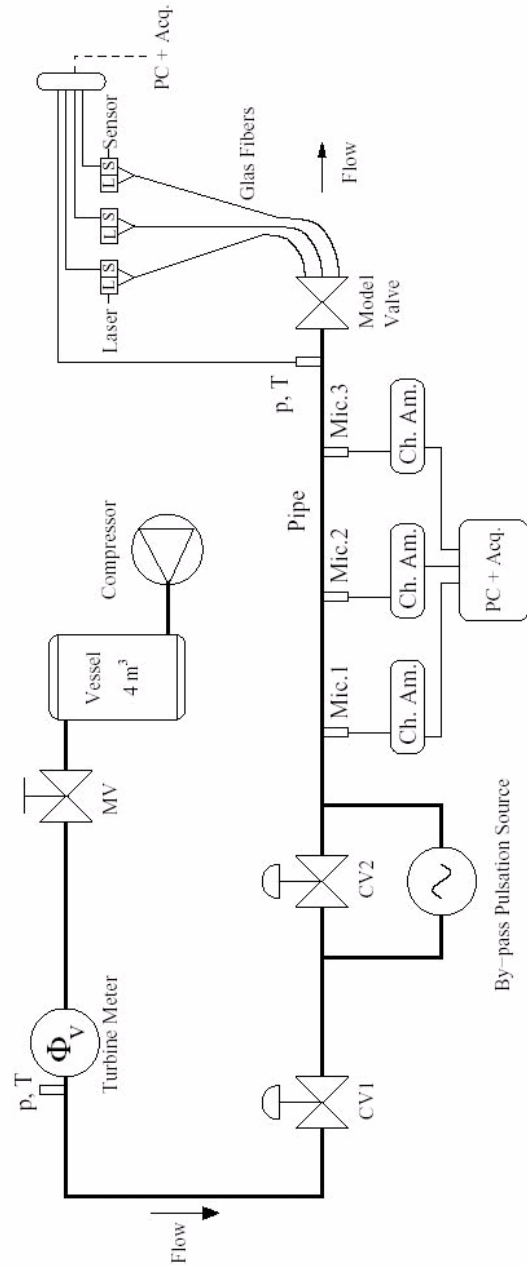


**Figure 3:** Experimental set-up (MV = manual valve, CV = control valve, Mic = microphone, ChAm = charge amplifier, PC+Acq = computer and acquisition interface)

Air is compressed by a screw compressor. The mean value of the volume-flow rate is measured by a turbine meter, where corrections for the compressibility of the air are taken into account. The pulsation source is a rotating cylinder, which blocks the flow periodically. To determine the fluctuations of the flow through the ring plate valve the so-called Two-Microphone Method<sup>4</sup> has been applied, which is based on dynamic pressure measurements at two positions on the pipe. As this method is normally applied in the frequency domain, the method has been extended to

reconstruct the dynamic components of  $\phi_v$  and  $\Delta p$  in the time domain.

The effective plate mass  $m$  is obtained by measuring the weight of the plate and adding the effective spring mass. The spring stiffness  $k_s$  is determined by measuring the static spring force balancing the gravity force of added objects. The damping constant  $\zeta$  is obtained by generating an underdamped oscillation without flow and subsequently measuring the amplitude decay. The parameters  $h_{pl}$ ,  $L_g$ ,  $h_{max}$  and  $A_p$  are determined by geometrical length scale measurements.

## 2.2 Two-Microphone Method

The unsteady values of  $\phi_v$  and  $\Delta p$  are obtained by making use of the linear theory of sound propagation and superposition of dynamic- and static quantities. The Two-Microphone Method is used to reconstruct the acoustic waves at the inlet of the model valve. Three pressure transducers, also referred to as microphones (typical sensitivity is 1400 pC/MPa), are mounted flush in the pipe wall. A pistonphone is used to calibrate the transducers and charge amplifiers with an accuracy better than 1 Pa for 250 Hz.

When the one-dimensional Euler equations are linearized, plane wave solutions for the pressure and velocity are obtained. The present flow is a low Mach number flow, which implies in first approximation identical wave numbers for the upstream- and downstream travelling waves, i.e.  $k = \omega/c_0$ , where  $\omega$  is the circular frequency and  $c_0$  is the speed of sound. The experiments are performed at conditions that corrections for i) Doppler effects and ii) visco-thermal effects are not necessary<sup>5</sup>, because i) the Mach number is much smaller than one (typically  $1.5 \times 10^{-2}$ ), and ii) the Shear number is much larger the one (typically  $2.3 \times 10^2$ ).

Consider the dynamic pressure in Fourier space, i.e.

$$p[x, \omega] \equiv p_+[x, \omega] + p_-[x, \omega] = \int_{-\infty}^{\infty} p[x, t] e^{-i\omega t} dt \quad (6)$$

where  $p_+$  and  $p_-$  are upstream- and downstream travelling pressure waves, respectively. See Fig. 4.

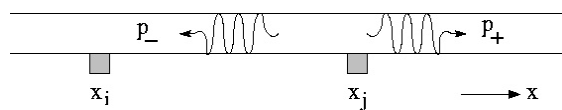


**Figure 4:** Wave decomposition in pipe ( $x_i$  and  $x_j$ : position of microphones)

This decomposition can be written as

$$\begin{aligned} p_+[x, \omega] &= \hat{p}_+[\omega] e^{-ikx}, \\ p_-[x, \omega] &= \hat{p}_-[\omega] e^{+ikx}, \end{aligned} \quad (7)$$

where  $i^2 \equiv -1$ . Two important quantities are defined: the reflection coefficient  $R_x$  and the transfer function  $H_{ij}$ , i.e.

$$\begin{aligned} R_x &\equiv \frac{p_-[x, \omega]}{p_+[x, \omega]}, \\ H_{ij} &\equiv \frac{p[x_i, \omega]}{p[x_j, \omega]}. \end{aligned} \quad (8)$$

Using Eqs. (6) – (8) the reflection coefficient at position  $x$  along the pipe can be determined as function of the transfer function and the wave number, i.e.

$$R_x = \frac{e^{-ik(x_i - x)} - H_{ij} e^{-ik(x_j - x)}}{H_{ij} e^{ik(x_j - x)} - e^{ik(x_i - x)}}. \quad (9)$$

After some algebra the dynamic pressure in Fourier space can be written as

$$p[x, \omega] = \frac{p[x_i, \omega] \sin[k(x_j - x)] + p[x_j, \omega] \sin[k(x - x_i)]}{\sin[k(x_j - x_i)]} \quad (10)$$

which shows that the pressure at position  $x$  is a weighed average of the pressures measured at positions  $x_i$  and  $x_j$ .

Volume-flow rate fluctuations can be determined by making use of the momentum equation of the linearized Euler equations, i.e.

$$\frac{\partial u}{\partial t} = -\frac{1}{\rho_0} \frac{\partial p}{\partial x} \quad (11)$$

where  $u = u[x, t]$  is the velocity amplitude and  $\rho_0$  is the mean density. By making use of Eqs. (6) – (7) the dynamic component of the volume-flow rate can be expressed as function of the reflection coefficient and the dynamic component of the pressure, i.e.

$$\Phi_v[x, \omega] = \frac{A}{\rho_0 c_0} \left( \frac{1 - R_x}{1 + R_x} \right) p[x, \omega] \quad (12)$$

where  $A$  is the cross-sectional area of the pipe.



Finally, the wave reconstruction in the *time* domain at any position  $x$  is obtained by taking the inverse Fourier transform, i.e.

$$p[x, t] = \frac{1}{2\pi} \int_{-\infty}^{\infty} p[x, \omega] e^{i\omega t} d\omega, \quad (13)$$

$$\Phi_v[x, t] = \frac{1}{2\pi} \int_{-\infty}^{\infty} \Phi_v[x, \omega] e^{i\omega t} d\omega.$$

Eq. (13) contains weight factors of the measured pressure fluctuations at positions  $x_i$  and  $x_j$  as function of  $\omega$ , yielding convolution integrals for time domain analysis. Fluctuations of the gas density are not reconstructed, although the evaluation of the valve coefficient  $\alpha$  (Eq. 1) requires the computation of the valve inlet density. Neglecting these fluctuations is justified by the acoustical approach, i.e.  $\rho[x, t]/\rho_0 \ll 1$ .

The acquisition interface samples data from the microphones. Therefore wave reconstruction (Eq. 13) is performed at a discrete level by using the (inverse) Fast Fourier Transform (FFT). Wrap-around (aliasing) errors are reduced by multiplying the dynamic pressure with the Bingham window. In order to prevent the introduction of large errors during reconstruction (Eq. 13 can become singular) the frequency filter of Bodén and Åbom<sup>4</sup> is applied, i.e.

$$0.1\pi < k |x_j - x_i| < 0.8\pi. \quad (14)$$

The remaining modes are zero-padded in Fourier space. In our case e.g.  $|x_j - x_i| = 0.60$  m, yielding  $28 \text{ Hz} < \omega/2\pi < 228 \text{ Hz}$ . This interval encloses typical valve resonance frequencies and typical pulsation source frequencies from the by-pass system (Fig. 3).

The issue of modelling the valve as a *black box*, naturally raises the question how to define the valve inlet, i.e. the upstream evaluation position of the state variables. Reconstruction of the root-mean-square pressure amplitude as function of coordinate  $x$  along the pipe (using Parseval's identity) reveals that the valve inlet can be defined at the geometrical inlet plane (valve port entrance). The valve has a port length  $L_p$  of 16 mm (which is much smaller than a typical wave length) and is therefore acoustically compact, see Fig. 5.

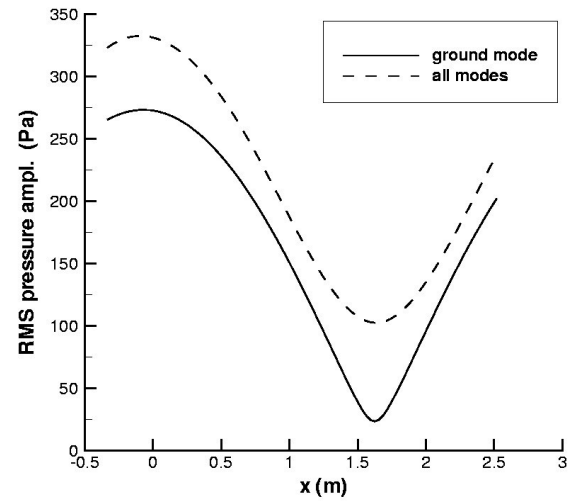


**Figure 5:** Example of the spatial wave reconstruction ( $x_i=0.50$  m and  $x_j=1.10$  m, sampling frequency is 800 Hz, valve inlet at  $x=-0.34$  m)

The dominant mode in the spectrum has a frequency of 50.4 Hz. It has been tested that there is no interference with electrical supply sources (50 Hz). The valve resonance frequency (27 Hz) is not observed in the spectrum. Therefore the valve oscillation is acoustically driven, in agreement with the experiments of Ziada *et al.*<sup>6</sup>.

Simultaneous pressure measurements at three different locations along the pipe makes it possible to illustrate the quality of the reconstruction procedure. The acoustic wave is reconstructed from microphones 1 and 2 at the location of microphone 3 (Fig. 3). A typical result of the reconstruction is shown in Fig. 6. Also the flow rate fluctuation at the same location can be reconstructed.

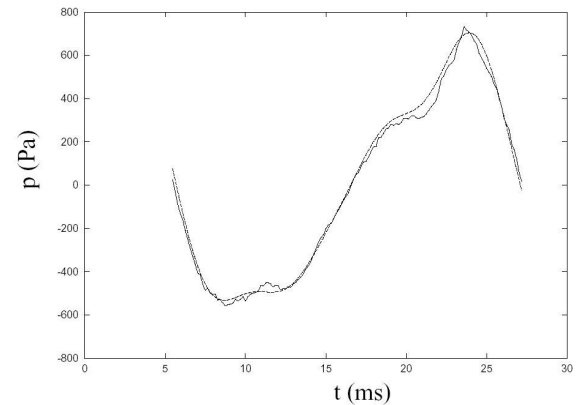


**Figure 6:** Dynamic pressure (— measurement, --- reconstruction)

### 3 Experimental Results

#### 3.1 Semi-Empirical Coefficients

The semi-empirical coefficients  $\alpha[h]$  and  $c_g[h]$  have been determined by generating a (quasi-)steady flow, i.e. the ring plate is ‘hovering’ at a certain opening  $h$ . In case of such a hovering plate the steady gas force  $F_g$  is balanced by the steady spring force  $k_s(h+h_{pi})$ . Steady flow could only be obtained by first forcing the valve plate fully open to its limiter and then reducing the flow rate to the required working point. In this way the onset of resonances resulting from the opening event of the ring plate valve is avoided. See Fig. 7.

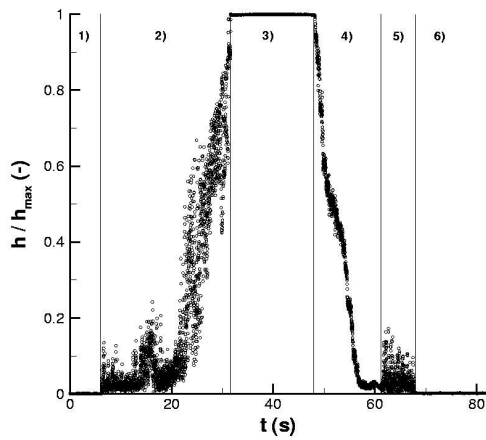


**Figure 7:** History of valve opening during slowly changing pressure difference (six states are distinguished: 1) fully closed, 2) resonance, 3) fully opened, 4) quasi-steady flow, 5) resonance, 6) fully closed; sampling frequency is 100 Hz)

During stage 4) the coefficients are determined. The standard deviation of  $h[t]$  is less than 1% of its mean value. Parabolic regression fits of  $\alpha$  and  $c_g$  as function of  $h$  appeared to be adequate from reproducibility point of view. See Fig. 8.

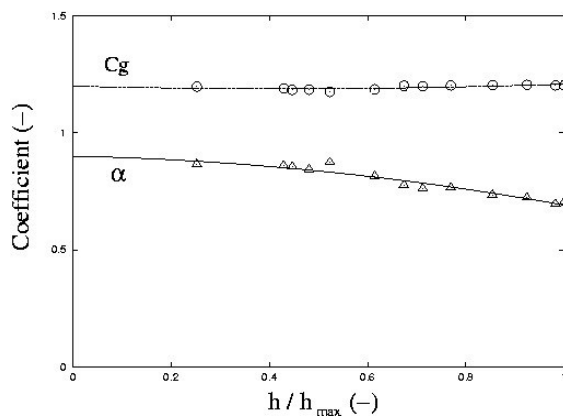


**Figure 8:** Measured semi-empirical coefficients for the model valve. The lines represent regression fits

It is expected that when a compressor valve experiences strong backflow pulsations during the discharge or suction process, flow reversal in the valve could occur. In order to estimate the flow coefficient  $\alpha$  for reverse flow, the valve-flanges system was mounted on the pipe end with the valve limiter upstream. The plate was *fixed* along the three guiding rods (by inserting nuts between plate and both limiter and seat) and the glasfibers were removed. Care has been taken that the flow is not disturbed by the modifications.

Some valve theories include the factor  $\text{sign}[\Delta p]$  in the algebraic flow rate equation, i.e.

$$\Phi_v = \alpha[h] \text{sign}[\Delta p] L_g h \sqrt{\frac{2}{\rho} |\Delta p|} \quad (15)$$

enforcing that the square-root operates on a non-negative number. However, it is expected that during flow reversal the flow experiences a higher resistance than in the case of normal flow direction (Fig. 9).

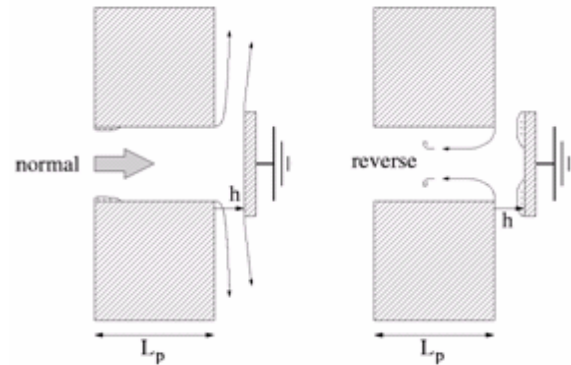


**Figure 9:** Sketch of flow around a fixed valve plate in (a) normal- and (b) reverse direction

Results of our model valve indeed show this behaviour (Fig. 10). The flow coefficient  $\alpha$  is plot as function of the Reynolds number defined by

$$\text{Re} \equiv \rho \frac{\Phi_v L_p}{A_p \mu} \quad (16)$$

where  $\mu$  is the dynamic viscosity.

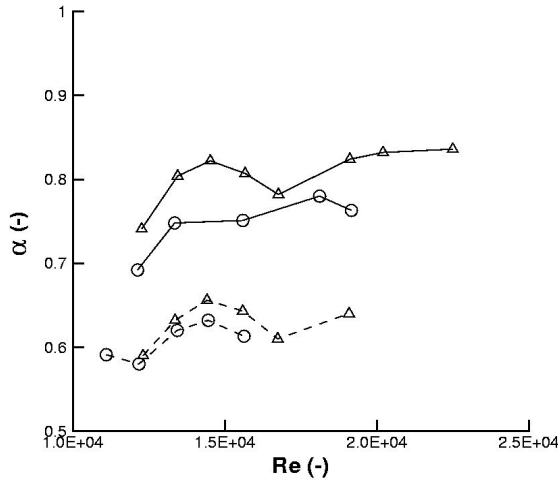


**Figure 10:** Steady flow through model valve with fixed opening: — normal flow; - - - reverse flow ( $h/h_{\max} = 0.26$  is denoted by o and  $h/h_{\max} = 0.54$  is denoted by  $\Delta$ )

In case of reverse flow, it is observed that  $\alpha$  decreases with approximately 0.2 within a wide range of Re.

### 3.2 Valve Dynamics

The Basic Valve Theory is closed when  $\alpha[h]$  and  $c_g[h]$  are known. Validation can be performed in several ways. In order to understand the valve dynamics, we wish to investigate various phenomena separately. In the following we will first consider a non-colliding oscillating valve plate. Plate collisions are investigated subsequently.

Consider the following experiment in which the model valve is mounted on the end of the pipe. Firstly, a steady flow is generated which includes a hovering valve plate. Secondly, the pulsation source is activated leading to a rotating hollow cylinder in the by-pass (Fig. 3). In order to avoid undesired acoustical oscillations, the control valve located just downstream of the pulsation source (not drawn in Fig. 3) was fully closed during the generation of the steady flow. Thirdly, this control valve is opened while the hollow cylinder is already rotating. We choose to integrate the equation of motion of the valve plate, Eq. (2), for prescribed experimentally measured  $\Delta p[t]$ . This will validate the gas force theory, Eq. (3). Fig. 11 shows a typical result.

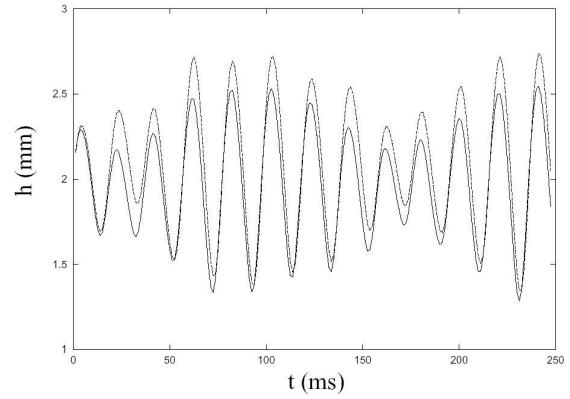


**Figure 11:** Validation of Basic Valve Theory: valve opening  $h$  (—experiment, - - - theory)

Furthermore we choose to compare the dynamic coefficient  $\alpha$  (from measurements of  $\phi_v[t]$ ,  $h[t]$  and  $\Delta p[t]$ ) with the semi-empirical coefficient  $\alpha$  (from measured  $h[t]$ ). Fig. 12 shows a typical result. It appears that there is a large difference between measured  $\alpha$  and theoretical  $\alpha$ . Employing the Extended Valve Theory (Sect. 1) yields no significant improvement of the predicted state variables.

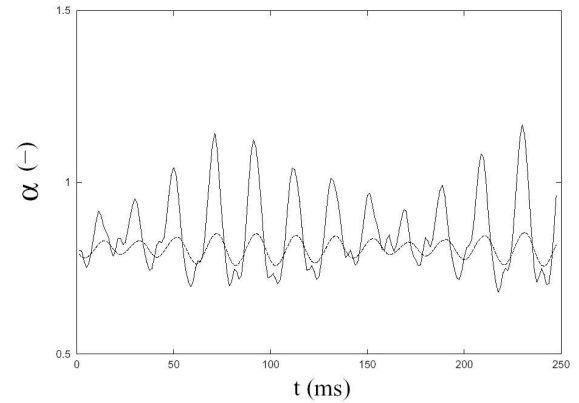


**Figure 12:** Validation of Basic Valve Theory: vena contracta factor  $\alpha$  (—experiment, - - - theory)

The valve plate is limited in its travel by the valve seat ( $h=0$ ) and by the limiter ( $h=h_{\max}$ ). When a moving body impacts a fixed wall it will bounce and reverse its direction of motion with a velocity that is generally lower than the velocity before impact. The restitution coefficient  $e_{\text{res}}$  (Eq. 2) cannot be predicted from the elastic properties of the valve material and geometry alone. There are many other (fluid-structure interaction) factors involved. In absence of flow, visual observation suggests inelastic ( $e_{\text{res}}=0$ ) impacts. When a mathematical model of a compressor system considers such inelastic valve plate collisions, conditions for transitions between several phases of operation (e.g. expansion, suction valve plate in motion, and suction valve fully open) have to be taken into account<sup>7</sup>. However, on-line sampling of

$h[t]$  reveals that at time scales of  $O(10^{-3})$  s and length scales of  $O(10^{-4})$  m semi-elastic collisions occur. Fig. 13 presents an example of the valve opening and plate speed as function of time for two collision events between the plate and limiter.

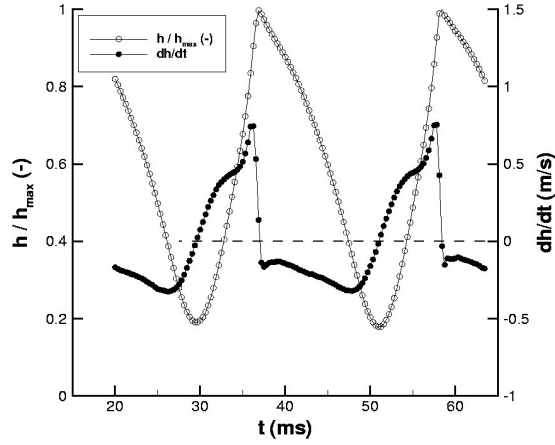


**Figure 13:** Collisions between plate and limiter for the model valve ( $h_{max} = 3.14$  mm, sampling frequency is 3.2 kHz)

Based on multiple rebounds the model valve has  $e_{res} = 0.2 \pm 0.1$  for the limiter and  $e_{res} = 0.3 \pm 0.1$  for the seat.

#### 4 Model Valve vs. Compressor Valve

The model valve has been designed in the parameter range (plate mass  $m$ , spring stiffness  $k_s$ , preload distance  $h_{pl}$ , port area  $A_p$ , sealing rim length, and maximum opening  $h_{max}$ ) of a commercial compressor valve. The latter will be referred to as 'compressor valve'. However, several differences can be distinguished (Table 1).

**Table 1:** Design differences between two valves

Item	Compressor Valve	Model Valve
Port channels	Convergent, multiple concentric	Prismatic, single ring
Valve plate	Disk with holes, non-metallic	Ring plate, aluminium
Discharge channels	Divergent	Prismatic
Guiding rods	Two, near center	Three, near pipe wall

The compressor valve plate has been coated on the downstream side with an aluminium layer in order to reflect the laser light with a high efficiency. The

two guiding rods of the compressor valve prevent plate rotation. Plate rotation could change the flow pattern significantly. However, for the compressor valve these rods are located at a small radius relative to the valve axis of symmetry, increasing the possibility of plate rocking (Fig. 14).

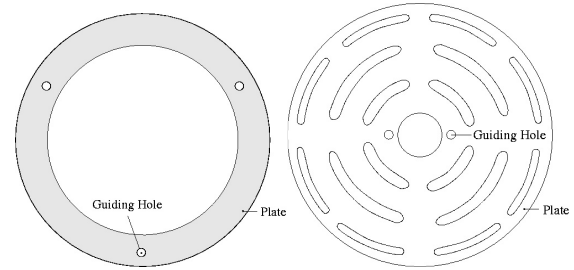


**Figure 14:** Guiding holes in valve plate for (a) model valve, and (b) compressor valve.

For the compressor valve the possibility of plate jamming during operation would be increased when these holes are located further away from the axis of symmetry. For both valves the plate has sharp edges at the upstream and downstream side, resulting in fixed flow separation lines. In both valves air cannot flow through the coil springs.

Fig. 15 shows the steady flow effects by comparison of the semi-empirical coefficients for the two valves.

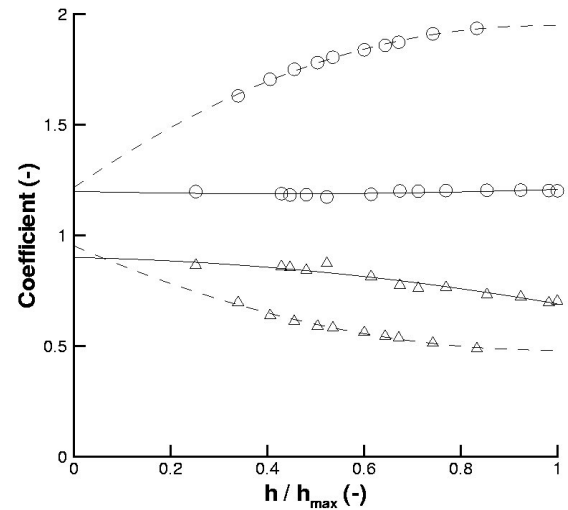


**Figure 15:** Semi-empirical coefficients (— model valve, - - - compressor valve);  $c_g$  is denoted by o and  $\alpha$  is denoted by  $\Delta$ )

The extrapolation of the coefficients for  $h \rightarrow 0$  is not meaningful because viscous effects are expected to give anomaly behaviour.



In our experimental method the valve plate displacement method can only be applied when the plate angle is not large. The model valve plate, however, is forced to move nearly translationally in which the angle cannot exceed approximately  $0.5^\circ$ . Light intensity measurements for oblique plate positions showed no significant dependence on this angle. Improving the present method by calibration for oblique plate positions could be useful for compressor valves. However, preliminary calibrations showed that only a few number of plate angles could be used, limited by the usage of feeler gauges.

For unsteady flow we observed considerable plate obliqueness (rocking) of the compressor valve. Because of the issues discussed in the preceding paragraph the Basic Valve Theory has not been validated for unsteady flow conditions. Fig. 16 shows typical time traces of the colliding plate of the compressor valve.

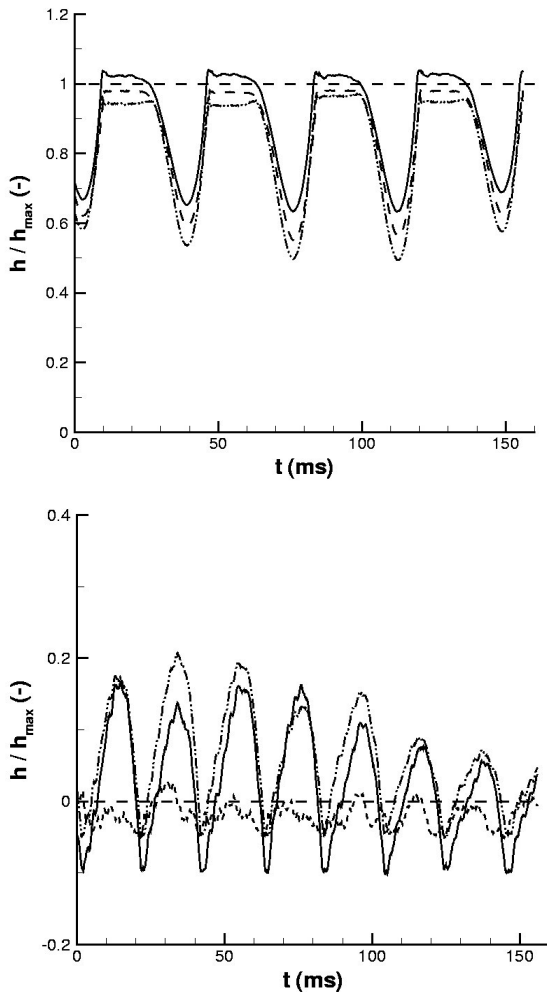


**Figure 16:** Collision events of compressor valve for (a) plate-limiter, and (b) plate-seat. Measured time traces are shown for three glassfiber bundles ( $h_{max} = 2.42$  mm, sampling frequency is 12.8 kHz)

## 5 Concluding Remarks

Semi-empirical description of the dynamical response of compressor valves use the valve opening  $h$ , the pressure difference  $\Delta p$  and the volume-flow rate  $\phi_v$  as basic state variables. This paper presents accurate dynamic measurements of these variables, i.e.  $\delta h/h_{max} < 2\%$ ,  $\delta \Delta p/\Delta p[h_{max}] < 1\%$  and  $\delta \phi_v/\phi_v[h_{max}] < 2\%$ .

Preliminary results for unsteady flow through the *model valve* show that the Basic Valve Theory (Sect. 1) is able to predict the gasforce acting on the plate reasonably accurately (Fig. 11). However, the flow rate through the valve is underpredicted (both mean value and fluctuating part) for given pressure difference (Fig. 12).

Furthermore an extension of the present theory (Sect. 1), incorporating flow inertia in the port and momentum injection by the moving plate, did not improve the predictions significantly. An important difference is found between  $\alpha[h]$  for unsteady and steady flow. A plot of  $\alpha[h]$  for unsteady flow (not shown in this paper) suggests that hysteretic changes in flow pattern are present. We expect this effect to be caused by a periodically detaching and reattaching separated flow from the seat.

It has been observed for both valves that the plate has almost parallel impacts against the limiter while the impacts against the seat often occur in severe oblique plate positions (Fig. 16). This suggests that there is an ‘air cushion’ between plate and limiter, that acts as a fluid damper. For the plate-seat interaction such a cushion is not present. Furthermore, the parallel impacts on the limiter are enhanced by the large spring force acting on the plate (suppressing small fluctuations of the unsteady gas force).

Further research is required to improve the present valve theories on the following items:

- 1) the ‘air cushion’ effect (by analysis of a new theory of unsteady flow between plate and limiter, including the dynamic vena contracta factor  $\alpha$  for  $dh/dt > 0$  vs.  $dh/dt < 0$ );
- 2) the difference between  $\alpha$  for steady and unsteady flow;
- 3) valve plate collisions (by dynamic measurements of all the valve state variables, in order to explore the dependence of parameters [valve eigen frequency  $\sqrt{k_s/m}$ , pulsation frequency, ...] on the valve dynamics [restitution coefficient  $e_{res}$ , mean valve pressure difference  $\Delta p_0$ , ...]).

A more elaborate discussion on the experimental method and the valve dynamics is presented in another paper<sup>8</sup>.

## 6 Acknowledgements

The authors are indebted to A. Hirschberg for helpful discussions, to J. van der List for construction of the ring plate valve and to M.C.A.M. Peters for using the Air Flow Test Facility at TNO TPD.

---

## References

- [1] Costagliola M. (1950) The theory of spring-loaded valves for reciprocating compressors, *J. Appl. Mech.*, 415-420.
- [2] Westphal M. (1893) Beitrag zur Grössenbestimmung von Pumpenventilen, *Z.d.V.D.I.* 37, 381-386.
- [3] St Hilaire A.O., Wilson T.A., Beavers G.S. (1971) Aerodynamic excitation of the harmonium reed, *J. Fluid Mech.* 49, 803-816.
- [4] Bodén H. and Åbom M. (1986) Influence of errors on the two-microphone method for measuring acoustic properties in ducts, *J. Acoust. Soc. Am.* 79, 541-549.
- [5] Peters M.C.A.M., Hirschberg A., Reijnen A.J., Wijnands A.P.J. (1993) Damping and reflection coefficient measurements for an open pipe at low Mach and low Helmholtz numbers, *J. Fluid Mech.* 256, 499-534.
- [6] Ziada S., Shine S.J., Bühlmann E.T. (1986) Self-excited vibrations of reciprocating compressor plate valves, *Proc. Int. Compr. Eng. Conf.*, Purdue, 398-414.
- [7] Toubert S. (1976) A contribution to the improvement of compressor valve design, PhD thesis, University of Delft, The Netherlands.
- [8] Habing R.A. (2005) An experimental method for validating compressor valve vibration theory, submitted to *J. Fluids Struct.*



# **Reciprocating Compressor Valve Plate Life and Performance Analysis**

by:

**Brun, Klaus**  
**Mechanical and Fluids Engineering**  
**Southwest Research Institute®**  
**San Antonio, Texas**  
**United States**  
**klaus.brun@swri.org**

**Nored, Marybeth G.**  
**Mechanical and Fluids Engineering**  
**Southwest Research Institute®**  
**San Antonio, Texas**  
**United States**  
**marybeth.nored@swri.org**

**Smalley, Anthony J.**  
**Tony Smalley Consulting, LLC**  
**Grand Junction, Colorado**  
**United States**  
**tony@tonysmalleyconsulting.com**

**Platt, John P.**  
**BP Company**  
**Houston, Texas**  
**United States**  
**plattjp2@bp.com**

**4<sup>th</sup> Conference of the EFRC**  
**June 9<sup>th</sup> / 10<sup>th</sup>, 2005, Antwerp**

## **Abstract:**

The operation of a reciprocating compressor is closely linked to the performance of its valves, in terms of both life and efficiency. To better understand the factors that affect reciprocating compressor valve performance and life, a Gas Machinery Research Council (GMRC) program has been initiated to systematically investigate the physical behavior of valve plates during compressor operation. A reciprocating compressor's valve plate life is generally considered to be a function of the plate's cyclic kinematics, transient stresses, and material properties. Thus, the valve research program aims to incorporate these fundamental factors into an analysis model that accurately predicts valve life for a given application, geometry, and plate material. The research will benefit users within the gas industry by providing a basis for improvements in applications engineering and operational decision-making related to reciprocating compressor valves. The analysis model developed by the research program is based on results from plate single impact tests, finite element (FE) calculations, optical valve plate 3-D motion measurements, and material high cycle fatigue testing. Some of the experimental and analytical results are discussed herein.

## 1 Introduction

In designing a reciprocating compressor valve, desirable functional attributes include good sealing, rapid opening and closing, sustained high flow area (when open), minimum bouncing upon impact, toleration of impact forces and maximum temperatures, and low flow resistance. Proper design choices, such as material, mass, spring constant, lift and flow area, will maximize the successfulness of the design. However, simple, passive valves do not tolerate wide operating ranges well. The challenge to the current research program is to achieve longer valve life with low loss and acceptable valve operation (including leak potential). Design improvements often come at a price because low flow resistance, which adds to longer life, conversely leads to excessive impact forces. Valve manufacturers have made many advances in materials and configuration. Yet, design tradeoffs, parameter selection and operation of valves are often mismanaged because applications engineering tools are not readily available.

Valve failures can be divided into two major categories: Environmental and Mechanical<sup>1</sup>. Environmental causes are those elements in the valve environment that can lead to valve failure, such as corrosive contaminants, foreign material, liquid slugs, or improper lubrication. Environmental failures can sometimes be prevented by the proper choice of valve material and conditioning of the gas stream (filtration, separation, etc.). Mechanical causes are valve failures that result from high cycle fatigue and abnormal mechanical motion of the valve, caused by high valve lift, valve operation at off-design conditions, valve flutter, pulsations, or spring failure. As impact velocities increase due to higher valve lift or valve operation at off-design conditions, the velocities cause excessive impact stresses and an accelerated damage rate to the valve. Some mechanical causes can be controlled with a good design of the valve components (guard, seat, moving element, and springs), although a valve's design is usually optimized for a single design point based on the fixed mass, stiffness, and damping of the valve plate and spring.

Perhaps the most common cause of plate or spring failure is valve operation at off-design conditions. In designing a valve to work reliably without failure, a range of operating conditions is assumed. The design, however, is optimized for a single set of operating pressures, temperatures, speed, cylinder clearance, gas molecular weight, lubrication rate, and pulsation level. When the operating conditions significantly deviate from the ideal case, the valve design reliability is not

necessarily ensured<sup>2</sup>. With the recent increased need for variable speed compressors in the reciprocating compressor market, the off-design operation of valves is more evident, seen by more failures in valves.

The efficiency of a reciprocating compressor also strongly depends on the performance of its suction and discharge valves. In high-speed units (600 RPM or more), valve performance is aggravated further by the increased frequency of valve impacts, higher impact velocities, and reduced flow areas. In general, the ideal compression cycle of a reciprocating compressor is affected directly by valve losses, which lower the adiabatic efficiency of the machine<sup>3</sup>. Valve performance is critical to both compressor efficiency and reliability. In turn, compressor efficiency has a direct impact on capacity when the driver is operating at its maximum power.

Several past studies have been conducted to understand valve failures and prolong valve life in order to improve compressor performance. In a 2003 study, engineers at El Paso Corporation investigated six different compressor valves from five manufacturers in order to determine valve efficiency, reliability, and cost of operation<sup>4</sup>. The six-month investigation found that valve efficiencies were directly related to compressor ratios, where inefficiency was attributed to valve leakage at low compression ratios. This finding highlights the critical problem in operating traditional valves at non-ideal (off-design) operating conditions. In addition, the El Paso study found that the losses through suction valves were approximately twice as great as the discharge valve losses<sup>4</sup>. Figure 1 shows an example of a P-V trace from a typical compressor with a pressure ratio of 1.4, tested in the El Paso study. The shaded gray area between the cylinder pressure trace and the suction and the discharge nozzle traces can be interpreted as the lost work required to pump gas into and out of the cylinder against the valve resistance.

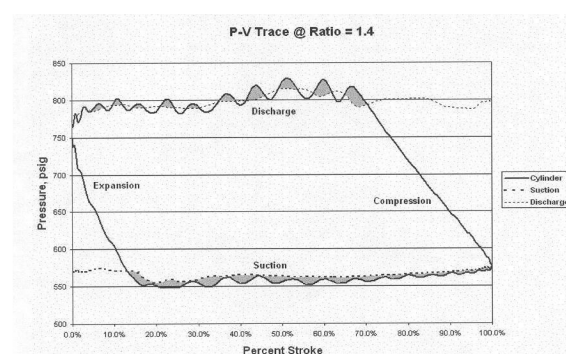


**Figure 1:** Typical P-V Chart Illustrating Valve Horsepower Losses



In 2001-2002, a GMRC program examined valve stresses in order to predict valve life. Southwest Research Institute® engineers tested a series of valves at the GMRC Reciprocating Compressor Test Facility (RCTF) and the Hoerbiger valve slapper facility. This program was initiated because of the need for improving analysis tools in valve application engineering<sup>5</sup>. Figure 2 shows the test setup at the Hoerbiger valve slapper facility. The program provided a limited set of data and yielded insight as to the effort required for future research. The research showed the need to validate a dynamic model of valve motion against actual test data. This previous GMRC research program provided a starting point for determining valve stress and modeling the valve's physical behavior.

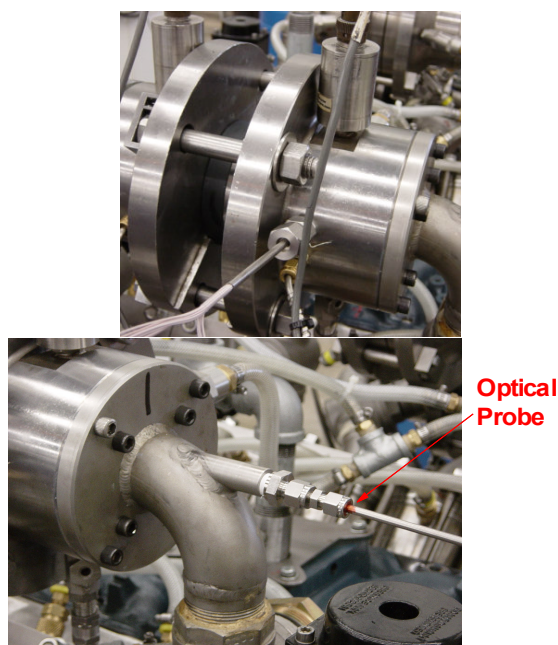


**Figure 2:** Previous GMRC Valve Testing at Hoerbiger Valve Slapper Facility

Beyond the current valve designs, a better tool is needed to predict valve life based on compressor operating profile, geometry, material, and valve type. This paper describes the GMRC research program, which aims to develop such a tool for valve behavior and performance. This program will enhance the understanding of valve motion and the consequent stresses created by the valve's operating behavior. Namely, through the integration of experimentally validated FE analysis of transient plate stresses, a probabilistic valve plate motion model based on real measured field data, and accurate plate material properties, a predictive tool for reciprocating compressor valve plate life can be developed. In combination with performance predictions, the predictive tool will support enhanced applications engineering for reciprocating compressor valves.

## 2 Reciprocating Compressor Valve Program

The objective of this research is to better understand the factors affecting reciprocating compressor valve performance. In meeting this objective, the research aims to develop a tool for predicting reciprocating compressor performance together with valve plate life. Valve life is considered to be a function of the plate cyclic 3-D kinematics and material properties. The program will investigate these two fundamental aspects of reciprocating compressor valves in developing a method to predict valve life. The benefit of the research is primarily to increase compressor efficiency and reduce downtime by allowing the user to optimize machine performance and valve life for a desired operating profile and valve material.

The components of the reciprocating valve program are outlined in Figure 3. In order to model the motion of a valve plate and the compressor performance, the compressor geometry, operating conditions, and valve parameters must be known. Although these parameters dominate the requirements for predicting valve motion and compressor performance, the flow resistance and pulsations in the piping are contributory factors. The influence of these conditions should be evaluated by measuring the motion of the plate under varied operating conditions (*Program Element 1*). The results of the first round of Program Element 1 testing will be discussed briefly for one set of operating conditions. The results provided an average impact velocity, angle and location for the opening and closing events. Future testing will examine other valve designs (varied plate designs, spring stiffness, etc.) and operating conditions (pressure ratio, speed, etc.).

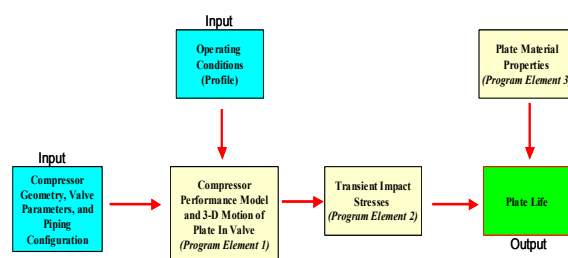


**Figure 3:** Roadmap for Reciprocating Compressor Valve Research

Characterizing the plate motion in three dimensions significantly differs from one-dimensional models of reciprocating compressor valve motion that the state of the art currently offers. Most of these one-dimensional models assume the plate to lift off the

seat and move towards the guard without any angularity to its movement. In reality, the plate moves toward the guard non-uniformly, with a significant level of angularity. The results of the research presented in this paper clearly show that the assumption of purely translatory motion of the plate is rarely valid. The precise motion of the plate is not yet sufficiently understood in order to use angular motion in deterministic valve motion predictions. This research aims to provide a more detailed understanding of the plate movement, in translation from the seat to the guard, with realistic angularity of the plate.

The 3-D motion of the plate can be used as an input to a finite element (FE) model that predicts plate transient impact stress as a function of impact velocity, angle of impact and location (*Program Element 2*). However, the FE model must be validated against real data in order to calibrate and verify the model. To validate the model, controlled single impact tests were completed using a burst-membrane shock-tube. These tests provided useful characterizations of the kinematic behavior of the plate. The single impact tests were recorded to determine plate impact velocity, angle and location. In addition, strain gauges provided strain measurements on the plate that correlated with the plate position recorded by displacement probes. Using the results from the single impact testing, the FE model was validated. The results of this program element will be discussed in detail.

Finally, a materials analysis of the plate material can be used in combination with a predictive model of plate stress to predict valve plate life (*Program Element 3*). The materials analysis is currently being conducted on PEEK material at various temperatures to characterize the fatigue behavior of PEEK. The results show conservative agreement with the manufacturer data. The fatigue testing will generate stress versus life data (SN curves) that can be tied to model estimations of plate impact stress to predict plate life.

### 3 Development of Model to Predict Valve Impact Stresses

One critical aspect of predicting valve plate life is linking the realistic physical behavior of the valve plate to a validated stress model. Obtaining useable results from compressor test data to validate the model can be challenging because of the high frequency of impacts and the complex non-uniform motion of the plate. To understand the plate kinematics and validate the model, single impact testing was performed using a burst-membrane shock-tube. This testing allowed a realistic single

impact event to be analyzed in detail without additional complicating valve motion characteristic of a typical reciprocating compressor.

A 12-inch diameter burst-membrane shock-tube was constructed, as shown in Figure 4. A typical reciprocating compressor valve was mounted 4.0 meters downstream of the shock-tube. The valve was instrumented with optical position probes (in order to measure displacement of the valve plate) and strain gauges (in order to measure strain on the plate). The instrumented valve is shown at the top in Figure 4. Three precision strain gauges (manufactured by Micro-Measurements with 120-ohm resistance) were mounted on the valve plate, which was affixed with reflective coating to optimize the available light for the optical probe measurement. The valve plate is shown in Figure 5. The high-speed optical probes were located on the outer diameter of the valve. This test setup provided detailed three-dimensional motion data and plate strain results.



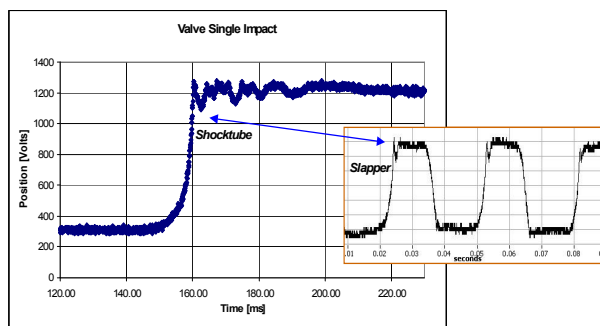
**Figure 4:** Burst-Membrane Shock-Tube (Top) and Instrumented Valve Fixture (Bottom)



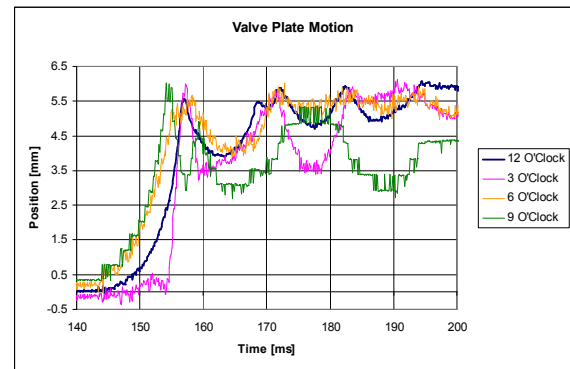
**Figure 5:** Valve Plate with Reflective Coating and Mounted Strain Gauges

The burst-membrane shock-tube testing was triggered with a plastic membrane and nichrome heat wire mounted to the membrane surface. Once the membrane burst, a normal shock traveled downstream and hit the valve assembly. The valve test fixture measured the movement of the valve plate as it impacted the guard and bounced multiple times after the shock. No springs were used in the valve in order to understand the plate motion completely without the influence of the spring elements. For each test, the data acquisition period began when the membrane burst. The data acquisition rate was approximately 10 kHz on six separate channels, which allowed sufficient sampling of the three high-speed optical position probes and the three strain gauges.

Four single impact tests were performed to capture a range of impact locations, angles, and velocities. The single impact profile matched previous plate profiles obtained in the Hoerbiger valve slapper. Figure 6 compares the two motion profiles. As the figure shows, the motion profile from single impact testing correlated with the multiple impacts recorded in the valve slapper. The three optical probe sensor measurements were used to determine how the plate impacted the guard, its subsequent motion and the impact velocity. Figure 7 shows the plate motion plot generated from the three optical position probes. The motion of the plate is not uniform and causes the plate to impact at an angle rather than flat. (However, valve springs tend to reduce the angularity of the impact.) The plate motion data also indicates that the plate bounces after the initial impact. In the first impact, the plate hits at the 9 o'clock position, followed by a more flat impact at the 12 o'clock and 3 o'clock positions, and then lastly at the 6 o'clock position. In the repeated hits after the initial impact and the subsequent “ringing” effect, different areas of the plate show varied amounts of movement, which confirms the plate’s angular movement.

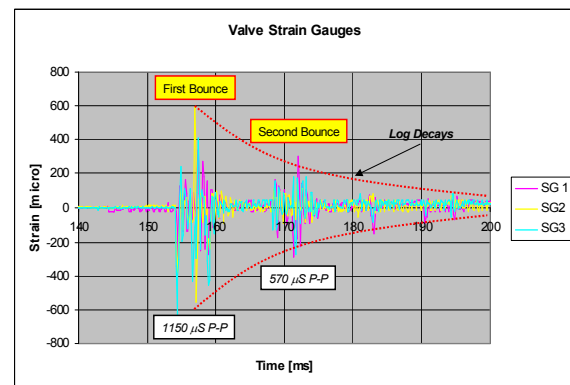


**Figure 6:** Comparison of Plate Motion Profile in Single Impact Shock-Tube Test and Hoerbiger Valve Slapper



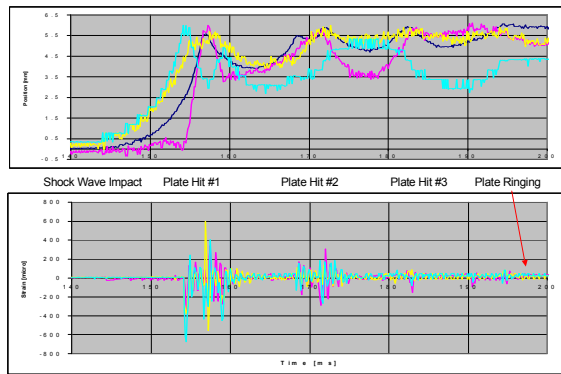
**Figure 7:** Valve Motion Recorded by Optical Position Probes, with Probe Coordinate Transformation

Figure 8 shows that the time traces from the strain gauges were consistent with the plate motion profile. The plate strain is at a maximum at the first impact at approximately 1,150  $\mu\epsilon$  peak-to-peak. The second and third bounce of the valve plate show significantly less strain and tend to follow a logarithmic decay in strain over time. This result is significant because it means that the primary impact causes the greatest strain on the valve plate and the resulting impacts are considerably weaker. Figure 9 compares the plate position to the valve strain to reveal the good correlation between the measured strain values and the plate displacement. The plot also shows the ringing phenomenon after the plate’s discrete impact points. The results from the shock-tube testing demonstrated a maximum plate impact velocity of 3.6 m/s, an impact location at 245°, and an impact angle of approximately 5.6°. Measurement uncertainties for velocity, impact angle and stress were around 20%, while the uncertainty for the stress measurement was slightly less at approximately 15%.



**Figure 8:** Corresponding Valve Strain Measured by Strain Gauges During Simple Impact Testing





**Figure 9:** Comparison of Measured Valve Position and Strain During Single Impact Test

An enhanced view of the initial impact (i.e., the first bounce) of the valve plate provides a detailed explanation of the strain generated by a single impact event. Figure 10 shows the strain of the valve plate at four locations during the first hit. From this strain plot, it is evident that the plate hits on its edge first at an angle of  $5.6^\circ$ , generating a peak-to-peak strain of approximately  $950 \mu\epsilon$ . The plate then hits almost flat with a maximum peak-to-peak strain of  $1140 \mu\epsilon$ . Last, the opposing edge strikes the guard at a less significant level ( $570 \mu\epsilon$  P-P). These values of strain show the initial edge impact, and the latter full plate hit generate the maximum strain in the valve plate. After the first impact events, the valve plate continues to bounce against the guard, but with a considerably reduced level of strain (and stress).

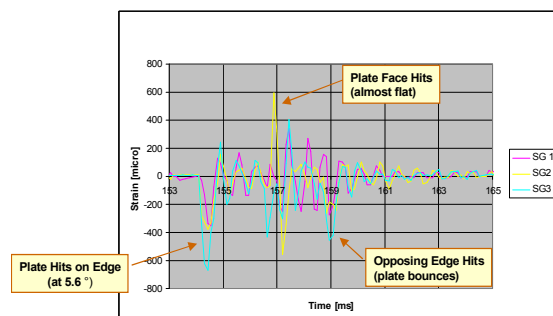


**Figure 10:** Expanded Valve Strain Measurements for Initial Plate “Bounce”

Thus, the single impact testing yielded a characterization of the valve plate kinematic behavior versus strain. The test results can be used to validate an FE model developed to simulate a single impact event for the valve plate. The FE model inputs were the impact velocity, angle, and location of the valve plate. To model the dynamic plate behavior, ANSYS was used to perform a transient stress calculation (typical valve plate geometry using 2438 elements). Model predictions for transient stress could be compared directly to

the calculated stress based on measured strain values. Figure 11 shows an example of the finite element model transient stress calculation. Model predictions of the plate movement could also be compared to the plate position plot. Table 1 highlights the good agreement between the FE model and the experimental data. The model predicted stress was slightly less than the measured stress in all cases, but within the uncertainty of the shock-tube test.

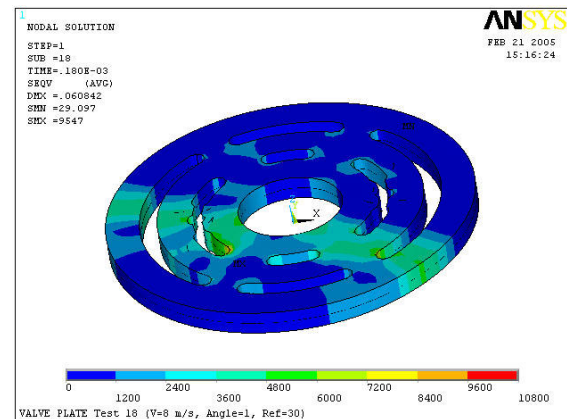


**Figure 11:** Finite Element Model of Valve Plate After Plate Single Impact and Resulting Stress Wave Propagation

**Table 1:** Summary of Results Comparing FE Model Performance to Measured Stress Data

Test No.	Test #25	Test #31	Test #45	Test #49
Velocity (m/s)	3.2	3.6	2.5	2.3
Impact Angle	$3.8^\circ$	$5.6^\circ$	$5.3^\circ$	$5.5^\circ$
Location	$74^\circ$	$245^\circ$	$251^\circ$	$247^\circ$
<b>Measured Stress (MPa)</b> (Closest SG, E = $4.3E4$ kPa)	38	41	26	27
<b>FE Model Stress (MPa)</b> (Closest SG, E = $4.3E4$ kPa)	33	36	24	23
<b>FE Model Deviation</b>	15%	14%	8%	17%
<i>FE Model Deviation is within stress measurement uncertainty (<math>U_{st}=20\%</math>)</i>				

To predict the stress levels at other impact angles and velocities, the FE model was used in a parametric study to determine the relationship between the plate kinematic behavior and transient stress levels. For a range of impact angles, velocities, and locations, the parametric study identified the highest stress location for a particular set of input values. The quarter symmetry about the plate allowed a detailed parametric evaluation of the plate to be performed on a single quarter



section. Maximum and minimum stress levels expected at particular locations were identified for specific impact angles and velocities. An example of the results obtained at an impact location of  $30^\circ$  is shown in Figure 12. The figure shows the increase in peak-to-peak stress as velocity increases. At an increased impact angle, the stress level increases more rapidly as velocity increases.

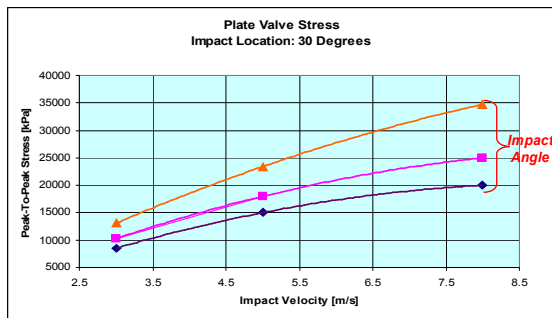


**Figure 12:** Parametric Study Results Using FE Model for Impact Plate Location of  $30^\circ$

Thus, the FE model will be used to predict valve life based on material stress-life properties and a characterization of the valve motion over a range of operating conditions. The testing proved to be worthwhile in understanding the kinematic behavior of the valve plate and the stress created by the differential pressure force across the plate. The single impact testing also provided the following conclusions about the kinematic motion of the plate:

- The valve plates were seen to *always* hit at an angle.
- The plate usually “bounces” at least one more time after the initial impact, but the subsequent impacts are softer.
- The highest stress events within each impact occur when the initial edge of the plate hits and the full plate hits, which is followed by the opposing edge hit.
- The initial edge and full plate hit generate the highest stresses (evident in Figure 10), and both of these hits create similar levels of stress (within 20% of magnitude).
- The highest stress levels decay quickly, but the plate continues to “ring” after impact, creating ongoing dynamic low stress.

## 4 Plate Motion Analysis

In order to effectively use the transient stress predictions of the FE model, the 3-D plate motion must be understood for a range of operating conditions and valve/piston designs. Thus, another critical element of the reciprocating compressor valve program is the study of the plate motion in

reciprocating compressor machines (Program Element 1, as shown in Figure 3). This element of the program will provide the data needed to characterize the three-dimensional motion of the valve plate. Once the characterization is complete for a range of operating conditions and design parameters, a probabilistic method can be developed to provide the necessary inputs (impact velocity, angle, and location) to the transient stress model.

To study the valve plate motion, a series of tests are being conducted at the SwRI<sup>®</sup> Metering Research Facility using an Ariel 250 HP reciprocating compressor, shown in Figure 13 (at top). Three optical position probes are used to monitor the position of the valve plate. The optical position probes were mounted on the discharge valve (see Figure 13 at bottom). The displacement data from the probes is then used to determine the plate velocity, angle of impact and impact location. An example of the calculated impact velocity determined from the optical position probe data is shown in Figure 14. Testing has been completed for a discharge valve with one particular set of springs at a speed of 900 RPM and a range of compression ratios. This testing indicates the most consistent empirical relationship is that between impact angle and plate velocity, as shown in Figure 15. This plot shows an increase in plate velocity for decreasing impact angle. Additional testing will provide the characteristic motion of the valve at different operating speeds, for both the suction and discharge valves, and for varied spring stiffness.

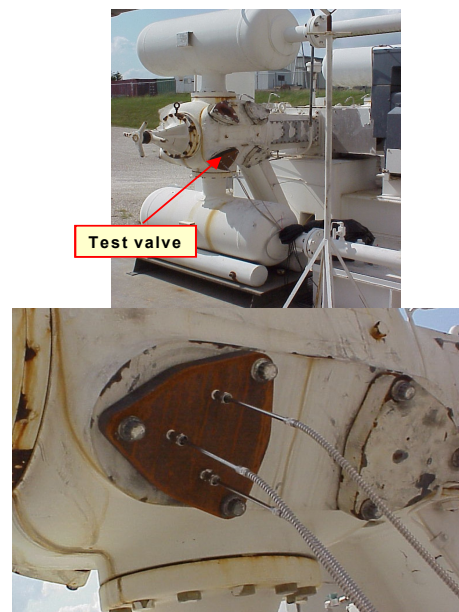


**Figure 13:** Ariel Reciprocating Compressor Used in Measuring Valve Motion (Top) with Optical Position Probes Mounted on Valve (Bottom)

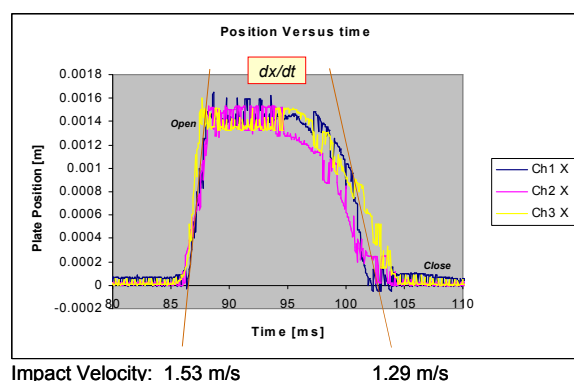


**Figure 14:** Typical Position Probe Data Used to Calculate Impact Velocity on SwRI Ariel Compressor

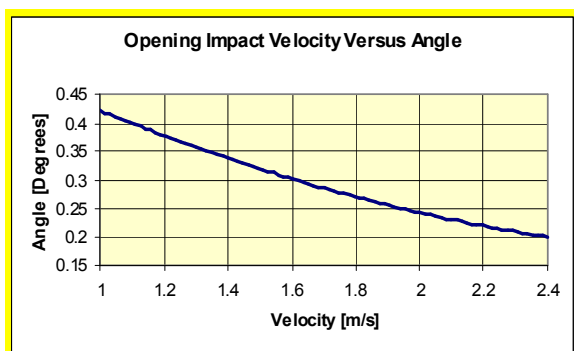


**Figure 15:** Correlation Between Impact Angle and Velocity for Valve Plate, Based on Displacement Probe Data

## 5 Materials Analysis

In addition to understanding the three-dimensional valve motion and predicting the transient stress, a stress-life analysis of the valve plate material is being performed. This analysis will be used to convert the predictions of the transient stress model into an estimation of valve life using S-N material curves. Fatigue life testing is being performed on PEEK material samples to determine the number of cycles to failure at various stress levels. Stress versus life curves (S-N curves) are then created for each set of tests.

The first fatigue tests were performed at room temperature at stress levels of 11.3 ksi and 16.3 ksi. The testing was consistent with manufacturer predictions, but also indicated that fatigue life is nearly infinite for very low stress levels. Additional stress levels will be tested at elevated temperatures to develop more S-N curves for PEEK (below and above the glass transition temperature). These tests will be run at similar stress levels to determine the effect of temperature on valve plate life.

## 6 Summary

The reciprocating compressor valve research aims to improve compressor efficiency and reduce downtime by enhancing valve performance. A dynamic finite element model has been developed and validated against single impact test data for plate transient stress analysis. Combining these stresses and valve motion predictions with material stress-life characteristics will yield valve plate life predictions. The resulting prediction capability should enable the reciprocating compressor user to tune the machine performance to reduce valve stress and prolong valve. In addition, the predictions will allow users to balance valve life and performance to meet a particular operation/business need for the compressor.

## 7 Acknowledgements

The authors would like to acknowledge the Gas Machinery Research Council, the United States Department of Energy, BP Corporation, and Hoerbiger Corporation for their financial and technical support of this valve research program.

## References

- <sup>1</sup> Hoerbiger Bulletin, HCA 8200-86, "How and Why Compressor Valves Fail," Hoerbiger Corporation of America, Inc.
- <sup>2</sup> Chaykosky, S., (2002), "Resolution of a Compressor Valve Failure: A Case Study," Dresser-Rand Literature, [www.dresserrand.com](http://www.dresserrand.com).
- <sup>3</sup> Gartmann, H., (1970), *De Laval Engineering Handbook*, Compiled by the engineering staff of De Laval Turbine, Inc., McGraw-Hill Book Company, New York, 1970.
- <sup>4</sup> Noall, M. and Couch, W., (2003), "Performance and Endurance Tests of Six Mainline Compressor Valves in Natural Gas Compression Service," Gas Machinery Conference Paper 2003.
- <sup>5</sup> Harris, R. E., Gernentz, R. S., Gomez-Leon, S., and Smalley, A. J., "Valve Life, Pressure Drop and Capacity," GMRC Report, June 2003.

# **Sizing and Optimization of Compressors in ldPE Plants and Validation by Measurement**

by:

**Andreas Allenspach and Carsten Krockner**

**Sizing Department**

**Burckhardt Compression**

**Winterthur**

**Switzerland**

**[andreas.allenspach@burckhardtcompression.com](mailto:andreas.allenspach@burckhardtcompression.com)**

**[carsten.krockner@burckhardtcompression.com](mailto:carsten.krockner@burckhardtcompression.com)**

**4<sup>th</sup> Conference of the EFRC  
June 9<sup>th</sup> / 10<sup>th</sup>, 2005, Antwerp**

## **Abstract:**

The sizing of compressors for ldPE plants is multifaceted. A multitude of parameters need to be determined that are linked with the layout of the whole plant. The present article gives an overview about compressor sizing and adaptation to the plant, gas properties under high pressure, design principles, gas pulsation analysis and a comparison between calculated and measured values of gas pulsation under high pressure.

## 1 Introduction

In low-density polyethylene (ldPE) plants ethylene or ethylene vinylacetat mixtures are compressed from 1 bara suction pressure up to over 3000 bara discharge pressure. For this duty two compressors are used that usually work with seven or eight compression stages. The typical feed pressure of the fresh ethylene is between 15 and 30 bara (figure 1). The compressor for the lower pressure range is divided into two parts, a booster part which compresses the recycled gas to fresh ethylene pressure, and a primary part, which compresses the gas up to the feed pressure of the hyper or secondary compressor (approx. 270 bara). The power saving regulation options are generally only applied on the booster/primary compressor. The two stage hyper compressor (secondary compressor) delivers the discharge pressure which is required at the reactor inlet.

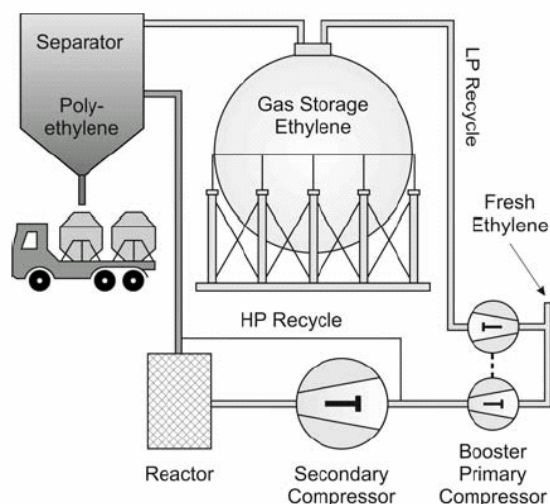


**Figure 1:** Principal schema of ldPE production

In this paper the influence of the secondary compressor design and compressor related parts of the plant will be discussed. Many compressor related design features have influence on the behavior and functionality of the whole plant. In a second part, the ways of calculation, optimization and some validations on the basis of an existing plant will be shown.

## 2 General aspects in ldPE plant design

There are various factors which influence the ldPE plant design. Many of these are related to the compressor design or compressor specific plant configurations like dampers, special supports or orifices.

On the other hand, there are various risks, technical and physical limitations, which should be considered for an ldPE plant design.

One of these is the temperature of the process gas. Due to the risk of polymerization of ethylene at higher pressures and temperatures, the gas temperature should not exceed a certain limit, which is about 110 °C for hyper compressors.

Depending on the support layout and because of the occurring temperatures, high thermal stress may be created in the piping.

As a result of the uncontinuous flow generated by the compressor, pressure pulsations occur inside the piping. These pulsations create forces, which can lead to vibration problems in the plant. Depending on the piping layout and compressor specific design features, these pulsations and vibrations can propagate more or less over the whole plant.

Additionally, vibrations may be caused not only by pulsations but also by unbalanced forces of the compressor, which are generated by the moving masses (like piston (plunger), piston rod, crosshead frame and connecting rod) of the compressor.

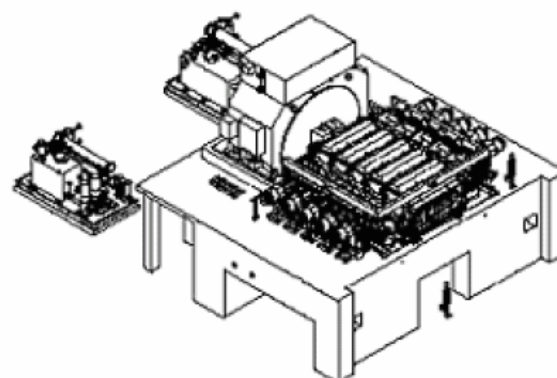


**Figure 2:** Picture of a hyper compressor with motor and foundation

The motor is chosen according to the required compressor torque. The motor inertia must be adapted to compensate the torsional irregularity of the compressor, which also depends on the chosen crank angles. A guaranteed maximum irregularity of rotation is required to limit the current pulsations in the electric circuit.

In addition, the method of flow regulation and recycle influences the compressor power consumption. The resulting discharge temperatures for each individual stage are relevant for the required intercooler and preheater capacity.



The goal of the compressor design is to respond to these problems and to get the best solution for the compressor and plant performance and reliability. It is important to know and consider all compressor design possibilities and their influences on the plant. The following two chapters will discuss the influences of compressor specific modifications on a ldPE plant design. It will also show the benefits and risks for the whole plant. Chapter 3 deals with the compressor design, chapter 4 with the specific plant design.

## 3 Compressor design

### 3.1 General design criteria

#### 3.1.1 Introduction

The basic compressor requirements to comply with the plant demands are the volume flow and gas temperature limits at specified pressures. To fulfill these limitations, the following compressor data's need to be adjusted for the two stage hyper compressor: the plunger diameter for each stage (2 parameters), the stroke for each stage (2 parameters), and the compressor speed (1 parameter).

The preliminary compressor design has these five basic parameters to choose, but only one binding limit (the compressor volume flow) and two maximum limits for the gas properties (the two discharge temperatures for both stages) on the plant side and some maximum limits for the compressor loading, like the allowable rod load of each stage and the compressor and piston speed on the compressor side. The limits on the compressor side can be fulfilled by the selection of an appropriate motion work respectively by the number of cylinders. But within these limitations, there are still many possibilities to design a compressor.

It is important to be aware of all the influences of these three (plunger diameter, stroke and compressor speed) main compressor parameters on the whole plant. The following subchapters will discuss their influences on all relevant compressor and plant properties.

#### 3.1.2 Plunger diameter

Neglecting valve losses and a variation of the clearance volume, the plunger area is proportional to the mass flow, but proportional to the rod load as well. Therefore, with a maximum pressure ratio and a given compressor frame (with an allowable plunger rod load) the maximum possible plunger area and the maximum diameter is given.

The plunger diameter determines a cylinder size that uses a size specific valve layout. The valve design together with the mass flow will create an average valve gas velocity. For a correct operation of the valve this velocity should not exceed a certain limit.

The valve design and the plunger diameter lead to a possible minimum clearance of the compression chamber. Depending on the pressure ratio of the stage and the polytropic coefficient of the compression, the influence of the clearance on the resulting mass flow of the compressor is different. The higher the polytropic coefficient and the lower the pressure ratio, the smaller is the influence of the clearance (figure 3). The pressure ratio is within the usual range for piston compressors but at the normal operating pressures for a hyper compressor the polytropic coefficient of ethylene is very high (between 6 and 8 depending on the pressures). Generally, the influence of the clearance on the mass flow is relatively small compared to other piston compressor applications. The detailed influence of the gas properties on the compressor design will be discussed in chapters 5 and 6.

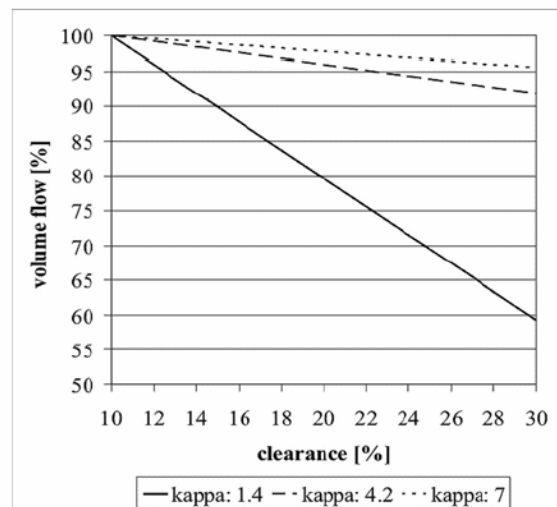
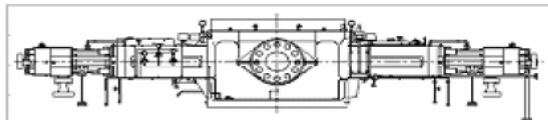


**Figure 3:** Influence of the clearance on the volume flow depending on the polytropic coefficient with a given pressure ratio of 4

A different plunger diameter results in a different plunger mass, if the same material is used for both diameters. Therefore, the selection of the plunger diameter has an influence on the unbalanced couples and forces. It also influences the foundation design. But compared to the weight of the crosshead frame and the connecting rod, the plunger mass is small. The influence of the stroke and the compressor speed on the unbalanced couples and forces is much higher than the influence of the plunger diameter.

Figure 4 shows typical relative weights of the moving masses of a hyper compressor (in percentage to the weight of a crosshead frame).



Crosshead frame:	100%
Connecting rod:	79%
Piston rod:	5%
Average plunger weight:	3%

**Figure 4:** List with the relative weights of the moving masses of a hyper compressor

In combination with the selection of the stroke, there is still a wide scope to size a plunger of a hyper compressor.

### 3.1.3 Stroke

Neglecting the valve losses, the stroke is as well proportional to the mass flow. But in comparison to the piston diameter for the stroke there is no influence on the rod load.

The stroke is proportional to the piston speed and the valve gas velocity. Both values may not exceed a certain limit. Therefore, the maximum possible stroke, with given cylinder size (valve design), piston diameter and compressor speed is given.

With a larger stroke the minimal required clearance percentage will get smaller, because the clearance required by the valves will stay the same, independent of the stroke. On the other hand, the ratio stroke to the connecting rod length will be higher what generally leads to a worse rotational irregularity. In addition, the shape of the flow (valve mass flow function) for the two sides of the compressor will be getting more different for high ratios of stroke to connecting rod length. Depending on the layout of the piping and of the crankshaft pin arrangement this influences more or less the pulsations.

Different strokes between the first and second stage in connection with the crankshaft pin arrangement, do have a significant influence on unbalanced couples and forces and therefore, on the foundation design as well.

Furthermore, the relation between first and second stage piston displacement influences the sizing of the intercooler and the preheater. With a lower ratio the first stage discharge pressure and temperature will be reduced and the second stage discharge pressure and temperature will be increased. Therefore, with a lower ratio the cooling and the heating capacity of the intercooler and preheater

can be reduced. On the other hand, the discharge temperatures must still stay beneath a maximum limit to avoid polymerization.

### 3.1.4 Compressor speed

As for the previous two compressor properties, the compressor speed is proportional to the mass flow, neglecting valve losses. The maximum possible compressor speed is given by the selected compressor frame or the allowable piston speed respectively the average valve gas velocity, which will raise proportionally to the compressor speed.

Unbalanced couples and forces will raise in squares with an increasing compressor speed.

The compressor speed has a main influence on the pulsation and vibration behavior of the plant, because all resonance conditions are in relation to the 1st harmonic order which is the compressor speed.

## 3.2 Detailed design criteria

### 3.2.1 Crankshaft pin arrangement

Another important design feature of a hyper compressor is the crankshaft pin arrangement. It has a huge influence on various plant and compressor properties such as on the pulsations, the unbalanced couples and forces and therewith the foundation design, the loads on the main bearings and the crankshaft loading, the tangential force on the crankshaft and therewith the irregularity and the sizing of the motor.

In general there is no solution which, regarding all criteria, leads to an optimal solution. The selection of the crankshaft pin arrangement is always a compromise between the above mentioned plant and compressor properties. The possible solutions depend directly from the number of cylinders.

### 3.2.2 Motion work

The following features are determined by the compressor design, but must always be considered for a new design of a hyper compressor.

For the unbalanced couples and forces the weights of the moving parts of the compressor are important.

The pulsations, unbalanced couples and forces and the rotational irregularity are influenced by the connecting rod length. In general with a longer rod length the pulsations, the higher orders of the unbalanced couples and forces and the irregularity are reduced, but the mass of this part and the overall length of the compressor unit is increased.

## 4 Plant design

The optimization process of the compressor continues for the layout of its pipe routing and the pipe fixation in the surrounding plant.

Attention must be paid to avoid any basic acoustical resonance length in the piping. The resonance length is one quarter of the wavelength for pipes closed at one end, and half of the wavelength for pipes between two vessels. The wavelength depends on the speed of sound and the harmonic order. Harmonic orders are multiples of the compressor speed. The number and the crank angle of all cylinders that are connected to the same piping system determine which harmonic order is dominating without the influence of a resonance condition.

In addition to the above resonance length, further resonance occurs if the piping length is a multiple of the half wavelength of a harmonic order. Especially for long lines, a multitude of resonance conditions of different harmonic orders might occur. The only possibility for a reliable investigation is to perform a pulsation study.

The piping system between the primary and the hyper compressor combines several unfavorable aspects: the lines are long, the discharge dampener and the separators in the high pressure recycle line are volumes that may form resonance conditions in the connecting line, and two compressors with different speed excite different harmonic orders. The pulsation study for this part must be done for both the primary and the hyper compressor. The calculated piping model will start at the primary discharge valve and finish with the hyper suction valve to avoid all possible resonance problems.

Independently from possible resonances, pulsation is always present due to the discontinuous operation of the compressor. The amount of the resulting pressure pulsation depends on the ratio of the compressor's mass flow and the piping diameter. Especially when the mass flow in an existing plant is increased but the same piping is kept, a higher pulsation will result under the assumption of the same operating conditions.

Orifices may be placed in the piping to reduce pressure pulsation (Figure 5). They act due to the pressure drop which depends on the density of the gas, the orifice design (length and diameter compared to piping diameter) and the mass flow through the orifice. The pressure pulsation damping benefit of the orifice for a specific order can be optimized, if the orifice is placed at the location with the maximum flow pulsation for this specific number of harmonics.

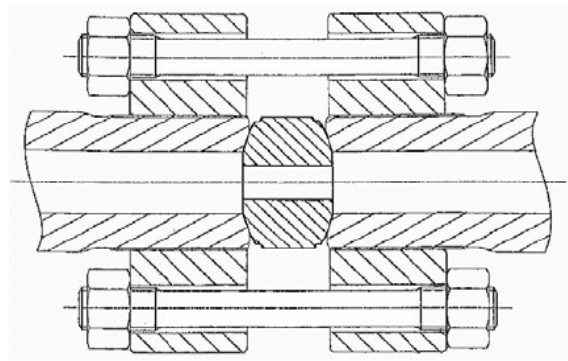


**Figure 5:** orifice in a high pressure line

Suitable locations can be determined by checking the flow and pressure pulsation in the pipe system by means of appropriate software [2].

The sizing of orifices is strongly limited to the acceptable pressure loss, which is usually in the range of less than one per cent of the line pressure (pressure drop is always coupled with power consumption). They are quite effective against pulsations caused by resonance conditions. The pressure pulsations caused by the uncontinuous flow out of the compression chamber and the superposition of the flow out of all cylinders which are connected by the piping can not be damped effectively by orifices. These pulsations can only be reduced by choosing a different piping layout (that means for example connecting different cylinders) or by adjusting the crankshaft pin angles (chapter 3.2.1)

A safe plant operation is assured if the cyclic stress in each point is small enough to remain within the limits of fatigue. A low pressure pulsation is not yet a guarantee for low stress. Parts of the piping and support structures might always have natural frequencies near the compressor's harmonic orders. If this occurs, even small excitation can lead to a strong vibration. Only the investigation of the mechanical behavior of the plant by a vibration study may discover and avoid possible resonances. The vibration study introduces the dynamic forces created by the pulsations and calculates the dynamic response.

If supports are modified to hold vibration forces, the stress due to dilatation must be checked. High pressure piping and supports are very stiff; therefore, special supports with springs should be used. Spring force will create a defined friction in the pipe support that can carry forces created by pulsation, but enables movements due to thermal dilatation.

If a common foundation structure for the interstage cooler and the hyper compressor exists, the displacements of the foundation due to the unbalanced couples and forces can be included in the vibration study as well. Therewith the mechanical study recognizes resonance condition due to unbalanced forces and due to pulsation forces.

The high pressure coolers and reactors are made of piles of thick-walled piping and easily reach very low natural frequencies in the order of the machine speed. Only early investigation will avoid excessive vibration caused by foundation excitation as well as by pulsation. Once the plant is finished, it is very difficult to shift the natural frequency because the heavy masses at heights of several meters are very difficult to stiffly support.

### 5 Calculation and validation

A good verification refers not only to the design operating data of the compressor, but takes possible deviations and uncertainties into account. There are sensible factors that influence results for either the compressor sizing, pulsation and vibration calculation.

#### 5.1 Influences on thermodynamic calculations

For thermodynamic calculations the first two thermodynamic main clauses are considered. The accurate calculation of the gas properties enthalpy and density is decisive. The different behavior of ethylene and ethylene/vinylacetat mixtures has a significant influence on the design of the compressor.

#### 5.2 Influences on pulsation analysis

The pulsation analysis is usually done according to the acoustic approximation. Therefore, the calculation program for example, uses the method of characteristics. It computes the propagation and reflection of pressure waves into one dimension: the piping axis. The main input parameter is the speed of sound of the gas in the piping.

The modeling of a piping system can be done with good accuracy. Only volumes are modeled in a simplified way, because a pulsation transversal to the main axis can not be calculated with a one-dimensional model. The error is rather small since for usual vessel diameters resonance conditions can only occur for high orders, which have only small amounts in the pulsation pulse. Typical values for a hyper compressor interstage system are a speed of sound between 1000 and 1500 m/s, and wavelengths between 300 and 450 m for a machine speed of 200 rpm.

It is desirable to verify calculation results that cover a field around the nominal operation conditions. Therefore, calculations are done for a varying speed of sound, usually  $\pm 12\%$ . In this way resonance conditions in the vicinity of operation cases can be detected and avoided.

### 5.3 Influences on vibration analysis

For a vibration analysis, a mechanical model of the plant must be built. This is where FEM-type programs have proven their utility.

The accuracy of the analysis depends widely if the model's mechanical properties correspond to those of the plant in operation. On the other hand, a certain degree of simplification is necessary to build the model with an acceptable effort. The main factors that may alter the model's properties are:

- Non-trivial 3D shapes that must not be modelled without approaches, e.g. at supports, valves, nozzles
- Varying friction in operation, due to corrosion and wear
- Quality of the construction: pre-stress due to alignment failures, varying material properties

The modeling represents a plant without initial stress. Pre-stressing a pipe or support when mounting, due e.g. to bad alignment, will give an effect of pretension and does shift the natural frequencies. Stress due to thermal expansion may act in a similar way. The result is a different behavior than predicted by the vibration study.

Most of those deviations have less influence on the basic natural modes, and more on modes at higher frequencies. A vibration analysis gives reliable information if main parts of the plant do not enter in resonance (e.g. coolers on a support structure). They cannot predict the exact behavior of small auxiliary parts, especially at higher frequencies (e.g. transmitters, drains).

### 6 Thermodynamic compressor calculation and gas properties

As seen in chapter 3 (with the discussed high polytropic exponent) the behavior of ethylene and ethylene vinylacetat mixtures is far beyond normal gas behavior for the discussed pressure range. The calculated gas property (density, enthalpy and speed of sound) have a significant influence on the compressor and the surrounding plant design.

The calculated speed of sound is the main input value for the pulsation study. An accurate calculated speed of sound is the basis to avoid any resonance conditions and problems in the piping of



the plant. Figure 6 shows measurements [according 1] of the speed of sound in the relevant pressure range for hyper compressors.

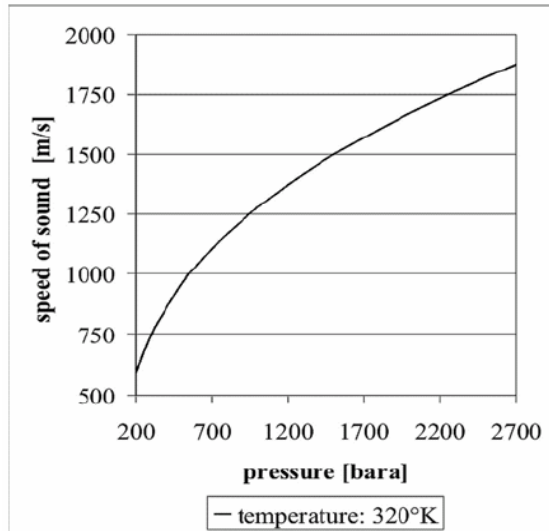


**Figure 6:** Speed of sound for pure ethylene

The calculated density is directly linked to the calculated interstage pressure, because without side stream the mass flow of the first and the second stage must be equal. The volume flow of each stage is given by the compressor design and the pressure ratio (interstage pressure). A different density behavior over the pressure range, for example for ethylene vinylacetat mixtures compared to pure ethylene, can increase the interstage pressure by more than 10%. Therefore, accurate rod and compressor loadings can only be calculated with an accurate density and knowledge of the operating gas compositions. Figure 7 shows the density (according 1) at higher pressures for pure ethylene.

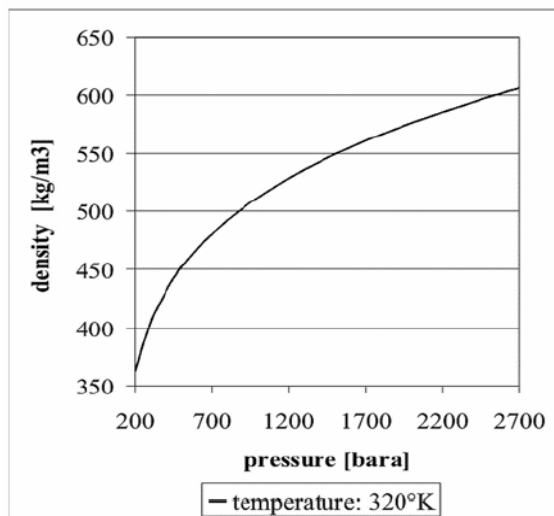


**Figure 7:** Density for pure ethylene

The source of correct gas behavior calculations are keenly measured gas properties in the required pressure range. The behavior of each gas property model has to be compared to accurate measurements or accurate measurements should be the source for a good gas property model.

## 7 Pulsation and vibration; comparison measurement calculation

A measurement of pulsation in high pressure plants is a task that requires a considerable effort. One possibility occurred while revamping an existing hyper compressor. In our example the 8-cylinder 2-stage hyper compressor has a shaft power of 9650 kW at 200 rpm and compresses ethylene from 220 to 2150 bar. It has been running at a customer site since 1975.

In the year 2000, the mass flow of this machine was raised to 72300 kg/h by installation of cylinders with larger bore. A pulsation study was done in advance to verify the modified system. High pulsation was calculated, that could be reduced to still admissible values up to 14 % peak to peak by installation of orifices. Further optimization was difficult because each 1st stage cylinder feeds via one line and cooler into one 2nd stage cylinder. The usual connection between two or more cylinders was not possible due to process conditions.

The vibrations that occurred after startup were the reason for the client's demand of further pulsation optimization. However, a measuring campaign should verify if the pulsation calculations were reliable.

One of the interstage lines was equipped with pressure gauges at special lens rings in existing flange connections. A scheme is shown in figure 8. The cooler consists of three parallel pipes of 32 mm inner diameter, the main piping has 58 mm inner diameter. The line pressure is 820 bara.

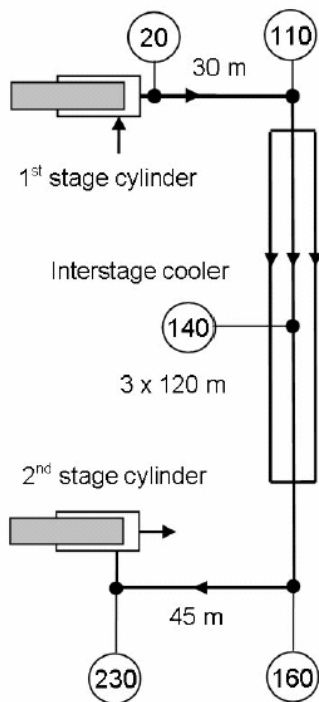


**Figure 8:** Scheme of the modeled interstage

The location of the PULSIM model nodes corresponds to those points where the pressure sensors are installed, see figure 9.

Location of measuring points	Node No. in model
1st stage discharge	20
Cooler inlet	110
Middle of cooler	140
Cooler outlet	160
2nd stage suction	230

**Figure 9:** Location of calculation nodes and measurement points in the system

Figure 10 shows the measured results as pressure at the measuring point over one revolution of the compressor crankshaft. The peak resulting from the 1st stage cylinder discharge pulse moves with speed of sound (1180 m/s) and appears at the following measuring points with a delay. After a line length of 195 m or roughly half a crankshaft revolution the peak reaches the 2nd stage suction cylinder.

The crank angles are arranged in a way that the depression caused by the suction pulse can partly compensate the incoming pressure peak.

Figure 11 shows results of the PULSIM calculation. Again, pressure is displayed over one crankshaft revolution. The overlaid columns show in addition the amounts of the first 10 harmonic orders. The

shape of the calculated curves shows a very good coincidence with the measured values.

The measurements show a high frequency overlay that could not be calculated by PULSIM, although harmonics up to 30<sup>th</sup> order were analyzed. A further investigation is in course.

The comparison shows that the calculation by means of methods of characteristics like PULSIM performs very well also under conditions of very high pressure. They prove to be a reliable tool for the optimization of polyethylene plants.

## 8 Conclusion

To avoid serious and time-consuming problems during the startup and operation of high pressure polyethylene plants, it is important to consider the whole plant and a multitude of aspects of compressor sizing. If the compressor manufacturer can verify the pressure pulsation by himself, the compressor can be adapted to the requirements of the plant more accurately and in a shorter time. Still better results can be achieved if both the booster-primary and the hyper compressor can be considered in the same optimization process.

Programs that use the method of characteristics have proven their reliability for high pressure application as it is shown in a comparison with measurements.

[1] ETHYLENE (Ethene) International  
Thermodynamic Tables of the Fluid State – 10,  
IUPAC Chemical Data Series No. 34, 1988,  
Blackwell Scientific Publications LTD

[2] PULSIM version 1.13, March 11 2002:  
calculation program developed by the Nederlandse  
Organisatie voor Toegepast-  
Natuurwetenschappelijk Onderzoek TNO

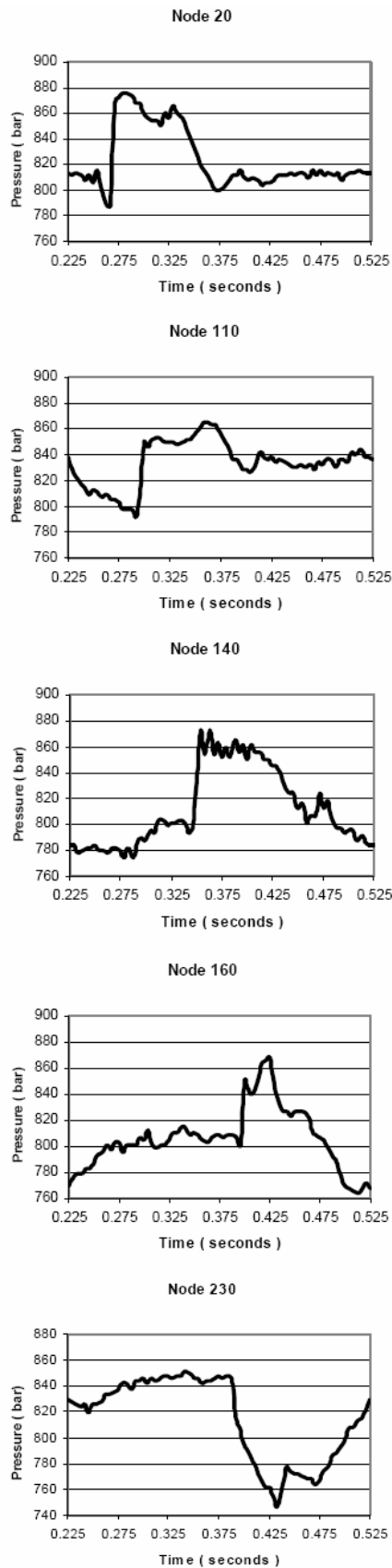


**Figure 10:** Measured values at points according to figure 9

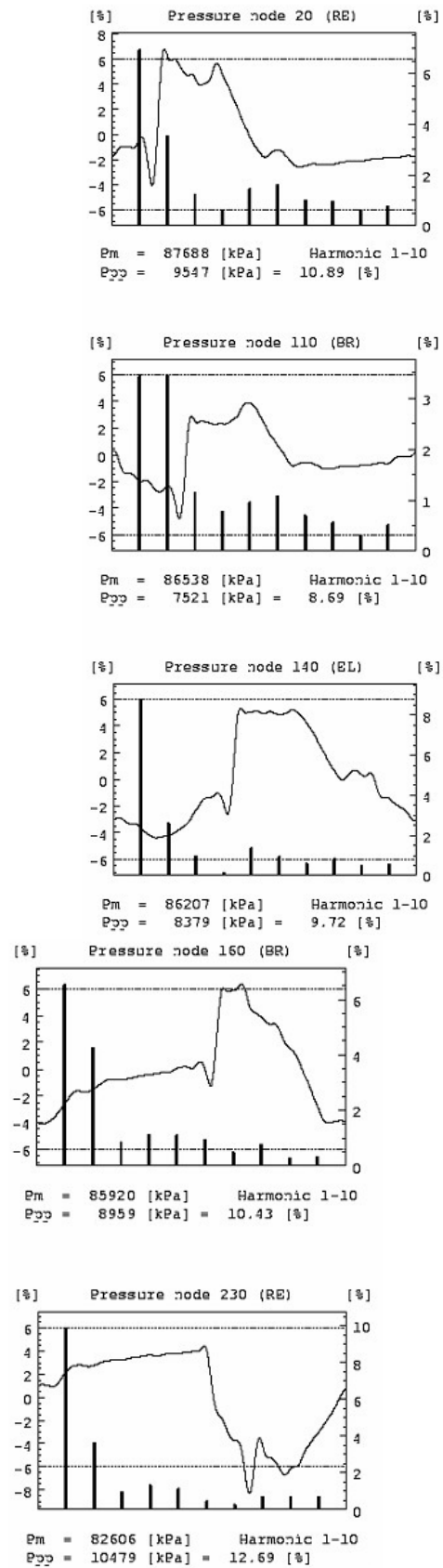


**Figure 11:** Calculated values at points according to figure 9



# **Economical Pipe Stress Analysis using Parametric Modelling and Design Standards**

by:

**V. Kacani, E. Huttar**  
**Leobersdorfer Maschinenfabrik AG**  
**VIENNA**  
**Austria**  
**vasillaq.kacani@lmf.at**

**4<sup>th</sup> Conference of the EFRC**  
**June 9<sup>th</sup> / 10<sup>th</sup>, 2005, Antwerp**

## **Abstract:**

For the optimal mechanical and acoustic selection and recalculation of the component parts of a compressor unit, generally, it is necessary to use available technical software as well as the manufacturer's own programs. It is important that this software should allow the compilation of user tools. This paper will present the parameterizing of the mechanical designing of compressor components, such as straight pipes, pipe elbows, flanges and pressure vessels under various types of loads, such as internal pressure, dead weight, wind and shaking forces. Great emphasis will be placed on the modelling of pulsation dampers. In general, shell elements are used to model these. For the area around nozzles and supports, a 3D model is performed with the help of the submodel technique. In this way both structure stress and notch stress are obtained. These figures are important not only for the endurance strength and the fatigue limit analysis, but also for comparison with various rules and standards. The carrying out of modal and mechanical forced harmonic analysis will also be dealt with, as well as the questions of the excitability of a mode and the dependence of the mechanical structural natural frequencies on the prestress.



## 1 General Remarks

Components of piston compressor units are exposed to loads from internal pressure, temperature and vibrations. In addition, and depending on the site location of the compressors, they also have to bear strain caused by acceleration, wind and seismic activity. Pressure pulsations within the unit also generate shaking forces that are of enormous importance. The first steps in designing the piping and its components, must therefore be based on flow considerations. To keep pressure loss, and with it the closely related power loss, to a minimum, relatively large nominal diameters are chosen as far as possible, but this is limited by high costs and lack of space. As the mass flow to be conveyed increases continually, the tendency is towards relatively small pipe cross sections.

The next step is to test the piping and its components, such as pipe elbows, T-pieces etc. under static internal pressure load. In doing this, the maximum operating temperature and allowances must be taken into consideration. The calculations are generally made in accordance with various standards and regulations, such as <sup>1</sup>, <sup>2</sup>, <sup>3</sup>, and in accordance with manufacturer specifications.

Next, the stress experienced under the loads described above is examined. As it is no longer possible to examine each individual component separately, a model of the whole system has to be performed. The quality of this model is crucial to the results.

## 2 Parametrical modelling of the piping system for FEA

The components of a compressor unit can generally be divided into the following groups:

- piping: straight pipes, pipe elbows, flanges, valves,
- pulsation dampers, separators, coolers
- supports for piping components
- cylinders, distance pieces, crankcase
- base frame
- other

In this paper, only the modelling of the piping system and the pulsation dampers will be dealt with i.e. only those components that are situated between the cylinder flanges.

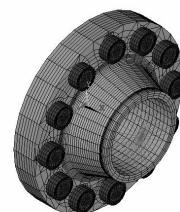
A section of a straight pipe is defined by its outside diameter, wall thickness and length. In most FEA Programs there are special elements, called PIPE elements. They are based on beam elements but

they nevertheless allow for internal pressure and, at the same time, it is also possible to subject them to transversal pressure in three directions (e.g. from wind, from snow and from seismic forces - in piping that is laid in the ground - etc.). The medium inside the pipe, and the insulation, can also be taken into consideration. There are also special elements for pipe elbows and T-pieces in ANSYS. For flanges and valves, the masses, and even the SIFs and FLX factors, can be entered, although the latter can also be entered by users.

To be able to perform an exact dynamic model of the flange connection, the flexibilities were calculated using a specially-made parametrical FEA 3D model. In addition to <sup>5</sup>, the axial, bending and torsional flexibility of the screw connection were also calculated here, taking into account the contact surfaces (between the gasket and the flange facing) and also the prestress of the bolts. To do this, a macro was programmed, as input parameter, containing the geometrical figures given in the standards (e.g. DIN 2627-2638).

To determine the flexibility, a spider is formed with MPC elements in the neck of the flange (at the joint where the pipe section meets the flange) and the required load is applied to its centre. The ratio of the load to the displacement of the centre node is then the corresponding flexibility. Figure 1 shows the FEA model of the flange connection with the dimensions of the DN150, PN160. Figure 2 shows the flexibilities calculated for a flange DN150, PN160 in accordance with DIN 2638.

The macro can in particular be used for cylinder flanges, which are usually different from standard flanges. Modelling the flange connection gives more exact results, both for the model analysis and for determining the thermal stresses. It is also possible to implement the 3D model of the flange connection into the model as a whole. Doing this does not however necessarily lead to more exact results, but the calculating time increases enormously.



0 PN160 D=355 b=50 k=290 h1=128 d3=210 s=12.5 d4=218

**Figure 1:** 3D geometric model of flange (PN160,DN150)

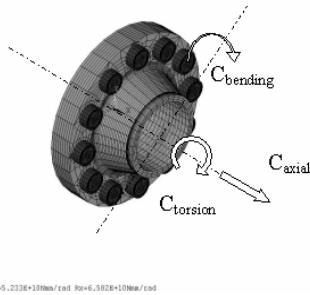
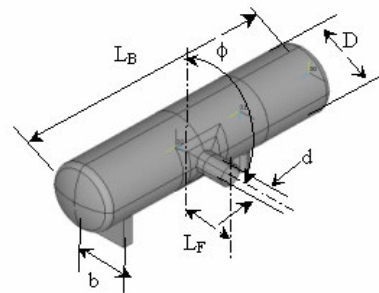


**Figure 2:** Axial, bending and torsional flexibility

In addition, those piping components that are exposed to the same pressure and temperature loads are grouped together in sub-systems. A two-stage machine has for example five sub-systems: compressor inlet, 1<sup>st</sup> stage discharge, 2<sup>nd</sup> stage suction, 2<sup>nd</sup> stage discharge and compressor outlet. Further parameters are the properties of the materials, allowances, etc.

In the next step, the pulsation dampers are modelled. To do this a very extensive macro was programmed, that could be called as often as required. Some of the parameters are listed here below:

- positioning the pressure vessel in space by means of three angles and three coordinates
- type of head (torispherical or ellipsoidal forms)
- outside diameters, wall thicknesses, shells, heads
- pressure vessel lengths
- pressure vessel supports in accordance with AD-Merkblätter S 3/1, S 3/2
- flange data, flanges on the shell (max. 5 at present)
- flange data, flanges on the heads (max. 2 at present)
- definitions of local systems of coordinates on the axes of pressure vessels and of flanges



Piping Technip, 13.447 Piping System=3

**Figure 3:** Model of pressure vessel for FEA

Pressure vessels are usually modelled using quadratic shell elements. These elements give good results when the ratio between thickness and the characteristic length of the system is greater than 10. For ratios of 5-10, the results are mostly acceptable. As these elements are two-dimensional, they cannot provide any notch stresses due to the bending part. Determining the local stress at the connection between the nozzle and the shell, is of extreme importance when determining the vessel's working life. Inaccuracy to the extent of  $\pm 10\%$  of the actual stress will, for steel, result in an increase/decrease in the endurance limit of  $+70/-40\%$ . For this reason the structure at the nozzles and the connections of the supports, has to be finely modelled using 3D elements. As the rough structure as a whole is sufficient for determining the displacement, the submodelling technique (the cut boundary displacement method) can be used for calculating the local stresses. A cut is made through the whole model around these areas. Displacements on this cut surface are calculated for the whole model and are then transferred to the submodel as boundary conditions. Figure 4 shows the volume submodel around the connection between the nozzle and the shell. This technique is parameterized and we obtain, as shown below, the stress along various paths both in the rough shell model and in the submodel. Meshing of these areas is carried out in accordance with <sup>6</sup>, in order to determine the structural stress directly. This means that the stresses can be determined directly at three points ( $0.4*s$ ,  $0.9*s$ , and  $1.4*s$ ;  $s$ =wall thickness), and from these three figures, the structural stress can be extrapolated.

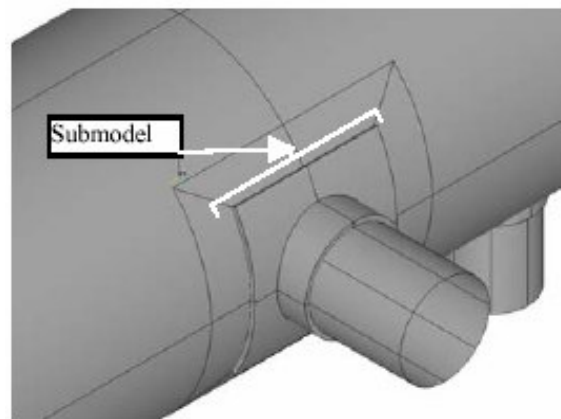


**Figure 4:** 3D submodel of a nozzle

Based on the parameterizing technique described above, Figure 5 shows the FEA model of the pipe with pulsation damper and its supports, of two compressor units in parallel operation. These units are single-stage balanced opposed B152 units with two throws, 490 rpm, 300 kW.

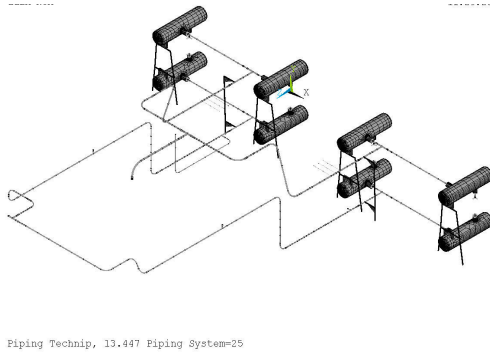


**Figure 5:** FEA model of piping system & vessels

## 3 Finite Element Analysis

### 3.1 Modal Analysis

It is recommended that the first step in the FEA analysis should be a modal analysis. This step in the calculation is important for the assessment of the whole system. It is here that the natural frequencies, vibration modes and the participation factors in 6 directions, that are used for the excitability of the vibration modes are determined.

The mechanical structural natural frequencies have to fulfil certain criteria. For example, according to the 5<sup>th</sup> edition of the API 618 (which is soon to appear), the first, mechanical, natural frequency must be 20 % above the second, harmonic of the reciprocating compressor. The system can of course be detuned by adapting (adding) supports until the required guidelines have been fulfilled.

The excitability of the model in various directions can also be assessed based on the vibration shapes and their participation coefficients. The following case history, Figure 6, is of a single-stage, natural gas, V-arrangement compressor with a single throw and two axes.

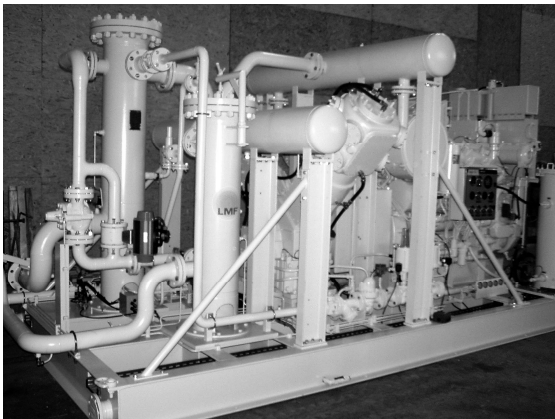
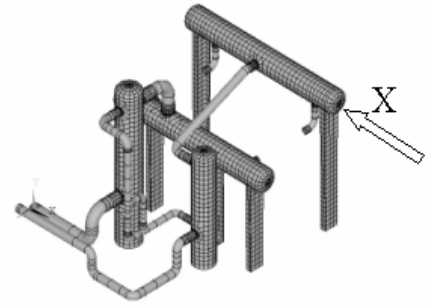


**Figure 6:** CNG VC compressor in V arrangement



PIPING, Zorlu Enerji, 13.418

**Figure 7:** Mode is excitable in direction X

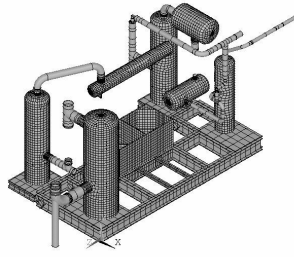
From the participation factors, it was clear that the vibration shape was excitable in direction X. The harmonic analysis then performed, showed relatively high dynamic stresses in the pipes attached to the pulsation dampers. Two corrective measures were decided upon:

- Additional supporting of the pulsation dampers on four beams, as shown in Figure 6 (greater distance from the compressor harmonic).
- Uncoupling the two cylinders acoustically by installing pulsation damper internals. This reduced the exciting force.

In this phase of the designing, it is also important to examine the effect of prestress (internal pressure). The following case history is of a two-stage balanced opposed compressor B252 with 250 mm stroke, 420 rpm, 650 kW, 1.5-2.5 bar inlet pressure and 24-28 bar discharge pressure. Figure 9 shows the corresponding FEA model of this unit.



**Figure 8:** B252 Compressor in the LMF assembly area



PIPING SYSTEM, BASELL, 13.303

**Figure 9:** FEA model of piping system, pressure vessels & base frame

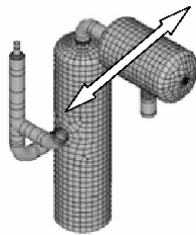


**Figure 10:** Lateral vibration mode of 2nd stage separator & pulsation damper

The modal analysis was carried out both in unloaded condition and under internal pressure/dead weight. In some of the natural frequencies, relatively large deviations were found. Under internal pressure, the lateral vibration of the second stage suction pulsation damper, Figure 10, had a natural frequency that was about 15 % higher than when it was in an unloaded condition. It is therefore important to take this phenomenon into account, not only in the difference between the natural frequencies from harmonics of the compressor, but also in the harmonic response of the structure.

### 3.2 Stress analysis under internal pressure/dead weight, temperature and external loads

The next step is the examination of the piping system under internal pressure/dead weight, stress from temperature and possible external loads. The aim of this calculation is to determine the stress and/or the stress components (depending on the rules) of the piping components, such as straight pipes, pipe elbows, tees, reducers etc., taking into consideration the SIFs and FLXs. The types of loads must here, be divided into two categories, primary and secondary, in accordance with the regulations (e.g. according to <sup>2</sup>, AD-S4). Then the

max. permissible stress can also be determined to be used to compare with the actual stresses.

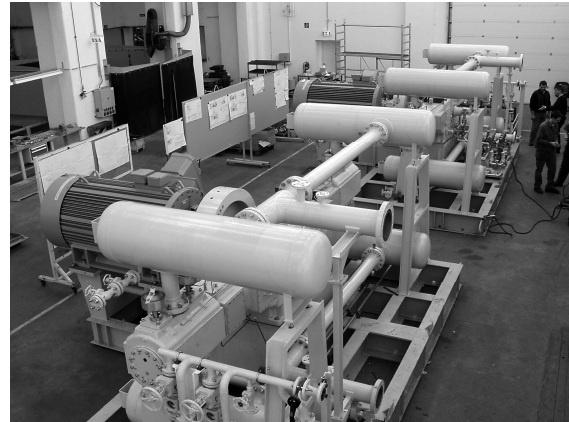


**Figure 11:** Two B152 compressors in the LMF assembly area

The forces and the moments on the flange connections and the stresses (principal stresses) around the nozzles and support areas of the pressure vessel are also determined here. Other important stress figures are structural stress and notch stress, which are necessary for a fatigue limit analysis, e.g. in accordance with FKM <sup>7</sup>. On the basis of the case history in Figure 11 and its FEA model, Figure 5, the following pictures show the stresses on the nozzles of a pressure vessel. The von Mises stresses and the principal stresses are the result given by the submodel technique. These results are also parameterised and can likewise be calculated on the shell model for purposes of comparison. Figure 12 shows the von Mises stress and Figures 13 and 14 the principal stresses along a path on the surface of the nozzle (Fig. 13) and the shell (Fig. 14) under internal pressure and dead weight. From the path results, the structural stress can easily be calculated.

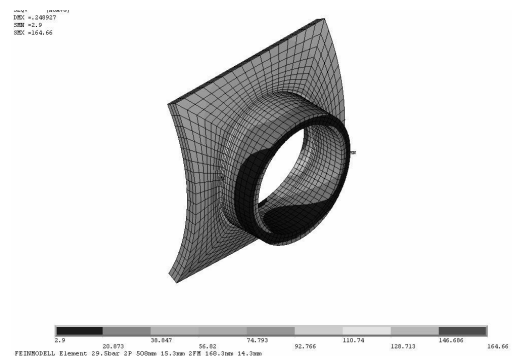


**Figure 12:** Von Mises stress in nozzle submodel



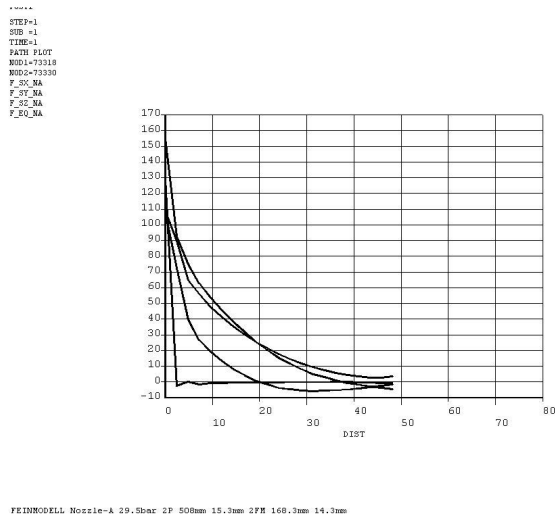


**Figure 13:** Path results in nozzle outer surface showing principal stresses and von Mises stress

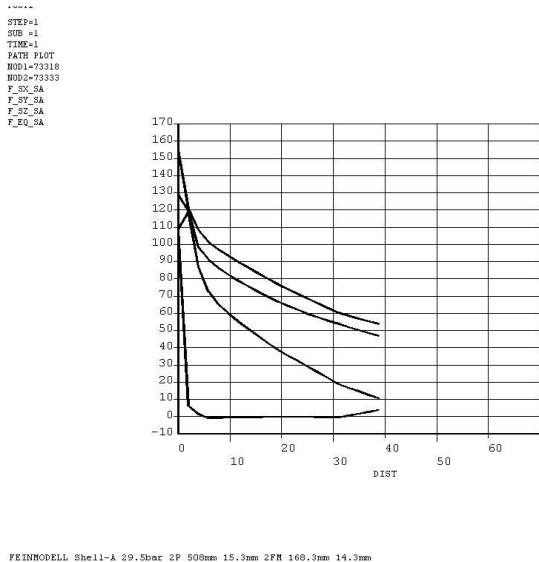


**Figure 14:** Path results in shell outer surface showing principal stresses and von Mises stress

### 3.3 Harmonic forced vibration analysis

Here the structural system response to the dynamic excitation resulting from pressure pulsation, dynamic gas forces, unbalanced dynamic forces and couples, is examined. To determine the pulsations in the compressor unit as a whole, it is necessary to use suitable, specially developed programs. This means that two software programs are generally needed for the complete analysis. The first for the flow calculation (acoustic) and the second for the mechanical structural examination (FEA program). Special software is also available to link the flow of a fluid to the movement of the structure. These

programs realise the fluid-structure interaction (so-called FSI) and generally lead to better results <sup>4</sup>.

Here the shaking forces calculated from the acoustic program, in the form of Fourier analysis (amplitude and phase of force), are transferred into the structure program (FEA). For this purpose, an interface was established to link the two programs. It is of crucial importance here to determine the shaking forces and their acting points correctly. As also described in <sup>4</sup>, the forces arise at the point where a change in flow direction and/or in cross section takes place. Figure 1 shows the typical places where shaking forces arise.

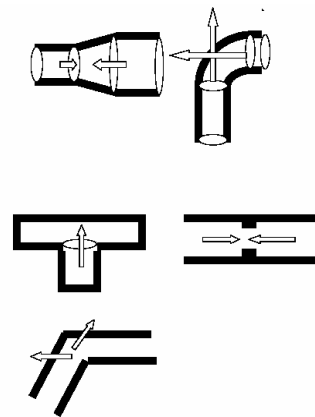


**Figure 15:** Typical shaking forces on piping systems

Figure 15 shows typical shaking forces on reducers, elbows, tees and orifice plates. In order to consider any variations in the gas parameters and geometry, the acoustic and harmonic analysis is done (even if the compressor speed is constant) for a range of  $\pm 20\%$  of the rated speed. This analysis gives, as its results, the dynamic stresses and the vibration velocities.

## 4 Summary

The parametric modelling of piping components and pulsation dampers described here, permits a systematic and particularly time-saving analysis of the mechanical system. The dynamic parameters of flange - particularly cylinder flanges, axial, torsional and bending flexibility - are determined using a separate macro and are then implemented into a model of the piping. Shell elements are used to model the pulsation dampers and the submodel technique is used for the area around the nozzles and supports. This allows the notch and structural stress to be more exactly determined. It is important that the modal analysis should be carried out both while the machine is unloaded (idling) and under operation conditions. The case histories examined showed deviations of 15 % from the natural

frequencies. With the help of modal analysis it is even possible to assess the dynamic excitability of the mechanical model. From the harmonic response of the mechanical model, the dynamic stress and vibration velocities can be determined.

---

### References

- <sup>1</sup> ASME Code for Pressure piping, B31 ASME B31.1
- <sup>2</sup> AD-Merkblätter
- <sup>3</sup> DIN 2413
- <sup>4</sup> VDI 3842 Schwingungen in Rohrleitungssysteme
- <sup>5</sup> A. Lifson, A.J.Smalley: Bending Flexibility of Bolted Flanges and Its Effect on Dynamical Behaviour of Structures
- <sup>6</sup> Hobbacher, Empfehlung zur Schwingfestigkeit geschweißter Verbindungen und Bauteilen
- <sup>7</sup> Rechnerischer Festigkeitsnachweis für Maschinenbauteile FKM